APPLICATION OF SIGNAL ANALYSIS TECHNIQUES TO CARDIAC ARRHYTHMIA DETECTION AND CLASSIFICATION

by

JYH-YUN WANG

B.S. in Physics, Fu Jen University, Taiwan
1970

M.S. in Physics, Northeastern University
1973

SUBMITTED IN PARTIAL FULFILLMENT OF THE
REQUIREMENTS FOR THE DEGREE OF
MASTER OF SCIENCE

at the

MASSACHUSETTS INSTITUTE OF TECHNOLOGY
January, 1976

Signature of Author_____
Department of Aeronautics and Astronautics, January 26, 1976

Certified by_____
Thesis Supervisor

Accepted by_____
Chairman, Departmental Graduate Committee

APPLICATION OF SIGNAL ANALYSIS TECHNIQUES TO CARDIAC ARRHYTHMIA DETECTION AND CLASSIFICATION

by

Jyh-Yun Wang

Submitted to the Department of Aeronautics and Astronautics on January 26, 1976, in partial fulfillment of the requirement for the degree of Master of Science.

ABSTRACT

A completely new approach to develop an automated program for rhythm analysis of electrocardiograms and vectorcardiograms using powerful statistical techniques of sequential estimation and detection theory is studied. The underlying cardiac rhythms are modeled as outputs of low-order linear stochastic dynamical systems. The relatively predictable persistent cardiac rhythms are detected and classified by using a multiple model hypothesis testing technique. Detection and classification of the relatively unpredictable transient cardiac arrhythmias are performed using a generalized likelihood ratio technique. Both the multiple model hypothesis testing and the generalized likelihood ratio identification techniques are tested extensively on a variety of actual data which includes normal sinus rhythm, bigeminy, trigeminy, PVC, PAC, dropped beat, SA block, tachycardia burst, multiple PVC, and slowing of heart rate. The results indicate that these cardiac events can be identified with great accuracy.

Thesis Supervisor: Alan S. Willsky, Ph.D.

Title: Assistant Professor of Electrical Engineering

ACKNOWLEDGMENTS

The author wishes to express his appreciation to his thesis advisor, Professor Alan S. Willsky, for his continued encouragement and constructive advice and comments throughout his thesis research. The author is particularly grateful to Dr. Donald E. Gustafson of the Charles Stark Draper Laboratory, for introducing him to this program and for providing continued assistance, support and encouragement. It was a great pleasure to work with them.

Special thanks go to Colonel M. Lancaster and his other associates at the United States Air Force School of Aerospace Medicine for giving their support and advice on medical matters, and for providing electrocardiographic records.

Finally, the author wishes to acknowledge the Charles Stark Draper Laboratory whose personnel and facilities contributed greatly to this work.

This thesis was prepared under CSDL Projects 52-65700 and 52-70000, sponsored by the United States Air Force School of Aerospace Medicine through contracts F41609-75-C-0013 and F41609-76-C-0004.

The publication of this work does not constitute approval by the United States Air Force or the Charles Stark Draper Laboratory of the findings or conclusions contained therein. It is published only for the exchange and stimulation of ideas.

TABLE OF CONTENTS

CHAPTER 1

INTRODUCTION

1.1 Principle of Electrocardiography

It has been known for many years that a measurable amount of potential variations within the electrical field on the body surface is associated with the electrical activity of the heart. As early as 1887, Ludwig and Waller [1] experimented with the capillary electroscope and recorded this electromotive force from the precordium. In 1899, Wenckebach [2] employed the polygraph to make simple but precise observations of the electrical events of atrial and ventricular activation. Einthoven's description [3], in 1903, of the string galvanometer for recording the potential variations, stimulated a sudden increase in both clinical and experimental studies of electrocardiography. This type of galvanometer has remained one of the most frequently used recording method because of its simplicity and portability, although other principles, such as the use of vacuum tube amplification, have been applied. Recording the potential difference between any two points on the body surface is accomplised by means of electrode from which the current is conducted to the galvanometer of the electrocardiograph via the lead wire, to be returned to the body by way of a second lead wire and its electrode. In clinical practice twelve leads are usually recorded routinely: (1) three bipolar extremity leads (standard limb leads), (2) three unipolar extremity leads, and (3) six unipolar precordial chest leads [4]. Using this standard twelve-lead system, the resulting potential difference record is called the Electrocardiogram (ECG).

Biophysical models of the heart and factor analysis of surface potentials have shown that the electrical effects on the surface of the body can largely be accounted for by a single equivalent electrical dipole free to rotate in three dimensions [5]-[7]. Under suitable homogeneity assumptions, the components of this equivalent dipole can be estimated by measuring three potential differences in perpendicular directions on the surface of the body, or by resolving non-orthogonal measurements. In practice, the Frank orthogonal lead system which consists of seven leads resolved along mutually orthogonal axes [8], is the most commonly used for this purpose. A record obtained by the use of this lead system is called a Vectorcardiogram (VCG).

While many differences occur in various leads from the same subject, and different persons yield distinctive curves, they all tend to conform to a common pattern illustrated in Figure 1.1. The normal electrocardiogram of a cardiac cycle consists of a series of waves arbitrarily designated by Einthoven as the P wave, the QRS complex, and the T wave. When the heart is at rest the electrocardiogram dis-

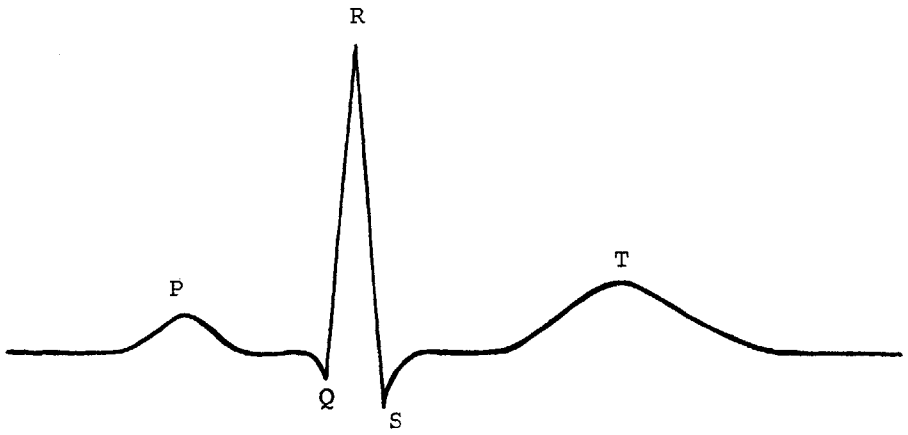

Figure 1.1 Waves of the Electrocardiogram

plays a straight horizontal line, the so-called iso-electric line or baseline. This baseline represents a constant direct current value produced by the recording device. Alternating current developed with myocardial activity is superimposed upon this baseline and is recorded as upward (positive) or downward (negative) deflections. The baseline may be shifted whenever there is movement of electrodes or a sudden change in skin resistance. In such a case the electrocardiographic signal is superimposed upon the baseline variations.

The P wave represents the depolarization wave of the auricular musculature which spreads radially from the sinoauricular (SA) node to the atrioventricular (AV) node. There is a delay in transmission of the impulse at the AV node, represented on the electrocardiogram by the P-R segment. The QRS complex is the depolarization of the ventricular musculature. It consists, usually, of an initial downward deflection, the Q wave, an initial upward deflection, the R wave, and an initial downward deflection after the R wave, the S wave. The T wave represents the ventricular repolarization and follows the QRS complex with a delay, the S-T segment, which represents, roughly, the duration of the excited state of the ventricular musculature, or the interval of time between completion of depolarization and the beginning of repolarization of the ventricular musculature [9].

Under pathological conditions the electrocardiogram undergoes some characteristic changes. The various resulting abnormalities in the electrocardiogram may be divided into two groups: (1) disturbances in the cardiac rhythm, and (2) changes in the electrocardiographic waveform. Abnormalities in the electrocardiographic

waveform are more or less related to the specific pathological process and its location in the heart, and thus, can be used to describe the state of the working muscle masses. The abnormalities in the order of the heart beat, known as cardiac arrhythmias, yields information concerning the sites and rates of cardiac pacemakers and the impulse propagation through the cardiac conduction system [9]. The electrocardiogram is the instrument "par excellence" in the diagnosis of the following clinical conditions: myocardial infection, atrial and ventricular hypertrophy, arrhythmias, pericarditis and systemic diseases which affect the heart. A complete analysis of the electrocardiogram should include both the rhythm analysis and the waveform analysis.

1.2 Computer-Aided Analysis of the Electrocardiogram

1.2.1 Background

Due to the high cost of labor, and the large amount of ECG/VCG records to be analyzed, the time available to the interpreting cardiologist is too limited for taking a multitude of measurements. In addition, due to the limited precision of hand measuring, which does not exceed 0.05 mm, and lack of well-defined criteria for determining the onset and end of waves especially in cases when waves are of low amplitude and have gradual slope, cardiologists are known to differ frequently in their measuring of electrocardiographic events. It is difficult to correlate mentally large numbers of ECG/VCG parameters, and extensive hand calculations for making use of efficient statistical classification techniques are also too time-consuming to be practical.

Careful studies have been made to assess the human variability in ECG interpretation. In one study, the results showed that in

repeated observations of one ECG the same cardiologist did not agree with his own diagnostic statements in 20% of the time, and different cardiologists did not agree with each other in nearly 25% of the statements [10]. Another study showed that 7 cardiologists completely agreed in only 28 out of 100 ECG's [11].

The advent of modern computer techniques changed this situation drastically. The unique ability of computers to perform a large number of numerical computations in a very short period of time enables one to apply a variety of mathematical operations for analyzing ECG/VCG records. ECG/VCG analysis from its engineering aspect is also an ideal field for automation. Some of the advantages of using computer-aided analysis of ECG/VCG are given in the following:

(1) Short-term and long-term cost saving.

(2) It become feasible and practical to obtain any number of ECG/VCG measurements. For instance, the slope of the wave at every point can be easily computed. Whether the signals are complex or simple, the measurements will be remarkably precise compared to those obtained manually.

(3) Best utilization of information already available on the scalar or vector electrocardiograms is obtained. Using high fidelity recording equipment, the computer can store and repeat the electrical signals of cardiogram; eliminating noise, interference, and other confusing artifacts which present difficulties in analysis.

(4) Application of complex statistical classification procedures no longer represent a limiting factor in ECG/VCG data evaluation.

(5) It is feasible to perform mass screening of large population groups which is absolutely necessary for the study and control of heart diseases.

Although the computer-aided analysis of ECG/VCG is an attractive one, problems do exist:

(1) In contrast to the human interpreter who possesses high pattern recognition capability, the computer finds this one of the most difficult operations to perform.

(2) The tremendous amount of variation that occurs among subjects, which we would like to classify into the same class, makes it very difficult to invent practical rules that include all instances.

(3) For a computer-aided ECG/VCG analysis program, the instructions must be listed in an orderly manner and followed precisely during interpretation. In contrast to this orderly, predetermined logical process, the human interpreter has the opportunity to review the record for any amount of time limited only by his own needs. He may review the data randomly, and even correct his initial diagnosis subject to further reviews.

(4) It is very difficult for the computer to identify the P waves, which have low amplitude and gradual slope, and thus may be buried in noise or masked by ventricular activity. This is also true of other subtleties of the cardiogram.

1.2.2 Historical Review

The concept of computerized analysis of the ECG/VCG is not new. The requirements for practical clinical applications of such programs include two parts: (1) analysis of cardiac rhythm, and (2) analysis of the contour or waveform of the complexes. Starting in the late 1950's there have been numerous efforts to automate the analysis of ECG/VCG's, resulting in many computer-aided programs for ECG/VCG analysis being used and developed [12]-[27]. Pattern recognition in these programs are almost exclusively done using a heirarchical computer logic structure. Much time is spent checking validity of the data, correcting measurement errors, and extrapolating for missing data. These tests are deterministic in that specific thresholds are set for the various tests, rather than statistical, wherein probabilistic statements are given based on statistical models of the temporal patterns. Thus, these schemes involve very complex logic structure which are difficult to debug and to modify. Another drawback in using the logic tree structure is the limitation of the rhythm analysis program in their assignment of severity levels. For example, arbitrary terms such as "severe", "mild", and "regular" are used. Thus, in spite of the amount of work done on this problem, the problem of computer-aided analysis of ECG/VCG is not yet completely solved.

Recent comparative studies on the performance of the available programs have indicated that the IBM program was the best overall [28]. On an overall basis, the program had a detection rate of 94.6% on a total of 1150 waveforms tested. However, the rate of correct identification was lower than this detection rate, because some of the arrhythmias detected by the program were assigned to "undetermined

rhythm" by the final identification logic. The program performed even worst on ventricular arrhythmias, for which the detection rate was only 86%. In the reproducibility study, the results showed that using two different digital representations of the same analog ECG record, the output rhythm statements generated by this program did not agree with each other about 10% of the time. It would appear that available programs are too highly tuned in that some features used for diagnosis actually contain more noise than information.

In more recent years, a variety of statistical analysis procedures for ECG/VCG analysis were studied to improve the performance of detection and classification for arrhythmias. Gersch, et al. [29],[30] transformed a sequence of 100 or 200 R-R intervals into a three-symbol (namely, short, regular, and long R-R interval) Markov chain sequence. The probability that the observed sequence was generated by each set of prototype models characteristic of different arrhythmia classes, was computed. That prototype corresponding to the largest probability of generating the observed sequence was classified as the disorder. The disorders considered were atrial fibrillation, PVC and PAC, bigeminy, sinus tachycardia with occasional bigeminy , sinus tachycardia, and ventricular tachycardia. Tests of this approach on patients with atrial fibrillation (AF) and atrial fibrillation with occasional PVC's (AFOCC) showed that 4 out of 15 AF records were misclassified as AFOCC using 200 heart-beats. The performance was worst when using 100 heat-beats. Pipberger, et al. [31] applied linear discriminat function analysis to training and independent sets of three common arrhythmias (namely, normal sinus rhythm, sinus rhythm plus premature beats, and atrial fibrillation) using R-R interval information only.

On an overall basis, this approach correctly classified 85% of the records tested. The performance for the premature beat classification was the worst, for which a correct identification rate of only 66% was obtained.

All the above statistical analysis procedures for classification have used fixed sample tests. Among the problems with a fixed sample test is the possibility that if the sample size is too large then a transient phenomenon may go undetected due to the large number of normal beats used in the average. Tsui and Wong [32] studied the feasibility of utilizing Wald's sequential probability test in cardiac rhythm classification. It has provisions for controlling error rate than sample size. The expected number of observations under pairwise testing of three selected rhythm classes (atrial fibrillation, normal sinus rhythm, and premature atrial and ventricular contractions) as a function of error rate were shown. However, no test of this approach on actual ECG data was given.

It is important to point out that, on an overall basis, arrhythmias were the greatest source of program errors of the three programs tested (IBM-1971, PHS-D, Mayo-1968) by Bailey, et al. [28]. The importance of the identification of arrhythmias is further underlined by the increasing recognition of the role of arrhythmias as a cause of sudden death [33]. Further, the reproducibility results of Bailey, et al. indicate that more robust computer algorithms are needed, and the statistical results suggest that more powerful statistical techniques should be used. These facts have provided much of the motivation for the work of developing an automated detection and classification program for rhythm analysis of ECG/VCG studied here.

1.3 Methods of Approach

The problem of automated arrhythmia analysis is, simply put, the problem of adequately reproducing the pattern recognition capabilities of the cardiologist. This problem may be only partially solvable, given the complexity of human pattern recognition capabilities and the limitations of even the most advanced computers. It seems fair to say that, given the exact timing of P waves and QRS complexes, together with gross descriptions of these waveforms, that arrhythmia diagnosis would be considerably simplified, since the electrophysiological mechanisms responsible for a large number of arrhythmia patterns have been described satisfactorily [34]. Theoretically at least, powerful pattern recognition techniques could then be brought to bear on the problem.

The techniques proposed in this research for arrhythmia detection and classification explicitly take into account uncertainties within each arrhythmia class in a systematic manner by using the very powerful statistical techniques of modern estimation and detection theory. This approach differs significantly from previous approaches to rhythm analysis in three ways; (1) the underlying rhythms are modeled as outputs of linear stochastic dynamical systems (2) rhythm classification will be done by hypothesis testing to find the most likely operating system, (3) unpredicted disturbances will be detected using a generalized likelihood ratio technique. Thus, the emphasis is on statistical modeling and testing of the data.

This approach has several advantages. First, since beat-to-beat variations are present and the wave intervals are never exactly regular, uncertainty has to be accommodated in any rhythm analysis scheme.

This can best be done by first obtaining detailed statistical information from actual data, which is readily available and quite extensive. Given a comprehensive statistical analysis of such data, it is natural to attempt to use it in the best possible manner. This can be done, for example, by trying to match the data to some dynamical model. Thus, if extensive correlation data were available and diagnostically significant, it would be feasible to construct dynamical models with the identical correlation characteristics. One can then bring the powerful techniques of sequential estimation and detection theory into action.

Alternatively, since the temporal patterns of many types of arrhythmias are known, a dynamical model may be subsumed for each "dynamically different" class. The parameters of the models can then be selected to best match the statistical characteristics of the model to the observed data. This approach has been taken in the present research and is covered in detail in subsequent chapters.

Of all of the data that can be obtained from an ECG or VCG, R-R interval data is by far the easiest to obtain and the "cleanest" in the sense of being almost error free. Such data possesses the highest "signal-to-noise ratio" and thus provides the most reliable information. On the other hand, data such as P-R and P-P intervals are inherently more noisy, as the detection of the smaller P waves introduces more errors. Considering this point, we have adopted the point of view that our first task is to understand fully the content of the more accurate R-R interval data. That is, we wish to determine precisely what information concerning arrhythmias is contained in R-R data and then to determine how to best extract this information

from the R-R intervals.

Our work along this direction has several natural subdivisions: (1) The Categorization of Arrhythmias - The determination of how various types of arrhythmic behavior manifest themselves in the observed signal. This involves the explicit determination of how various arrhythmias affect R-R interval histories (we do not categorize the effects of arrhythmias on other observable quantities, such as P-R intervals, P-P intervals, shapes of QRS complexes, etc.; because, for the purpose of this initial study we are mostly concerned with the R-R data). (2) Statistical Analysis of Arrhythmic R-R data - The purpose of this task is to obtain further and more quantitative information about the manifestation of various arrhythmias. Certain simple statistics related to the R-R data are computed, and these statistics can be used either to identify certain arrhythmias or to provide useful inputs in the design of more sophisticated mathematical models. (3) Determination of Dynamic Models for the Generation of R-R Interval Data for Different Arrhythmias - Based on the information in (1) and (2), we can obtain relatively simple dynamic models that generate R-R intervals with the desired statistical properties. The purpose of this task is to construct models to which we can apply the powerful tools of sequential estimation, detection, and hypothesis testing. (4) The Development and Testing of Estimation, Detection, and Hypothesis Testing Algorithms for Arrhythmia Detection Based on R-R Data - We apply several signal processing techniques to the mathematical models developed in (3).

1.4 Synopsis of Following Chapters

In Chapter 2, an algorithm for fiducial point detection of the QRS complex for the ECG/VCG record utilizing both slope and amplitude information is present. The detection is done using a single lead only. Results on experimental tests using actual data are presented.

The categorization of arrhythmias into different distinctive classes is the subject of Chapter 3. This involves the determination of how various types of arrhythmias manifest themselves in the observed signal, and how various arrhythmias affect the R-R intervals. Further and more quantitative information about the manifestation of various arrhythmias is studied in Chapter 4, by performing statistical analysis on the R-R intervals of different arrhythmia classes.

Based on the information obtained in Chapters 3 and 4, we determine the dynamical models for the generation of R-R interval data for different arrhythmias in Chapter 5. The purpose of this task is to construct models to which we can apply the powerful statistical analysis tools for detection and classification.

In Chapter 6, the multiple model hypothesis testing algorithm for the detection and classification of persistent rhythms is discussed. Numerical results obtained using actual data are presented. The generalized likelihood ratio detector system for the detection and classification of the transient rhythms is studied in Chapter 7. The necessary GLR equations are derived in detail. Actual data are tested, and the results are presented. Finally, some further discussion and conclusions are given in Chapter 8. Several areas which need further research are also pointed out, and discussed.

All the data used in the tests were digitized at a rate of 250 samples per second, and were provided by USAF/SAM personnel. The computer used to remove the baseline drifts, to locate fiducial point for the QRS complex, and to perform the statistical analysis, was a Nova 2 minicomputer. An IBM/360 computer was used for performing both the multiple model hypothesis and GLR detection tests.

CHAPTER 2

DATA PREPROCESSING

Data preprocessing refers herein to the sequence of steps required to obtain the R-R interval sequence from the digitized ECG/VCG record being processed. The preprocessor may be conveniently divided into two steps: (1) remove the low frequency baseline drifts, (2) detect the fiducial points of QRS complexes. These are discussed separately in the following sections.

2.1 Baseline Removal

A crucial step in the computer analysis of ECG/VCG's is the removal of low frequency baseline drifts. These disturbances can be quite severe and, if not eliminated, can cause significant errors in fiducial point detection and area computation of the QRS complex, which will be used in arrhythmia detection and classification. The slow varying baseline drift is caused by a combination of factors including:

(1) DC bias of the ECG/VCG output amplifiers
(2) slow changes in temperature
(3) coding/decoding mismatch of the FM tape recording
(4) variations in tape speed during data digitization
(5) electrode polarization changes
(6) geometric changes of torso due to respiration of patient

For the present purposes, the baseline will be defined as any unwanted low frequency components of the measured cardiographic signals. Let the measured signal at time t_i be m(i) and denote the underlying cardiographic signal by v(i). Then,

$$m(i) = v(i) + b(i) \tag{2.1}$$

where the baseline b(i) is an additive disturbance which includes both physiological and non-physiological effects. In order to remove this disturbance b(i) in the data preprocessing, we need to design a baseline estimator, which will take the measured signal m(i) as input and give an estimated baseline $\hat{b}(i)$ as output. Then we can get the underlying cardiographic signal $\hat{v}(i)$ by subtracting the estimated baseline $\hat{b}(i)$ from the measured signal m(i). The structure of this recursive baseline removal process is illustrated in Figure 2.1.

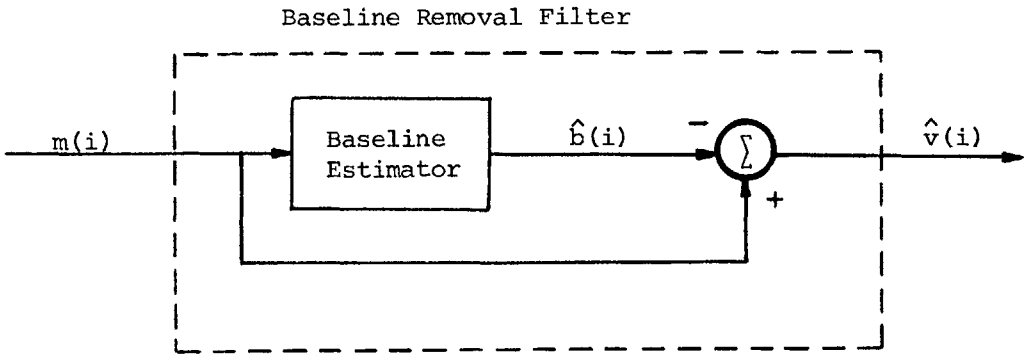

Figure 2.1 Recursive Baseline Removal Process

Several recursive baseline removal processes have been designed and tried in [35], [36]. The results showed that an efficient data preprocessor can best be realized by using a moving average non-causal filter for baseline removal. It is further tested in [37] on arrhythmic data. The experimental data indicate that very little diagnostic information is lost. Since the problem of baseline removal has been studied in detail in [35]-[37], no further discussion is given here.

2.2 Fiducial Point Detection for the QRS Complex

The high slope segments of the QRS complex relative to the remainder of the waveform appear to be the most reliable indicator to identify this complex. In order to have a well defined fiducial point for the QRS complex, we use the maximum startup slope point or the maximum slope point before the maximum amplitude of the R wave as the fiducial point (see Figure 2.2). The maximum slope at the fiducial point varies markedly from lead to lead. However, most of the QRS complexes on a given lead have a higher slope at the fiducial point than any part of the P and T waves in that lead. Accordingly, the first step in detecting the fiducial point is to find the slope for each lead which distinguishes P's and T's from QRS's.

Although this method is generally quite reliable, some problems do exist. Occasionally a small number of aberrant QRS complexes are present in a record. The maximum slope at the fiducial point on these QRS complexes may be markedly lower than the maximum slope on the complexes representing the dominant rhythm, and comparable to the high slope parts of the T waves. In this case it is not possible to find a slope which will distinguish all of the T waves from the QRS complexes. In order to detect all the QRS complexes, we therefore have to set the slope threshold at a very low value. Although we will be able to detect all the QRS complexes by doing this, at the same time we will also detect those T waves which have their maximum slopes greater than the slope threshold. The easiest way to avoid this difficulty is to

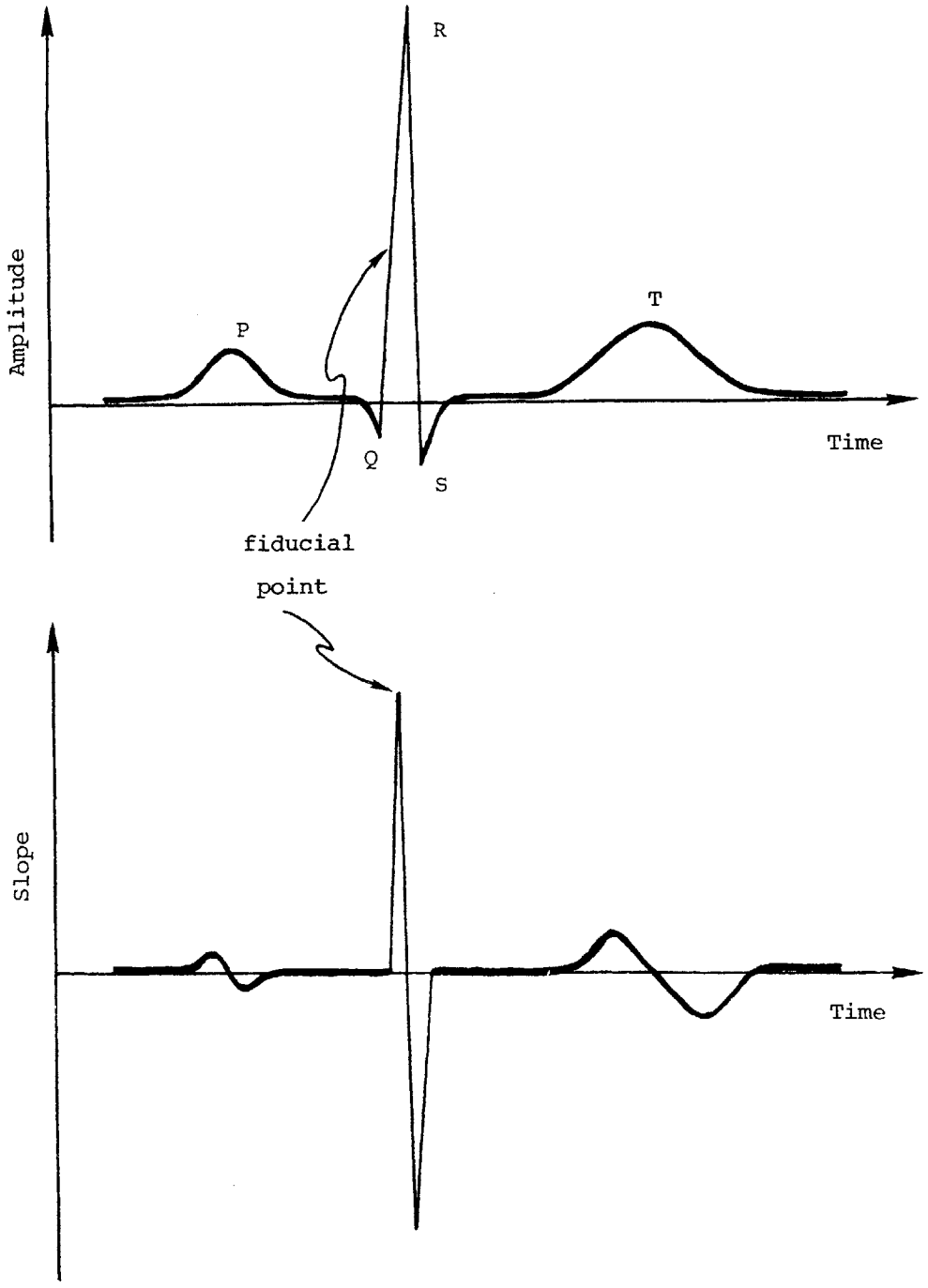

Figure 2.2 Fiducial Point Detection

skip a selected number of data points after the fiducial point is detected. We choose the number of data points to be skipped to insure skipping of the T wave, yet small enough so as not to miss any QRS complexes.

Another problem caused by using the low slope threshold is that we will detect noise bursts which have slopes greater than the slope threshold and which are not in the region skipped after the detection of the fiducial point. Since these have amplitudes much lower than the amplitudes at the fiducial points, we can thus reject them by requiring that the fiducial point should also satisfy the condition that the product of its amplitude and slope be greater than a positive threshold. This condition will not only reject noise bursts, but also insure that the fiducial points of the R waves detected are at the points before the maximum amplitudes of the R waves, since we require slope times amplitude to be positive.

2.3 Algorithm for Fiducial Point Detection

A program, RRFILE, has been developed based on the concept described above for detecting the fiducial points of the QRS complexes for both the arrhythmic and non-arrhythmic data from which the low frequency baseline shifts have been removed. A detailed description of the algorithm is given in the following, and a flow chart of this program is shown in Figures 2.3(a) and 2.3(b).

First, three data points are read into REM(1), REM(2) and REM(3). The slope of a best fit straight line over these three points is calculated as: REM(3) - REM(1). The window REM moves forward by dropping its trailing point REM(1), shifting REM(2) to REM(1), etc.,

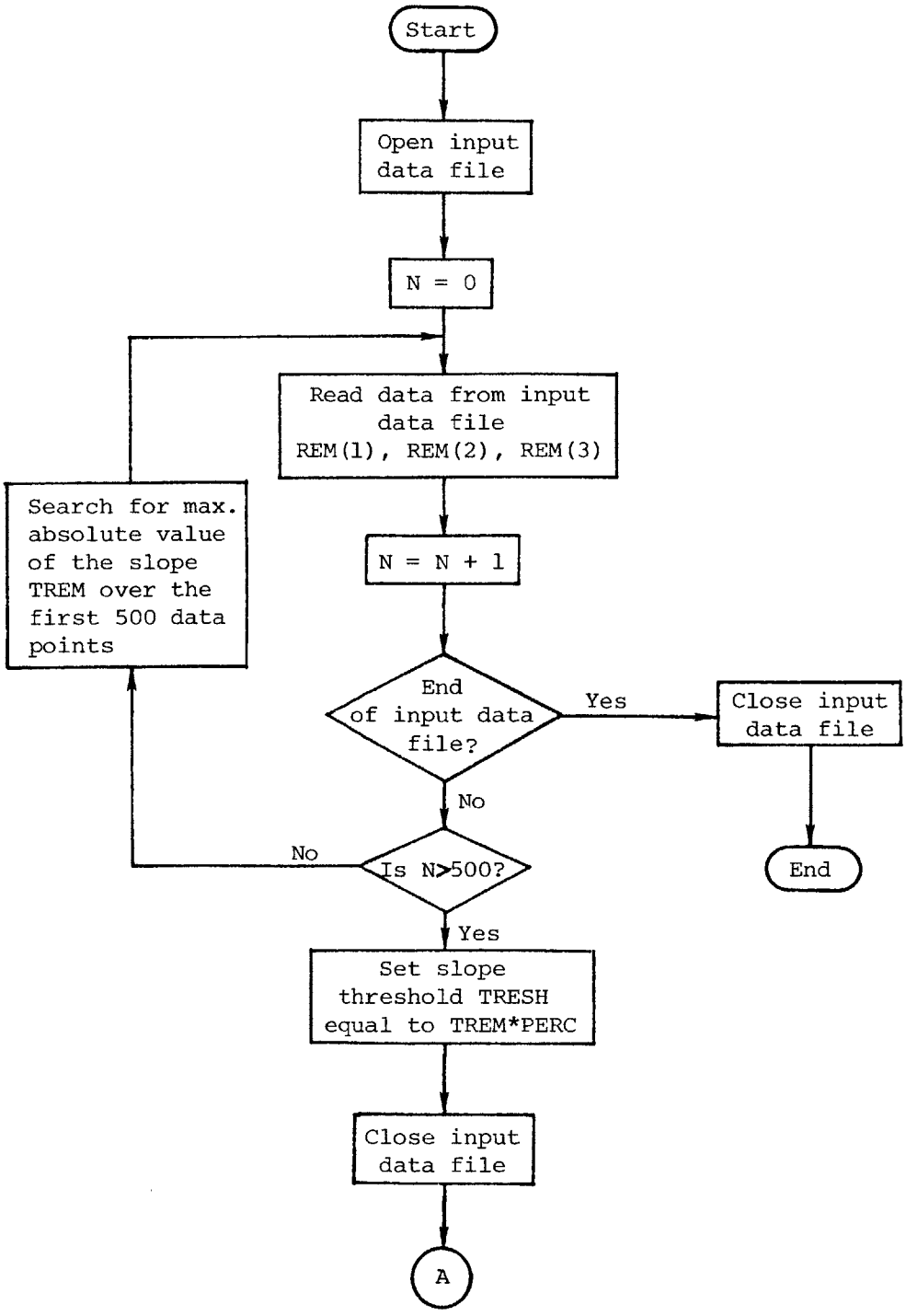

Figure 2.3(a) Flow Chart for Program RRFILE

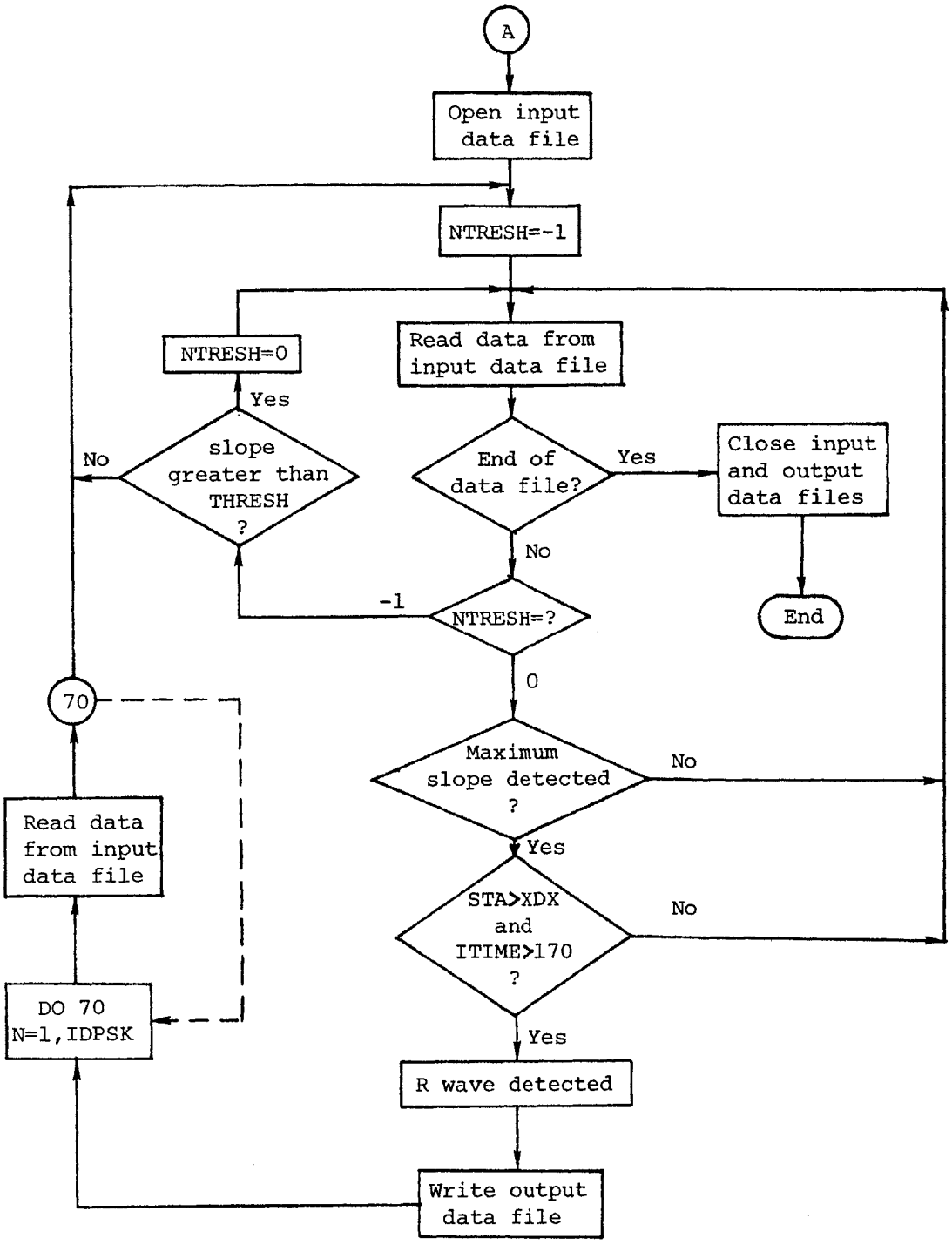

Figure 2.3(b) Flow Chart for Program RRFILE

and reading in a new data point as REM(3). The maximum absolute value of the slope, TREM, over the first 500 data points in the input data file is searched. The slope threshold, TRESH, is then set at a certain percent PERC of the maximum absolute value of the slope TREM. The value of PERC is an adjustable parameter.

Once the slope threshold is set for this record, we can start searching for the fiducial points from the very beginning of this input data file. When the absolute value of the slope TSUM is greater than the slope threshold TRESH, the maximum slope is searched. This maximum slope point is not the fiducial point of an R wave, unless the product, STA, of its amplitude REM(3) and slope TSUM is greater than a threshold XDX. The value of XDX is a design parameter.

Finally, we require ITIME, the point where a fiducial point is detected, to be greater than 170 before we can declare that an R wave has been detected. The reason for imposing this condition is due to the fact that some records may start in the middle of a QRS complex; in this case the fiducial point may be in error for this QRS complex. A safe way to avoid this problem is to neglect the fiducial point detected within the first 50 data points, which is greater than the width of a QRS complex. All the input data files used in this program must have their baseline shifts removed first. That is, the input to the program RRFILE is the output data file from the baseline removal filter BSLNFT, in which a moving window average is used to estimate the baseline. The baseline at the midpoint of the overall window is estimated as the average of all the data points within this window. Thus, at the start of a record no baseline estimates can be made for the first 120 data points which are used to fill the window. Hence a

value of zero is assigned to the first 120 output data points for the baseline removal filter. Therefore, in order to avoid false detection we neglect the fiducial point detected within the first 170 data points in a record.

When a fiducial point is detected, a selected number of data points IDPSK are not searched for R waves. This will not only skip the high slope part of the T waves but also speed up the overall processing. The value of IDPSK is a design parameter.

2.4 Experiments and Results

The algorithm for R wave detection RRFILE was tested for both arrhythmic and non-arrhythmic data. A summary of all these data files is given in Table 2.1.

Data file name	Diagnosis
IN.5 IN.20 IN.30	Normal Rhythm
HUANPVCS	Premature ventricular contractions
HARNETPVCS	Premature ventricular contractions
SPOONPAC	Premature atrial contractions
BLOOM	Supraventricular arrhythmia
CUNATFIB	Atrial fibrillation

Table 2.1 Summary of Data Files Used for Testing the Fiducial Point Detector RRFILE

The objective of this test was to determine whether the algorithm described in Section 2.3 could detect all of the R waves and reject all T waves and noises in each record for a proper choice of the parameters PERC, XDX, and IDPSK, where PERC is the percentage of the maximum absolute value of the slope TREM over the first 500 data points for the slope threshold TRESH, (TRESH=TREM*PERC), XDX is the slope times amplitude threshold for REM(3)*TSUM, and IDPSK is the number of data points skipped after a fiducial point is detected. We also wished to find a set (or sets) of numbers for the parameters PERC, XDX and IDPSK which are good in the sense that no R waves are missed in any of the data files we have on hand (see Table 2.1). This will aid in our evaluating the robustness of the detector with respect to these parameters.

The input data files to the R wave detector RRFILE were the third lead of those in Table 2.1, from which the baseline shifts have been removed, and the output data files were the R-R intervals detected in each lead. A total of 1,000 sampling data points (250 data points =1 second) in the third lead of all the arrhythmia data files both before and after the baseline shifts have been removed are shown in Figures 2.4 - 2.8). From these figures we can see that there are aberrant R waves present in all these data files. Note also that the filtered waveforms appear unaffected from a diagnostic viewpoint. All these data files were tested individually at first for different values of parameters. The R waves detected for each different set of parameters were then checked visually with the data files, which were displayed on the Tektronics 4010 digital display. Finally, a satisfactory set of values for the parameters were found, which were good for all the data files being tested. These are given in the following:

PERC = 0.20

XDX = 3,000

IDPSK = 70

The results are given in Tables 2.2-2.9 for all the data files in Table 2.1. The fourth and fifth columns give the fiducial point detected and the intervals between the two consecutive fiducial points (or the so called R-R intervals), respectively. We also give the slope and slope* amplitude at the fiducial point in column two and three, respectively. The R-R interval data in column five is in the output data file from program RRFILE. This R-R interval data file will be used in subsequent chapters for arrhythmia analysis.

In this section we have developed a simple procedure for the determination of fiducial points of the QRS complexes. Although good performance was obtained for the data files tested, more data should be tested to evaluate this fiducial point detector in a wide variety of situations. These tests will either be used to adjust parameters of the present detector, or suggest more robust detector designs.

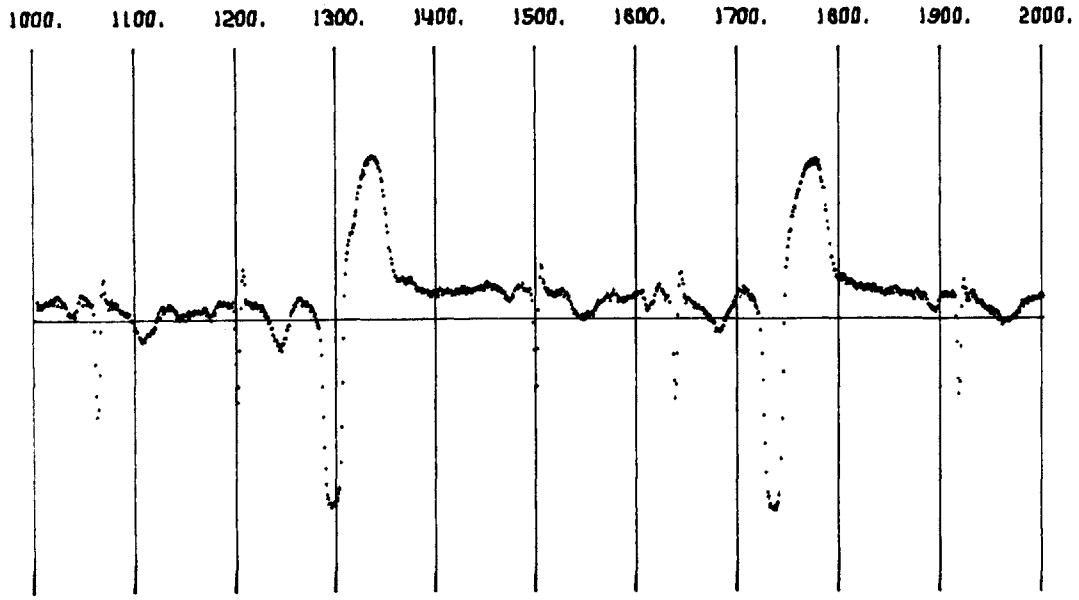

Figure 2.4(a) Unfiltered Data File HUANPVCS

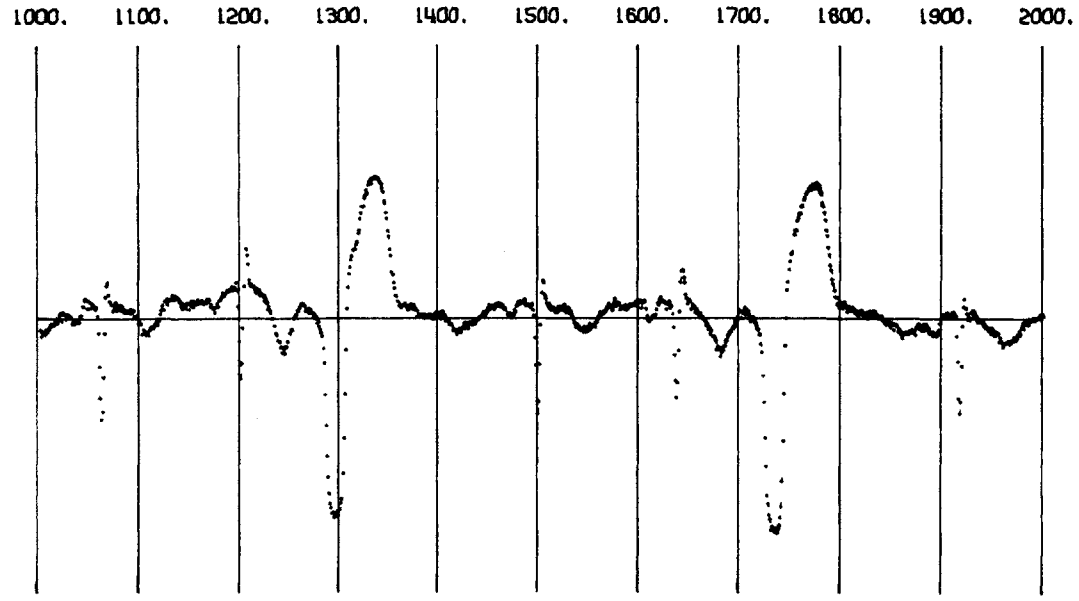

Figure 2.4(b) Filtered Data File HUANPVCS

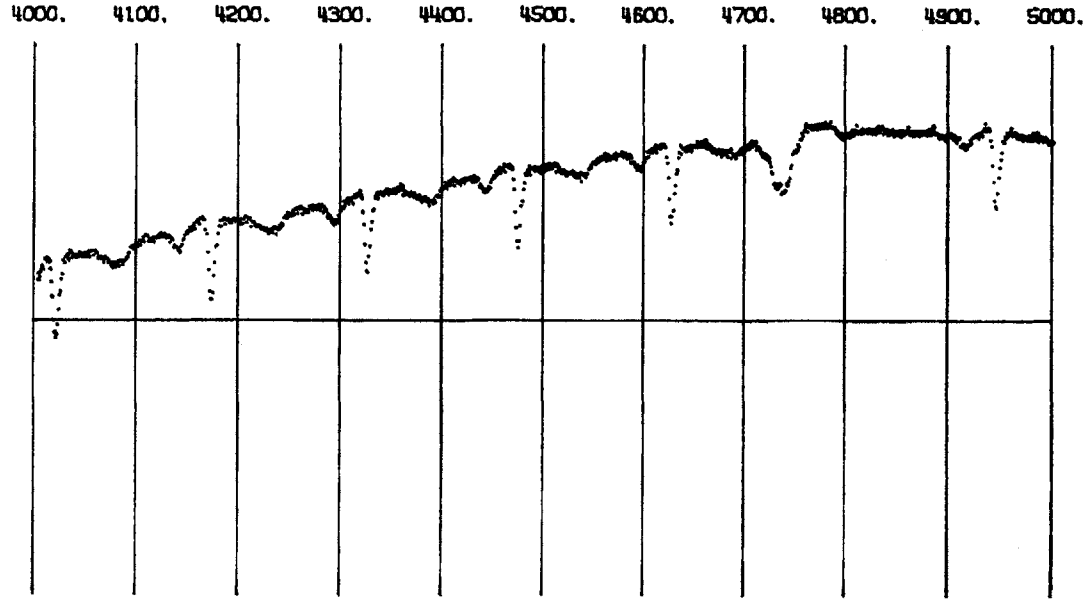

Figure 2.5(a) Unfiltered Data File HARNETPVCS

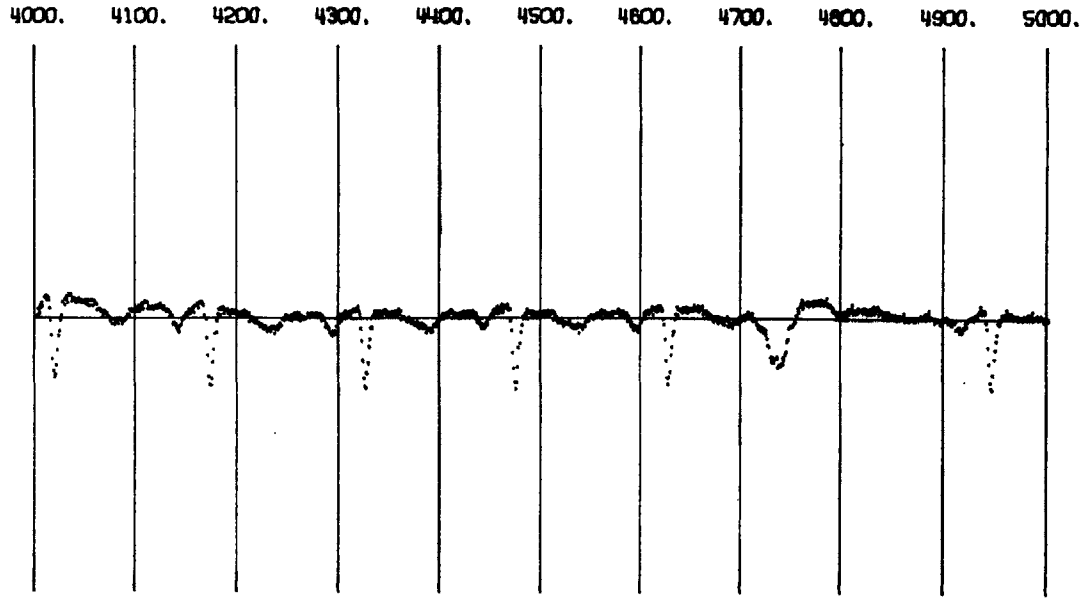

Figure 2.5(b) Filtered Data File HARNETPVCS

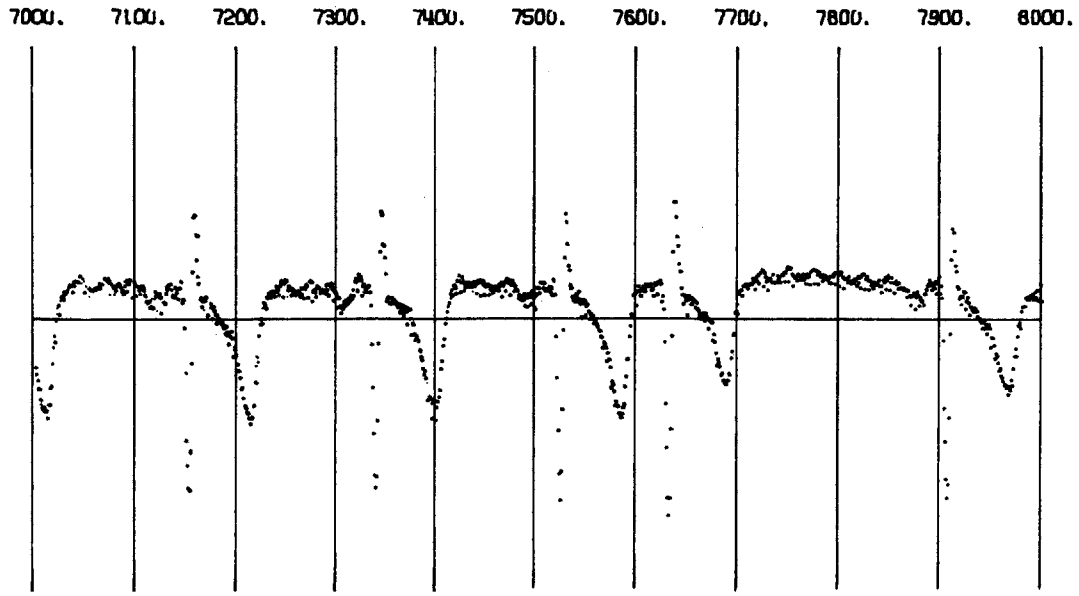

Figure 2.6(a) Unfiltered Data File SPOONPAC

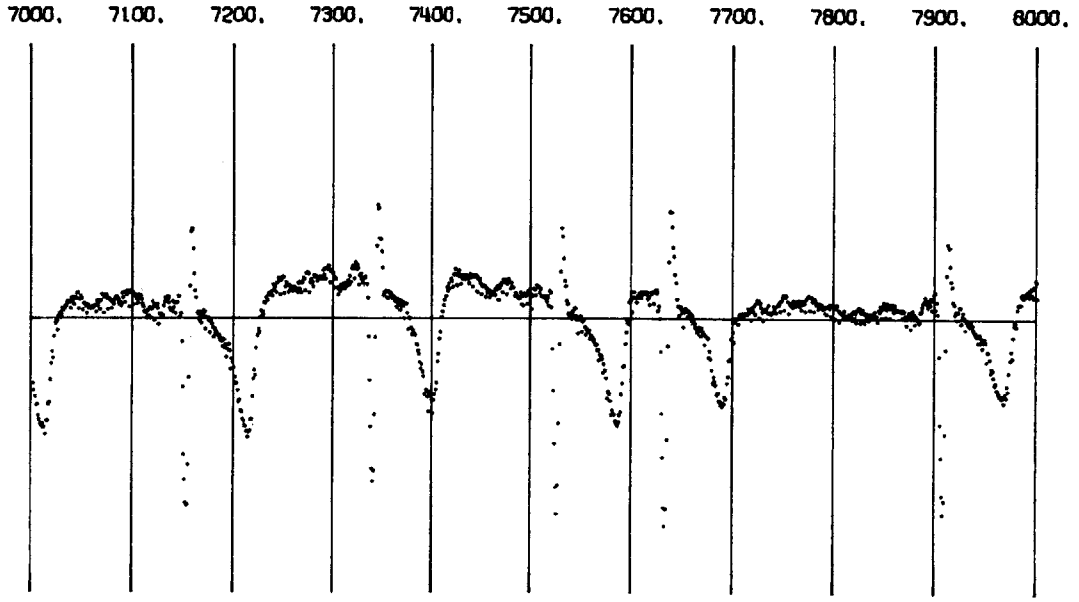

Figure 2.6(b) Filtered Data File SPOONPAC

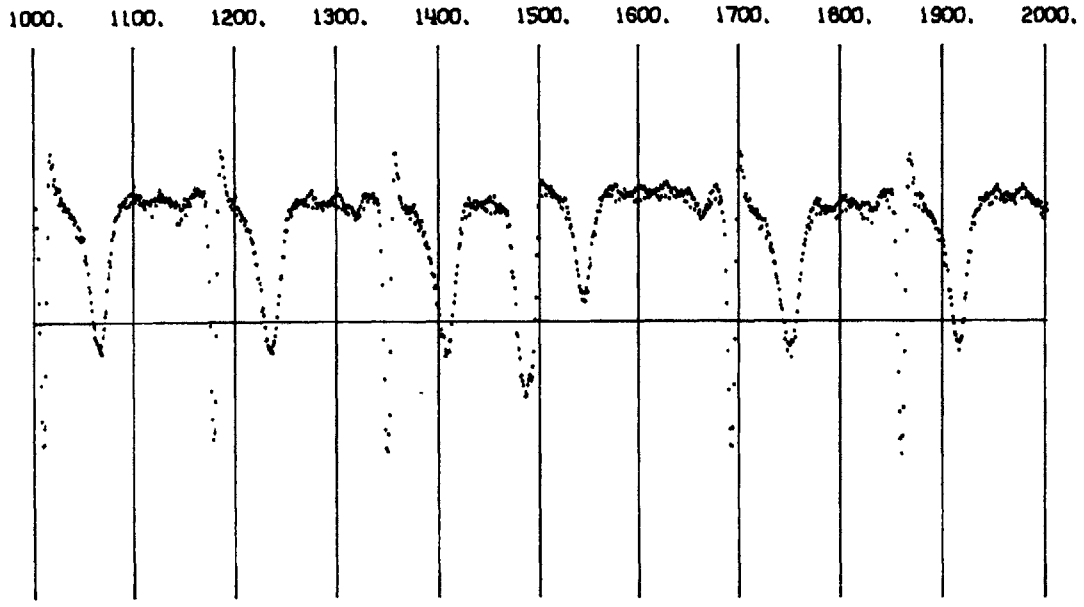

Figure 2.7(a) Unfiltered Data File BLOOM

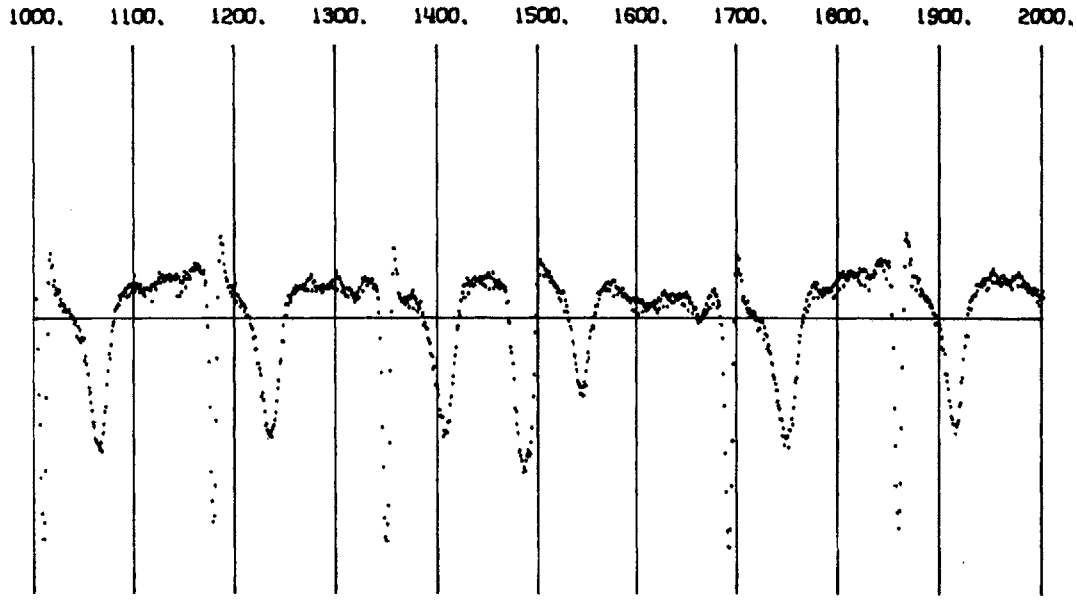

Figure 2.7(b) Filtered Data File BLOOM

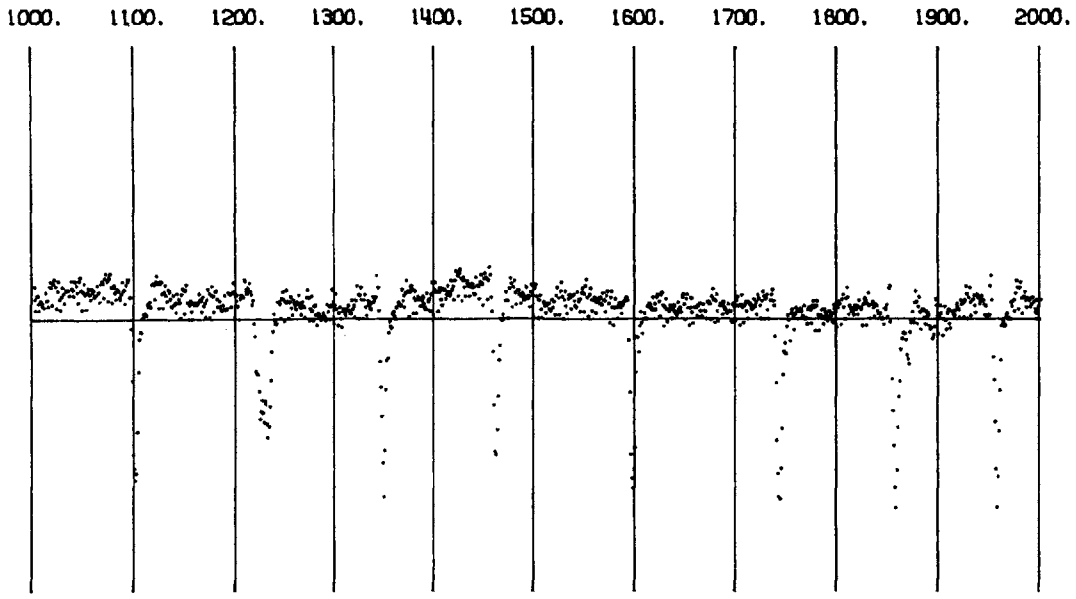

Figure 2.8(a) Unfiltered Data File CUNATFIB

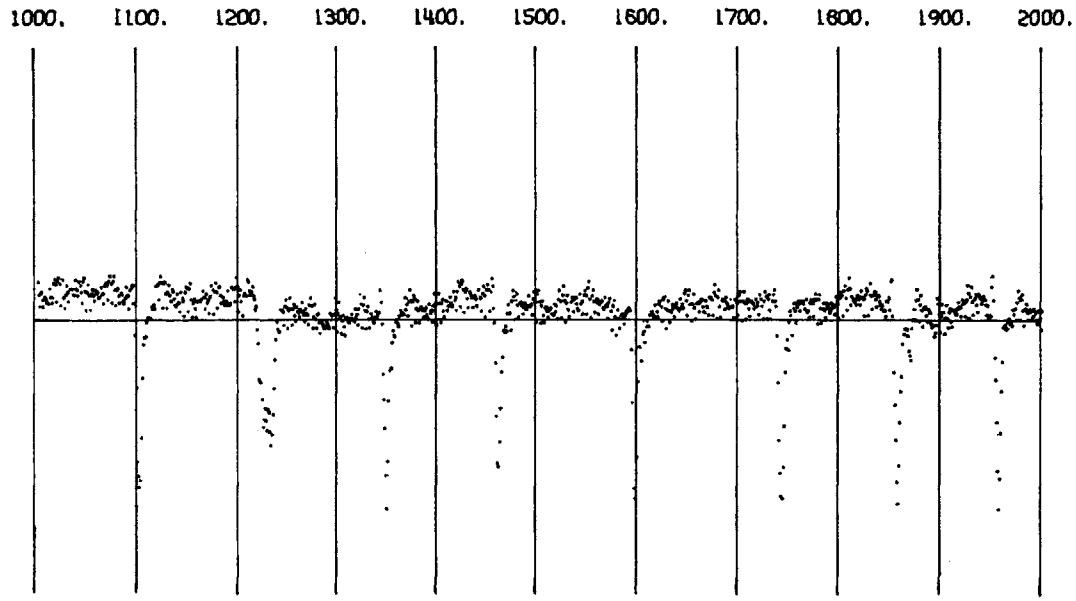

Figure 2.8(b) Filtered Data File CUNATFIB

N	AMP*SLOPE	SLOPE	R	R-R
1	309222.00	486	343	
2	142400.00	467	524	181
3	289014.00	517	706	182
4	335369.00	524	893	187
5	410010.00	503	1081	188
6	302316.00	491	1266	185
7	251758.00	486	1446	180
8	383176.00	518	1629	183
9	318708.00	528	1814	185
10	371700.00	514	2001	187
11	302670.00	506	2186	185
12	179740.00	463	2366	180
13	420332.00	479	2549	183
14	384524.00	522	2735	186
15	240672.00	514	2921	186
16	167268.00	479	3101	180
17	254380.00	477	3275	174
18	362604.00	509	3448	173
19	250332.00	534	3624	176
20	289333.00	529	3804	180
21	314730.00	475	3980	176
22	377762.00	451	4153	173
23	284400.00	526	4330	177
24	387660.00	507	4506	176
25	272847.00	520	4683	177
26	187322.00	479	4854	171
27	315792.00	474	5019	165
28	322848.00	524	5187	168
29	356580.00	536	5357	170
30	227416.00	496	5533	176
31	375221.00	454	5705	172
32	234720.00	493	5871	166
33	197358.00	488	6044	173
34	292734.00	545	6218	174
35	237870.00	513	6395	177
36	307572.00	506	6567	172
37	338845.00	473	6733	166
38	283974.00	506	6903	170
39	355200.00	530	7075	172
40	324407.00	544	7248	173
41	363540.00	470	7421	173
42	283745.00	483	7592	171
43	174523.00	467	7763	171

Table 2.2 Results from R Wave Detector for Data File IN.5

N	AMP*SLOPE	SLOPE	R	R-R
1	638420,00	639	224	
2	601198,00	631	423	199
3	700036,00	636	629	206
4	624162,00	630	834	205
5	625779,00	634	1028	194
6	678700,00	619	1226	198
7	658125,00	635	1431	205
8	642178,00	622	1634	203
9	635680,00	653	1828	194
10	646323,00	625	2022	194
11	600392,00	632	2222	200
12	666357,00	633	2422	200
13	583128,00	630	2614	192
14	522886,00	629	2807	193
15	570960,00	631	3006	199
16	656057,00	632	3202	196
17	607910,00	629	3387	185
18	554228,00	630	3577	190
19	625443,00	645	3777	200
20	638352,00	655	3980	203
21	538248,00	622	4176	196
22	500185,00	636	4378	202
23	612315,00	633	4586	208
24	605402,00	640	4790	204
25	602147,00	624	4989	199
26	525800,00	626	5194	205
27	522110,00	635	5398	204
28	585972,00	641	5593	195
29	590187,00	636	5791	198
30	604144,00	641	5997	206
31	685035,00	661	6204	207
32	544208,00	638	6405	201
33	609224,00	642	6613	208
34	548886,00	640	6828	215
35	593388,00	637	7038	210
36	578716,00	617	7239	201

Table 2.3 Results from R Wave Detector for Data File IN.20

N	AMP*SLOPE	SLOPE	R	R-R
1	575901.00	647	376	
2	601650.00	606	612	236
3	557118.00	619	854	242
4	579723.00	614	1093	239
5	550745.00	652	1325	232
6	660050.00	659	1548	223
7	304010.00	594	1778	230
8	461610.00	600	2009	231
9	608854.00	637	2239	230
10	670735.00	680	2464	225
11	653016.00	626	2692	228
12	556665.00	587	2936	244
13	624193.00	624	3185	249
14	562100.00	662	3420	235
15	473295.00	640	3655	235
16	474240.00	593	3899	244
17	616701.00	607	4142	243
18	664796.00	640	4373	231
19	586440.00	663	4596	223
20	620730.00	632	4821	225
21	540855.00	605	5055	234
22	571340.00	611	5294	239
23	638400.00	663	5526	232
24	567120.00	629	5758	232
25	567862.00	601	5998	240
26	544840.00	617	6235	237
27	463246.00	632	6465	230
28	653646.00	683	6680	215
29	592620.00	682	6892	212
30	601620.00	614	7105	213
31	529440.00	553	7323	218
32	667454.00	657	7544	221
33	640648.00	656	7771	227

Table 2.4 Results from R Wave Detector for Data File IN.30

N	AMP*SLOPE	SLOPE	R	R-R
1	49617.00	220	196	
2	37504.00	200	534	138
3	120696.00	219	424	90
4	37760.00	211	637	213
5	35600.00	199	776	139
6	98580.00	200	867	91
7	58290.00	215	1060	193
8	24278.00	189	1198	138
9	92112.00	207	1285	87
10	50560.00	208	1497	212
11	36942.00	175	1635	138
12	110187.00	209	1725	90
13	53694.00	204	1915	190
14	20737.00	186	2052	137
15	103500.00	202	2145	93
16	66774.00	202	2351	206
17	24628.00	180	2497	146
18	102567.00	233	2584	87
19	49395.00	190	2799	215
20	19662.00	169	2935	136
21	90280.00	187	3028	93
22	35772.00	200	3218	190
23	20806.00	167	3362	144
24	94952.00	197	3449	87
25	54008.00	190	3658	209
26	20336.00	189	3792	134
27	85250.00	169	3888	96
28	53298.00	194	4093	205
29	27950.00	196	4242	149
30	107712.00	219	4330	88
31	63640.00	191	4535	205
32	30414.00	167	4666	131
33	100992.00	200	4766	100
34	55566.00	216	4933	167
35	44082.00	198	5058	125
36	49725.00	209	5182	124
37	86673.00	173	5299	117
38	63168.00	194	5461	162
39	37515.00	176	5631	170
40	49700.00	201	5805	174
41	40467.00	190	5964	159
42	97658.00	195	6051	87

Table 2.5 Results from R Wave Detector for Data File HUANPVCS

N	AMP*SLOPE	SLOPE	R	R-R
1	18792,00	116	227	
2	14833,00	98	381	154
3	16791,00	116	533	152
4	12388,00	101	692	159
5	3276,00	45	798	106
6	15662,00	115	1028	230
7	17255,00	110	1190	162
8	14175,00	100	1348	158
9	5280,00	108	1502	154
10	4312,00	57	1649	147
11	18291,00	101	1800	151
12	26924,00	126	1951	151
13	32712,00	133	2105	154
14	28476,00	140	2257	152
15	34075,00	158	2416	159
16	24252,00	136	2581	165
17	38148,00	165	2744	163
18	29555,00	131	2901	157
19	30702,00	150	3061	160
20	10595,00	65	3166	105
21	30492,00	135	3395	229
22	24910,00	152	3550	155
23	31255,00	142	3712	162
24	28320,00	150	3866	154
25	27744,00	146	4016	150
26	28896,00	150	4170	154
27	27132,00	144	4323	153
28	27664,00	146	4471	148
29	23552,00	146	4624	153
30	3132,00	38	4725	101
31	32562,00	135	4942	217
32	30222,00	141	5092	150
33	25864,00	135	5246	154
34	16566,00	133	5395	149
35	30702,00	148	5545	150
36	21156,00	147	5686	141
37	23544,00	128	5831	145
38	17776,00	107	5983	152
39	4968,00	65	6086	103
40	24696,00	126	6300	214
41	30226,00	136	6451	151
42	25338,00	147	6602	151
43	29348,00	116	6759	157

Table 2.6(a) Results from R Wave Detector for Data File HARNETPVCS

N	AMP*SLOPE	SLOPE	R	R-R
44	15453,00	112	6911	152
45	25920,00	148	7068	157
46	32508,00	132	7226	158
47	25122,00	139	7375	149
48	16920,00	111	7537	162
49	20300,00	123	7695	158
50	18928,00	131	7860	165
51	22272,00	130	8036	176
52	20384,00	140	8211	175
53	22018,00	140	8378	167
54	28800,00	136	8543	165

Table 2.6(b) Results from R Wave Detector for Data File HARNETPVCS

N	AMP*SLOPE	SLOPE	R	R-R
1	76744,00	211	212	
2	57330,00	251	396	184
3	70152,00	224	499	103
4	62900,00	232	792	293
5	73486,00	225	982	190
6	87636,00	222	1212	230
7	66132,00	219	1457	245
8	61246,00	230	1696	239
9	63040,00	207	1936	240
10	49348,00	192	2147	211
11	73481,00	213	2346	199
12	81719,00	220	2561	215
13	64500,00	234	2767	206
14	66946,00	207	2964	197
15	75601,00	227	3171	207
16	65520,00	238	3379	208
17	80832,00	229	3582	203
18	70218,00	243	3808	226
19	54927,00	202	4019	211
20	79758,00	220	4236	217
21	63954,00	243	4458	222
22	81204,00	213	4661	203
23	65824,00	202	4794	133
24	72618,00	236	5070	276
25	69888,00	232	5254	184
26	60750,00	220	5445	191
27	73905,00	226	5627	182
28	60990,00	208	5802	175
29	85690,00	226	5919	117
30	67840,00	232	6174	255
31	70434,00	237	6357	183
32	51480,00	197	6538	181
33	51060,00	173	6735	197
34	56496,00	239	6949	214
35	72420,00	248	7149	200
36	64214,00	198	7336	187
37	66066,00	212	7523	187
38	85490,00	232	7629	106
39	67488,00	242	7903	274
40	61182,00	252	8078	175
41	89880,00	214	8252	174

Table 2.7 Results from R Wave Detector for Data File SPOONPAC

N	AMP*SLOPE	SLOPE	R	R-R
1	12136,00	128	171	
2	95046,00	229	334	163
3	90288,00	205	502	168
4	57035,00	196	670	168
5	55420,00	206	835	165
6	38280,00	167	1003	168
7	82000,00	241	1174	171
8	86724,00	207	1344	170
9	3600,00	65	1471	127
10	79050,00	187	1687	216
11	61685,00	214	1854	167
12	71857,00	213	2024	170
13	85140,00	220	2193	169
14	72581,00	221	2357	164
15	73146,00	173	2524	167
16	87435,00	208	2692	168
17	79346,00	199	2868	176
18	90153,00	210	3047	179
19	54522,00	197	3225	178
20	36600,00	151	3400	175
21	69680,00	199	3582	182
22	74382,00	201	3752	170
23	58320,00	210	3918	166
24	75647,00	222	4089	171
25	41478,00	187	4257	168
26	84534,00	205	4427	170
27	64288,00	184	4596	169
28	68442,00	207	4762	166
29	86112,00	209	4928	166
30	71526,00	204	5095	167
31	59004,00	197	5257	162
32	74666,00	230	5419	162
33	87480,00	229	5590	171
34	104594,00	232	5764	174
35	9591,00	95	5923	159
36	64148,00	186	6128	205
37	71940,00	235	6302	174
38	13125,00	95	6440	138
39	73617,00	201	6634	194
40	58100,00	180	6788	154
41	67868,00	195	6944	156
42	75990,00	230	7102	158
43	65330,00	205	7273	171

Table 2.8(a) Results from R Wave Detector for Data File BLOOM

N	AMP*SLOPE	SLOPE	R	R-R
44	65564,00	202	7442	169
45	6862,00	78	7589	147
46	75164,00	201	7802	213
47	59940,00	185	7975	173
48	4560,00	62	8097	122

Table 2.8(b) Results from R Wave Detector for Data File BLOOM

N	AMP*SLOPE	SLOPE	R	R-R
1	33228,00	163	235	
2	41440,00	207	336	101
3	42884,00	176	460	124
4	38478,00	167	559	99
5	30870,00	178	652	93
6	30856,00	157	740	88
7	27090,00	185	852	112
8	30784,00	175	969	117
9	37668,00	209	1098	129
10	6489,00	82	1219	121
11	16020,00	125	1345	126
12	20169,00	165	1460	115
13	39198,00	188	1594	134
14	37697,00	172	1739	145
15	20440,00	153	1852	113
16	12969,00	134	1952	100
17	40764,00	209	2085	133
18	29344,00	152	2178	93
19	31536,00	169	2314	136
20	17622,00	139	2417	103
21	32809,00	196	2556	139
22	5216,00	100	2708	152
23	48944,00	177	2800	92
24	29832,00	199	2885	85
25	33142,00	149	2998	113
26	36608,00	181	3085	87
27	36580,00	166	3177	92
28	19992,00	118	3327	150
29	35133,00	206	3439	112
30	34875,00	165	3546	107
31	56980,00	221	3642	96
32	14231,00	140	3735	93
33	41216,00	158	3905	170
34	35086,00	163	4025	120
35	30115,00	149	4134	109
36	52052,00	179	4223	89
37	49517,00	231	4343	120
38	53130,00	175	4474	131
39	34750,00	164	4581	107
40	43875,00	185	4675	94
41	44892,00	228	4768	93
42	39732,00	183	4856	88
43	47894,00	190	5006	150

Table 2.9(a) Results from R Wave Detector for Data File CUNATFIB

N	AMP*SLOPE	SLOPE	R	R-R
44	36224.00	174	5114	108
45	34299.00	191	5251	137
46	38440.00	214	5347	96
47	34320.00	176	5435	88
48	25536.00	152	5535	100
49	47922.00	229	5626	91
50	19836.00	124	5730	104
51	34036.00	176	5864	134
52	57510.00	183	5957	93
53	8307.00	123	6076	119
54	43245.00	224	6176	100
55	33371.00	170	6268	92
56	38870.00	235	6351	83
57	33396.00	157	6437	86
58	3344.00	78	6522	85
59	39249.00	161	6638	116
60	29304.00	163	6758	120
61	21090.00	143	6869	111
62	25872.00	143	6994	125
63	33288.00	142	7096	102
64	35179.00	136	7212	116
65	44688.00	154	7308	96
66	34844.00	143	7450	142
67	3479.00	80	7555	105
68	30315.00	176	7652	97
69	31970.00	166	7764	112
70	68250.00	182	7850	86
71	29868.00	163	7938	88
72	31005.00	154	8023	85
73	48504.00	200	8109	86
74	48620.00	172	8192	83
75	28900.00	194	8284	92
76	49319.00	182	8371	87
77	34026.00	190	8459	88
78	23364.00	148	8552	93
79	34866.00	159	8667	115
80	33672.00	190	8755	88
81	32960.00	154	8845	90
82	31772.00	176	8984	139
83	24378.00	173	9097	113
84	5626.00	107	9209	112
85	47793.00	188	9288	79
86	27572.00	154	9367	79

Table 2.9(b) Results from R Wave Detector for Data File CUNATFIB

N	AMP*SLOPE	SLOPE	R	R-R
87	37845.00	200	9484	117
88	30429.00	150	9597	113
89	35720.00	194	9687	90
90	30130.00	184	9780	93
91	21888.00	132	9881	101
92	29344.00	143	9964	83
93	40081.00	187	10074	110
94	42174.00	219	10159	85
95	45510.00	230	10238	79
96	32034.00	183	10355	117
97	38280.00	151	10444	89
98	35340.00	191	10542	98

Table 2.9(c) Results from R Wave Detector for Data File CUNATFIB

CHAPTER 3

CATEGORIZATION OF CARDIAC ARRHYTHMIAS

3.1 Introduction

The main goal of cardiac rhythm analysis is to classify ECG/VCG's into various diagnostic categories or arrhythmic patterns. Cardiac arrhythmias result from disturbances or alterations in the normal mechanisms of cardiac activity. Such disturbances manifest themselves as changes in the contours of the P waves and QRS complexes, absence of the P or QRS complexes, or irregularity of the P-P, P-R, or R-R intervals. Therefore, a complete categorization of cardiac arrhythmias must take all these characteristics into account. However, since only the R-R interval data will be used in this study to test feasibility of the proposed detection methods. Thus, in the following an attempt is made to categorize cardiac arrhythmias based on the use of R-R intervals only. Due to the fact that no P wave information is used in this classification, all the arrhythmic patterns which have the same R-R interval characteristics will be classified into the same category. No QRS contour information is considered either; hence the abnormality of the QRS complex is not of interest in this study.

All the arrhythmic patterns are first divided into two distinct families: (1) persistent rhythms, (2) transient events. In each family, further classification into various classes are made, based on the clearly identifiable R-R interval patterns. We have attempted to devise a set of classes that include most arrhythmias. These classes will form the basis for our statistical analysis and detection schemes.

3.2 Persistent Rhythms

All the cardiac arrhythmias which have a persistent rhythmic pattern belong to this family. Four classes are further identified in this family.

(1) Small Variation

This is the category for R-R intervals which exhibit small but random deviations from the mean value of the R-R intervals and its R-R interval pattern is shown in Figure 3.1. Here only the QRS complexes, which are represented by impulses, are shown.

Figure 3.1 R-R Interval Pattern for Small Variation

This class includes:

(a) normal sinus rhythm (60-100 beats/min)

(b) sinus tachycardia (>100 beats/min)

(c) sinus bradycardia (<60 beats/min).

The rate used to distinguish between these three cases is based on the mean value of the R-R interval. Note that 2:1 SA block may be indistinguishable from sinus bradycardia here.

(2) Large Variation

This class is characterized by a large but random variation in the R-R interval sequence from the mean value. This class contains, among others:

(a) sinus arrhythmia

(b) atrial fibrillation

The R-R interval pattern for large variations, is shown in Figure 3.2 .

Figure 3.2 R-R Interval Pattern for Large Variation

(3) Bigeminy

This class is characterized by R-R intervals which are alternately long and short as shown in Figure 3.3. The causes for this cardiac arrhythmia are:

(a) a premature contraction following every normal contraction (coupling)

(b) the presence of an AV block of every third auricular impulse.

long-short

Figure 3.3 R-R Interval Pattern for Bigeminy

(4) Trigeminy

This class is characterized by R-R interval sequence which takes one of the following patterns: normal-short-long, normal-long-short, short-short-long or long-long-short. The causes for these patterns are due to the following cardiac disturbances:

(a) a premature contraction that regularly follows every two normal heart beats

(b) two consecutive premature contractions following a normal heart beat

(c) a complete AV block of every fourth impulse.

The four possible patterns in this class are show in Figure 3.4.

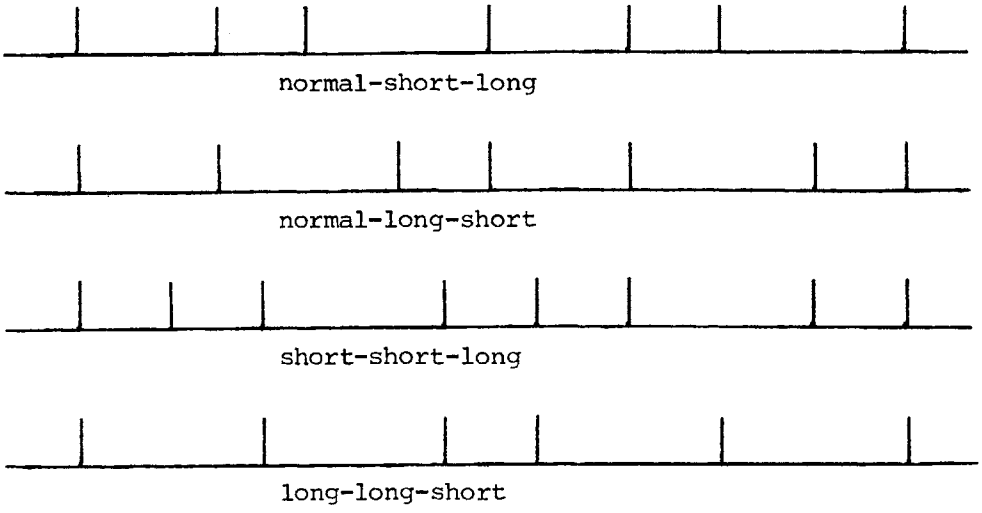

Figure 3.4 R-R Interval Patterns for Trigeminy

3.3 Transient Events

All the cardiac arrhythmias which do not have a persistent pattern shall be included in this family. The occurances of the cardiac arrhythmias in this family are totally unpredictable. Several classes are also identified in the following.

(1) Rhythm Jump

This class is characterized by a sudden change of the heart rate, which occurs in the case of onset of bradycardia or tachycardia. The R-R interval patterns are shown in Figure 3.5.

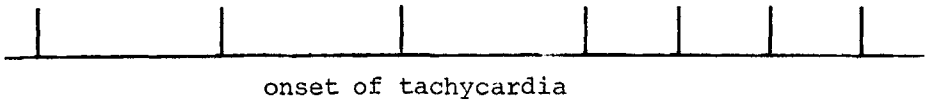

onset of bradycardia

Figure 3.5 R-R Interval Patterns for Rhythm Jump

(2) Non-Compensatory Beat

This class is characterized by intermittent premature QRS complexes in which there is incomplete compensation of the R-R interval subsequent to the premature beat or by dropped QRS complexes in which a much longer than normal R-R interval results. The patterns are shown in Figure 3.6. This class includes:

(a) sinus arrest (persistent loss of impulses)

(b) SA block

(c) atrial prematures

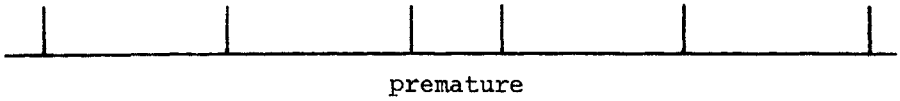

premature

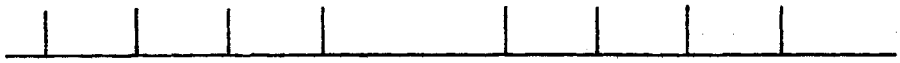

block

Figure 3.6 R-R Interval Patterns for Non-Compensatory Beats

(3) Compensatory Beat

This class of arrhythmias is characterized by intermittent premature QRS complexes in which complete compensation of the R-R interval is achieved subsequent to the premature beat. Thus, the interval between the QRS complex preceeding the premature and the post-premature QRS complex is equal to two normal R-R intervals. The associated

R-R interval pattern is shown in Figure 3.7.

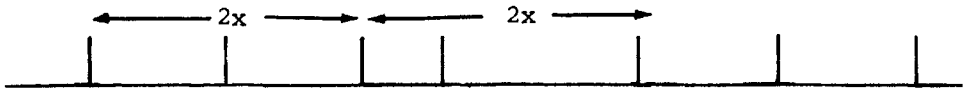

Figure 3.7 R-R Interval Pattern for Compensatory Beat

This class includes:

(a) AV nodal prematures

(b) ventricular prematures

(4) Double Non-Compensatory Beat

This arrhythmia class is characterized by one of the following patterns: (1) an underlying uniform R-R interval upon which is superposed intermittent extra or ectopic beats called interpolated beats (these extra beats do not interfere with the normal ventricular rhythm); (2) a double premature, or (3) two consecutive dropped beats. The patterns are shown in Figure 3.8.

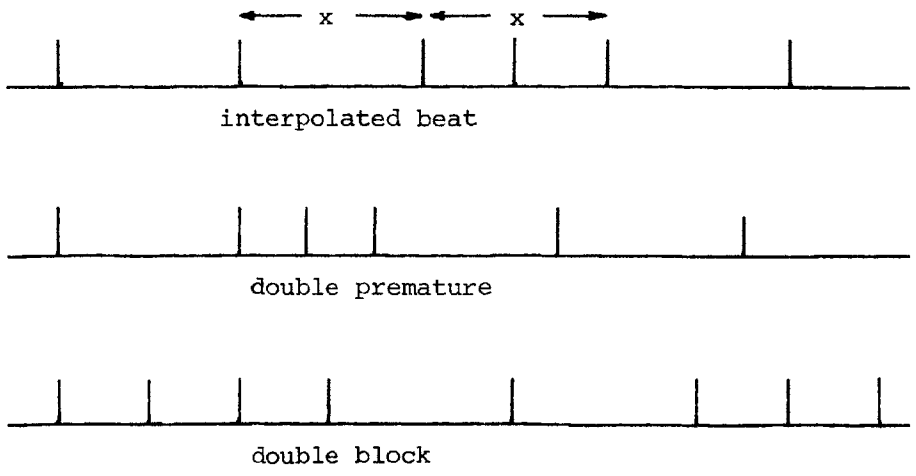

Figure 3.8 R-R Interval Patterns for Double Non-Compensatory Beat

It should be emphasized that the choice of classes made here reflects significantly different structural characteristics of the R-R interval pattern only and does not include either P-R or R-P intervals, or the equally important P-P intervals.

There is another important class of arrythmias which can be detected without resorting to detection of P waves. This is the important class in which there is an unusually large amount of high-frequency energy. This class includes fibrillation and flutter and it appears that detection can be accomplished by use of digital high pass filters. It should be pointed out that the classes described in this chapter are used to form the basis for our detection and classification techniques. There may be other classes which are not considered here. Any further classes can be handled in a similar manner.

CHAPTER 4

STATISTICAL ANALYSIS OF R-R INTERVAL DATA

4.1 Introduction

In this chapter we will discuss some statistical tests for the analysis of R-R interval data. The motivation for this statistical analysis of the R-R interval data is to determine the statistical characteristics of each different arrhythmia class that we wish to detect and identify. These statistical characteristics could possibly be used by themselves in performing the detection and classification of the arrhythmias, or they could be used as important information in the development of more detailed dynamical models of R-R interval behavior. Having such mathematical models, we could design more sophisticated statistical detection and identification algorithms for performing the automatic rhythm analysis (several such techniques are discussed in Chapters 6 and 7). A detailed description of each statistical tests we wish to perform on the R-R interval data is given first in Section 4.2. The formula needed to perform the tests are also derived. Finally, a wide variety of actual data are tested, and the results are given in Section 4.3.

4.2. Analysis

4.2.1 Histogram, Sample Mean and Sample Variance

Assume that we are given a sequence of R-R intervals: $y(1), y(2), \ldots, y(k), \ldots y(n)$, where $y(k)$ is the kth R-R interval and n is the total number of R-R intervals in the ECG/VCG record which we would like to analyze. The onset of the ventricular activity is random

in the sense that even for a regular normal rhythm the R-R intervals are not exactly the same; rather they have small random deviations from their mean value. Therefore, the given R-R interval sequence, y(i), i=1,...,n, should be treated as a discrete random process. However, if we do not care about the order in which these R-R intervals are given, y(i), i=1,...,n, can then be considered as samples of a random variable Y. All the possible samples form the sample space of this random variable, and the probability that Y will assume a particular value lying in this sample space is given by the frequency function or the probability density function. Hence a random variable is completely specified by giving its sample space and frequency function. In our case, the random variable Y is the R-R interval, which can only take positive integer values (because our digitized approach quantize the intervals),therefore the sample space is the set of all positive integers. From this statistical standpoint, the different arrhythmia classes are then characterized by different frequency functions only, because their underlying sample spaces are all identical. Therefore if we can find the frequency functions associated with each arrhythmia classes, then the problem of detection and classification of arrhythmias would be simplified considerably. Although an analytical form of the frequency function is usually hard to get, we can graphically display this function by generating a histogram of the R-R intervals in the record. For different arrhythmia classes the associated R-R interval histogram patterns would hopefully be quite different; hence by examining the R-R interval histogram pattern we obtain useful classification information.

One would also like to know some of the simple statistical

parameters associated with the frequency functions, as these few numbers often provide useful information and are far more easily dealt with than an entire histogram. The most obvious statistic one would like to get is the sample mean, m_s, over all the R-R intervals contained in a record. The mean thus gives the average value of the R-R intervals one would expect to see and is computed as

$$m_s = \frac{1}{n} \sum_{i=1}^{n} y(i) \tag{4.1}$$

Such a piece of information can be useful in detecting tachycardia, or bradycardia.

In many cases, the information in the sample mean is not sufficient to distinguish all the arrhythmia patterns we wish to identify. For example, a regular normal rhythm may have the same mean R-R interval as a bigeminy, even though their R-R interval patterns are very different (one is very regular and the other has frequency function with two peaks). Therefore, one would like to have a measure of the variation of the R-R intervals away from the mean value. One such measure is provided by the sample variance over all the R-R intervals contained in the record.

The sample variance σ_s^2 is the mean-squared value of the R-R intervals about the sample mean, and σ_s is the r.m.s. deviation or standard deviation; thus,

$$\sigma_s^2 = \frac{1}{n-1} \sum_{i=1}^{n} [y(i)-m_s]^2 \tag{4.2}$$

The reason for using (n-1) instead of n for the average in Equation (4.2) is we want an unbiased measure of the variance [38]. From Equation (4.2) we see that a large variance means that the data may vary widely from the mean value, and a small variance means that the sample mean is a pretty good estimate of the data. Thus, by computing the sample variance, we can distinguish, for example, a bigeminy or sinus arrhythmia from a normal rhythm which has regular R-R intervals.

4.2.2 Running Mean and Running Variance

Thus far we have introduced the statistical concepts of R-R interval histogram, sample mean, and sample variance by considering that the given R-R intervals, y(i), i=1,2,...,n, are samples of a random variable Y. These simple statistical concepts provide us with some very important information for use in the detection and classification of the cardiac arrhythmias. However, due to the fact that we have not considered the order in which these R-R intervals occur we will not be able to distinguish, for example, a sudden rhythm jump from a bigeminal rhythm, or a gradually slowing normal rhythm from a sinus arrhythmia. Therefore, other statistical concepts are necessary that in some sense take into account the sequential variations of the given R-R interval sequence. In other words, we are also interested in knowing the values of some of the simple statistical parameters at each instant of time k. In principle, one might wish to compute the mean and variance at each time k, k=1,...,n; however this is not possible, since we only have one sample at each time. One alternative might be to use the running mean, m(k), which is given by:

$$m(k) = \frac{1}{k} \sum_{i=1}^{k} y(i) \qquad k=1,\ldots,n \tag{4.3}$$

In the case when k=n, Equation (4.3) reduces to Equation (4.1), thus we have

$$m(n) = m_s \tag{4.4}$$

It is more efficient for computing to put Equation (4.3) into a recursive form. Rewriting Equation (4.3) in the following form

$$m(k) = \frac{1}{k} \left[\sum_{i=1}^{k-1} y(i) + y(k) \right] \qquad k=1,\ldots,n \tag{4.5}$$

and using Equation (4.3) for k=k-1, Equation (4.5) becomes

$$m(k) = \frac{1}{k} [(k-1)m(k-1)+y(k)] \qquad k=1,\ldots,n \tag{4.6}$$

Equation (4.6) thus gives us the desired recursive form for computing the running means. The running mean m(k) gives the mean value of the R-R intervals up to time k; hence if the running mean m(k) begins to change markedly, one might be able to detect the onset of tachycardia or the presence of some other arrhythmic activity.

The variance of the R-R intervals at each time k, $\sigma^2(k)$, is given as

$$\sigma^2(k) = \frac{1}{k-1} \sum_{i=1}^{k} [y(i) - m(k)]^2 \qquad k=2,\ldots,n \tag{4.7}$$

where m(k) is computed from Equation (4.6). For k=n, Equation (4.7)

is just Equation (4.2); thus,

$$\sigma^2(n) = \sigma_s^2 \tag{4.8}$$

One would also like to write the running variance, $\sigma^2(k)$, in a recursive form. Expanding the square in Equation (4.7), we have

$$\sigma^2(k) = \frac{1}{k-1} \sum_{i=1}^{k} [y^2(i) - 2y(i)m(k) - m^2(k)] \quad k=2,\ldots,n \tag{4.9}$$

or

$$\sigma^2(k) = \frac{1}{k-1}\left[\sum_{i=1}^{k} y^2(i) - 2 \sum_{i=1}^{k} y(i)m(k) + km^2(k)\right] \quad k=2,\ldots,n \tag{4.10}$$

Upon using Equation (4.3), Equation (4.10) becomes

$$\sigma^2(k) = \frac{1}{k-1}\left[\sum_{i=1}^{k} y^2(i) - km^2(k)\right] \quad k=2,\ldots,n \tag{4.11}$$

Equation (4.11) is still not in a recursive form, because of the first term in the bracket; therefore we define a new quantity as follows

$$R_0(k) = \frac{1}{k} \sum_{i=1}^{k} y^2(i) \tag{4.12}$$

Where $R_0(k)$ is another statistical quantity, the mean-squared value.

Equation (4.11) can then be rewritten in the following form, by substituting Equation (4.12) in Equation (4.11):

$$\sigma^2(k) = \frac{k}{k-1}\left[R_0(k) - m^2(k)\right] \tag{4.13}$$

with k=2,...,n. The mean-squared value, $R_0(k)$, can be computed using the following recursive equation

$$R_0(k) = \frac{1}{k}\left[(k-1)R_0(k-1) + y^2(k)\right] \tag{4.14}$$

Therefore, using Equation (4.13) we can compute the running variance recursively, where $R_0(k)$ and $m(k)$ are given by Equations (4.6) and (4.14), respectively.

4.2.3 Sliding Window Mean, Variance, and Outlier Test

One problem with the computation of the running mean and running variance at each time k over all the k R-R intervals is that they are very slow in responding to a change in R-R interval behavior. By examining Equations (4.6) and (4.7) we can see that as k gets larger, the new piece of R-R interval $y(k)$ is weighted by a small factor $1/k$ and $1/k-1$ for computation of running mean and running variance, respectively. Therefore a sudden change of the R-R interval behavior at large k will not change the running mean and running variance by much, and thus we might not be able to detect this change. This is not surprising, since the running mean $m(k)$ and variance $\sigma^2(k)$ are statistics based on the assumption that the first k intervals have similar probabilistic properties.

In order to overcome this problem, we can compute a sliding window mean and variance, i.e., at any instant of time k, we only use the last ℓ R-R intervals, and ℓ is the sliding window width. This is equivalent to assuming that the R-R intervals are slowly varying (quasi-stationary) in a statistical sense. Thus, the equation for computing the mean can

be written as:

$$m(k) = \frac{1}{\ell} \sum_{i=k-\ell+1}^{k} y(i) \qquad k=\ell,\ell+1,\ldots,n \tag{4.15}$$

Again, rewriting Equation (4.15) in a recursive form, we have

$$m(k) = m(k-1) + \frac{1}{\ell} [y(k)-y(k-\ell)] \qquad k=\ell,\ell+1,\ldots,n \tag{4.16}$$

where $m(k)$ for $k \leq \ell$ is computed using Equation (4.6). The equation for computing the sliding window variance of width ℓ is

$$\sigma^2(k) = \frac{1}{\ell-1} \sum_{i=k-\ell+1}^{k} [y(i)-m(k)]^2 \qquad k=\ell,\ell+1,\ldots,n \tag{4.17}$$

In order to get a recursive relation for $\sigma^2(k)$, we define

$$R_0(k) = \frac{1}{\ell} \sum_{i=k-\ell+1}^{k} y^2(i) \tag{4.18}$$

which can be rewritten as:

$$R_0(k) = R_0(k-1) + \frac{1}{\ell} [y^2(k)-y^2(k-\ell)] \tag{4.19}$$

Substituting Equation (4.18) into Equation (4.17), we have

$$\sigma^2(k) = \frac{\ell}{\ell-1} [R_0(k) - m^2(k)] \qquad k=\ell,\ell+1,\ldots,n \tag{4.20}$$

Where $R_0(k)$ and $m(k)$ are computed from Equations (4.19) and (4.16), respectively.

From Equations (4.16) and (4.17) we can see that all the R-R interval data are weighted with the same factors $1/\ell$ and $1/\ell-1$ for sliding mean and variance, respectively. These factors are not changed with the time k, and therefore, these statistical parameters will respond to behavior of the R-R interval sequence that is not constant over the entire time sequence of interest, and the instant at which this erratic behavior happens will be more easily detected.

At this point we would like to discuss another statistical test that is useful for detecting the transient events in an R-R interval sequence. From Chapter 3, we see that all the transient arrhythmia classes are characterized by either a longer or shorter R-R interval (relative to the preceding pattern), or a combination of both. Therefore a satisfactory test should detect both the magnitude and sign of the change of the aberrant R-R interval. A simple statistical test which will perform this task is an outlier test, which is an effective test for distinguishing a piece of data from a particular ensemble, which is specified by some statistical parameters.

In our case, we wish to detect the ectopic event on top of an underlying normal sinus rhythm; hence, the ensemble is formed by all the R-R intervals of this underlying normal rhythm. For an ectopic event, we would expect that the R-R interval is very different from the ensemble which contains the usual R-R intervals and is characterized by the running mean $m(k)$ and standard deviation $\sigma(k)$. Therefore, an outlier test on a new R-R interval $y(k+1)$ is given as:

$$\frac{y(k+1) - m(k)}{\sigma(k)} \triangleq \alpha \tag{4.21}$$

for $\alpha > \varepsilon$: declare an ectopic event with a longer R-R interval

$\alpha < -\varepsilon$: declare an ectopic event with a shorter R-R interval

where ε is a positive valued threshold that represents how many standard deviations of variation we are willing to tolerate before declaring an interval to be an outlier. The quantities $\mathbf{m}(k)$ and $\sigma(k)$ in Equation (4.21) are computed according to Equations (4.6) and (4.13), respectively, for the case that $|\alpha| \leq \varepsilon$. However, in the case that $|\alpha| > \varepsilon$ we will exclude this new R-R interval $y(k+1)$ from the computations of $m(k)$ and $\sigma(k)$.

By using this simple outlier test one could in principle detect the various transient rhythms described in Chapter 3. For example, an $\alpha < -\varepsilon$ follows by an $\alpha > \varepsilon$ is the indictive of a compensatory beat, and two consecutive $\alpha > \varepsilon$ might be classified as a double non-compensatory event.

4.2.4 Correlation Functions and Scatter Diagram

All the statistical tests described so far do not tell us anything about the sequential nature of the pattern of the R-R intervals. (although those just described in Section 4.2.3 do deal time variations.) In other words, if the given R-R interval sequence has a periodic pattern, one will not be able to identify it using the previously introduced statistical tests. However a test to identify a periodic R-R interval pattern in arrhythmia analysis is very important, since two of the arrhythmic classes we wish to detect and identify - **bigeminy**

and trigeminy - are of this nature. For a bigeminal rhythm, the R-R interval sequential pattern is: long, short, long, short, etc., thus we have

$$y(i) \cong y(i+2) \qquad i=1,2,... \tag{4.22}$$

(where $\cong$ is used to indicate "to within small random variations"), which is a periodic function of period two. Similarly for a trigeminal rhythm of a period of three, we have

$$y(i) \cong y(i+3) \qquad i=1,2,... \tag{4.23}$$

An available statistical test which could be used to aid in detecting these periodic patterns is the sample correlation. For a given sequence of data points, y(i), i=1,...,n, the correlation function $R_\tau(k)$ is defined as follows:

$$R_\tau(k) = \frac{1}{k-\tau} \left[\sum_{i=1}^{k-\tau} y(i)y(i+\tau) \right] \qquad k>\tau \tag{4.24}$$

which is the average over data points up to time k of the correlation between data points τ time units apart. These numbers are computed in general for several values of τ. For $\tau=0$, Equation (4.24) becomes

$$R_0(k) = \frac{1}{k} \sum_{i=1}^{k} y^2(i) \tag{4.25}$$

which is identical to the mean-squared value defined earlier in Section

4.2.2. Equation (4.24) can be rewritten recursively as

$$R_\tau(k) = \frac{1}{k-\tau}\,[(k-1-\tau)R_\tau(k-1) + y(k-\tau)y(k)] \qquad k>\tau \tag{4.26}$$

A possible method of utilizing these correlation functions to detect a periodic function is illustrated by an example. Suppose we are given a bigeminal R-R interval sequence y(i), i=1,...,n, which has a pattern of long, short, long, short, etc. In the ideal case we have the equality

$$y(i) = y(i+2) \qquad i=1,2,\ldots,n-2 \tag{4.27}$$

or, upon rewriting Equation (4.27) out explicitly:

$$y(1) = y(3) = y(5) \ldots\ldots\ldots \tag{4.28}$$

$$y(2) = y(4) = y(6) \ldots\ldots\ldots \tag{4.29}$$

and $y(1) > y(2)$.

The sample correlation functions are then computed for different values of τ using Equation (4.24) for k=n:

$$\begin{aligned}
R_0(n) &= \frac{1}{n}\left[\sum_{i=1}^{n} y(i)y(i)\right] && \text{for } \tau=0 \\
R_1(n) &= \frac{1}{n-1}\left[\sum_{i=1}^{n-1} y(i)y(i+1)\right] && \text{for } \tau=1 \\
R_2(n) &= \frac{1}{n-2}\left[\sum_{i=1}^{n-2} y(i)y(i+2)\right] && \text{for } \tau=2 \\
&\ \ \vdots
\end{aligned} \tag{4.30}$$

Using Equations (4.27) through (4.29), and assuming that n is even, Equation (4.30) can be reduced to:

$$R_0(n) = \frac{1}{n}\left[\frac{n}{2}\,y^2(1) + \frac{n}{2}\,y^2(2)\right] = \frac{1}{2}\left[y^2(1) + y^2(2)\right]$$

$$R_1(n) = \frac{1}{n-1}[(n-1)y(1)y(2)] = y(1)y(2)$$

$$R_2(n) = \frac{1}{n-2}\left[\frac{n-2}{2}\,y^2(1) + \frac{n-2}{2}\,y^2(2)\right] = \frac{1}{2}\,[y^2(1) + y^2(2)] \tag{4.31}$$

$$R_3(n) = \frac{1}{n-3}\,[(n-3)y(1)y(2)] = y(1)y(2)$$

$$\vdots$$

which implies

$$R_0(n) = R_2(n) = R_4(n) = \ldots. \tag{4.32}$$

and

$$R_1(n) = R_3(n) = R_5(n) = \ldots \tag{4.33}$$

Note that since a squared quantity is alway greater or equal to zero, we have

$$[y(1) - y(2)]^2 \geq 0 \tag{4.34}$$

or,

$$\frac{1}{2}\,[y^2(1) + y^2(2)] \geq y(1)y(2) \tag{4.35}$$

where the equality holds for $y(1) = y(2)$ (where all of the beats are of the same length). Hence from Equation (4.31), we have

$$R_0(n) > R_1(n) \tag{4.36}$$

The relations given by Equations (4.32), (4.33) and (4.36) are thus the condition for a bigeminal rhythm.

From these relations, we can devise simple tests for bigeminy. For example, as we have seen bigeminy is characterized by

$$R_0(n) = R_2(n) \tag{4.37}$$

and we may have a rule that we declare an R-R interval sequence to be bigeminy if

$$R_2(n) \geq (1-\varepsilon)R_0(n) \tag{4.38}$$

where ε is a small positive number. One could, of course, consider more complex tests - involving R_4, R_0, etc., but these will entail more and more calculations on-line. In addition, from Equation (4.30) we see that $R_\tau(n)$ has only $n-\tau$ terms in it. Thus, the higher order correlations, such as R_4, are more apt to have large errors due to small sample sizes. In any event, the main point of this example is to illustrate that the correlation function contains extremely useful diagnostic information concerning the sequential correlation of a string of R-R intervals.

Another mechanism which could also be used to detect a cardiac rhythm which has some periodicity is considered here. From Equations (4.22) and (4.23), we see that the R-R intervals of a rhythmic pattern which has a periodicity of two have the following relations:

$$y(1) = y(3) = y(5) = \ldots\ldots$$
$$y(2) = y(4) = y(6) = \ldots\ldots \tag{4.39}$$

and for the R-R intervals of a periodic pattern of period three, we have

$$y(1) = y(4) = y(7) = \ldots\ldots$$
$$y(2) = y(5) = y(8) = \ldots\ldots \tag{4.40}$$
$$y(3) = y(6) = y(9) = \ldots\ldots$$

This motivates the computation of statistics for every qth beat, i.e., the original R-R interval sequence y(i), i=1,2,..., is broken up into q strings

$$\begin{aligned} &y(1), y(q+1), y(2q+1), \ldots\ldots \\ &y(2), y(q+2), y(2q+2), \ldots\ldots \\ &\quad\vdots \\ &y(q), y(2q), y(3q), \ldots\ldots\ldots \end{aligned} \tag{4.41}$$

and then compute the statistics of these strings. Note that Equation (4.41) reduces to Equation (4.39) for q=2, and to Equation (4.40) for q=3. For a periodic pattern of periodicity q, the mean of the overall pattern would differ markedlly from the means computed based on the q substrings, and the variance of the overall would be much larger than the variances of the q substrings. In this way, one could detect a pattern that has some periodicity.

In Section 4.2.2 we have introduced a simple method to display the R-R interval data graphically by using an R-R interval histogram. The

histogram gives us useful information for use in the detection of different cardiac arrhythmias, but it yields no information as to the sequence of occurrance of various size intervals. Another available graphical method which will display the correlations between the adjacent intervals is the scatter diagram. A scatter diagram is a plot of points, which have the adjacent intervals as their coordinates, on a two-dimensional space. This graphical technique will provide us with more diagnostic information. For instance, since the R-R interval histogram does not display the sequence of occurrance of the R-R intervals, a bigeminal rhythm may not be distinguishable from a sudden rhythm jump. However, their scatter diagrams will be markedlly different due to the fact that the sequences of occurrance of the R-R intervals for these two rhythms are not the same. Therefore a bigeminy and a sudden rhythm jump will be easily identified by using a scatter diagram. Identification of different arrhythmia classes using scatter diagrams will be demonstrated in the next section.

4.3 Experiments and Results

A program RRARAN was written to perform the R-R interval statistical analysis described in Section 4.2. A wide variety of both persistent and transient rhythm data was tested. In addition to the data files given in Table 2.1, we have also run tests for the data files listed in Table 4.1. As before the R waves were found using the R wave detector RRFILE described in Chapter 2.

Data File Name	Diagnosis
#503	Atrial premature contractions
#476	Graduate Slowing of heart rate
#463	Second degree AV block of the Wenckebach type
#492-1	Atrial premature contraction

Table 4.1 A Summary of Part of the Data Files Used in the R-R Interval Statistical Analysis

In order to study the characteristics of each different arrhythmia class, all the data files given in Tables 2.1 and 4.1 are reclassified into different arrhythmic classes according to the categorization concept described in Chapter 3. This categorization is given in Table 4.2.

Arrhythmia Category	Data File Names
Small Variation	IN.5, IN.20, IN.30
Large Variation	CUNATFIB
Trigeminy	HUANPVCS, HUANTRI(1)
Bigeminy	#503
Compensatory Beat	HARNETPVCS, SPOONPAC, BLOOM
Rhythm Jump	IN.5+30(2), #476(3)
Non-Compensatory Beat	#463
Double Non-Compensatory Beat	#492-1

Table 4.2 Categorization of the Date Files Given in Tables 2.1 and 4.1

Notes:

(1) A study of the R-R intervals of data file HUANPVCS in Table 2.5 shows that the trigeminal pattern persists only over the first 31 R-R intervals. Thus, in order to study the statistical characteristics of a trigeminal pattern, we creat a new pure trigeminal data file HUANTRI using the first 31 R-R intervals in data file HUANPVCS.

(2) Since none of the data files given in Tables 2.1 and 4.1 has a rhythm jump pattern as we described in Chapter 3, a pattern of this type was created artificially by adding data file IN.30 which has a slower heart rate to data file IN.5 which has a faster heart rate. This new data file is denoted by IN.5+30.

(3) We do not have an exactly matched category for data file #476, which exhibits a gradually slowing heart rate. For the present study, we classify it in the rhythm jump category.

All the data files were studied in the order given in Table 4.2. First an R-R interval histogram for each of the data files was generated. For all the date files except #476 and #463, the range of the R-R intervals covered were from 0 to 300 sampling points (250 sampling points = 1 second). With 10 sampling points in each bin, the whole range was divided into 30 bins. There was an extra bin, which gave all the R-R intervals which exceeded 300. Therefore, this histogram shows 31 bins altogether. For data files #476 and #463, since there were many R-R intervals exceeding 300, the R-R interval range covered was changed to the range of 60 to 400 sampling points. The resulting histograms are shown in Figures 4.1 - 4.14. A two-dimensional

R-R interval scatter diagram was generated next for all the data files with the nth R-R interval as the abscissa, and (n+1)st R-R interval as the ordinate. The range covered by both coordinates was from 0 to 400 sampling points. These scatter diagrams are shown in Figures 4.15 - 4.28.

Next, the running mean, running variance and deviation (α) defined in Equation (4.21) were computed and are given in Tables 4.3 - 4.16. The results of sliding window statistics using a window width of five are given in Tables 4.17 - 4.29. Next the statistics of every qth R-R intervals were computed for $q=1,\ldots,5$, and the results are given in Tables 4.30 - 4.42. Finally ten correlation functions, $\tau=0,1,\ldots,9$ in Equation (4.24), were computed, and the associated normalized correlation functions were also calculated. The results are given in Tables 4.43 - 4.55. From these results, we can make the following observations:

(1) R-R Interval Histogram

The R-R interval histograms have very small r.m.s. (root mean square) deviations for the non-arrhythmic data (see Figures 4.1 - 4.3) compared with those of the arrhythmic data (Figures 4.4 - 4.14). For the fourteen data files studied, the r.m.s. deviations for the non-arrhythmic data varied from 6.2 to 9.3, while those for the arrhythmic data varied from 16.7 to 71.2. There is a clear separation between the arrhythmic and non-arrhythmic data for these fourteen data files, but if we put too much emphasis on these r.m.s. deviations we may be misled. An example will demonstrate this point. Suppose in our data file all the R-R intervals are almost the same, with very

small r.m.s. deviation, except for one R-R interval, which is due to the presence of an aberrant R wave, say an atrial premature beat. In this case, since there is only one premature beat, the r.m.s. deviation of those regular R-R intervals will not be changed by much. This implies that even for a single arrhythmic beat the r.m.s. deviation over all the data would be small. Therefore, while it is safe to say that if the r.m.s. deviation of a record is greater than a given threshold, the record contains arrhythmic data, a small r.m.s. deviation does not necessarily imply that the data is non-arrhythmic.

The range over which the R-R intervals vary is small for non-arrhythmic data. It only covers 3 to 4 bins, while the arrhythmic data will cover at least ten bins (see Figures 4.4 - 4.14). Therefore, it seems reasonable to say that if the range of R-R intervals in the histogram is greater than 5 or 6 bins, this data is arrhythmic.

The R-R interval histogram tells us more than just whether the data is arrhythmic or non-arrhythmic; it also indicates to some extent what type of arrhythmia is in the record. Figure 4.4 clearly shows the large R-R interval variations about its mean value which is the indicative of a sinus arrhythmia or atrial fibrillation. Note that the histogram measures frequency of occurrance of various size intervals but yields no information as to their sequence. Thus for those arrhythmias that are characterized by a particular sequencing of events, the histogram can not be used to make a definite diagnosis. Of course the histogram can give indications of the presence of such arrhythmias.

Consider Figure 4.5, where the short R-R intervals correspond

to premature beats, and the long ones to the compensatory beats. However the trigeminal rhythm pattern is not so obviously identified in this histogram. This is due to the fact that the trigeminal pattern in HUANPVCS persists only over the first 31 R-R intervals; thus the non-trigeminal part of the data clouds the pattern. A trigeminal pattern is clearly evident for HUANTRI (Figure 4.6) by the three clearly separated R-R interval clusters representing the premature beats, normal intervals, and compensatory beats. Figure 4.7 clearly shows that a bigeminal rhythm may be present in data file #503. Figure 4.8 shows clearly the premature ventricular contractions with the short intervals and long compensatory intervals. Figure 4.9 and 4.10 are similar to Figure 4.8, with the regular R-R intervals centered in the histogram and a group of short premature beats and group of long compensatory beats around it.

A sudden rhythm jump of data file IN.5+30 manifests itself in the histogram (Figure 4.11); however, this is indistinguishable from a bigeminal rhythm (Figure 4.7). This again indicates the limited usefulness of the histogram. Graduate slowing in Figure 4.12 shows the R-R intervals cover a large range, which is from 160 to 340 sampling points for data file #476. The non-compensatory beats are all clearly identified from the R-R interval histograms (Figures 4.13 and 4.14), however a double non-compensatory is indistinguishable from a non-compensatory beat.

(2) Scatter Diagram

Scatter diagrams display the correlations between two consecutive R-R intervals. If all the R-R intervals are regular with small random

variations, then all the points in the scatter diagram should be confined to a small region and its distribution should be circular because of the randomness. Figures 4.15 - 4.17 show that the points in the scatter diagrams are confined in a rather small region, but they are elliptically distributed roughly along the diagonal line x=y, rather than a circle. This implies that the R-R intervals are somewhat serially correlated for normal rhythms. The scatter diagrams for the arrhythmic data spread over a large region compared with those of the non-arrhythmic data.

The random variations of the R-R intervals for atrial fibrillation are shown clearly for CUNATFIB in Figure 4.18. For HUANPVCS (Figure 4.19), a triangular shaped distribution is shown with many points in three outlying clusters roughly forming the triangle. This pattern is more obvious for HUANTRI (Figure 4.20). This is indicative of trigeminy and is of diagnostic use, since the scatter diagram does reflect the sequencing of the R-R intervals. Two clusters which are symmetric about the diagonal line x=y are observed for #503 in Figure 4.21. This is suggestive of bigeminy. In Figure 4.22, the compensatory beats are obvious, with the underlying regular R-R intervals close to the center of the triangle and the premature and compensatory beats at the vertices of the triangle. Every time there is a premature beat the point will move down from the center. The next point, with the short premature beat followed by a long compensatory beat, will move up and to the left. After the long compensatory beat, the R-R interval is back to normal again, and the point will move to the right of the center first and then back to the center. The distributions

of Figures 4.23 and 4.24 are similar to that of Figure 4.22, except that in Figure 4.23 the triangle is bigger and the variations of the points in each group are larger, and in Figure 4.24 the points in the vertices have relatively large variations.

A rhythm jump is characterized by two clusters along the diagonal line x=y, and a single point which has its coordinates approximately equal to the mean values of the two clusters as shown in Figure 4.25. Using a scatter diagram, a bigeminal rhythm (Figure 4.21) is clearly distinguishable from a rhythm jump. In Figure 4.26 a gradually slowing heart rate has all its points near the diagonal line x=y. This shows a strong serially correlation in the R-R intervals for graduate slowing rhythm. In Figure 4.27 the non-compensatory beats are obvious, with the underlying normal R-R intervals confined to a small region which is located on the diagonal x=y line. Every time there is a dropped (premature) beat, the point will move up (down) first from the normal R-R interval cluster. The next point, with the heart rate back to normal again, will move to the right (left) of the center cluster, and then back to the center. However, for a double non-compensatory beat an extra point is shown along the diagonal line x=y for data file #492-1 in Figure 4.28, representing the two consecutive shorter intervals.

(3) Deviation (α)

It appears that monitoring the deviation (α) provides a very simple way of detecting an ectopic change in the R-R intervals. In table 4.7, the deviations clearly show a rhythm pattern of period three. For instance, at N=3, α=2.92, a longer interval (213) is

detected, at N=5, α= -1.06, a shorter interval (91) is detected, and at N=6, α=1.17, a longer interval (193) is again detected. In table 4.9, a bigeminal pattern is shown by the changing of signs of the deviations. In Tables 4.10 - 4.12, the compensatory beats are identified by a large negative deviation followed by a large positive one. For instance, in Table 4.10 for N=19,20, the deviations are -2.37 and 3.02, respectively, which is indictive of a compensatory beat. More compensatory beats are detected at N=29,38 in Table 4.10, at N=22,28,37 in Table 4.11, and at N=8,34,37 and 44 in Table 4.12. Other ectopic events are detected by monitoring α (see Tables 4.13 - 4.16). Therefore, it is clear that a study of the behavior of these deviations will provide useful information in the design of an arrhythmia detection and classification system. Note however that this algorithm cannot detect ectopic beats prior to the third beat, since it has no basis for computing a running variance until two intervals have been processed (see Table 4.11 for an example of a missed premature beat at N=2).

(4) Sliding Window Statistics

As we discussed in Section 4.2, the advantage of using sliding window is to get a faster response to a sudden change in R-R interval behavior. This is clearly shown in Tables 4.17 - 4.29 by the dramatic changes in the variances of the R-R intervals compared to those computed using overall R-R interval data.

(5) Statistics of Every qth Beat

In Tables 4.30 - 4.42, the normal rhythms are indicated by approximately the same mean values and same (small) variances. On

the other hand, for CUNATFIB we observed approximately the same but larger variances, which are given in Table 4.33. As indicated earlier, HUANPVCS and #503 are indicative of trigeminy and bigeminy, respectively. These are clearly shown by the statistics in Tables 4.34 - 4.36. For example, in Table 4.34 we see that we obtain markedly smaller variances for the "every 3rd beat" calculations. This is clearly indicative of trigeminy. Since this algorithm is designed particularly to detect R-R interval sequences which have a certain period, Tables 4.37 - 4.42 do not suggest any detection and classification information for these periodic patterns.

(6) Correlation Function

The periodic pattern of HUANPVCS is clearly reflected in the correlation function in Tables 4.47 and 4.48, which peak strongly at τ=0,3,6, and 9. For #503, the correlation function in Table 4.49 peaks strongly at τ=0,2,4,6,8, which suggests a periodic function of period two. Note also that the correlation function falls off very slowly for normal rhythms (Tables 4.43 - 4.45) and somewhat faster for the slightly less correlated rhythms (such as in Tables 4.46 and 4.51). Note that the correlation function is an average statistic. Thus, transient events are often masked in this statistic. As an example, consider the jump between two normal rhythms as shown in Table 4.53. Since the only temporal deviation is at the one point at which the rhythm shifts, the correlation function is dominated by the remaining regular pattern.

In this chapter we have described and tested a variety of statistical tests for the analysis of R-R interval data. These tests

provide both qualitative and quantitative information that will be useful in the design of an overall detection system. However, as we have seen each of the tests has its limitations, and the output of the tests is not particularly amenable to simple decision rules. In the next chapters, with the aid of the knowledge gained from these tests, we will put together two compact and systematic techniques for the detection and classification of arrhythmias.

```
INTERVAL     NUMBER        R-R INTERVAL HISTO

  0 TO  10       0
 10 TO  20       0
 20 TO  30       0
 30 TO  40       0
 40 TO  50       0
 50 TO  60       0
 60 TO  70       0
 70 TO  80       0
 80 TO  90       0
 90 TO 100       0
100 TO 110       0
110 TO 120       0
120 TO 130       0
130 TO 140       0
140 TO 150       0
150 TO 160       0
160 TO 170       6      XXXXXX
170 TO 180      24      XXXXXXXXXXXXXXXXXXXXXXXX
180 TO 190      12      XXXXXXXXXXXX
190 TO 200       0
200 TO 210       0
210 TO 220       0
220 TO 230       0
230 TO 240       0
240 TO 250       0
250 TO 260       0
260 TO 270       0
270 TO 280       0
280 TO 290       0
290 TO 300       0
  GT.  300       0


NUMBER OF R-R INTERVALS IN INPUT DATAFILE =   42
SAMPLE MEAN = 176.7   RMS DEVIATION =  6.4
```

Figure 4.1 R-R Interval Histogram for Data File IN.5

```
INTERVAL     NUMBER        R-R INTERVAL HISTO

  0 TO  10       0
 10 TO  20       0
 20 TO  30       0
 30 TO  40       0
 40 TO  50       0
 50 TO  60       0
 60 TO  70       0
 70 TO  80       0
 80 TO  90       0
 90 TO 100       0
100 TO 110       0
110 TO 120       0
120 TO 130       0
130 TO 140       0
140 TO 150       0
150 TO 160       0
160 TO 170       0
170 TO 180       0
180 TO 190       2      XXXX
190 TO 200      16      XXXXXXXXXXXXXXXXXXXXXXXXXXXXXXXX
200 TO 210      16      XXXXXXXXXXXXXXXXXXXXXXXXXXXXXXXX
210 TO 220       1      XX
220 TO 230       0
230 TO 240       0
240 TO 250       0
250 TO 260       0
260 TO 270       0
270 TO 280       0
280 TO 290       0
290 TO 300       0
  GT.  300       0

 NUMBER OF R-R INTERVALS IN INPUT DATAFILE =    35
 SAMPLE MEAN = 200.4    RMS DEVIATION =  6.2
```

Figure 4.2 R-R Interval Histogram for Data File IN.20.

```
INTERVAL     NUMBER        R-R INTERVAL HISTO

  0 TO  10      0
 10 TO  20      0
 20 TO  30      0
 30 TO  40      0
 40 TO  50      0
 50 TO  60      0
 60 TO  70      0
 70 TO  80      0
 80 TO  90      0
 90 TO 100      0
100 TO 110      0
110 TO 120      0
120 TO 130      0
130 TO 140      0
140 TO 150      0
150 TO 160      0
160 TO 170      0
170 TO 180      0
180 TO 190      0
190 TO 200      0
200 TO 210      0
210 TO 220      4      XXXXXXXX
220 TO 230     10      XXXXXXXXXXXXXXXXXX
230 TO 240     13      XXXXXXXXXXXXXXXXXXXXXXXXX
240 TO 250      5      XXXXXXXXXX
250 TO 260      0
260 TO 270      0
270 TO 280      0
280 TO 290      0
290 TO 300      0
 GT.  300       0


NUMBER OF R-R INTERVALS IN INPUT DATAFILE =    32
SAMPLE MEAN = 231.1   RMS DEVIATION =  9.3
```

Figure 4.3 R-R Interval Histogram for Data File IN.30.

```
INTERVAL     NUMBER        R-R INTERVAL HISTO

  0 TO  10      0
 10 TO  20      0
 20 TO  30      0
 30 TO  40      0
 40 TO  50      0
 50 TO  60      0
 60 TO  70      0
 70 TO  80      3      XXX
 80 TO  90     22      XXXXXXXXXXXXXXXXXXXXX
 90 TO 100     22      XXXXXXXXXXXXXXXXXXXXX
100 TO 110     11      XXXXXXXXXXX
110 TO 120     20      XXXXXXXXXXXXXXXXXXXX
120 TO 130      5      XXXXX
130 TO 140      8      XXXXXXXX
140 TO 150      4      XXXX
150 TO 160      1      X
160 TO 170      1      X
170 TO 180      0
180 TO 190      0
190 TO 200      0
200 TO 210      0
210 TO 220      0
220 TO 230      0
230 TO 240      0
240 TO 250      0
250 TO 260      0
260 TO 270      0
270 TO 280      0
280 TO 290      0
290 TO 300      0
 GT.  300       0

NUMBER OF R-R INTERVALS IN INPUT DATAFILE =   97
SAMPLE MEAN = 106.3   RMS DEVIATION = 19.7
```

Figure 4.4 R-R Interval Histogram for Data File CUNATFIB.

```
INTERVAL     NUMBER        R-R INTERVAL HISTO

  0 TO  10       0
 10 TO  20       0
 20 TO  30       0
 30 TO  40       0
 40 TO  50       0
 50 TO  60       0
 60 TO  70       0
 70 TO  80       0
 80 TO  90       7      XXXXXXXXXXXXX
 90 TO 100       5      XXXXXXXXXX
100 TO 110       0
110 TO 120       1      XX
120 TO 130       2      XXXX
130 TO 140       8      XXXXXXXXXXXXXXXX
140 TO 150       3      XXXXXX
150 TO 160       1      XX
160 TO 170       3      XXXXXX
170 TO 180       1      XX
180 TO 190       2      XXXX
190 TO 200       1      XX
200 TO 210       4      XXXXXXXX
210 TO 220       3      XXXXXX
220 TO 230       0
230 TO 240       0
240 TO 250       0
250 TO 260       0
260 TO 270       0
270 TO 280       0
280 TO 290       0
290 TO 300       0
  GT.  300       0


 NUMBER OF R-R INTERVALS IN INPUT DATAFILE =    41
 SAMPLE MEAN = 142.8   RMS DEVIATION = 43.4
```

Figure 4.5 R-R Interval Histogram for Data File HUANPVCS

```
INTERVAL     NUMBER        R-R INTERVAL HISTO

  0 TO  10       0
 10 TO  20       0
 20 TO  30       0
 30 TO  40       0
 40 TO  50       0
 50 TO  60       0
 60 TO  70       0
 70 TO  80       0
 80 TO  90       6      XXXXXXXXXXXX
 90 TO 100       4      XXXXXXXX
100 TO 110       0
110 TO 120       0
120 TO 130       0
130 TO 140       8      XXXXXXXXXXXXXXXX
140 TO 150       3      XXXXXX
150 TO 160       0
160 TO 170       0
170 TO 180       0
180 TO 190       2      XXXX
190 TO 200       1      XX
200 TO 210       4      XXXXXXXX
210 TO 220       3      XXXXXX
220 TO 230       0
230 TO 240       0
240 TO 250       0
250 TO 260       0
260 TO 270       0
270 TO 280       0
280 TO 290       0
290 TO 300       0
  GT.  300       0


 NUMBER OF R-R INTERVALS IN INPUT DATAFILE =   31
 SAMPLE MEAN = 144.2   RMS DEVIATION = 47.0
```

Figure 4.6 R-R Interval Histogram for Data File HUANTRI.

```
INTERVAL     NUMBER        R-R INTERVAL HISTO

  0 TO  10       0
 10 TO  20       0
 20 TO  30       0
 30 TO  40       0
 40 TO  50       0
 50 TO  60       0
 60 TO  70       0
 70 TO  80       0
 80 TO  90       0
 90 TO 100       0
100 TO 110       0
110 TO 120       0
120 TO 130       5      XXXXXXXXXX
130 TO 140      14      XXXXXXXXXXXXXXXXXXXXXXXXXX
140 TO 150       1      XX
150 TO 160       0
160 TO 170       0
170 TO 180       0
180 TO 190       0
190 TO 200       0
200 TO 210       0
210 TO 220       0
220 TO 230       0
230 TO 240       0
240 TO 250       0
250 TO 260       1      XX
260 TO 270       7      XXXXXXXXXXXXX
270 TO 280       7      XXXXXXXXXXXXX
280 TO 290       2      XXXX
290 TO 300       2      XXXX
  GT.  300       0

  NUMBER OF R-R INTERVALS IN INPUT DATAFILE =   39
  SAMPLE MEAN = 201.1   RMS DEVIATION = 71.2
```

Figure 4.7 R-R Interval Histogram for Data File #503.

```
INTERVAL     NUMBER        R-R INTERVAL HISTO

  0 TO  10      0
 10 TO  20      0
 20 TO  30      0
 30 TO  40      0
 40 TO  50      0
 50 TO  60      0
 60 TO  70      0
 70 TO  80      0
 80 TO  90      0
 90 TO 100      0
100 TO 110      4      XXXX
110 TO 120      0
120 TO 130      0
130 TO 140      0
140 TO 150      9      XXXXXXXXX
150 TO 160     26      XXXXXXXXXXXXXXXXXXXXXXXXXX
160 TO 170      8      XXXXXXXX
170 TO 180      2      XX
180 TO 190      0
190 TO 200      0
200 TO 210      0
210 TO 220      2      XX
220 TO 230      2      XX
230 TO 240      0
240 TO 250      0
250 TO 260      0
260 TO 270      0
270 TO 280      0
280 TO 290      0
290 TO 300      0
  GT.  300      0


NUMBER OF R-R INTERVALS IN INPUT DATAFILE =    55
SAMPLE MEAN = 156.9   RMS DEVIATION = 24.4
```

Figure 4.8 R-R Interval Histogram for Data File HARNETPVCS.

```
INTERVAL     NUMBER        R-R INTERVAL HISTO


  0 TO  10       0
 10 TO  20       0
 20 TO  30       0
 30 TO  40       0
 40 TO  50       0
 50 TO  60       0
 60 TO  70       0
 70 TO  80       0
 80 TO  90       0
 90 TO 100       0
100 TO 110       2       XXXX
110 TO 120       1       XX
120 TO 130       0
130 TO 140       1       XX
140 TO 150       0
150 TO 160       0
160 TO 170       0
170 TO 180       3       XXXXXX
180 TO 190       8       XXXXXXXXXXXXXXX
190 TO 200       5       XXXXXXXXXX
200 TO 210       5       XXXXXXXXXX
210 TO 220       5       XXXXXXXXXX
220 TO 230       3       XXXXXX
230 TO 240       2       XXXX
240 TO 250       1       XX
250 TO 260       1       XX
260 TO 270       0
270 TO 280       2       XXXX
280 TO 290       0
290 TO 300       1       XX
  GT.  300       0


NUMBER OF R-R INTERVALS IN INPUT DATAFILE =    40
SAMPLE MEAN = 201.0   RMS DEVIATION = 40.8
```

Figure 4.9 R-R Interval Histogram for Data File SPOONPAC.

```
INTERVAL     NUMBER        R-R INTERVAL HISTO

  0 TO  10       0
 10 TO  20       0
 20 TO  30       0
 30 TO  40       0
 40 TO  50       0
 50 TO  60       0
 60 TO  70       0
 70 TO  80       0
 80 TO  90       0
 90 TO 100       0
100 TO 110       0
110 TO 120       0
120 TO 130       2      XX
130 TO 140       1      X
140 TO 150       1      X
150 TO 160       4      XXXX
160 TO 170      25      XXXXXXXXXXXXXXXXXXXXXXXXX
170 TO 180      11      XXXXXXXXXXX
180 TO 190       1      X
190 TO 200       1      X
200 TO 210       1      X
210 TO 220       2      XX
220 TO 230       0
230 TO 240       0
240 TO 250       0
250 TO 260       0
260 TO 270       0
270 TO 280       0
280 TO 290       0
290 TO 300       0
  GT,  300       0


 NUMBER OF R-R INTERVALS IN INPUT DATAFILE =    47
 SAMPLE MEAN = 168,6   RMS DEVIATION = 16,7
```

Figure 4.10 R-R Interval Histogram for Data File BLOOM.

```
INTERVAL     NUMBER        R-R INTERVAL HISTO

  0 TO  10      0
 10 TO  20      0
 20 TO  30      0
 30 TO  40      0
 40 TO  50      0
 50 TO  60      0
 60 TO  70      0
 70 TO  80      0
 80 TO  90      0
 90 TO 100      0
100 TO 110      0
110 TO 120      0
120 TO 130      0
130 TO 140      0
140 TO 150      0
150 TO 160      0
160 TO 170      6      XXXXXX
170 TO 180     24      XXXXXXXXXXXXXXXXXXXXXXXX
180 TO 190     12      XXXXXXXXXXXX
190 TO 200      0
200 TO 210      0
210 TO 220      4      XXXX
220 TO 230     10      XXXXXXXXXX
230 TO 240     13      XXXXXXXXXXXXX
240 TO 250      5      XXXXX
250 TO 260      0
260 TO 270      0
270 TO 280      0
280 TO 290      0
290 TO 300      0
 GT. 300        0


NUMBER OF R-R INTERVALS IN INPUT DATAFILE =   74
SAMPLE MEAN = 200.2   RMS DEVIATION = 28.2
```

Figure 4.11 R-R Interval Histogram for Data File IN.5+30.

```
INTERVAL     NUMBER        R-R INTERVAL HISTO

 60 TO  70      0
 70 TO  80      0
 80 TO  90      0
 90 TO 100      0
100 TO 110      0
110 TO 120      0
120 TO 130      0
130 TO 140      0
140 TO 150      0
150 TO 160      0
160 TO 170      0
170 TO 180      4      XXXXXXXXXXXXXXXXXXX
180 TO 190      1      XXXXX
190 TO 200      0
200 TO 210      2      XXXXXXXXXX
210 TO 220      1      XXXXX
220 TO 230      0
230 TO 240      1      XXXXX
240 TO 250      0
250 TO 260      1      XXXXX
260 TO 270      0
270 TO 280      0
280 TO 290      0
290 TO 300      1      XXXXX
300 TO 310      1      XXXXX
310 TO 320      0
320 TO 330      1      XXXXX
330 TO 340      2      XXXXXXXXXX
340 TO 350      0
350 TO 360      0
360 TO 370      0
370 TO 380      0
380 TO 390      0
390 TO 400      0

NUMBER OF R-R INTERVALS IN INPUT DATAFILE =   15
SAMPLE MEAN = 239.3   RMS DEVIATION = 63.1
```

Figure 4.12 R-R Interval Histogram for Data File #476.

```
INTERVAL     NUMBER        R-R INTERVAL HISTO

 60 TO  70      0
 70 TO  80      0
 80 TO  90      0
 90 TO 100      0
100 TO 110      0
110 TO 120      0
120 TO 130      0
130 TO 140      0
140 TO 150      0
150 TO 160      0
160 TO 170      0
170 TO 180      0
180 TO 190      1      XXXXX
190 TO 200      3      XXXXXXXXXXXXXXX
200 TO 210      3      XXXXXXXXXXXXXXX
210 TO 220      5      XXXXXXXXXXXXXXX
220 TO 230      0
230 TO 240      0
240 TO 250      0
250 TO 260      0
260 TO 270      0
270 TO 280      0
280 TO 290      0
290 TO 300      0
300 TO 310      0
310 TO 320      0
320 TO 330      1      XXXXX
330 TO 340      0
340 TO 350      1      XXXXX
350 TO 360      0
360 TO 370      1      XXXXX
370 TO 380      0
380 TO 390      0
390 TO 400      0

NUMBER OF R-R INTERVALS IN INPUT DATAFILE =   15
SAMPLE MEAN = 256.5   RMS DEVIATION = 63.4
```

Figure 4.13 R-R Interval Histogram for Data File #463.

```
INTERVAL     NUMBER        R-R INTERVAL HISTO

  0 TO  10      0
 10 TO  20      0
 20 TO  30      0
 30 TO  40      0
 40 TO  50      0
 50 TO  60      0
 60 TO  70      0
 70 TO  80      0
 80 TO  90      0
 90 TO 100      0
100 TO 110      1      XXXXX
110 TO 120      0
120 TO 130      0
130 TO 140      1      XXXXX
140 TO 150      0
150 TO 160      0
160 TO 170      0
170 TO 180      0
180 TO 190      0
190 TO 200      0
200 TO 210      0
210 TO 220      0
220 TO 230      0
230 TO 240      1      XXXXX
240 TO 250      2      XXXXXXXXXX
250 TO 260      3      XXXXXXXXXXXXXXX
260 TO 270      0
270 TO 280      0
280 TO 290      0
290 TO 300      0
 GT.  300       0

 NUMBER OF R-R INTERVALS IN INPUT DATAFILE =     8
 SAMPLE MEAN = 218.4   RMS DEVIATION = 59.4
```

Figure 4.14 R-R Interval Histogram for Data File #492-1.

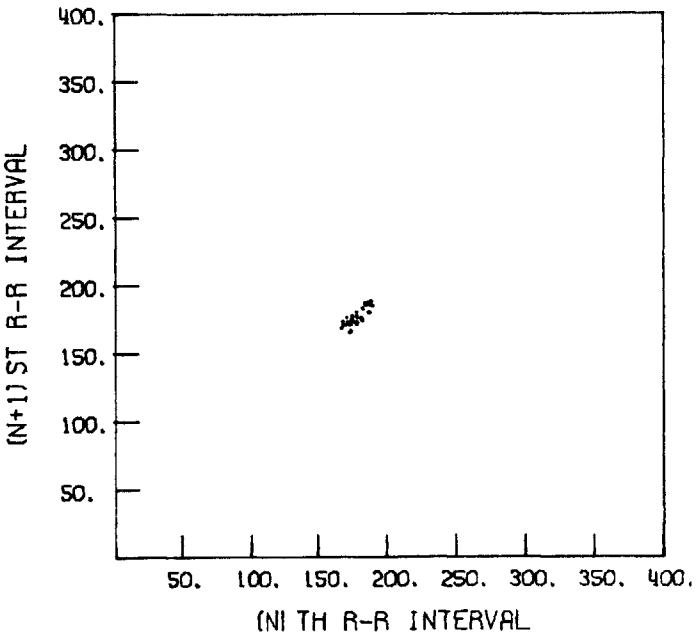

Figure 4.15 R-R Interval Scatter Diagram for Data File IN.5.

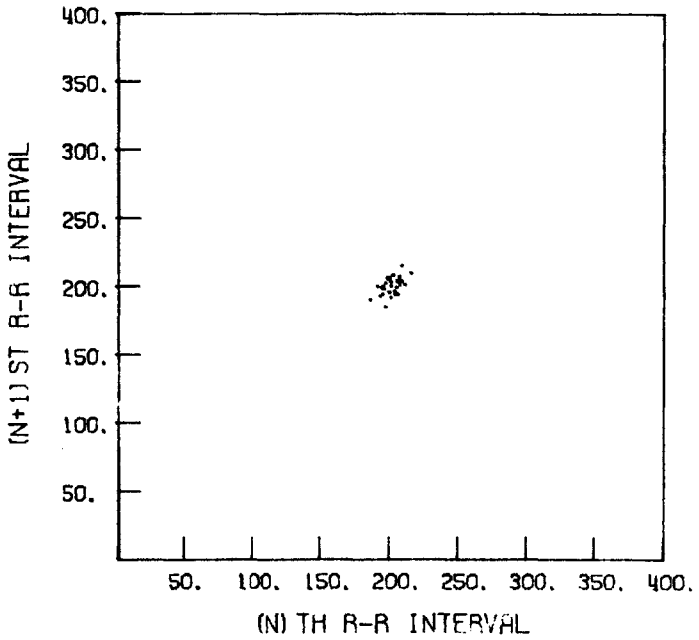

Figure 4.16 R-R Interval Scatter Diagram for Data File IN.20.

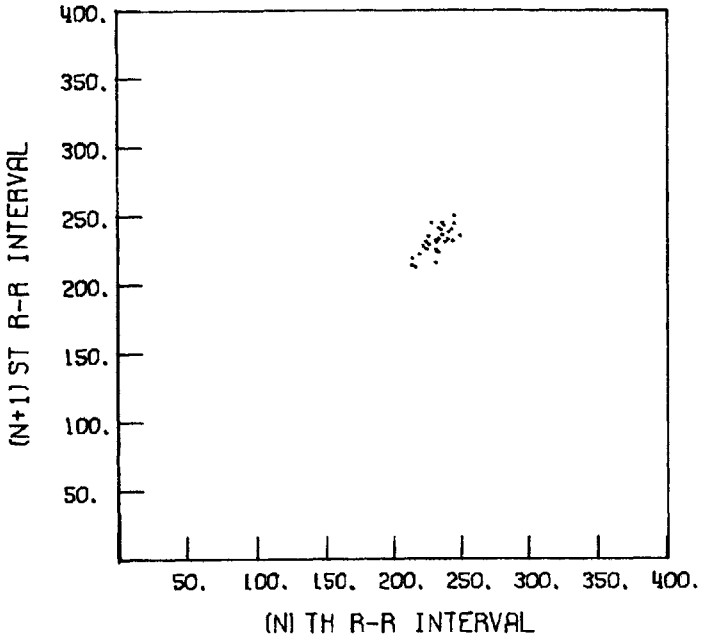

Figure 4.17 R-R Interval Scatter Diagram for Data File IN.30.

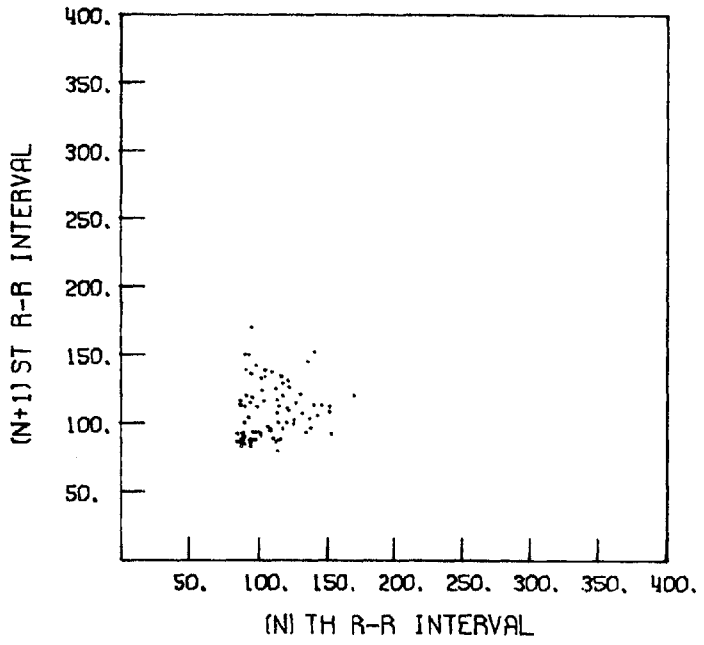

Figure 4.18 R-R Interval Scatter Diagram for Data File CUNATFIB.

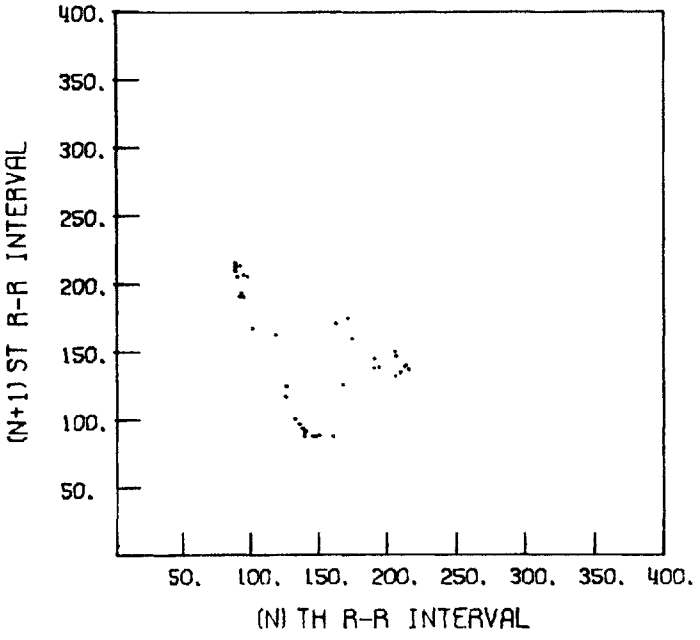

Figure 4.19 R-R Interval Scatter Diagram for Data File HUANPVCS.

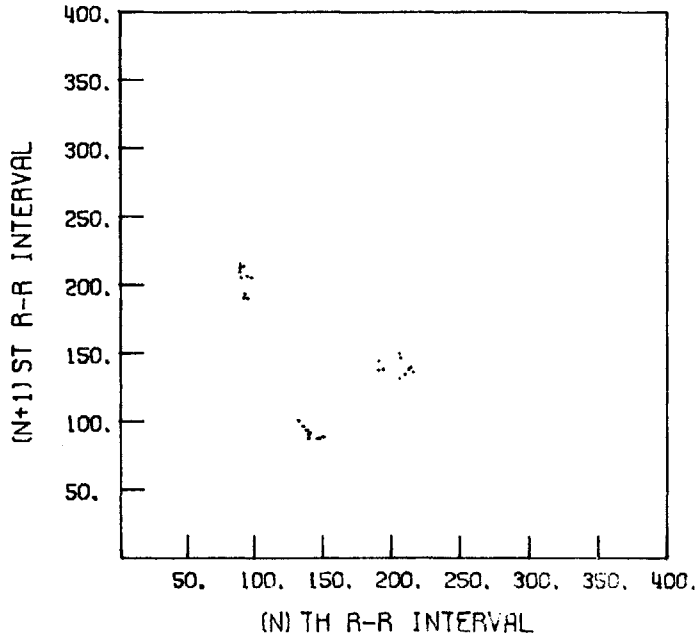

Figure 4.20 R-R Interval Scatter Diagram for Data File HUANTRI.

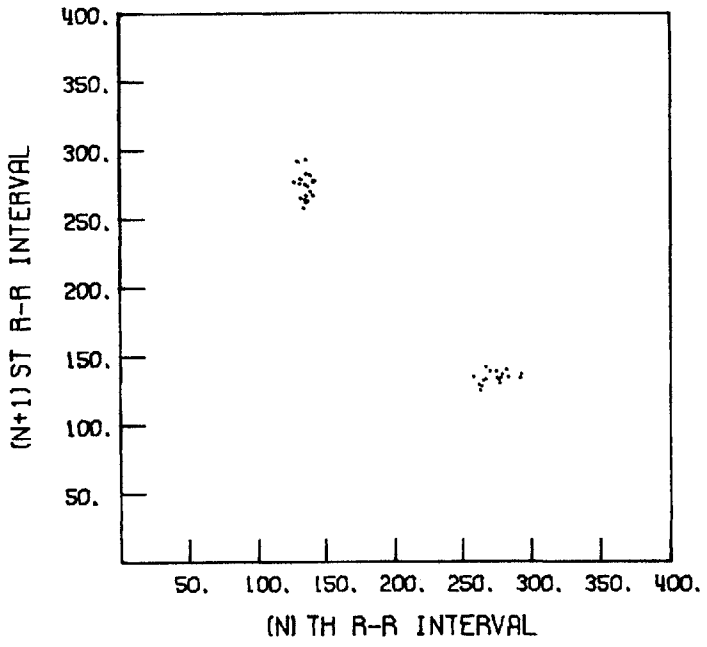

Figure 4.21 R-R Interval Scatter Diagram for Data File #503.

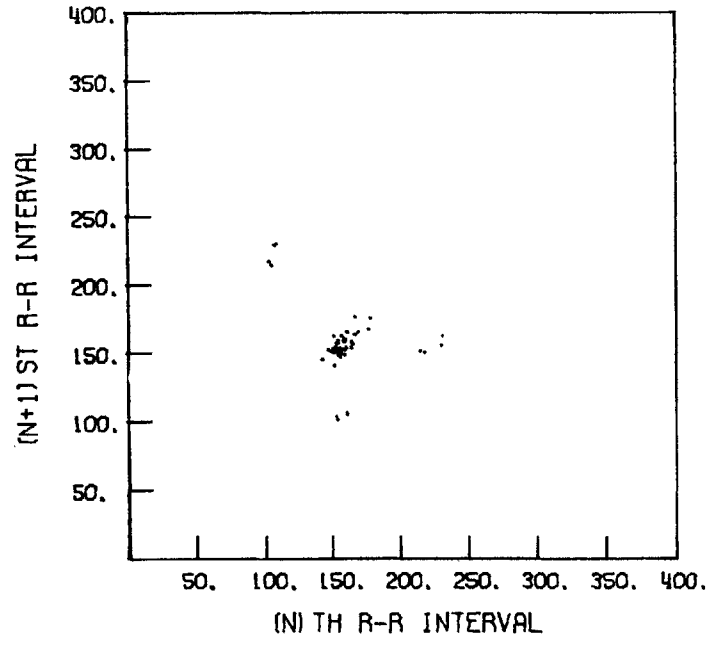

Figure 4.22 R-R Interval Scatter Diagram for Data File HARNETPVCS.

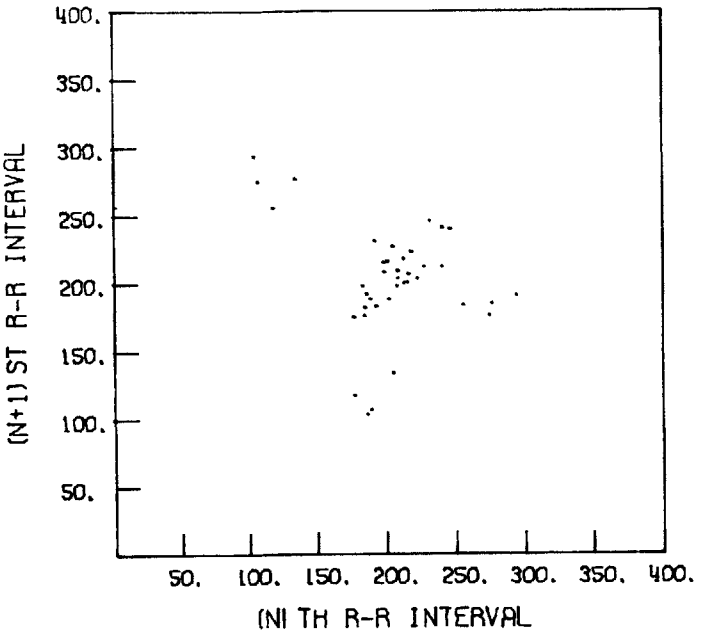

Figure 4.23 R-R Interval Scatter Diagram for Data File SPOONPAC.

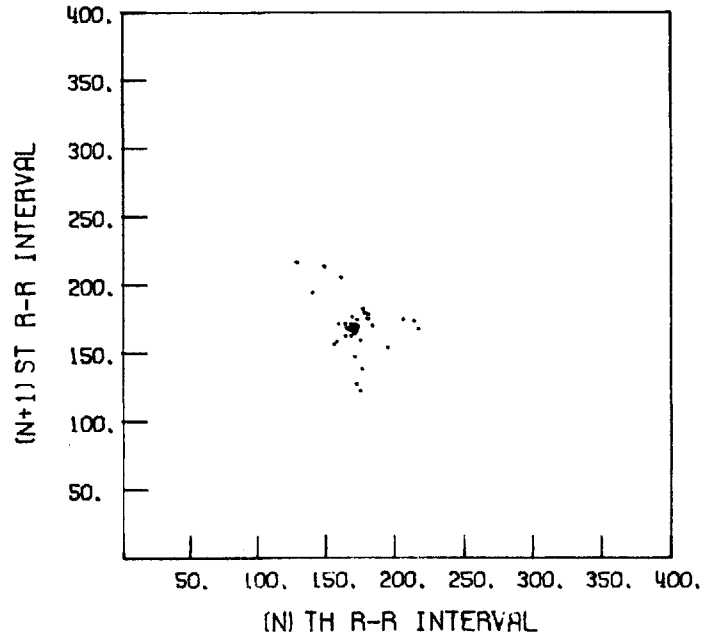

Figure 4.24 R-R Interval Scatter Diagram for Data File BLOOM.

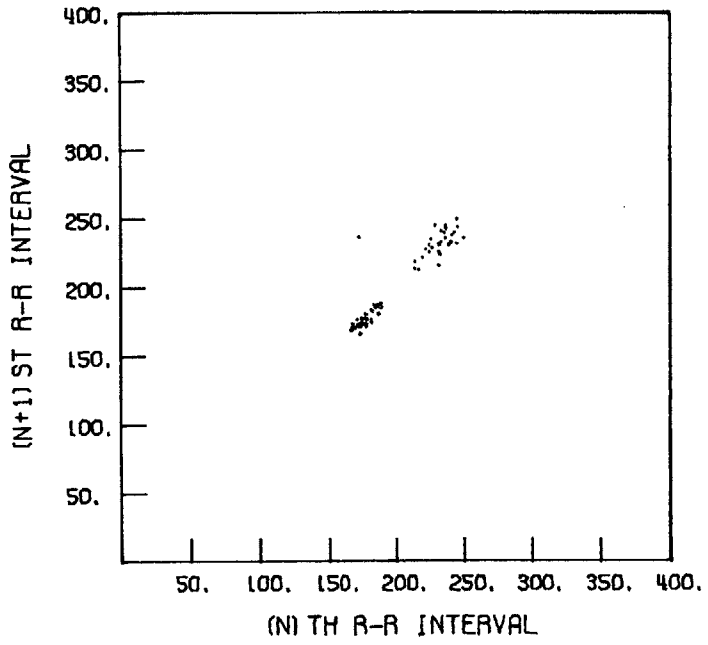

Figure 4.25 R-R Interval Scatter Diagram for Data File IN.5+30.

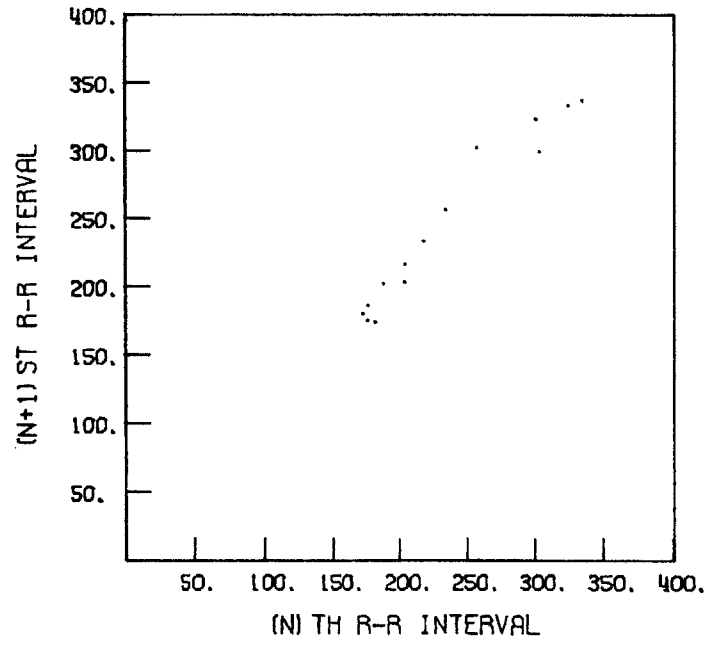

Figure 4.26 R-R Interval Scatter Diagram for Data File #476.

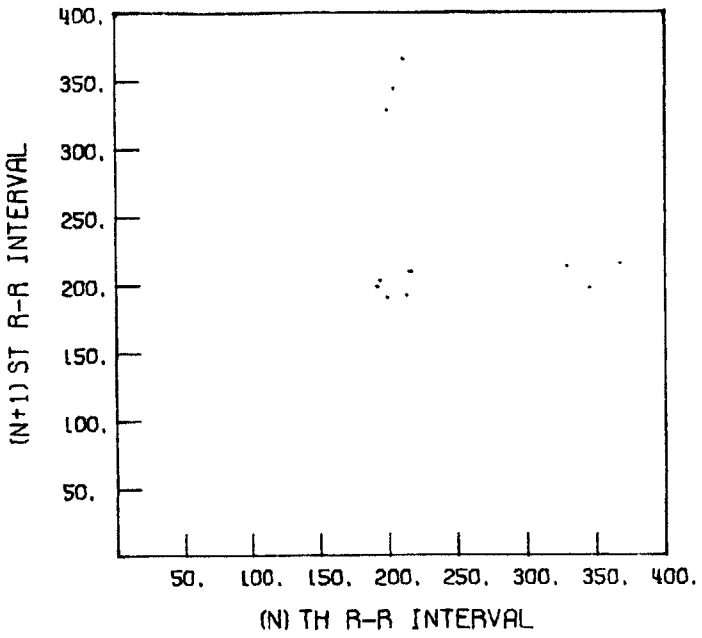

Figure 4.27 R-R Interval Scatter Diagram for Data File #463.

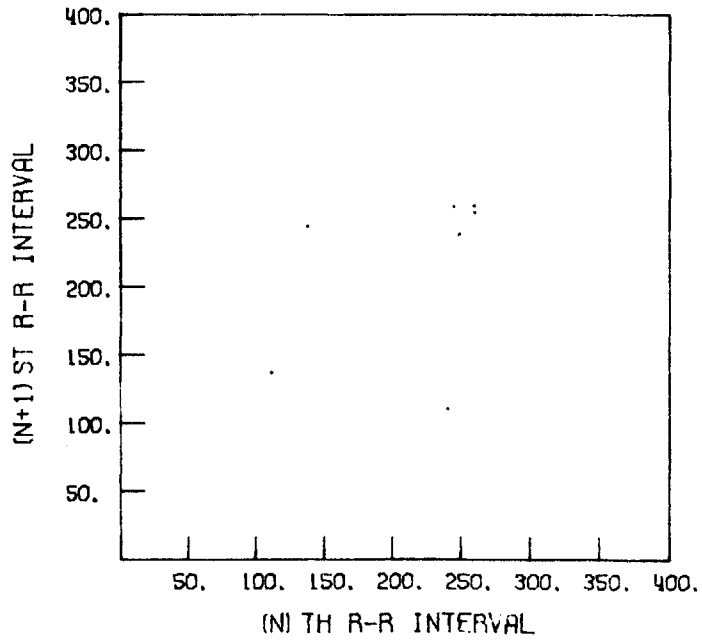

Figure 4.28 R-R Interval Scatter Diagram for Data File #492-1.

N	R-R INTER	RUNNING MEAN	RUNNING RMS DEV	RUNNING VARIANCE	DEVIATION (α)
1	181	181.00			
2	182	181.50	0.71	0.50	
3	187	183.33	3.21	10.33	7.78
4	188	184.50	3.51	12.33	1.45
5	185	184.60	3.05	9.30	0.14
6	180	185.83	3.51	10.97	-1.51
7	183	183.71	3.04	9.24	-0.25
8	185	183.88	2.85	8.12	0.42
9	187	184.22	2.86	8.19	1.10
10	185	184.30	2.71	7.34	0.27
11	180	183.91	2.88	8.29	-1.59
12	183	183.83	2.76	7.60	-0.32
13	186	184.00	2.71	7.33	0.79
14	186	184.14	2.66	7.06	0.74
15	180	183.87	2.77	7.69	-1.56
16	174	183.25	3.64	13.27	-3.56
17	173	182.65	4.31	18.62	-2.81
18	176	182.28	4.47	19.98	-1.54
19	180	182.16	4.37	19.14	-0.51
20	176	181.85	4.48	20.03	-1.41
21	173	181.43	4.77	22.75	-1.98
22	177	181.23	4.75	22.57	-0.93
23	176	181.00	4.77	22.72	-1.10
24	177	180.83	4.74	22.42	-0.84
25	171	180.44	5.03	25.33	-2.08
26	165	179.85	5.79	33.49	-3.07
27	168	179.41	6.11	37.39	-2.05
28	170	179.07	6.26	39.19	-1.54
29	176	178.97	6.17	38.10	-0.49
30	172	178.73	6.20	38.41	-1.13
31	166	178.32	6.51	42.36	-2.05
32	173	178.16	6.47	41.88	-0.82
33	174	178.03	6.41	41.08	-0.64
34	177	178.00	6.31	39.88	-0.16
35	172	177.83	6.30	39.71	-0.95
36	166	177.50	6.52	42.48	-1.88
37	170	177.30	6.54	42.82	-1.15
38	172	177.16	6.51	42.42	-0.81
39	173	177.05	6.46	41.74	-0.64
40	173	176.95	6.41	41.08	-0.63
41	171	176.80	6.40	40.91	-0.93
42	171	176.67	6.38	40.72	-0.91

Table 4.3 Running Statistics of Data File IN.5.

N	R-R INTER	RUNNING MEAN	RUNNING RMS DEV	RUNNING VARIANCE	DEVIATION (α)
1	199	199.00			
2	206	202.50	4.95	24.50	
3	205	203.33	3.79	14.33	0.51
4	194	201.00	5.60	31.33	-2.47
5	198	200.40	5.03	25.30	-0.54
6	205	201.17	4.88	23.78	0.91
7	203	201.43	4.50	20.29	0.38
8	194	200.50	4.93	24.29	-1.65
9	194	199.78	5.09	25.94	-1.52
10	200	199.80	4.80	23.07	0.04
11	200	199.82	4.56	20.76	0.04
12	192	199.17	4.90	23.96	-1.72
13	193	198.69	4.99	24.90	-1.26
14	199	198.71	4.80	23.00	0.06
15	196	198.53	4.67	21.85	-0.57
16	185	197.69	5.64	31.84	-2.90
17	190	197.24	5.77	33.32	-1.56
18	200	197.39	5.64	31.80	0.48
19	203	197.68	5.63	31.68	1.00
20	196	197.60	5.49	30.16	-0.30
21	202	197.81	5.44	29.57	0.80
22	208	198.27	5.74	32.90	1.87
23	204	198.52	5.73	32.81	1.00
24	199	198.54	5.61	31.42	0.08
25	205	198.80	5.64	31.76	1.15
26	204	199.00	5.62	31.55	0.92
27	195	198.85	5.56	30.90	-0.71
28	198	198.82	5.46	29.80	-0.15
29	206	199.07	5.52	30.50	1.32
30	207	199.33	5.62	31.55	1.44
31	201	199.39	5.53	30.61	0.30
32	208	199.66	5.65	31.92	1.56
33	215	200.12	6.17	38.05	2.72
34	210	200.41	6.31	39.77	1.60
35	201	200.43	6.21	38.64	0.09

Table 4.4 Running Statistics of Data File IN.20.

N	R-R INTER	RUNNING MEAN	RUNNING RMS DEV	RUNNING VARIANCE	DEVIATION (α)
1	236	236.00			
2	242	239.00	4.24	18.00	
3	239	239.00	3.00	8.99	0.00
4	232	237.25	4.27	18.25	-2.33
5	223	234.40	7.37	54.30	-3.34
6	230	233.67	6.83	46.68	-0.60
7	231	233.29	6.32	39.92	-0.39
8	230	232.87	5.96	35.55	-0.52
9	225	232.00	6.16	38.00	-1.32
10	228	231.60	5.95	35.37	-0.65
11	244	232.73	6.77	45.81	2.08
12	249	234.08	7.98	63.70	2.40
13	235	234.15	7.65	58.47	0.11
14	235	234.21	7.35	54.02	0.11
15	244	234.87	7.52	56.55	1.33
16	243	235.37	7.54	56.92	1.08
17	231	235.12	7.38	54.49	-0.58
18	223	234.44	7.71	59.44	-1.64
19	225	233.95	7.80	60.82	-1.22
20	234	233.95	7.59	57.63	0.00
21	239	234.19	7.48	55.96	0.67
22	232	234.09	7.32	53.53	-0.29
23	232	234.00	7.16	51.28	-0.29
24	240	234.25	7.11	50.56	0.84
25	237	234.36	6.98	48.75	0.39
26	230	234.19	6.89	47.53	-0.62
27	215	233.48	7.70	59.32	-2.78
28	212	232.71	8.58	73.62	-2.79
29	213	232.03	9.19	84.40	-2.30
30	218	231.57	9.38	88.05	-1.53
31	221	231.23	9.42	88.73	-1.13
32	227	231.09	9.30	86.42	-0.45

Table 4.5 Running Statistics of Data File IN.30.

N	R-R INTER	RUNNING MEAN	RUNNING RMS DEV	RUNNING VARIANCE	DEVIATION (α)
1	101	101.00			
2	124	112.50	16.26	264.50	
3	99	108.00	13.89	193.00	-0.83
4	93	104.25	13.60	184.92	-1.08
5	88	101.00	13.84	191.50	-1.19
6	112	102.83	13.17	173.37	0.79
7	117	104.86	13.16	173.14	1.08
8	129	107.87	14.88	221.27	1.85
9	121	109.55	14.59	212.76	0.88
10	126	111.00	14.73	216.89	1.14
11	115	111.36	14.02	196.66	0.27
12	134	113.25	14.88	221.48	1.61
13	145	115.69	16.75	280.57	2.13
14	113	115.50	16.11	259.50	-0.16
15	100	114.47	16.03	256.98	-0.96
16	133	115.62	16.17	261.32	1.16
17	93	114.29	16.59	275.10	-1.40
18	136	115.50	16.88	285.09	1.51
19	103	114.84	16.66	277.47	-0.74
20	139	116.05	17.09	292.05	1.45
21	152	117.76	18.41	338.99	2.10
22	92	116.59	18.79	353.02	-1.40
23	85	115.22	19.50	380.36	-1.68
24	113	115.12	19.08	364.04	-0.11
25	87	114.00	19.51	380.50	-1.47
26	92	113.15	19.59	383.91	-1.13
27	154	114.52	20.48	419.41	1.88
28	112	114.43	20.10	404.11	-0.12
29	107	114.17	19.79	391.58	-0.37
30	96	113.57	19.75	389.08	-0.92
31	93	112.90	19.74	389.76	-1.04
32	170	114.69	21.89	479.06	2.69
33	120	114.85	21.56	464.94	0.24
34	109	114.68	21.26	451.87	-0.27
35	89	113.94	21.39	457.40	-1.21
36	120	114.11	21.10	445.36	0.28
37	131	114.57	20.99	440.71	0.80
38	107	114.37	20.74	430.31	-0.36
39	94	113.85	20.73	429.61	-0.98
40	93	113.32	20.72	429.47	-1.01
41	88	112.71	20.84	434.36	-1.22
42	150	113.60	21.37	456.88	1.79
43	108	113.47	21.14	446.72	-0.26

Table 4.6(a) Running Statistics of Data File CUNATFIB.

N	R-R INTER	RUNNING MEAN	RUNNING RMS DEV	RUNNING VARIANCE	DEVIATION (α)
44	137	114.00	21.19	448.91	1.11
45	96	113.60	21.12	445.92	-0.85
46	88	113.04	21.22	450.26	-1.21
47	100	112.77	21.07	444.10	-0.61
48	91	112.31	21.08	444.49	-1.03
49	104	112.14	20.90	436.67	-0.39
50	134	112.58	20.91	437.31	1.05
51	93	112.20	20.88	436.08	-0.94
52	119	112.33	20.70	428.42	0.33
53	100	112.09	20.57	423.05	-0.60
54	92	111.72	20.56	422.57	-0.98
55	83	111.20	20.73	429.71	-1.40
56	86	110.75	20.81	433.24	-1.22
57	85	110.30	20.91	437.14	-1.24
58	116	110.40	20.74	430.04	0.27
59	120	110.56	20.60	424.16	0.46
60	111	110.57	20.42	416.99	0.02
61	125	110.80	20.33	413.45	0.71
62	102	110.66	20.20	407.92	-0.43
63	116	110.75	20.05	401.80	0.26
64	96	110.52	19.97	398.82	-0.74
65	142	111.00	20.19	407.83	1.58
66	105	110.91	20.05	402.13	-0.30
67	97	110.70	19.97	398.89	-0.69
68	112	110.72	19.82	392.99	0.06
69	86	110.36	19.90	396.05	-1.25
70	88	110.04	19.94	397.48	-1.12
71	85	109.69	20.02	400.61	-1.26
72	86	109.36	20.07	402.78	-1.18
73	83	109.00	20.17	406.70	-1.31
74	92	108.77	20.13	405.03	-0.84
75	87	108.48	20.15	405.86	-1.08
76	88	108.21	20.15	405.95	-1.02
77	93	108.01	20.09	403.64	-0.75
78	115	108.10	19.98	399.01	0.35
79	88	107.85	19.98	399.02	-1.01
80	90	107.63	19.95	397.96	-0.89
81	139	108.01	20.13	405.13	1.57
82	113	108.07	20.01	400.44	0.25
83	112	108.12	19.89	395.72	0.20
84	79	107.77	20.03	401.06	-1.46
85	79	107.44	20.15	406.03	-1.44
86	117	107.55	20.06	402.33	0.47

Table 4.6(b) Running Statistics of Data File CUNATFIB.

N	R-R INTER	RUNNING MEAN	RUNNING RMS DEV	RUNNING VARIANCE	DEVIATION (α)
87	113	107.61	19.95	397.97	0.27
88	90	107.41	19.92	396.98	-0.88
89	95	107.25	19.87	394.77	-0.72
90	101	107.18	19.77	390.75	-0.51
91	83	106.91	19.82	392.81	-1.22
92	110	106.95	19.71	388.64	0.16
93	85	106.71	19.74	389.59	-1.11
94	79	106.41	19.84	393.56	-1.40
95	117	106.55	19.76	390.53	0.53
96	89	106.34	19.74	389.70	-0.89
97	98	106.26	19.65	386.29	-0.42

Table 4.6(c) Running Statistics of Data File CUNATFIB

N	R-R INTER	RUNNING MEAN	RUNNING RMS DEV	RUNNING VARIANCE	DEVIATION (α)
1	138	138.00			
2	90	114.00	33.94	1152.00	
3	213	147.00	61.99	3843.00	2.92
4	139	145.00	50.77	2578.00	-0.13
5	91	134.20	50.17	2516.70	-1.06
6	193	144.00	50.89	2589.60	1.17
7	138	143.14	46.51	2165.14	-0.12
8	87	136.12	47.41	2248.12	-1.21
9	212	144.56	51.06	2606.77	1.60
10	138	143.90	48.18	2321.43	-0.13
11	90	139.00	48.51	2353.39	-1.12
12	190	143.25	48.54	2356.19	1.05
13	137	142.77	46.51	2162.85	-0.13
14	93	139.21	46.62	2173.41	-1.07
15	206	143.67	48.12	2315.53	1.43
16	146	143.81	46.49	2161.50	0.05
17	87	140.47	47.08	2216.27	-1.22
18	215	144.61	48.93	2394.49	1.58
19	136	144.16	47.60	2265.36	-0.18
20	93	141.60	47.72	2276.99	-1.07
21	190	143.90	47.69	2274.69	1.01
22	144	143.91	46.54	2166.39	0.00
23	87	141.43	47.00	2208.71	-1.22
24	209	144.25	47.99	2302.90	1.44
25	134	143.84	47.02	2211.15	-0.21
26	96	142.00	47.02	2210.72	-1.02
27	205	144.33	47.67	2272.67	1.34
28	149	144.50	46.79	2189.30	0.09
29	88	142.55	47.13	2221.19	-1.21
30	205	144.63	47.69	2274.59	1.33
31	131	144.19	46.95	2204.76	-0.29
32	100	142.81	46.85	2194.67	-0.94
33	167	143.55	46.30	2143.81	0.52
34	125	143.00	45.71	2088.97	-0.40
35	124	142.46	45.14	2037.84	-0.42
36	117	141.75	44.69	1997.61	-0.56
37	162	142.30	44.20	1953.21	0.45
38	170	143.03	43.83	1920.63	0.63
39	174	143.82	43.53	1894.68	0.71
40	159	144.20	43.03	1851.86	0.35
41	87	142.80	43.42	1885.57	-1.33

Table 4.7 Running Statistics of Data File HUANPVCS.

N	R-R INTER	RUNNING MEAN	RUNNING RMS DEV	RUNNING VARIANCE	DEVIATION (α)
1	138	138.00			
2	90	114.00	33.94	1152.00	
3	213	147.00	61.99	3843.00	2.92
4	139	145.00	50.77	2578.00	-0.13
5	91	134.20	50.17	2516.70	-1.06
6	193	144.00	50.89	2589.60	1.17
7	138	143.14	46.51	2163.14	-0.12
8	87	136.12	47.41	2248.12	-1.21
9	212	144.56	51.06	2606.77	1.60
10	138	143.90	48.18	2321.45	-0.13
11	90	139.00	48.51	2353.39	-1.12
12	190	143.25	48.54	2356.19	1.05
13	137	142.77	46.51	2162.85	-0.13
14	93	139.21	46.62	2173.41	-1.07
15	206	143.67	48.12	2315.53	1.43
16	146	143.81	46.49	2161.50	0.05
17	87	140.47	47.08	2216.27	-1.22
18	215	144.61	48.93	2394.49	1.58
19	136	144.16	47.60	2265.56	-0.18
20	93	141.60	47.72	2276.99	-1.07
21	190	143.90	47.69	2274.69	1.01
22	144	143.91	46.54	2166.59	0.00
23	87	141.43	47.00	2208.71	-1.22
24	209	144.25	47.99	2302.90	1.44
25	134	143.84	47.02	2211.15	-0.21
26	96	142.00	47.02	2210.72	-1.22
27	205	144.33	47.67	2272.67	1.34
28	149	144.50	46.79	2189.50	0.09
29	88	142.55	47.13	2221.19	-1.21
30	205	144.63	47.69	2274.59	1.33
31	131	144.19	46.95	2204.76	-0.29

Table 4.8 Running Statistics of Data File HUANTRI.

N	R-R INTER	RUNNING MEAN	RUNNING RMS DEV	RUNNING VARIANCE	DEVIATION (α)
1	133	133,00			
2	261	197,00	90,51	8192,00	
3	128	174,00	75,39	5683,00	-0,76
4	275	199,25	79,62	6338,92	1,34
5	132	185,80	75,22	5658,70	-0,84
6	274	200,50	76,31	5823,51	1,17
7	133	190,86	74,19	5505,81	-0,88
8	266	200,25	73,64	5423,36	1,01
9	132	192,67	72,55	5263,00	-0,93
10	263	199,70	71,92	5172,89	0,97
11	127	193,09	71,67	5136,08	-1,01
12	291	201,25	73,95	5468,00	1,37
13	133	196,00	73,28	5370,66	-0,92
14	292	202,86	74,94	5615,81	1,31
15	136	198,40	74,25	5512,67	-0,89
16	281	203,56	74,64	5571,58	1,11
17	139	199,76	73,95	5468,57	-0,86
18	277	204,06	74,02	5478,29	1,04
19	133	200,32	73,75	5439,65	-0,96
20	282	204,40	74,07	5486,97	1,11
21	134	201,05	73,81	5448,63	-0,95
22	275	204,32	73,65	5424,51	0,97
23	138	201,43	73,27	5369,15	-0,90
24	276	204,54	73,26	5367,39	1,02
25	129	201,52	73,29	5371,99	-1,03
26	264	203,92	72,85	5307,27	0,85
27	131	201,22	72,80	5300,08	-1,00
28	257	203,21	72,21	5214,90	0,77
29	134	200,83	72,07	5193,84	-0,96
30	262	202,87	71,69	5139,50	0,85
31	124	200,32	71,89	5168,82	-1,10
32	276	202,69	71,98	5181,05	1,05
33	129	200,45	72,00	5183,68	-1,02
34	278	202,74	72,13	5205,46	1,08
35	136	200,83	71,96	5177,64	-0,93
36	269	202,72	71,82	5158,82	0,95
37	138	200,97	71,62	5128,75	-0,90
38	266	202,68	71,42	5101,42	0,91
39	141	201,10	71,17	5064,72	-0,86

Table 4.9 Running Statistics of Data File #503.

N	R-R INTER	RUNNING MEAN	RUNNING RMS DEV	RUNNING VARIANCE	DEVIATION (α)
1	154	154.00			
2	152	153.00	1.41	2.00	
3	159	155.00	3.61	13.00	4.24
4	106	142.75	24.68	608.92	-13.59
5	230	160.20	44.49	1979.20	3.54
6	162	160.50	39.80	1583.90	0.04
7	158	160.14	36.34	1320.81	-0.06
8	154	159.37	33.72	1136.84	-0.17
9	147	158.00	31.81	1011.75	-0.37
10	151	157.30	30.07	904.23	-0.22
11	151	156.73	28.59	817.40	-0.21
12	154	156.50	27.27	743.72	-0.09
13	152	156.15	26.14	683.31	-0.17
14	159	156.36	25.13	631.35	0.11
15	165	156.93	24.31	591.21	0.34
16	163	157.31	23.54	554.10	0.25
17	157	157.29	22.79	519.47	-0.01
18	160	157.44	22.12	489.53	0.12
19	105	154.68	24.64	606.89	-2.37
20	229	158.40	29.17	851.10	3.02
21	155	158.24	28.44	809.10	-0.12
22	162	158.41	27.77	771.23	0.15
23	154	158.22	27.15	737.01	-0.16
24	150	157.87	26.60	707.79	-0.30
25	154	157.72	26.06	678.89	-0.15
26	153	157.54	25.55	652.58	-0.18
27	148	157.19	25.12	630.85	-0.37
28	153	157.04	24.66	608.11	-0.17
29	101	155.10	26.36	694.67	-2.27
30	217	157.17	28.26	798.44	2.35
31	150	156.94	27.81	773.47	-0.25
32	154	156.84	27.36	748.79	-0.11
33	149	156.61	26.97	727.25	-0.29
34	150	156.41	26.58	706.51	-0.24
35	141	155.97	26.32	692.50	-0.58
36	145	155.67	26.00	676.05	-0.42
37	152	155.57	25.64	657.65	-0.14
38	103	154.18	26.69	712.61	-2.05
39	214	155.72	28.03	785.58	2.24
40	151	155.60	27.68	766.00	-0.17
41	151	155.49	27.34	747.36	-0.17
42	157	155.52	27.00	729.20	0.06
43	152	155.44	26.69	712.11	-0.15

Table 4.10(a) Running Statistics of Data File HARNETPVCS.

N	R-R INTER	RUNNING MEAN	RUNNING RMS DEV	RUNNING VARIANCE	DEVIATION (α)
44	157	155.46	26.37	695.58	0.06
45	158	155.53	26.08	679.94	0.09
46	149	155.39	25.80	665.78	-0.25
47	162	155.53	25.54	652.23	0.26
48	158	155.58	25.27	638.44	0.09
49	165	155.78	25.04	626.99	0.37
50	176	156.18	24.95	622.36	0.81
51	175	156.55	24.84	616.84	0.75
52	167	156.75	24.63	606.87	0.42
53	165	156.91	24.42	596.48	0.33

Table 4.10(b) Running Statistics of Data File HARNETPVCS.

N	R-R INTER	RUNNING MEAN	RUNNING RMS DEV	RUNNING VARIANCE	DEVIATION (α)
1	184	184.00			
2	103	143.50	57.28	3280.50	
3	293	193.33	95.34	9090.33	2.61
4	190	192.50	77.87	6063.00	-0.03
5	230	200.00	69.49	4828.50	0.48
6	245	207.50	64.81	4200.31	0.65
7	239	212.00	60.35	3642.01	0.49
8	244	215.50	56.74	3219.71	0.46
9	211	215.00	53.10	2819.50	-0.07
10	199	213.40	50.32	2531.83	-0.30
11	215	213.55	47.74	2278.86	0.03
12	206	212.92	45.57	2076.43	-0.16
13	197	211.69	43.85	1922.90	-0.35
14	207	211.36	42.15	1776.55	-0.11
15	208	211.13	40.65	1650.42	-0.08
16	203	210.62	39.30	1544.52	-0.20
17	226	211.53	38.23	1461.89	0.59
18	211	211.50	37.09	1375.92	-0.01
19	217	211.79	36.07	1301.06	0.15
20	222	212.30	35.18	1237.80	0.28
21	203	211.86	34.35	1180.02	-0.26
22	133	208.27	37.50	1406.51	-2.30
23	276	211.22	39.27	1541.99	1.81
24	184	210.08	38.81	1505.84	-0.69
25	191	209.32	38.18	1457.63	-0.49
26	182	208.27	37.79	1428.05	-0.72
27	175	207.04	37.60	1414.10	-0.88
28	117	203.82	40.64	1651.27	-2.39
29	255	205.59	41.02	1682.61	1.26
30	133	204.83	40.52	1641.60	-0.55
31	181	204.06	40.06	1605.19	-0.59
32	197	203.84	39.43	1554.97	-0.18
33	214	204.15	38.85	1509.49	0.26
34	200	204.03	38.27	1464.26	-0.11
35	187	203.54	37.81	1429.46	-0.45
36	187	203.08	37.37	1396.23	-0.44
37	106	200.46	40.15	1612.20	-2.60
38	274	202.39	41.36	1710.96	1.83
39	175	201.69	41.05	1685.14	-0.66
40	174	201.00	40.76	1661.12	-0.67

Table 4.11 Running Statistics of Data File SPOONPAC.

N	R-R INTER	RUNNING MEAN	RUNNING RMS DEV	RUNNING VARIANCE	DEVIATION (α)
1	163	163.00			
2	168	165.50	3.54	12.50	
3	168	166.33	2.89	8.33	0.71
4	165	166.00	2.45	6.00	-0.46
5	168	166.40	2.30	5.31	0.82
6	171	167.17	2.79	7.77	2.00
7	170	167.57	2.76	7.62	1.02
8	127	162.50	14.57	212.29	-14.70
9	216	168.44	22.44	503.77	3.67
10	167	168.30	21.17	448.01	-0.06
11	170	168.45	20.09	403.47	0.08
12	169	168.50	19.15	366.81	0.03
13	164	168.15	18.38	337.82	-0.23
14	167	168.07	17.66	311.92	-0.06
15	168	168.07	17.02	289.64	-0.00
16	176	168.56	16.56	274.26	0.47
17	179	169.18	16.23	263.53	0.63
18	178	169.67	15.89	252.35	0.54
19	175	169.95	15.49	239.85	0.54
20	182	170.55	15.31	234.47	0.78
21	170	170.52	14.92	222.75	-0.04
22	166	170.32	14.60	213.10	-0.30
23	171	170.35	14.26	203.42	0.05
24	168	170.25	13.96	194.82	-0.16
25	170	170.24	13.66	186.68	-0.02
26	169	170.19	13.39	179.28	-0.09
27	166	170.04	13.15	173.04	-0.31
28	166	169.89	12.93	167.21	-0.31
29	167	169.79	12.71	161.53	-0.22
30	162	169.53	12.57	157.98	-0.61
31	162	169.29	12.43	154.54	-0.60
32	171	169.34	12.23	149.65	0.14
33	174	169.48	12.07	145.63	0.38
34	159	169.18	12.02	144.45	-0.87
35	205	170.20	13.50	176.85	2.98
36	174	170.31	13.12	172.21	0.29
37	138	169.43	13.99	195.64	-2.46
38	194	170.08	14.36	206.24	1.76
39	154	169.67	14.40	207.42	-1.12
40	156	169.33	14.38	206.77	-0.95
41	158	169.05	14.31	204.74	-0.79
42	171	169.10	14.14	199.83	0.14
43	169	169.09	13.97	195.07	-0.00

Table 4.12(a) Running Statistics of Data File BLOOM.

N	R-R INTER	RUNNING MEAN	RUNNING RMS DEV	RUNNING VARIANCE	DEVIATION (α)
44	147	168.59	14.20	201.60	-1.58
45	213	169.58	15.52	240.87	3.13
46	173	169.65	15.36	235.78	0.22
47	122	168.64	16.70	278.97	-3.10

Table 4.12(b) Running Statistics of Data File BLOOM.

N	R-R INTER	RUNNING MEAN	RUNNING RMS DEV	RUNNING VARIANCE	DEVIATION (α)
1	181	181.00			
2	182	181.50	0.71	0.50	
3	187	183.33	3.21	10.33	7.78
4	188	184.50	3.51	12.33	1.45
5	185	184.60	3.05	9.30	0.14
6	180	183.83	3.31	10.97	-1.51
7	183	183.71	3.04	9.24	-0.25
8	185	183.88	2.85	8.12	0.42
9	187	184.22	2.86	8.19	1.10
10	185	184.30	2.71	7.34	0.27
11	180	183.91	2.88	8.29	-1.59
12	183	183.83	2.76	7.60	-0.32
13	186	184.00	2.71	7.33	0.79
14	186	184.14	2.66	7.06	0.74
15	180	183.87	2.77	7.69	-1.56
16	174	183.25	3.64	13.27	-3.56
17	173	182.65	4.31	18.62	-2.81
18	176	182.28	4.47	19.98	-1.54
19	180	182.16	4.37	19.14	-0.51
20	176	181.85	4.48	20.03	-1.41
21	173	181.43	4.77	22.75	-1.98
22	177	181.23	4.75	22.57	-0.93
23	176	181.00	4.77	22.72	-1.10
24	177	180.83	4.74	22.42	-0.84
25	171	180.44	5.03	25.33	-2.08
26	165	179.85	5.79	33.49	-3.07
27	168	179.41	6.11	37.39	-2.05
28	170	179.07	6.26	39.19	-1.54
29	176	178.97	6.17	38.10	-0.49
30	172	178.73	6.20	38.41	-1.13
31	166	178.32	6.51	42.36	-2.05
32	173	178.16	6.47	41.88	-0.82
33	174	178.03	6.41	41.08	-0.64
34	177	178.00	6.31	39.88	-0.16
35	172	177.85	6.30	39.71	-0.95
36	166	177.50	6.52	42.48	-1.88
37	170	177.30	6.54	42.82	-1.15
38	172	177.16	6.51	42.42	-0.81
39	173	177.05	6.46	41.74	-0.64
40	173	176.95	6.41	41.08	-0.63
41	171	176.80	6.40	40.91	-0.93
42	171	176.67	6.38	40.72	-0.91
43	236	178.05	11.05	121.61	9.30

Table 4.13(a) Running Statistics of Data File IN.5+30.

N	R-R INTER	RUNNING MEAN	RUNNING RMS DEV	RUNNING VARIANCE	DEVIATION (α)
44	242	179.50	14.55	211.72	5.80
45	239	180.82	16.90	285.61	4.09
46	232	181.95	18.34	336.20	3.03
47	223	182.81	19.10	364.76	2.24
48	230	183.79	20.08	403.37	2.47
49	231	184.76	20.99	440.48	2.35
50	230	185.66	21.74	472.42	2.16
51	225	186.43	22.21	493.31	1.81
52	228	187.25	22.74	516.89	1.87
53	244	188.30	23.83	567.75	2.50
54	249	189.43	25.01	625.29	2.55
55	235	190.25	25.52	651.45	1.82
56	235	191.05	25.99	675.35	1.75
57	244	191.98	26.69	712.47	2.04
58	245	192.86	27.29	744.88	1.91
59	231	193.51	27.51	756.64	1.40
60	225	194.00	27.54	758.34	1.07
61	225	194.51	27.59	761.47	1.13
62	234	195.15	27.82	774.14	1.43
63	239	195.84	28.15	792.17	1.58
64	232	196.41	28.28	800.02	1.28
65	232	196.95	28.41	807.03	1.26
66	240	197.61	28.68	822.69	1.52
67	237	198.19	28.87	833.58	1.37
68	230	198.66	28.91	835.81	1.10
69	215	198.90	28.76	827.38	0.57
70	212	199.09	28.60	817.89	0.46
71	213	199.28	28.44	808.90	0.49
72	218	199.54	28.33	802.38	0.66
73	221	199.84	28.24	797.53	0.76
74	227	200.20	28.22	796.56	0.96

Table 4.13(b) Running Statistics of Data File IN.5+30.

N	R-R INTER	RUNNING MEAN	RUNNING RMS DEV	RUNNING VARIANCE	DEVIATION (α)
1	171	171.00			
2	180	175.50	6.36	40.50	
3	174	175.00	4.58	21.00	-0.24
4	175	175.00	3.74	14.00	0.00
5	186	177.20	5.89	34.70	2.94
6	202	181.33	11.41	130.27	4.21
7	203	184.43	13.25	175.62	1.90
8	216	188.37	16.59	275.12	2.38
9	233	193.33	21.49	462.00	2.69
10	256	199.60	28.34	805.39	2.92
11	302	208.91	40.94	1676.28	3.61
12	299	216.42	46.91	2200.25	2.20
13	323	224.62	53.77	2890.75	2.27
14	333	232.36	59.22	3507.48	2.02
15	337	239.33	63.14	3986.94	1.77

Table 4.14 Running Statistics of Data File #476.

N	R-R INTER	RUNNING MEAN	RUNNING RMS DEV	RUNNING VARIANCE	DEVIATION (α)
1	211	211,00			
2	192	201,50	13,44	180,50	
3	203	202,00	9,54	91,00	0.11
4	344	237,50	71,43	5101,67	14.89
5	197	229,40	64,45	4154,30	-0.57
6	190	222,83	59,85	3582,18	-0.61
7	198	219,29	55,44	3073,25	-0.41
8	328	232,87	64,12	4111,55	1.96
9	213	230,67	60,34	3641,49	-0.31
10	209	228,50	57,30	3285,83	-0.36
11	366	241,00	68,37	4674,19	2.40
12	215	238,83	65,62	4305,60	-0.38
13	209	236,54	63,37	4015,27	-0.45

Table 4.15 Running Statistics of Data File #463.

N	R-R INTER	RUNNING MEAN	RUNNING RMS DEV	RUNNING VARIANCE	DEVIATION (α)
1	247	247.00			
2	238	242.50	6.36	40.50	
3	110	198.33	76.63	5872.33	-20.82
4	137	183.00	69.68	4855.33	-0.80
5	244	195.20	66.22	4385.70	0.88
6	258	205.67	64.54	4165.87	0.95
7	259	213.29	62.27	3877.90	0.83
8	254	218.37	59.42	3531.12	0.65

Table 4.16 Running Statistics of Data File #492-1.

N	R-R INTER	RUNNING MEAN	RUNNING RMS DEV	RUNNING VARIANCE	DEVIATION (α)
5	185	184.60	3.05	9.30	
6	180	184.40	3.36	11.30	-1.51
7	183	184.60	3.21	10.30	-0.42
8	185	184.20	2.95	8.70	0.12
9	187	184.00	2.64	6.99	0.95
10	185	184.00	2.64	6.99	0.38
11	180	184.00	2.64	6.99	-1.51
12	183	184.00	2.64	6.99	-0.38
13	186	184.20	2.77	7.70	0.76
14	186	184.00	2.55	6.49	0.65
15	180	183.00	3.00	8.99	-1.57
16	174	181.80	5.02	25.19	-3.00
17	173	179.80	6.26	39.19	-1.75
18	176	177.80	5.51	28.19	-0.61
19	180	176.60	3.28	10.79	0.41
20	176	175.80	2.68	7.19	-0.18
21	173	175.60	2.88	8.29	-1.04
22	177	176.40	2.51	6.29	0.49
23	176	176.40	2.51	6.29	-0.16
24	177	175.80	1.64	2.69	0.24
25	171	174.80	2.68	7.19	-2.93
26	165	173.20	5.21	27.19	-3.65
27	168	171.40	5.13	26.30	-1.00
28	170	170.20	4.44	19.70	-0.27
29	176	170.00	4.06	16.49	1.31
30	172	170.20	4.15	17.20	0.49
31	166	170.40	3.85	14.80	-1.01
32	173	171.40	3.71	13.80	0.68
33	174	172.20	3.77	14.19	0.70
34	177	172.40	4.04	16.30	1.27
35	172	172.40	4.04	16.30	-0.09
36	166	172.40	4.04	16.30	-1.59
37	170	171.80	4.15	17.20	-0.59
38	172	171.40	3.97	15.80	0.05
39	173	170.60	2.79	7.80	0.40
40	173	170.80	2.95	8.70	0.86
41	171	171.80	1.30	1.70	0.06
42	171	172.00	1.00	1.00	-0.61

Table 4.17 Statistics of Sliding Window Width 5 for Data File IN.5.

N	R-R INTER	RUNNING MEAN	RUNNING RMS DEV	RUNNING VARIANCE	DEVIATION (α)
5	198	200.40	5.03	25.30	
6	205	201.60	5.32	28.30	0.91
7	203	201.00	4.85	23.51	0.26
8	194	198.80	5.07	25.71	-1.44
9	194	198.80	5.07	25.71	-0.95
10	200	199.20	5.07	25.71	0.24
11	200	198.20	4.03	16.21	0.16
12	192	196.00	3.74	14.01	-1.54
13	193	195.80	3.90	15.21	-0.80
14	199	196.80	3.96	15.71	0.82
15	196	196.00	3.54	12.51	-0.20
16	185	193.00	5.24	27.51	-3.11
17	190	192.60	5.41	29.30	-0.57
18	200	194.00	6.36	40.51	1.37
19	203	194.80	7.33	53.71	1.41
20	196	194.80	7.33	53.71	0.16
21	202	198.20	5.31	28.21	0.98
22	208	201.80	4.38	19.21	1.85
23	204	202.60	4.34	18.81	0.50
24	199	201.80	4.60	21.21	-0.83
25	205	203.60	3.36	11.30	0.69
26	204	204.00	3.24	10.51	0.12
27	195	201.40	4.28	18.31	-2.78
28	198	200.20	4.21	17.71	-0.79
29	206	201.60	4.83	23.31	1.38
30	207	202.00	5.25	27.52	1.12
31	201	201.40	5.13	26.32	-0.19
32	208	204.00	4.30	18.52	1.29
33	215	207.40	5.03	25.32	2.56
34	210	208.20	5.07	25.72	0.52
35	201	207.00	6.04	36.51	-1.42

Table 4.18 Statistics of Sliding Window Width 5 for Data File IN.20.

N	R-R INTER	RUNNING MEAN	RUNNING RMS DEV	RUNNING VARIANCE	DEVIATION (α)
5	223	234.40	7.37	54.30	
6	230	233.20	7.53	56.70	-0.60
7	231	231.00	5.70	32.50	-0.29
8	230	229.20	3.56	12.70	-0.18
9	225	227.80	3.56	12.70	-1.18
10	228	228.80	2.59	5.70	0.06
11	244	231.60	7.30	53.30	6.37
12	249	235.20	10.62	112.69	2.38
13	235	236.20	10.23	104.69	-0.02
14	235	238.20	8.29	68.69	-0.12
15	244	241.40	6.19	38.29	0.70
16	243	241.20	6.10	37.19	0.26
17	231	237.60	5.64	31.80	-1.67
18	223	235.20	8.73	76.19	-2.59
19	225	233.20	9.86	97.19	-1.17
20	234	231.20	7.95	63.19	0.08
21	239	230.40	6.54	42.79	0.98
22	232	230.60	6.58	43.30	0.24
23	232	232.40	5.03	25.29	0.21
24	240	235.40	3.85	14.79	1.51
25	237	236.00	3.81	14.49	0.42
26	230	234.20	4.15	17.20	-1.58
27	215	230.80	9.68	93.69	-4.63
28	212	226.80	12.72	161.69	-1.94
29	213	221.40	11.37	129.29	-1.09
30	218	217.60	7.30	53.29	-0.30
31	221	215.80	3.70	13.69	0.47
32	227	218.20	6.14	37.70	3.03

Table 4.19 Statistics of Sliding Window Width 5 for Data File IN.30.

N	R-R INTER	RUNNING MEAN	RUNNING RMS DEV	RUNNING VARIANCE	DEVIATION (α)
5	88	101,00	13,84	191,50	
6	112	103,20	14,69	215,70	0,79
7	117	101,80	12,36	152,70	0,94
8	129	107,80	17,05	290,70	2,20
9	121	113,40	15,50	240,30	0,77
10	126	121,00	6,82	46,49	0,81
11	115	121,60	5,90	34,79	-0,88
12	134	125,00	7,31	53,49	2,10
13	145	128,20	11,69	136,69	2,73
14	113	126,60	13,35	178,30	-1,30
15	100	121,40	17,92	321,30	-1,99
16	133	125,00	18,12	328,50	0,65
17	93	116,80	21,91	480,20	-1,77
18	136	115,00	19,22	369,50	0,88
19	103	113,00	19,99	399,50	-0,62
20	139	120,80	21,22	450,20	1,30
21	152	124,60	25,26	638,29	1,47
22	92	124,40	25,58	654,29	-1,29
23	85	114,20	29,64	878,69	-1,54
24	113	116,20	29,03	842,69	-0,04
25	87	105,80	28,12	790,70	-1,01
26	92	93,80	11,17	124,70	-0,49
27	150	105,40	27,30	745,29	5,03
28	112	110,80	24,81	615,69	0,24
29	107	109,60	24,83	616,29	-0,15
30	96	111,40	23,04	530,79	-0,55
31	93	111,60	22,83	521,29	-0,80
32	170	115,60	31,39	985,29	2,56
33	120	117,20	31,36	983,69	0,14
34	109	117,60	31,21	974,29	-0,26
35	89	116,20	32,55	1059,69	-0,92
36	120	121,60	29,87	892,29	0,12
37	131	113,80	15,90	252,69	0,31
38	107	111,20	15,69	246,19	-0,43
39	94	108,20	17,54	307,69	-1,10
40	93	109,00	16,51	272,49	-0,87
41	88	102,60	17,36	301,29	-1,27
42	150	106,40	25,36	643,29	2,73
43	108	106,60	25,37	643,79	0,06

Table 4.20(a) Statistics of Sliding Window Width 5 for Data File CUNATFIB.

N	R-R INTER	RUNNING MEAN	RUNNING RMS DEV	RUNNING VARIANCE	DEVIATION (α)
44	137	115.20	27.25	742.69	1.20
45	96	115.80	26.67	711.19	-0.70
46	88	115.80	26.67	711.19	-1.04
47	100	105.80	18.87	356.19	-0.59
48	91	102.40	19.88	395.29	-0.78
49	104	95.80	6.50	42.19	0.08
50	134	103.40	18.30	334.78	5.88
51	93	104.40	17.36	301.28	-0.57
52	119	108.20	18.21	331.68	0.84
53	100	110.00	16.45	270.48	-0.45
54	92	107.60	18.51	335.28	-1.09
55	83	97.40	13.50	182.28	-1.34
56	86	96.00	14.40	207.48	-0.84
57	85	89.20	6.91	47.68	-0.76
58	116	92.40	13.61	185.28	3.88
59	120	98.00	18.54	356.48	2.05
60	111	103.60	16.83	283.28	0.71
61	125	111.40	15.63	244.27	1.27
62	102	114.80	8.81	77.68	-0.60
63	116	114.80	8.81	77.68	0.14
64	96	110.00	11.42	130.48	-2.13
65	142	116.20	18.39	338.18	2.80
66	105	112.20	18.17	330.18	-0.61
67	97	111.20	18.99	360.68	-0.84
68	112	110.40	18.82	354.28	0.04
69	86	108.40	21.13	446.28	-1.30
70	88	97.60	11.06	122.29	-0.97
71	85	93.60	11.33	128.29	-1.14
72	86	91.40	11.57	133.78	-0.67
73	83	85.60	1.81	3.29	-0.73
74	92	86.80	3.42	11.69	3.53
75	87	86.60	3.36	11.29	0.06
76	88	87.20	3.27	10.69	0.42
77	93	88.60	4.04	16.29	1.77
78	115	95.00	11.47	131.49	6.54
79	88	94.20	11.86	140.69	-0.61
80	90	94.80	11.48	131.69	-0.35
81	139	105.00	21.87	478.48	3.85
82	113	109.00	20.94	438.48	0.37
83	112	108.40	20.77	431.29	0.14
84	79	106.60	23.22	539.29	-1.42
85	79	104.40	25.59	654.78	-1.19
86	117	100.00	19.26	370.99	0.49

Table 4.20(b) Statistics of Sliding Window Width 5 for Data File CUNATFIB.

N	R-R INTER	RUNNING MEAN	RUNNING RMS DEV	RUNNING VARIANCE	DEVIATION (α)
87	113	100,00	19,26	370,99	0,67
88	90	95,60	18,32	335,78	-0,52
89	93	98,40	16,09	258,78	-0,14
90	101	102,80	11,92	142,19	0,16
91	83	96,00	11,49	131,99	-1,66
92	110	95,40	10,41	108,29	1,22
93	85	94,40	11,26	126,79	-1,00
94	79	91,60	13,26	175,79	-1,37
95	117	94,80	17,38	302,19	1,92
96	89	96,00	16,55	273,99	-0,33
97	98	93,60	14,79	218,79	0,12

Table 4.20(c) Statistics of Sliding Window Width 5 for Data File CUNATFIB.

N	R-R INTER	RUNNING MEAN	RUNNING RMS DEV	RUNNING VARIANCE	DEVIATION (α)
5	91	134,20	50,17	2516,70	
6	193	145,20	56,80	3226,20	1,17
7	138	154,80	48,60	2362,20	-0,13
8	87	129,60	43,25	1870,80	-1,39
9	212	144,20	57,27	3279,70	1,91
10	138	153,60	49,71	2471,50	-0,11
11	90	135,00	50,64	2564,00	-1,28
12	190	143,40	56,88	3234,81	1,13
13	137	153,40	48,22	2324,81	-0,11
14	93	129,60	40,87	1670,51	-1,25
15	206	143,20	53,67	2880,70	1,87
16	146	154,40	44,93	2018,30	0,05
17	87	133,80	48,03	2306,71	-1,50
18	215	149,40	60,40	3648,30	1,69
19	136	158,00	52,97	2805,50	-0,22
20	93	135,40	51,45	2647,30	-1,23
21	190	144,20	57,16	3267,70	1,06
22	144	155,60	47,83	2287,50	-0,00
23	87	130,00	41,98	1762,50	-1,43
24	209	144,60	55,20	3047,30	1,88
25	134	152,80	48,23	2325,70	-0,19
26	96	134,00	48,42	2344,50	-1,18
27	205	146,20	58,26	3393,70	1,47
28	149	158,60	48,24	2327,51	0,05
29	88	134,40	46,97	2206,31	-1,46
30	205	148,60	56,57	3200,31	1,50
31	131	155,60	50,25	2524,81	-0,31
32	100	134,60	46,22	2136,31	-1,11
33	167	138,20	48,28	2330,71	0,70
34	125	145,60	40,94	1675,81	-0,27
35	124	129,40	24,13	582,51	-0,53
36	117	126,60	24,70	610,31	-0,51
37	162	139,00	23,55	554,51	1,43
38	170	139,60	24,46	598,31	1,32
39	174	149,40	26,85	720,81	1,41
40	159	156,40	22,85	521,31	0,36
41	87	150,40	35,95	1292,31	-3,04

Table 4.21 Statistics ofSliding Window Width 5 for Data File HUANPVCS.

N	R-R INTER	RUNNING MEAN	RUNNING RMS DEV	RUNNING VARIANCE	DEVIATION (α)
5	91	134.20	50.17	2516.70	
6	193	145.20	56.80	3226.20	1.17
7	138	154.80	48.60	2362.20	-0.13
8	87	129.60	43.25	1870.80	-1.39
9	212	144.20	57.27	3279.70	1.91
10	138	153.60	49.71	2471.30	-0.11
11	90	153.00	50.64	2564.00	-1.28
12	190	143.40	56.88	3234.81	1.13
13	137	153.40	48.22	2324.81	-0.11
14	93	129.60	40.87	1670.31	-1.25
15	206	143.20	53.67	2880.70	1.87
16	146	154.40	44.93	2018.50	0.05
17	87	133.80	48.03	2306.71	-1.50
18	215	149.40	60.40	3648.30	1.69
19	136	158.00	52.97	2805.50	-0.22
20	93	135.40	51.45	2647.30	-1.23
21	190	144.20	57.16	3267.70	1.06
22	144	155.60	47.83	2287.30	-0.00
23	87	130.00	41.98	1762.50	-1.43
24	209	144.60	55.20	3047.30	1.88
25	134	152.80	48.23	2325.70	-0.19
26	96	134.00	48.42	2344.50	-1.18
27	205	146.20	58.26	3393.70	1.47
28	149	158.60	48.24	2327.31	0.05
29	88	134.40	46.97	2206.31	-1.46
30	205	148.60	56.57	3200.31	1.50
31	131	155.60	50.25	2524.81	-0.31

Table 4.22 Statistics of Sliding Window Width 5 for Data File HUANTRI.

N	R-R INTER	RUNNING MEAN	RUNNING RMS DEV	RUNNING VARIANCE	DEVIATION (α)
5	132	185.80	75.22	5658.70	
6	274	214.00	76.89	5912.50	1.17
7	133	188.40	78.62	6181.30	-1.05
8	266	216.00	76.31	5822.50	0.99
9	132	187.40	75.46	5695.80	-1.10
10	263	213.60	74.14	5497.50	1.00
11	127	184.20	73.55	5379.70	-1.17
12	291	215.80	79.55	6327.70	1.46
13	133	189.20	80.79	6527.20	-1.04
14	292	221.20	84.09	7071.20	1.27
15	136	195.80	87.42	7642.70	-1.01
16	281	226.60	84.19	7088.50	0.97
17	139	196.20	82.55	6814.69	-1.04
18	277	225.00	80.07	6411.49	0.98
19	135	193.20	78.37	6141.19	-1.15
20	282	222.40	78.92	6228.80	1.13
21	134	195.00	79.02	6243.49	-1.12
22	273	219.80	78.85	6216.69	1.01
23	138	192.00	78.14	6105.50	-1.04
24	276	220.60	77.31	5976.79	1.08
25	129	190.00	77.21	5961.49	-1.18
26	264	216.00	75.51	5701.49	0.96
27	131	187.60	75.41	5687.29	-1.13
28	257	211.40	74.62	5568.29	0.92
29	134	183.00	70.81	5014.48	-1.04
30	262	209.60	70.44	4961.28	1.12
31	124	181.60	71.23	5073.28	-1.22
32	276	210.60	74.90	5609.78	1.33
33	129	185.00	76.92	5916.98	-1.09
34	278	213.80	79.95	6392.18	1.21
35	136	188.60	80.81	6530.78	-0.97
36	269	217.60	77.80	6052.28	0.99
37	138	190.00	76.36	5831.48	-1.02
38	266	217.40	73.55	5406.79	1.00
39	141	190.00	70.78	5009.48	-1.04

Table 4.23 Statistics of Sliding Window Width 5 for Data File #503.

N	R-R INTER	RUNNING MEAN	RUNNING RMS DEV	RUNNING VARIANCE	DEVIATION (α)
5	230	160,20	44,49	1979,20	
6	162	161,80	44,35	1967,20	0,04
7	158	163,00	44,10	1945,00	-0,08
8	154	162,00	44,27	1960,00	-0,20
9	147	170,20	33,89	1148,20	-0,34
10	151	154,40	5,86	34,30	-0,57
11	151	152,20	4,09	16,70	-0,58
12	154	151,40	2,88	8,30	0,44
13	152	151,00	2,55	6,50	0,21
14	159	153,40	3,36	11,30	3,14
15	165	156,20	5,81	33,70	3,45
16	163	158,60	5,59	31,30	1,17
17	157	159,20	5,12	26,20	-0,29
18	160	160,80	3,19	10,20	0,16
19	105	150,00	25,34	642,00	-17,47
20	229	162,80	44,06	1941,20	3,12
21	155	161,20	44,20	1953,20	-0,18
22	162	162,20	44,13	1947,70	0,02
23	154	161,00	44,29	1961,50	-0,19
24	150	170,00	33,26	1106,50	-0,25
25	154	155,00	4,36	19,00	-0,48
26	153	154,60	4,45	19,80	-0,46
27	148	151,80	2,68	7,20	-1,48
28	153	151,60	2,51	6,30	0,45
29	101	141,80	22,93	525,70	-20,16
30	217	154,40	41,28	1703,80	3,28
31	150	153,80	41,32	1707,70	-0,11
32	154	155,00	41,20	1697,50	0,00
33	149	154,20	41,29	1704,70	-0,15
34	150	164,00	29,69	881,50	-0,10
35	141	148,80	4,76	22,70	-0,77
36	145	147,80	4,97	24,70	-0,80
37	152	147,40	4,39	19,30	0,85
38	103	138,20	20,14	405,70	-10,11
39	214	151,00	40,03	1602,49	3,76
40	151	153,00	39,65	1572,49	-0,00
41	151	154,20	39,44	1555,69	-0,05
42	157	155,20	39,44	1555,19	0,07
43	152	165,00	27,50	756,49	-0,08

Table 4.24(a) Statistics of Sliding Window Width 5 for Data File HARNETPVCS.

N	R-R INTER	RUNNING MEAN	RUNNING RMS DEV	RUNNING VARIANCE	DEVIATION (α)
44	157	153.60	3.13	9.79	-0.29
45	158	155.00	3.24	10.50	1.41
46	149	154.60	3.91	15.29	-1.85
47	162	155.60	5.13	26.29	1.89
48	158	156.80	4.76	22.70	0.47
49	165	158.40	6.02	36.29	1.72
50	176	162.00	9.87	97.49	2.92
51	175	167.20	7.98	63.69	1.32
52	167	168.20	7.46	55.69	-0.03
53	165	169.60	5.46	29.79	-0.43

Table 4.24(b) Statistics of Sliding Window Width 5 for Data File HARNETPVCS.

N	R-R INTER	RUNNING MEAN	RUNNING RMS DEV	RUNNING VARIANCE	DEVIATION (α)
5	230	200.00	69.49	4828.50	
6	245	212.20	71.31	5084.70	0.65
7	239	239.40	36.86	1358.30	0.38
8	240	228.80	22.35	499.71	0.02
9	211	233.00	13.44	180.51	-0.80
10	199	226.80	20.47	419.20	-2.55
11	215	220.80	18.06	326.20	-0.58
12	206	214.20	15.61	243.71	-0.82
13	197	205.60	7.67	58.81	-1.10
14	207	204.80	7.16	51.21	0.16
15	208	206.60	6.43	41.31	0.45
16	203	204.20	4.44	19.71	-0.56
17	226	208.20	10.85	117.71	4.91
18	211	211.00	8.86	78.51	0.26
19	217	213.00	8.86	78.51	0.68
20	222	215.80	9.09	82.71	1.02
21	203	215.80	9.09	82.71	-1.41
22	133	197.20	36.58	1338.21	-9.10
23	276	210.20	51.30	2631.71	2.15
24	184	203.60	52.32	2737.31	-0.51
25	191	197.40	51.42	2644.31	-0.24
26	182	193.20	51.71	2675.71	-0.30
27	175	201.60	41.98	1762.31	-0.35
28	117	169.80	30.06	903.71	-2.02
29	255	184.00	49.15	2416.02	2.83
30	183	182.40	49.00	2400.82	-0.02
31	181	182.20	49.00	2401.22	-0.03
32	197	186.60	49.18	2418.82	0.30
33	214	206.00	30.41	925.02	0.56
34	200	195.00	13.51	182.52	-0.20
35	187	195.80	12.72	161.72	-0.59
36	187	197.00	11.16	124.52	-0.69
37	106	178.80	42.20	1780.72	-8.15
38	274	190.80	59.64	3556.72	2.26
39	175	185.80	59.72	3566.72	-0.26
40	174	183.20	59.94	3592.72	-0.20

Table 4.25 Statistics of Sliding Window Width 5 for Data File SPOONPACS.

N	R-R INTER	RUNNING MEAN	RUNNING RMS DEV	RUNNING VARIANCE	DEVIATION (α)
5	168	166.40	2.30	5.30	
6	171	168.00	2.12	4.50	2.00
7	170	168.40	2.30	5.50	0.94
8	127	160.20	18.70	349.70	-17.99
9	216	170.40	31.50	992.50	2.98
10	167	170.20	31.52	993.70	-0.11
11	170	170.00	31.52	993.50	-0.00
12	169	169.80	31.52	993.69	-0.05
13	164	177.20	21.81	475.69	-0.18
14	167	167.40	2.30	5.30	-0.47
15	168	167.60	2.50	5.30	0.26
16	176	168.80	4.44	19.70	3.65
17	179	170.80	6.38	40.70	2.30
18	178	173.60	5.68	32.30	1.13
19	175	175.20	4.32	18.70	0.25
20	182	178.00	2.74	7.50	1.57
21	170	176.80	4.55	20.69	-2.92
22	166	174.20	6.34	40.20	-2.37
23	171	172.80	6.06	36.69	-0.50
24	168	171.40	6.23	38.79	-0.79
25	170	169.00	2.00	3.99	-0.22
26	169	168.80	1.92	3.69	-0.00
27	166	168.80	1.92	3.69	-1.46
28	166	167.80	1.78	3.19	-1.46
29	167	167.60	1.81	3.28	-0.45
30	162	166.00	2.55	6.49	-3.09
31	162	164.60	2.41	5.79	-1.57
32	171	165.60	3.78	14.29	2.66
33	174	167.20	5.36	28.68	2.22
34	159	165.60	6.50	42.29	-1.55
35	205	174.20	18.29	334.68	6.06
36	174	176.60	17.04	290.28	-0.01
37	138	170.00	24.50	600.49	-2.27
38	194	174.00	26.84	720.49	0.98
39	154	173.00	27.62	762.99	-0.75
40	156	165.20	21.43	459.19	-0.62
41	158	160.00	20.59	423.99	-0.24
42	171	166.60	16.70	278.78	0.55
43	169	161.60	7.83	61.28	0.14

Table 4.26(a) Statistics of Sliding Window Width 5 for Data File BLOOM.

N	R-R INTER	RUNNING MEAN	RUNNING RMS DEV	RUNNING VARIANCE	DEVIATION (α)
44	147	160,20	9,88	97,68	-1,87
45	213	171,60	25,06	627,79	5,34
46	173	174,60	23,89	570,79	0,06
47	122	164,80	33,75	1139,19	-2,20

Table 4.26(b) Statistics of Sliding Window Width 5 for Data File BLOOM.

N	R-R INTER	RUNNING MEAN	RUNNING RMS DEV	RUNNING VARIANCE	DEVIATION (α)
5	185	184.60	3.05	9.30	
6	180	184.40	3.36	11.30	-1.51
7	183	184.60	3.21	10.30	-0.42
8	185	184.20	2.95	8.70	0.12
9	187	184.00	2.64	6.99	0.95
10	185	184.00	2.64	6.99	0.38
11	180	184.00	2.64	6.99	-1.51
12	183	184.00	2.64	6.99	-0.38
13	186	184.20	2.77	7.70	0.76
14	186	184.00	2.55	6.49	0.65
15	180	183.00	3.00	8.99	-1.57
16	174	181.80	5.02	25.19	-3.00
17	173	179.80	6.26	39.19	-1.75
18	176	177.80	5.31	28.19	-0.61
19	180	176.60	3.28	10.79	0.41
20	176	175.80	2.68	7.19	-0.18
21	173	175.60	2.88	8.29	-1.04
22	177	176.40	2.51	6.29	0.49
23	176	176.40	2.51	6.29	-0.16
24	177	175.80	1.64	2.69	0.24
25	171	174.80	2.68	7.19	-2.93
26	165	173.20	5.21	27.19	-3.65
27	168	171.40	5.13	26.30	-1.00
28	170	170.20	4.44	19.70	-0.27
29	176	170.00	4.06	16.49	1.31
30	172	170.20	4.15	17.20	0.49
31	166	170.40	3.85	14.80	-1.01
32	173	171.40	3.71	13.80	0.68
33	174	172.20	3.77	14.19	0.70
34	177	172.40	4.04	16.30	1.27
35	172	172.40	4.04	16.30	-0.09
36	166	172.40	4.04	16.30	-1.59
37	170	171.80	4.15	17.20	-0.59
38	172	171.40	3.97	15.80	0.05
39	173	170.60	2.79	7.80	0.40
40	173	170.80	2.95	8.70	0.86
41	171	171.80	1.30	1.70	0.06
42	171	172.00	1.00	1.00	-0.61
43	236	184.80	28.64	820.20	63.97

Table 4.27(a) Statistics of Sliding Window Width 5 for Data File IN.5+30.

N	R-R INTER	RUNNING MEAN	RUNNING RMS DEV	RUNNING VARIANCE	DEVIATION (α)
44	242	198.60	36.95	1365.30	2.00
45	239	211.80	37.31	1391.70	1.09
46	232	224.00	29.86	891.50	0.54
47	223	234.40	7.37	54.30	-0.03
48	230	233.20	7.53	56.70	-0.60
49	231	231.00	5.70	32.50	-0.29
50	230	229.20	3.56	12.70	-0.18
51	225	227.80	3.56	12.70	-1.18
52	228	228.80	2.39	5.70	0.06
53	244	231.60	7.30	53.30	6.37
54	249	235.20	10.62	112.69	2.38
55	235	236.20	10.23	104.69	-0.02
56	235	238.20	8.29	68.69	-0.12
57	244	241.40	6.19	38.29	0.70
58	243	241.20	6.10	37.19	0.26
59	231	237.60	5.64	31.80	-1.67
60	223	235.20	8.73	76.19	-2.59
61	225	233.20	9.86	97.19	-1.17
62	234	231.20	7.95	63.19	0.08
63	239	230.40	6.54	42.79	0.98
64	232	230.60	6.58	43.30	0.24
65	232	232.40	5.03	25.29	0.21
66	240	235.40	3.85	14.79	1.51
67	237	236.00	3.81	14.49	0.42
68	230	234.20	4.15	17.20	-1.58
69	215	230.80	9.68	93.69	-4.63
70	212	226.80	12.72	161.69	-1.94
71	213	221.40	11.37	129.29	-1.09
72	218	217.60	7.30	53.29	-0.30
73	221	215.80	3.70	15.69	0.47
74	227	218.20	6.14	37.70	3.03

Table 4.27(b) Statistics of Sliding Window Width 5 for Data File IN.5+30.

N	R-R INTER	RUNNING MEAN	RUNNING RMS DEV	RUNNING VARIANCE	DEVIATION (α)
5	186	177.20	5.89	34.70	
6	202	183.40	11.44	130.81	4.21
7	203	188.00	14.05	197.50	1.71
8	216	196.40	16.01	256.51	1.99
9	233	208.00	17.56	308.51	2.29
10	256	222.00	22.77	518.51	2.73
11	302	242.00	38.97	1518.51	3.51
12	299	261.20	38.60	1489.72	1.46
13	323	282.60	36.90	1361.42	1.60
14	333	302.60	29.69	881.43	1.37
15	337	318.80	17.50	306.41	1.16

Table 4.28 Statistics of Sliding Window Width 5 for Data File #476.

N	R-R INTER	RUNNING MEAN	RUNNING RMS DEV	RUNNING VARIANCE	DEVIATION (α)
5	197	224,40	64,45	4154,30	
6	190	225,20	66,60	4435,70	-0,61
7	198	226,40	65,90	4343,30	-0,41
8	328	251,40	77,50	6005,84	1,54
9	213	225,20	58,08	3372,73	-0,50
10	209	227,60	56,85	3232,34	-0,28
11	366	262,80	78,22	6118,69	2,43
12	215	266,20	75,00	5625,74	-0,61
13	209	242,40	69,14	4780,85	-0,76

Table 4,29 Statistics of Sliding Window Width 5 for Data File #463.

q	GROUP* NUMBER	SAMPLE MEAN	SAMPLE RMS DEV	SAMPLE VARIANCE
1	1	176.67	6.38	40.71
2	1 2	176.76 176.57	6.44 6.48	41.49 41.96
3	1 2 3	177.21 176.57 176.21	6.83 6.24 6.51	46.65 38.88 42.34
4	1 2 3 4	177.00 176.64 176.50 176.50	6.51 6.39 6.70 6.92	42.40 40.85 44.94 47.83
5	1 2 3 4 5	172.89 175.56 178.25 180.50 176.75	6.41 5.88 6.73 5.73 5.85	41.11 34.53 45.36 32.86 34.21

Table 4.30 Statistics of Every qth R-R Interval for Data File IN.5

* For q=k, the R-R interval sequence is broken up into k substrings (see Equation (4.41)). Each of these substrings is indicated by the "Group number".

q	GROUP NUMBER	SAMPLE MEAN	SAMPLE RMS DEV	SAMPLE VARIANCE
1	1	200.45	6.21	38.60
2	1 2	200.56 200.29	5.82 6.78	33.91 45.97
3	1 2 3	199.92 200.50 200.91	6.89 5.42 6.79	47.54 29.37 46.09
4	1 2 3 4	200.22 204.33 200.89 195.75	7.74 3.91 3.44 6.56	59.94 15.25 11.86 43.07
5	1 2 3 4 5	199.43 200.29 201.29 200.71 200.43	6.70 7.76 7.57 5.99 4.28	44.95 60.24 57.24 35.91 18.28

Table 4.31 Statistics of Every qth R-R Interval for Data File IN.20.

q	GROUP NUMBER	SAMPLE MEAN	SAMPLE RMS DEV	SAMPLE VARIANCE
1	1	231.09	9.30	86.41
2	1 2	230.62 231.56	9.51 9.36	90.52 87.60
3	1 2 3	230.18 231.00 232.20	8.49 8.50 11.61	72.16 72.20 134.85
4	1 2 3 4	229.87 229.75 231.37 233.37	8.90 7.27 10.65 11.29	79.27 52.79 113.41 127.41
5	1 2 3 4 5	234.71 232.43 228.50 228.33 230.67	8.24 10.83 9.69 9.50 9.54	67.91 117.28 93.94 90.27 91.06

Table 4.32 Statistics of Every qth R-R Interval for Data File IN.30.

q	GROUP NUMBER	SAMPLE MEAN	SAMPLE RMS DEV	SAMPLE VARIANCE
1	1	106.26	19.65	386.30
2	1 2	103.84 108.73	19.22 19.98	369.51 399.31
3	1 2 3	101.82 108.78 108.31	17.22 20.44 20.99	296.59 417.79 440.42
4	1 2 3 4	105.64 108.29 101.96 109.17	22.09 17.40 15.96 22.64	487.99 302.91 254.74 512.67
5	1 2 3 4 5	105.20 113.85 108.47 101.00 102.42	20.40 23.45 17.32 15.25 19.83	416.17 549.71 300.04 232.44 393.04

Table 4.33 Statistics of Every qth R-R Interval for Data File CUNATFIB.

q	GROUP NUMBER	SAMPLE MEAN	SAMPLE RMS DEV	SAMPLE VARIANCE
1	1	142.80	43.42	1885.36
2	1 2	142.71 142.90	44.86 43.02	2012.31 1850.94
3	1 2 3	141.14 98.79 192.00	10.15 22.65 27.04	103.06 513.10 731.33
4	1 2 3 4	135.73 146.90 150.40 138.90	44.12 47.11 46.73 40.65	1946.82 2219.21 2183.38 1652.77
5	1 2 3 4 5	132.00 139.50 153.12 147.00 143.75	39.73 44.94 49.15 47.61 44.30	1578.50 2019.43 2416.12 2266.29 1962.21

Table 4.34 Statistics of Every qth R-R Interval for Data File HUANPVCS.

q	GROUP NUMBER	SAMPLE MEAN	SAMPLE RMS DEV	SAMPLE VARIANCE
1	1	144.19	46.95	2204.76
2	1 2	142.69 145.80	48.20 47.22	2323.43 2229.74
3	1 2 3	139.09 90.20 203.80	5.28 3.08 9.48	27.89 9.51 89.95
4	1 2 3 4	154.62 146.75 150.75 144.71	46.93 52.04 51.26 45.17	2202.27 2708.50 2627.93 2040.24
5	1 2 3 4 5	140.57 142.33 148.00 146.17 144.50	40.55 49.03 57.06 54.12 51.20	1643.95 2404.27 3255.60 2929.36 2621.90

Table 4.35 Statistics of Every qth R-R Interval for Data File HUANTRI.

q	GROUP NUMBER	SAMPLE MEAN	SAMPLE RMS DEV	SAMPLE VARIANCE
1	1	201.10	71.17	5064.72
2	1 2	133.00 272.79	4.29 9.74	18.42 94.92
3	1 2 3	196.15 208.69 198.46	72.60 72.16 73.93	5270.14 5206.73 5464.94
4	1 2 3 4	133.30 271.00 132.70 274.78	3.27 9.76 5.29 9.89	10.68 95.35 28.01 97.90
5	1 2 3 4 5	200.75 205.25 199.25 207.62 191.45	76.38 75.31 72.15 77.86 72.89	5834.21 5671.64 5206.21 6061.98 5313.29

Table 4.36 Statistics of Every qth R-R Interval for Data File #503

q	GROUP NUMBER	SAMPLE MEAN	SAMPLE RMS DEV	SAMPLE VARIANCE
1	1	156.91	24.42	596.48
2	1 2	156.44 157.38	24.56 24.75	603.26 612.81
3	1 2 3	149.67 158.28 163.12	16.99 31.98 21.05	288.59 1022.69 443.24
4	1 2 3 4	156.43 157.77 156.46 157.00	26.11 24.36 23.85 26.15	681.65 593.53 568.61 682.83
5	1 2 3 4 5	155.27 156.64 150.82 145.40 177.20	8.43 5.46 16.50 34.34 34.63	71.02 29.85 272.17 1178.93 1199.51

Table 4.37 Statistics of Every qth R-R Interval for Data File HARNETPVCS.

q	GROUP NUMBER	SAMPLE MEAN	SAMPLE RMS DEV	SAMPLE VARIANCE
1	1	201,00	40,76	1661,13
2	1 2	209,15 192,85	40,22 40,65	1617,82 1652,03
3	1 2 3	180,79 216,46 207,31	37,57 45,28 32,26	1411,41 2049,94 1040,90
4	1 2 3 4	201,70 193,70 216,60 192,00	39,55 49,20 41,56 32,64	1564,46 2420,68 1727,60 1065,35
5	1 2 3 4 5	200,00 173,12 227,75 204,87 199,25	21,97 53,22 56,76 24,71 19,49	482,57 2831,84 3222,21 610,70 379,93

Table 4.38 Statistics of Every qth R-R Interval for Data File SPOONPAC.

q	GROUP NUMBER	SAMPLE MEAN	SAMPLE RMS DEV	SAMPLE VARIANCE
1	1	168,64	16,70	278,98
2	1	170,00	20,03	401,22
	2	167,22	12,64	159,72
3	1	164,94	9,01	81,13
	2	166,56	21,12	446,13
	3	174,80	17,04	290,46
4	1	173,33	21,73	472,24
	2	170,42	8,91	79,35
	3	166,67	18,50	342,42
	4	163,73	15,44	238,42
5	1	168,60	5,78	33,38
	2	162,00	17,66	312,00
	3	167,89	17,76	315,36
	4	168,67	19,62	384,75
	5	176,78	19,63	385,20

Table 4.39 Statistics of Every qth R-R Interval for Data File BLOOM.

q	GROUP NUMBER	SAMPLE MEAN	SAMPLE RMS DEV	SAMPLE VARIANCE
1	1	200,20	28,22	796,58
2	1 2	200,05 200,35	28,15 28,68	792,61 822,62
3	1 2 3	200,52 200,52 199,54	27,85 28,49 29,52	775,42 811,51 871,65
4	1 2 3 4	199,89 200,53 200,22 200,17	28,78 30,01 28,31 28,08	828,44 900,59 801,24 788,38
5	1 2 3 4 5	195,07 197,60 204,60 204,73 198,93	29,09 28,87 30,03 28,03 27,58	846,21 833,25 901,97 785,78 760,84

Table 4.40 Statistics of Every qth R-R Interval for Data File IN.5+30.

q	GROUP NUMBER	SAMPLE MEAN	SAMPLE RMS DEV	SAMPLE VARIANCE
1	1	239.33	63.14	3986.96
2	1 2	241.12 237.29	69.26 60.80	4797.55 3696.57
3	1 2 3	225.60 243.40 249.00	64.15 69.87 67.70	4115.80 4881.80 4583.52
4	1 2 3 4	228.25 242.75 254.00 230.00	68.47 68.11 77.88 63.17	4687.58 4639.58 6064.67 3991.00
5	1 2 3 4 5	225.00 227.33 237.67 247.00 259.67	68.46 63.12 76.83 79.92 75.57	4687.00 3984.34 5902.33 6388.00 5714.31

Table 4.41 Statistics of Every qth R-R Interval for Data File #476.

q	GROUP NUMBER	SAMPLE MEAN	SAMPLE RMS DEV	SAMPLE VARIANCE
1	1	236,54	63,37	4015,27
2	1 2	228,14 246,33	61,11 70,50	3734,14 4941,87
3	1 2 3	234,20 270,75 205,25	61,59 89,43 11,44	3793,70 7996,92 130,92
4	1 2 3 4	207,50 197,00 255,67 295,67	7,19 10,44 95,58 70,32	51,67 109,00 9136,30 4944,27
5	1 2 3 4 5	255,67 201,67 246,67 278,50 203,00	96,13 11,93 70,50 92,63 8,49	9240,36 142,33 4970,33 8580,50 72,00

Table 4.42 Statistics of Every qth R-R Interval for Data File #463.

τ	CORRELATION FUNCTION	NORMALIZED CORRELATION FUNCTION
0	0.131253E 7	0.100000E 1
1	0.131219E 7	0.999739E 0
2	0.131179E 7	0.999436E 0
3	0.131162E 7	0.999305E 0
4	0.131168E 7	0.999350E 0
5	0.131178E 7	0.999429E 0
6	0.131151E 7	0.999221E 0
7	0.131112E 7	0.998927E 0
8	0.131100E 7	0.998829E 0
9	0.131107E 7	0.998889E 0

Table 4.43 Correlation Functions for Data File IN.5

τ	CORRELATION FUNCTION	NORMALIZED CORRELATION FUNCTION
0	0.140731E 7	0.100000E 1
1	0.140665E 7	0.999531E 0
2	0.140600E 7	0.999067E 0
3	0.140643E 7	0.999374E 0
4	0.140676E 7	0.999607E 0
5	0.140605E 7	0.999100E 0
6	0.140558E 7	0.998769E 0
7	0.140614E 7	0.999168E 0
8	0.140647E 7	0.999401E 0
9	0.140587E 7	0.998972E 0

Table 4.44 Correlation Functions for Data File IN.20.

τ	CORRELATION FUNCTION	NORMALIZED CORRELATION FUNCTION
0	0.171161E 7	0.100000E 1
1	0.171077E 7	0.999505E 0
2	0.170946E 7	0.998742E 0
3	0.170891E 7	0.998423E 0
4	0.170889E 7	0.998407E 0
5	0.170847E 7	0.998161E 0
6	0.170778E 7	0.997761E 0
7	0.170785E 7	0.997802E 0
8	0.170898E 7	0.998461E 0
9	0.170997E 7	0.999041E 0

Table 4.45 Correlation Functions for Data File IN.30

τ	CORRELATION FUNCTION	NORMALIZED CORRELATION FUNCTION
0	0.113228E 7	0.100000E 1
1	0.110095E 7	0.972330E 0
2	0.109811E 7	0.969825E 0
3	0.109708E 7	0.968914E 0
4	0.109580E 7	0.967780E 0
5	0.110299E 7	0.974154E 0
6	0.110008E 7	0.971560E 0
7	0.109458E 7	0.966701E 0
8	0.109922E 7	0.970805E 0
9	0.109590E 7	0.967874E 0

Table 4.46 Correlation Functions for Data File CUNATFIB.

τ	CORRELATION FUNCTION	NORMALIZED CORRELATION FUNCTION
0	0.911537E 6	0.100000E 1
1	0.803674E 6	0.881669E 0
2	0.806747E 6	0.885040E 0
3	0.889520E 6	0.975846E 0
4	0.804125E 6	0.882163E 0
5	0.811316E 6	0.890052E 0
6	0.888813E 6	0.975070E 0
7	0.812154E 6	0.890972E 0
8	0.811228E 6	0.889956E 0
9	0.881890E 6	0.967475E 0

Table 4.47 Correlation Functions for Data File HUANPVCS

τ	CORRELATION FUNCTION	NORMALIZED CORRELATION FUNCTION
0	0.710688E 6	0.100000E 1
1	0.611490E 6	0.860419E 0
2	0.616511E 6	0.867484E 0
3	0.697579E 6	0.981554E 0
4	0.623659E 6	0.877542E 0
5	0.614075E 6	0.864057E 0
6	0.690736E 6	0.971925E 0
7	0.630871E 6	0.887690E 0
8	0.616431E 6	0.867372E 0
9	0.678404E 6	0.954573E 0

Table 4.48 Correlation Functions for Data File HUANTRI.

τ	CORRELATION FUNCTION	NORMALIZED CORRELATION FUNCTION
0	0.176970E 7	0.100000E 1
1	0.139541E 7	0.788502E 0
2	0.175252E 7	0.990292E 0
3	0.141260E 7	0.798216E 0
4	0.173232E 7	0.978878E 0
5	0.143148E 7	0.808881E 0
6	0.171226E 7	0.967538E 0
7	0.145199E 7	0.820469E 0
8	0.169283E 7	0.956561E 0
9	0.147237E 7	0.831988E 0

Table 4.49 Correlation Functions for Data File #503

τ	CORRELATION FUNCTION	NORMALIZED CORRELATION FUNCTION
0	0.133584E 7	0.100000E 1
1	0.129213E 7	0.967279E 0
2	0.130753E 7	0.978808E 0
3	0.130405E 7	0.976201E 0
4	0.130263E 7	0.975143E 0
5	0.130557E 7	0.977338E 0
6	0.130462E 7	0.976626E 0
7	0.130439E 7	0.976460E 0
8	0.130398E 7	0.976146E 0
9	0.130806E 7	0.979204E 0

Table 4.50 Correlation Functions for Data File HARNETPVCS.

τ	CORRELATION FUNCTION	NORMALIZED CORRELATION FUNCTION
0	0.168082E 7	0.100000E 1
1	0.159831E 7	0.950910E 0
2	0.162566E 7	0.967181E 0
3	0.162240E 7	0.965242E 0
4	0.160987E 7	0.957790E 0
5	0.162667E 7	0.967783E 0
6	0.161573E 7	0.961272E 0
7	0.160943E 7	0.957525E 0
8	0.160847E 7	0.956957E 0
9	0.162688E 7	0.967907E 0

Table 4.51 Correlation Functions for Data File SPOONPAC.

τ	CORRELATION FUNCTION	NORMALIZED CORRELATION FUNCTION
0	0.134946E 7	0.100000E 1
1	0.133297E 7	0.987786E 0
2	0.133411E 7	0.988630E 0
3	0.133940E 7	0.992550E 0
4	0.133580E 7	0.989878E 0
5	0.133549E 7	0.989647E 0
6	0.133542E 7	0.989596E 0
7	0.133952E 7	0.992636E 0
8	0.133773E 7	0.991308E 0
9	0.133268E 7	0.987568E 0

Table 4.52 Correlation Functions for Data File BLOOM.

τ	CORRELATION FUNCTION	NORMALIZED CORRELATION FUNCTION
0	0.302415E 7	0.100000E 1
1	0.301988E 7	0.998588E 0
2	0.301515E 7	0.997023E 0
3	0.301215E 7	0.996035E 0
4	0.301061E 7	0.995521E 0
5	0.300898E 7	0.994985E 0
6	0.300566E 7	0.993886E 0
7	0.300202E 7	0.992683E 0
8	0.299977E 7	0.991939E 0
9	0.299832E 7	0.991459E 0

Table 4.53 Correlation Functions for Data File IN.5+30

τ	CORRELATION FUNCTION	NORMALIZED CORRELATION FUNCTION
0	0.915024E 6	0.100000E 1
1	0.899096E 6	0.982592E 0
2	0.883430E 6	0.965471E 0
3	0.866015E 6	0.946459E 0
4	0.850695E 6	0.929696E 0
5	0.835008E 6	0.912553E 0
6	0.828222E 6	0.905156E 0
7	0.824072E 6	0.900601E 0
8	0.824072E 6	0.900601E 0
9	0.828222E 6	0.905136E 0

Table 4.54 Correlation Functions for Data File #476.

τ	CORRELATION FUNCTION	NORMALIZED CORRELATION FUNCTION
0	0.775539E 6	0.100000E 1
1	0.715681E 6	0.922817E 0
2	0.711164E 6	0.916993E 0
3	0.734015E 6	0.946457E 0
4	0.730161E 6	0.941488E 0
5	0.714299E 6	0.921035E 0
6	0.734723E 6	0.947370E 0
7	0.734723E 6	0.947370E 0
8	0.714299E 6	0.921035E 0
9	0.730161E 6	0.941488E 0

Table 4.55 Correlation Functions for Data File #463.

CHAPTER 5

DYNAMICAL MODELLING OF CARDIAC RHYTHMS BASED ON THEIR R-R INTERVAL CHARACTERISTICS

5.1 Introduction

In Chapter 4 we have demonstrated that we could detect and identify different arrhythmia classes by their statistical characteristics, which are expressed in terms of some simple statistical parameters. However, a completely automated computer algorithm for rhythm analysis of ECG/VCG's using these statistics would be quite complex. The reason for this is the fact that in order to detect and identify positively the presence of a certain rhythm pattern, we need to perform several threshold tests. For instance, some tests for identifing a bigeminal rhythm would be: (1) sample variance greater than a preset threshold, (2) sample variance of every other R-R intervals less than a preset threshold, and (3) the difference of the two sample means of every other R-R intervals greater than a preset threshold. Thus for each arrhythmia class we wish to detect, we need to set up some necessary threshold tests just for the purpose of detecting this particular rhythm. Therefore the final structure of the algorithm is formed by putting all the threshold tests needed to detect and identify all the arrhythmia classes together, and since all these tests are of threshold type, the final detection logic is deterministic. In other words, an ECG/VCG record will be classified into a particular rhythm pattern based solely on certain threshold tests, and this decision structure does not take into account the margins by which the thresholds passed or failed. What would be preferable would be a decision rule that

(1) contains a minimum number of threshold tests, since it is extremely difficult to modify and analyze decision rules that contain numerous (and extraneous) logical branches

(2) is based on statistics that somehow reflect and quantify our confidence in our decision - i.e. We would like to use quantities such as the probability or likelihood that a certain decision is the correct one. In this case one will have a much more rational basis for the setting of thresholds.

There is a more sophisticated statistical method for the detection and identification of the arrhythmias, as we will see in Chapters 6 and 7. The final structure of the algorithm using this approach is extremely unified and the decision tests are done statistically rather than deterministically. However, in order to utilize this powerful statistical method, we need to develop mathematical models for each of the rhythm patterns we wish to detect. The models developed in this chapter are based upon the categorization concepts described in Chapter 3, and the dynamical descriptions defined in a qualitative manner in Chapter 4. (As we will see, the statistical analysis of the preceding chapter provides a method for choosing certain parameters in these mathematical models). In the rest of this chapter we will discuss the modelling concept and the mathematical models for both the persistent and transient rhythms described in Chapter 3.

5.2 Dynamical Models for Persistent Rhythms

For this class of rhythms, our conceptual picture for the models

is illustrated in Figure 5.1.

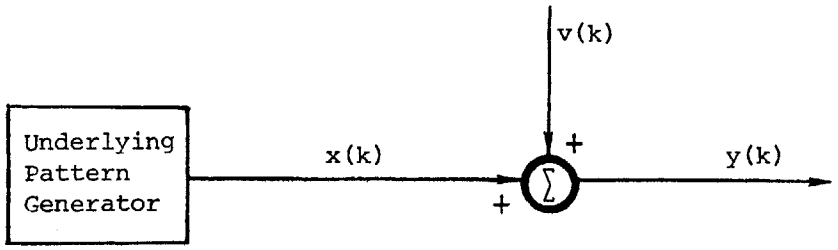

Figure 5.1 Conceptual Diagram of the Dynamical Model for Persistent Rhythms

Here we imagine that an underlying pattern generator generates a sequence of R-R intervals, x(k), k=1,2,..., according to a particular ideal pattern. This ideal R-R interval sequence is what we called "nominal R-R interval sequence" or "state sequence" which is different from the actually observed R-R interval sequence, y(k), k=1,2,... . The actual R-R interval, y(k), is the nominal R-R interval x(k) corrupted by an additive noise v(k), which comes from two sources. The first of these is the unavoidable errors in computing the R-R intervals, caused by inaccuracies in locating the fiducial points of the QRS complexes. In addition, as we have discussed in Chapter 4, even for a regular normal rhythm the R-R intervals are not exactly the same; rather there are normal variations about the ideal underlying rhythmic pattern. Thus, a second source of noise is included to represent these normal variations.

Using this conceptual picture, a persistent rhythm class can then be modelled mathematically by using two discrete-time relations. The

first equation describes the mechanism in which the ideal underlying rhythm pattern is generated and is called the process equation, which describes the state of a system at every instant of time. The second equation, which is called the observation equation, gives the relation between the actually observed data and the state of the system. In our case, the actually observed R-R interval is given by the state plus an additive noise term. In the following we will describe the mathematical models of this form for the persistent rhythm classes discussed in Chapter 3.

(1) Dynamical Model for Small Variation

For this class of rhythm, the given R-R interval sequence, $y(k)$, $k=1,2,\ldots$, has only small, random variations about its mean value. Thus, we can model this class of rhythms by an ideal pattern consisting of exactly equal R-R intervals, generated by an underlying pattern generator, and an additive noise, which represents the small variation, is then added to the nominal R-R interval and gives the actually observed R-R interval data.

Therefore the mathematical model for this class of rhythms is given as:

$$x(k) = x(k-1) \tag{5.1}$$

$$y(k) = x(k) + v(k) \tag{5.2}$$

where Equation (5.1) is the process equation which describes an ideal state sequence consists of exactly equal states, $x(k)$, $k=1,2,\ldots$, and the actually observed data is given by the observation equation, Equation (5.2), which is the sum of the state and a noise term $v(k)$.

Here the initial state x(0) is thought of as a random variable with given mean m(0) and covariance P(0). The noise v(k) is assumed to be unbiased and uncorrelated with itself, thus we have

$$E[v(k)]=0 \tag{5.3}$$

$$E[v(k)v(j)]=R_s\delta_{kj} \tag{5.4}$$

where R_s is the noise variance for the small variation rhythm and δ_{kj} is the Kronecker delta, $\delta_{kj}=0$ if $k\neq j$ and 1 if $k=j$. In addition we assume that the noise at any time k is independent of the underlying rhythm state, thus

$$E[v(k)x(j)]=0 \tag{5.5}$$

We also assume that all random variables have Gaussian probability density functions.

The quantities P(0), m(0), and R_s are free parameters to be determined from the statistical tests of Chapter 4. It is <u>not</u> true that we will determine these for each patient individually from the statistical tests. Rather, we will use these tests on a number of records to determine <u>reasonable values in general</u> (the role of these parameters will become clearer in Chapters 6 and 7).

(2) <u>Dynamical Model for Large Variation</u>

For this class of rhythms the observed R-R intervals have large variations about the mean value. Therefore, we can model this class of rhythms using the same model we used for the small variation rhythm, and increase the noise variance of v to account for the larger variations in this class. The mathematical model is then identical to Equations (5.1)

and (5.2) and is rewritten here for convenience

$$x(k) = x(k-1) \tag{5.6}$$

$$y(k) = x(k) + v(k) \tag{5.7}$$

Here the observation noise v(k) has variance R_ℓ, which is greater than R_s, or

$$E[v(k)v(j)] = R_\ell \delta_{kj} \qquad R_\ell > R_s \tag{5.8}$$

(3) Dynamical Model for Bigeminy

For a bigeminal rhythm, the observed R-R intervals oscillate between two different R-R interval sizes, i.e., the R-R interval sequence has a pattern of short, long, short, long, etc. Thus we need a mathematical relation which will generate an ideal underlying pattern of this form, and the variations observed in the R-R intervals will again be modelled as additive noise. A second order model which describes this rhythm pattern is

$$x(k) = \begin{bmatrix} 0 & 1 \\ 1 & 0 \end{bmatrix} x(k-1) \tag{5.9}$$

$$y(k) = [1\ 0]x(k) + v(k) \tag{5.10}$$

where x(k) is the nominal R-R interval and is a two-dimensional vector

$$x(k) = \begin{bmatrix} x_1(k) \\ x_2(k) \end{bmatrix} \tag{5.11}$$

The initial state x(0) is a two-dimensional random vector with given mean m(0) and covariance P(0), and the noise $\{v(k)\}$ is again a white Gaussian sequence with the following statistics

$$E[v(k)]=0 \tag{5.12}$$

$$E[v(k)v(j)] = R_b \delta_{kj} \tag{5.13}$$

Again, P(0), m(0), and R_b are free parameters to be determined by some statistical means.

Assuming that we are given the initial state,

$$x(0) = \begin{bmatrix} x_1(0) \\ x_2(0) \end{bmatrix} \tag{5.14}$$

then the state sequence given by the process equation, Equation (5.9), is

$$x(1) = \begin{bmatrix} x_2(0) \\ x_1(0) \end{bmatrix} \quad x(2) = \begin{bmatrix} x_1(0) \\ x_2(0) \end{bmatrix} \quad x(3) = \begin{bmatrix} x_2(0) \\ x_1(0) \end{bmatrix} \ldots \tag{5.15}$$

The observation equation, Equation (5.10), then gives

$$\begin{aligned} y(1) &= x_2(0) + v(1) \\ y(2) &= x_1(0) + v(2) \\ y(3) &= x_2(0) + v(3) \\ &\vdots \end{aligned} \tag{5.16}$$

which is an alternation between $x_1(0)$ and $x_2(0)$, and the correct model for a bigeminal rhythm.

(4) Dynamical Model for Trigeminy

In this case we have an R-R interval sequence which has a period of three; hence we need a process equation which can generate such a pattern. A model which describes this class of rhythms is

$$x(k) = \begin{bmatrix} 0 & 0 & 1 \\ 1 & 0 & 0 \\ 0 & 1 & 0 \end{bmatrix} x(k-1) \tag{5.17}$$

$$y(k) = [1\ 0\ 0]\ x(k) + v(k) \tag{5.18}$$

where $x(k)$ is a three dimensional vector

$$x(k) = \begin{bmatrix} x_1(k) \\ x_2(k) \\ x_3(k) \end{bmatrix} \tag{5.19}$$

and the noise process is again a white Gaussian sequence with statistics

$$E[v(k)]=0 \tag{5.20}$$

$$E[v(k)v(j)] = R_t \delta_{kj} \tag{5.21}$$

It is easily seen that this model is appropriate for the trigeminal rhythm we wish to model.

5.3 Dynamical Models for Transient Rhythms

In order to model the transient rhythm classes we use again a conceptual picture for the models as we did in the case of persistent rhythms. A transient rhythm can always be viewed dynamically as an abrupt change, additively superimposed upon an underlying small variational rhythm. Using this concept, we can then model the transient rhythms by imagining that a noise free ideal underlying pattern, which includes the abrupt changes is generated first, and the actually observed R-R interval sequence $\{y(k)\}$ is then obtained by superimposing a noise sequence $\{v(k)\}$ upon the underlying nominal R-R interval pattern. This conceptual picture is illustrated in Figure 5.2.

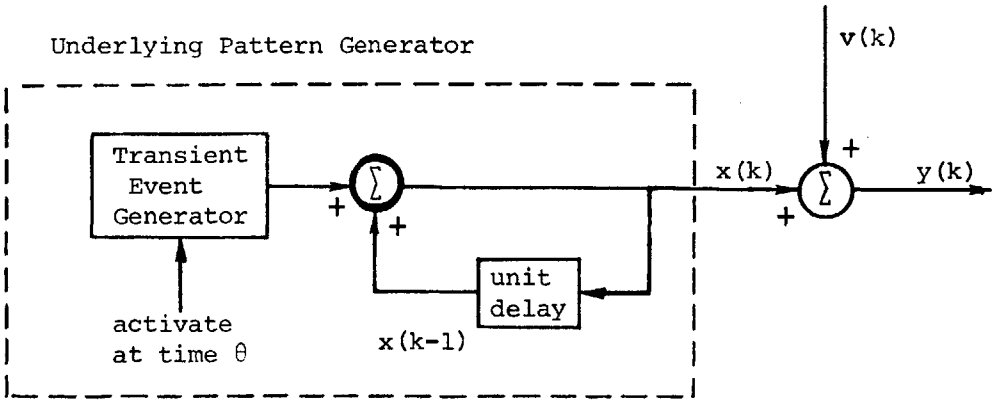

Figure 5.2 Conceptual Diagram of the Dynamical Model for Transient Rhythms

Here the underlying pattern generator is driven by a randomly activated transient event generator, which generates one of the four abrupt R-R interval changes described in Chapter 3 at activating time θ. For $k<\theta$, the unit delayed feedback loop will generate an R-R interval sequence, $x(k)$, $k=1,\ldots\theta-1$, which are all exactly equal. However for

$k \geq \theta$, the underlying nominal R-R interval is given as the sum of the outputs from the transient even generator and the unit delayed feedback. Using this conceptual diagram, we will describe the mathematical models for the transient rhythm classes in the following.

(1) Dynamical Model for Rhythm Jump

In this class of rhythm, there is a sudden change of the size of the R-R intervals. The model for this is

$$x(k) = x(k-1) + \nu\delta_{\theta,k} \tag{5.22}$$

$$y(k) = x(k) + v(k) \tag{5.23}$$

where ν is an unknown jump in the normal R-R interval, and θ is the unknown time at which this jump occurs. Here $\delta_{\theta,k}$ is the Kronecker delta defined earlier. The nominal R-R interval pattern given by Equation (5.22) is

$$\begin{aligned} x(1) &= x(0) \\ x(2) &= x(0) \\ &\vdots \\ x(\theta-1) &= x(0) \\ x(\theta) &= x(0) + \nu \\ x(\theta+1) &= x(0) + \nu \\ &\vdots \end{aligned} \tag{5.24}$$

Note that for $\nu>0$ there is a sudden jump to a slower heart rate, and for $\nu<0$ a sudden jump to a faster heart rate; thus the model given by

Equations (5.22) and (5.23) describes both the onset tachycardia and bradycardia.

(2) Dynamical Model for Non-Compensatory Beat

For this class of ectopic events, there is either a shortened or lengthened R-R interval, followed by a return to the regular pattern. Thus a mathematical model which describes this pattern is

$$x(k) = x(k-1) + \nu[\delta_{\theta,k} - \delta_{\theta,k-1}] \tag{5.25}$$

$$y(k) = x(k) + v(k) \tag{5.26}$$

Equation (5.25) gives the following state sequence:

$$\begin{aligned} x(1) &= x(0) \\ x(2) &= x(0) \\ &\vdots \\ x(\theta-1) &= x(0) \\ x(\theta) &= x(0) + \nu \\ x(\theta+1) &= x(0) \\ &\vdots \end{aligned} \tag{5.27}$$

which has a non-compensatory beat at time θ.

(3) Dynamical Model for Compensatory Beat

In this case, there is either a shortened or lengthened R-R interval, followed by a compensatory pause, such that the sum of these two successive R-R intervals equals twice the regular R-R interval. The model for this is

$$x(k) = x(k-1) + \nu[\delta_{\theta,k} - 2\delta_{\theta,k-1} + \delta_{\theta,k-2}] \tag{5.28}$$

$$y(k) = x(k) + v(k) \tag{5.29}$$

The sequence of the states given by Equation (5.28) is

$$x(1) = x(0)$$

$$x(2) = x(0)$$

$$\vdots$$

$$x(\theta-1) = x(0)$$

$$x(\theta) = x(0) + \nu$$

$$x(\theta+1) = x(0) - \nu$$

$$x(\theta+2) = x(0)$$

$$\vdots$$

(4) Dynamical Model for Double Non-Compensatory Beat

For this case, we are seeking a model which is characterized by two successive lengthened or shortened R-R intervals. The model for this is

$$x(k) = x(k-1) + \nu[\delta_{\theta,k} - \delta_{\theta,k-2}] \tag{5.31}$$

$$y(k) = x(k) + v(k) \tag{5.32}$$

The nominal R-R interval sequence from Equation (5.31) has the following pattern

$$
\begin{aligned}
x(1) &= x(0) \\
x(2) &= x(0) \\
&\vdots \\
x(\theta-1) &= x(0) \\
x(\theta) &= x(0) + \nu \\
x(\theta+1) &= x(0) + \nu \\
x(\theta+2) &= x(0) \\
&\vdots
\end{aligned}
\tag{5.33}
$$

which is precisely the model we need. Note also that if $\nu = -x(0)/2$, Equation (5.33) gives the state sequence for an interpolated beat.

CHAPTER 6

DETECTION AND CLASSIFICATION OF PERSISTENT RHYTHMS

6.1 The Multiple Model Hypothesis Testing Technique

In Chapter 5, we have developed dynamical models for several persistent arrhythmia classes, namely, small variation, large variation, bigeminy and trigeminy. All the dynamical models for these arrhythmia classes can be considered as special cases of a more general discrete dynamical system of the following form:

$$x(k) = \Phi(k,k-1)x(k-1) + \Gamma(k)W(k) \tag{6.1}$$

$$y(k) = H(k)x(k) + v(k) \tag{6.2}$$

where $x(k) \in R^n$ is the state, with initial condition $x(0)$ being a Gaussian random variable with mean

$$E[x(0)] = \bar{x}(0) \tag{6.3}$$

and covariance

$$E[(x(0)-\bar{x}(0))(x(0)-\bar{x}(0))^T] = P(0) \tag{6.4}$$

and the driving noise, $w(k)$, is an m-dimensional white Gaussian sequence with statistics

$$E[w(k)]=0 \tag{6.5}$$

$$E[w(k)w^T(j)]=Q(k)\delta_{kj} \tag{6.6}$$

$y(k) \in R^p$ is the observation, and $\{v(k)\}$ is a p-dimensional white Gaussian measurement noise sequence with statistics

$$E[v(k)]=0 \tag{6.7}$$

$$E[v(k)v^T(j)]=R(k)\delta_{kj} \tag{6.8}$$

Furthermore, $x(0)$, $w(k)$, and $v(j)$ are mutually independent, i.e.,

$$E[w(k)v^T(j)]=0 \tag{6.9}$$

$$E[w(k)x^T(0)]=0 \tag{6.10}$$

$$E[v(k)x^T(0)]=0 \tag{6.11}$$

Referring to Equations (6.1) through (6.11), the dynamical models for the persistent rhythms are specified by Φ,Γ,H,Q, and R. Since no driving noise is included in the state equation of the dynamical models, Q is set equal to zero for all these four persistent rhythm classes. The other parameters for different classes are given as

(1) <u>small variation</u>

$$\Phi(k,k-1)=1 \qquad H(k)=1$$
$$R(k)=R_s \tag{6.12}$$

(2) large variation

$$\Phi(k,k-1)=1 \qquad H(k)=1$$
$$R(k) = R_{\ell}(>R_s) \tag{6.13}$$

(3) bigeminy

$$\Phi(k,k-1) = \begin{bmatrix} 0 & 1 \\ 1 & 0 \end{bmatrix} \quad H(k) = [1\ 0] \tag{6.14}$$

$$R(k) = R_b$$

(4) trigeminy

$$\Phi(k,k-1) = \begin{bmatrix} 0 & 0 & 1 \\ 1 & 0 & 0 \\ 0 & 1 & 0 \end{bmatrix} \quad H(k) = [1\ 0\ 0] \tag{6.15}$$

$$R(k) = R_t$$

the R's, P(0), and $\bar{x}(0)$ are design parameters.

We now consider the problem of detection and classification for these classes of arrhythmias, i.e., given a sequence of R-R intervals, we wish to determine which one of the several possible persistent rhythms is present. Our design of the detection and classification of this class of problems is based on the Multiple Model Hypothesis Testing technique. The method of approach of using this Multiple Model Hypothesis Testing technique is described in detail in the following.

Given the dynamical model [(6.1)-(6.2)], we wish to design a system that will estimate the state $x(k)$ given the measurements $y(1), y(2), \ldots y(k)$. Let $\hat{x}(i|j)$ denote the estimate of $x(i)$ given observations $y(1),\ldots,y(j)$. Then these state estimates for the system [(6.1)-(6.2)] can be computed by the Kalman filter equation [39].

$$\hat{x}(k|k-1) = \Phi(k,k-1)\hat{x}(k-1|k-1) \tag{6.16}$$

$$\hat{x}(k|k) = \hat{x}(k|k-1) + M(k)\gamma(k) \tag{6.17}$$

with initial condition

$$\hat{x}(0|0) = \bar{x}(0) \tag{6.18}$$

where $M(k)$ is the filter gain, and $\gamma(k)$ is the measurement residual or innovations process

$$\gamma(k) = y(k) - H(k)\hat{x}(k|k-1) \tag{6.19}$$

with statistics

$$E[\gamma(k)]=0 \tag{6.20}$$

$$E[\gamma(k)\gamma^T(j)] = V(k)\delta_{kj} \tag{6.21}$$

the associated error covariance matrix, $P(i|j)$, residual covariance, and the filter gain, $M(k)$, can be computed according to the following recursive relations:

$$P(k|k-1) = \Phi(k,k-1)P(k-1|k-1)\Phi^T(k,k-1) + \Gamma(k)Q(k)\Gamma^T(k) \quad (6.22)$$

$$V(k) = H(k)P(k|k-1)H^T(k) + R(k) \quad (6.23)$$

$$M(k) = P(k|k-1)H^T(k)V^{-1}(k) \quad (6.24)$$

$$P(k|k) = P(k|k-1) - M(k)H(k)P(k|k-1) \quad (6.25)$$

with initial condition

$$P(0|0) = P(0) \quad (6.26)$$

Since we do not know a priori which of the possible arrhythmia classes will occur, we hypothesize several possible arrhythmia classes, namely, small variation, large variation, bigeminy and trigeminy, and wish to determine which one of these possible models is the correct one. In this case, we can employ the technique described in [40], [41]. We have several possible models, which are specified by Φ_i, Γ_i, H_i, Q_i and R_i as given by Equations (6.12) through (6.15). Here subscript i is used to indicate different persistent rhythm classes. Using Equations (6.16) through (6.26), we construct a Kalman filter for each of these models. The measurement residuals $\gamma_i(k)$, and the associated covariance $V_i(k)$ from each of these Kalman filters are then used to compute the probabilities, $Pr_i(k)$, that each of the models is correct. Assuming there are n possible models, then the probability, $Pr_j(k)$, that the jth model is the correct one can be calculated from the following recursive relation

$$Pr_j(k) = \frac{N(\gamma_j(k),V_j(k))Pr_j(k-1)}{\sum_{i=1}^{n} N(\gamma_i(k),V_i(k))Pr_i(k-1)} \tag{6.27}$$

with initial probabilities $Pr_j(0)$, $j=1,2,...n$, where $N(\gamma,V)$ is the normal density function

$$N(\gamma,V) = \frac{1}{(2\pi)^{p/2}(\det V)^{1/2}} \exp\left[-\frac{1}{2}\gamma^T V^{-1}\gamma\right] \tag{6.28}$$

The $Pr(0)$'s are design parameters, detV is the determinant of V, and γ is a p-dimensional vector.

By determining which model has the largest probability, we are able to determine the correct underlying persistent rhythm pattern. Therefore, this Multiple Hypothesis Testing technique will enable us to perform both the detection and classification of the persistent arrhythmia classes we wish to detect. The structure of this method of approach is shown in Figure 6.1.

6.2 The Multiple Model Hypothesis Testing Algorithm

A program has been developed and tested for performing the multiple model hypothesis tests on the persistent rhythm classes, which include small variation, large variation, bigeminy and trigeminy. The dynamical models for these four classes are given in Chapter 5,

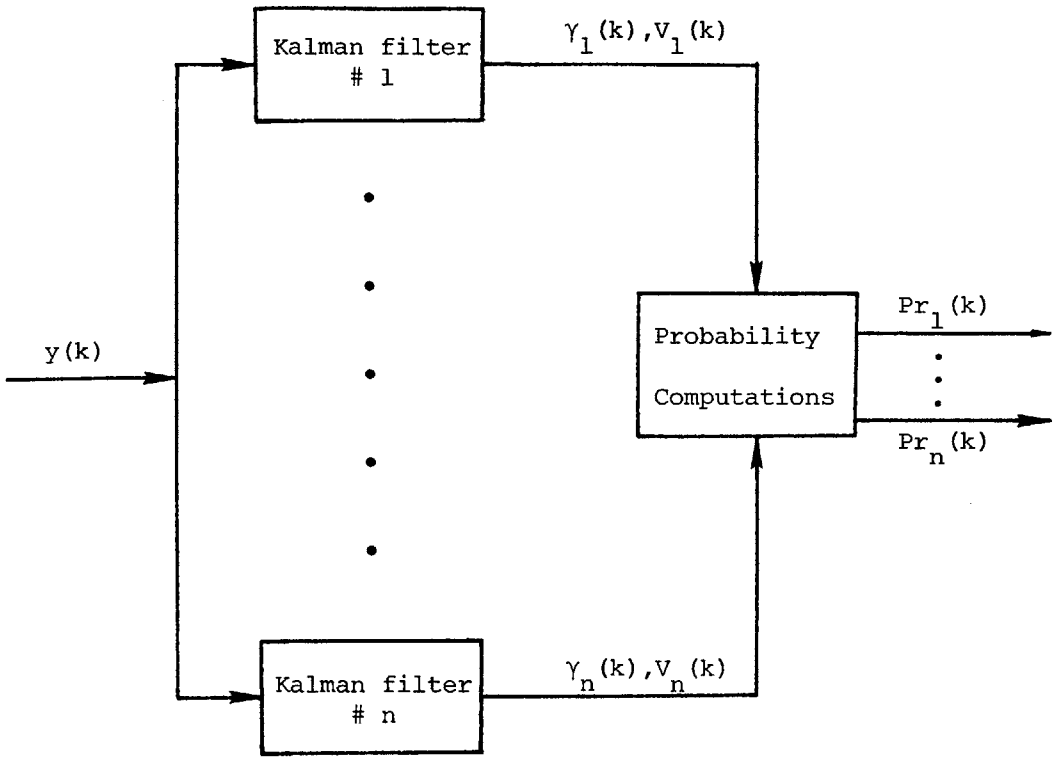

Figure 6.1 The Multiple Model Hypothesis Testing Structure

and the associated Kalman filter equations can be implemented using Equations (6.16) through (6.26). Using the R-R interval data as input, we can then compute the innovations, $\gamma_i(k)$, and the associated covariance, $V_i(k)$, for each of these four models from their Kalman filter equations. The probabilities that the R-R interval data being tested belong to different arrhythmic classes are then computed

recursively using Equations (6.27).

In practice, we want our multiple hypothesis testing system to lock onto the correct model as fast as possible, i.e., we wish to achieve the detection and classification of the underlying persistent rhythm for the R-R interval data being tested using as few R-R intervals as possible. However in some cases, after the system has locked onto a persistent underlying rhythm, the probability, Pr (k), that this underlying rhythm model is the correct one can be very large, hence the probabilities for the other models to be true are very small. In this case, if there is a sudden change of the rhythm pattern in the R-R interval sequence being tested, our system will respond to this change by adjusting the probabilities. However, this adjustment is slow according to Equation (6.27), since Pr(k+1) is proportional to Pr(k), which can be very small. Therefore in order to improve the adaptability of the filters in our system, both upper and lower bounds should be put on the probabilities. An upper bound of 97%, and a lower bound of 1% are used for all probabilities, with the constraint that the sum of all the probabilities is 100%.

Although for given initial error covariance matrices and measurement noises the filter gain sequence associated with each rhythm models can be computed "off-line" using Equations (6.22) through (6.26), in order to study the effects on the response of the system for different values of initial error covariances and measurement noises we will compute all the gians "on-line" instead.

Due to the fact that the gains of the Kalman filters will decrease monotonically with time, a sudden change of the R-R interval data (for instance, R-R interval data which starts with trigeminy, and suddenly switches to regular rhythm) will not be rapidly adapted to by the filters. In order to overcome this difficulty, we have to be able to detect the sudden changes and reinitialize the probabilities and filter parameters, which include initial error covariance matrices, measurement noises and overall mean values of the R-R intervals. The easiest way to detect a sudden change is to set a threshold on the factor $\gamma^2(k)/2V(k)$ of the most probable model. Here, the most probable model is defined as the one with probability greater than 80%. After a sudden change has been detected, a reasonable period of time should pass before searching for the next sudden rhythm change, since, as mentioned above, a sudden rhythm change will not be adapted to rapidly by the filters. That is, this threshold test is good only when the multiple model filter has been locked onto the correct model.

As we have mentioned earlier in this section, we wish to achieve the detection and classification of the underlying persistent rhythm for the R-R interval record being tested using as few R-R intervals as possible. However due to the fact that the process equation for bigeminal and trigeminal rhythms can also be used to describe the R-R interval pattern for a small variational rhythm, the a posteriori probabilities for both bigeminal and trigeminal filters are too high in the presence of a small variational underlying rhythm. This will result in a low detection and classification rate for small variational

underlying rhythms (see experimental results in Section 6.3). In this case all components of the filter states are about the same, which would indicate that a small variational rhythm is present. Therefore a test incorporating the differences between filter states to aid in the discrimination of small variational rhythms is developed and implemented as follows:

First, we compute

$$\Delta B = \frac{|\hat{x}_b^1(k|k) - \hat{x}_b^2(k|k)|}{MAX(\hat{x}_b^1(k|k), \hat{x}_b^2(k|k))} \tag{6.29}$$

and

$$\Delta T = \frac{|\hat{x}_t^1(k|k) - \hat{x}_t^2(k|k)| + |\hat{x}_t^2(k|k) - \hat{x}_t^3(k|k)| + |\hat{x}_t^3(k|k) - \hat{x}_t^1(k|k)|}{MAX(\hat{x}_t^1(k|k), \hat{x}_t^2(k|k), \hat{x}_t^3(k|k))} \tag{6.30}$$

where $\hat{x}_b^i$ and $\hat{x}_t^i$ are the ith components of the filter state estimates for the bigeminal and trigeminal models, respectively.

If $\Delta B(\Delta T)$ is small, we know that the underlying rhythm is not bigeminy (trigeminy). Therefore the a posteriori probability for the bigeminal (trigeminal) model computed using Equation (6.27) should be reduced. However if $\Delta B(\Delta T)$ is fairly large, which is indicative of a bigeminal (trigeminal) rhythm, no reduction on the a posteriori probability for the bigeminal (trigeminal) model is needed. Thus Equation (6.27) is modified as follow for the a posteriori probability computations.

$$Pr_j(k) = \frac{N(\gamma_j(k), V_j(k)) Pr_j(k-1) C_j}{\sum_{i=1}^{4} N(\gamma_i(k), V_i(k)) Pr_i(k-1) C_i} \qquad (6.31)$$

where i=1,...4 are for small variation, large variation, bigeminy, and trigeminy, respectively. The values for C_1 and C_2 are both set equal to 1, and the values for C_2, and C_4 for different values of ΔB and ΔT are given in Tables 6.1, and 6.2.

ΔB	C_3
≤ 0.1	0.2
>0.1 and <0.3	$0.2 + 4(\Delta B - 0.1)$
≥ 0.3	1.0

Table 6.1 The values of C_3 as a function of ΔB

ΔT	C_4
≤ 0.5	0.2
>0.5 and <0.8	$0.2 + \frac{8}{3} (\Delta T - 0.5)$
≥ 0.8	1.0

Table 6.2 The values of C_4 as a function of ΔT

A detailed description of the algorithm is given in the following, and a flow chart of this program is shown in Figures 6.2(a) and 6.2(b). This program can not only accept real R-R interval data, but also has the ability to generate artificial data for testing purposes. The filter parameters and initial probabilities for all four models are read in first. Reading in zero for the initial error covariance of the regular rhythm will terminate the program. The data code IRCODE, which indicates what type of data is being used, is then read in. The codes for different data types are given in Table 6.3. If IRCODE is not equal to 9 more information is needed in order to generate R-R interval data. Before generating a new R-R interval, the total number of R-R intervals required , NRR, is checked. An R-R interval is then generated according to the data code specified.

IRCODE	TYPE OF DATA
1	Generate small or large variation data according to the variance and the R-R intervals mean value specified
2	Generate bigeminal data
3	Generate trigeminal data
9	Use real data

Table 6.3 Data Codes and Types of Data Used in Multiple Hypothesis Testing Program.

For IRCODE equal to 9, a real R-R interval is read in directly. The end of the data is indicated by a zero R-R interval. After all the

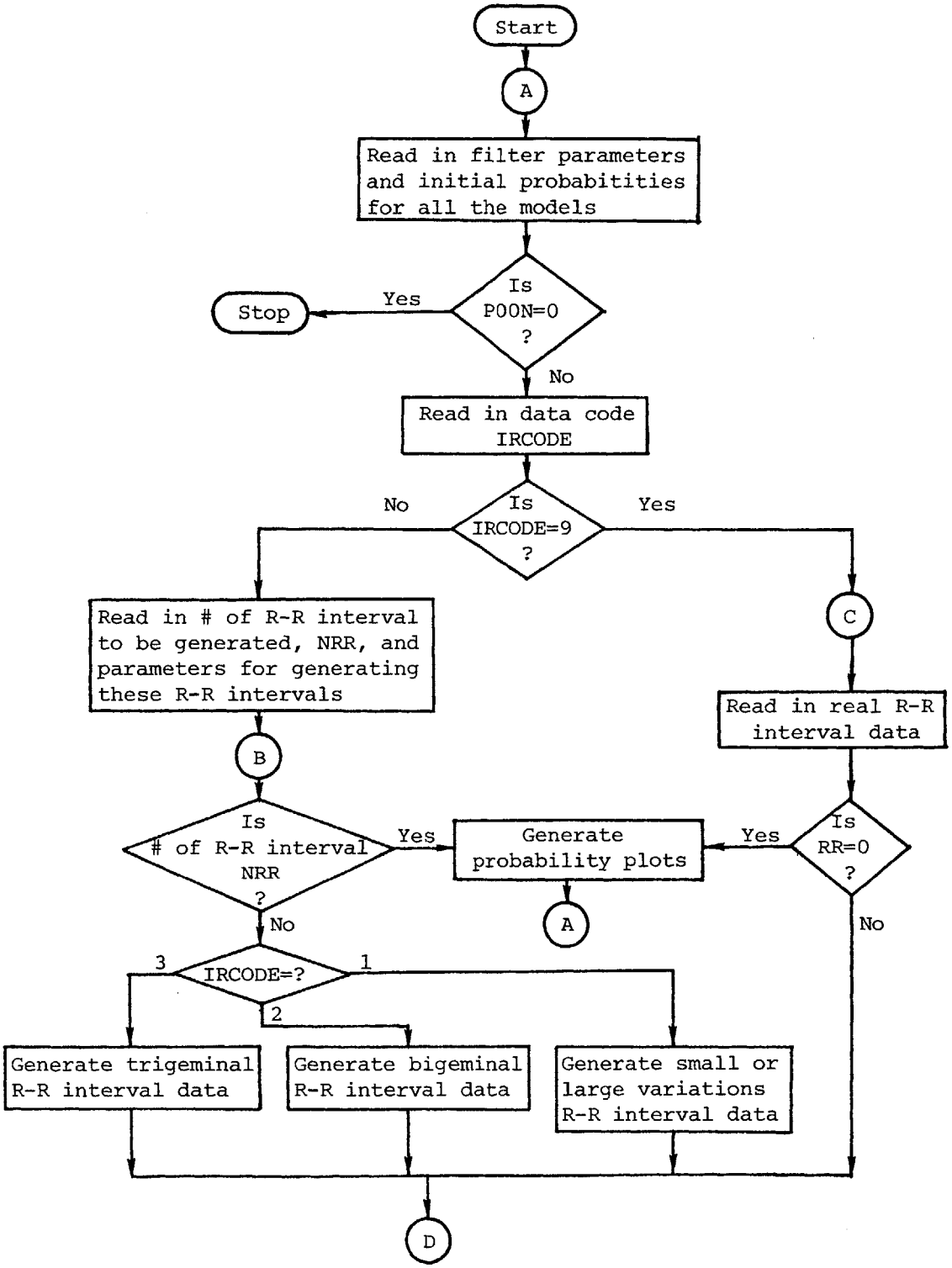

Figure 6.2(a) Flow Chart of Multiple Hypothesis Testing Algorithm

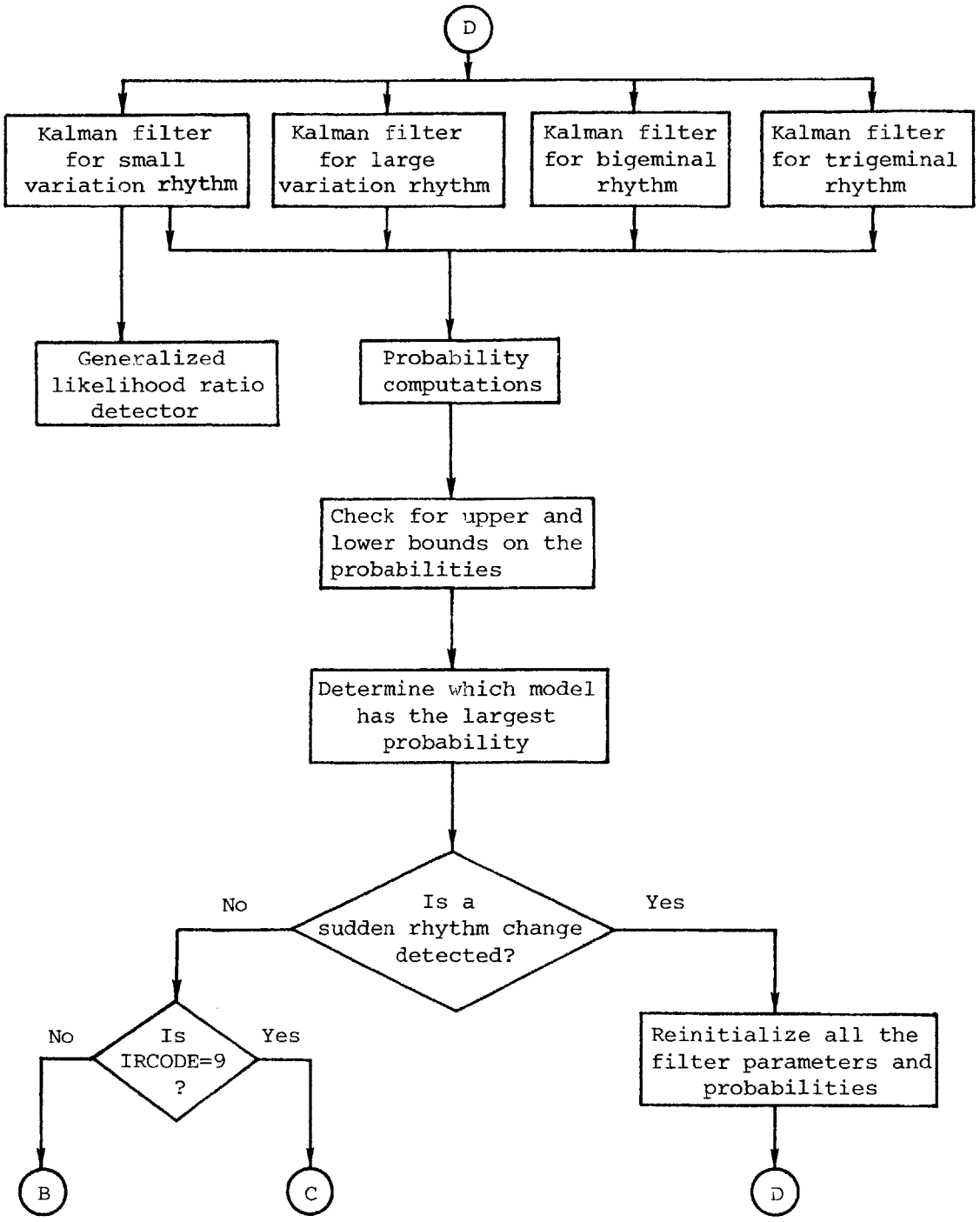

Figure 6.2(b) Flow Chart of Multiple Hypothesis Testing Algorithm

R-R intervals are processed, a probability plot will be generated. For each new R-R interval, the Kalman filters for small variation, large variation, bigeminy, and trigeminy will run in parallel, and the innovations and associated covariances are computed. The probabilities are then calculated, based on the outputs from the Kalman filters. Note that the outputs from the Kalman filter for small variation rhythm is also used as the input to a generalized likelihood ratio detector, which is used to detect the transient rhythms and is discussed in Chapter 7. Next the probabilities are checked against the upper and lower bounds. After the most probable model has been decided upon, a search for sudden rhythm changes of the R-R interval data can be made. Once a sudden change is detected, all the filter parameters and probabilities are reinitialized, and the probabilities are computed again. If no sudden change is detected, the program will continue and will read in the next R-R interval.

6.3 Experiments and Results

The algorithm described in Section 6.2 was tested on the available R-R interval data files. The objective of this test was to determine whether the multiple model hypothesis testing algorithm described in Section 6.2 could detect and classify the arrhythmic R-R interval data files being tested. We also wished to find a best set of filter parameters and initial probabilities for all four models, such that the multiple hypothesis testing program would detect and classify the R-R interval data file being tested in the

shortest time. Finally, we wished to test the filter adaptability to the R-R interval data when the input rhythm pattern is suddenly switched. In this set of tests, we used data files IN.5 and IN.30 as small variational data, CUNATFIB as large variational data, HUANPVCS as trigeminal data, and data file #503 as bigeminal data. For each of these data files only the first twenty R-R intervals were used in testing the multiple hypothesis testing algorithm. The mean value, variance, and standard deviation of these twenty R-R intervals for each of these data files are given in Tables 4.3, 4.5, 4.6 and 4.9, and are summarized in Table 6.4 for convenience. Using these actual R-R interval data, a series of tests were made.

Data File Name	Mean	Variance	Standard Deviation
IN.5	181.85	20.03	4.48
IN.30	233.95	57.63	7.59
CUNATFIB	116.05	292.05	17.09
#503	204.40	5486.97	74.07
HUANPVCS	141.60	2276.99	47.72

Table 6.4 Statistics of the Data Files Used in Testing the Multiple Hypothesis Testing Algorithm

The results are given in Figures 6.3-6.59. In the figures, the a posteriori probability of each of the four possible persistent rhythm states, namely, small variation, large variation, bigeminy, and trigeminy, is plotted vs. time. The time is not explicitly given, rather, the locations of the fiducial points of the QRS complexes are shown and the R-R intervals are printed along the time axis.

One of the most important aspects of the filter design and subsequent a posteriori probability computations is the sensitivity of the filter performance to parameter variations. It is desirable that the detection performance be relatively unchanged over a wide range of variation of filter parameters, so that the filter can be used with confidence. Thus, a nominal set of filter parameters was selected first, based on the statistical results given in Chapter 4 and a series of tests were then made to: (1) study the effects of filter performance to parameter variations about these nominal values, (2) determine a best set of filter parameters. The design parameters for the multiple hypothesis testing filter were the initial error covariance P(0), initial estimate of the mean R-R interval $\hat{x}(0|0)$, the a priori probability Pr(0), and the measurement noise variance R for each of the four persistent rhythm models.

The heart rate is determined by the rate at which the SA node initiates the depolarization pulses, and in general this rate is approximately equal to 75 beats per minute. For a data sampling rate of 250/sec, this is equivalent to an R-R interval of 200 sampling

points. Therefore the initial estimate of the mean of the state, denoted by x_0 in the figures, for all models were set equal, with a nominal value of 200. Since we have no a priori information as to which of the possible persistent rhythm classes the data file being tested belongs; the initial probabilities, $Pr_j(0)$, $j=1,\ldots,4$, were all set equal, with a value of 0.25 such that the sum of all probabilities is 1. In other words, this is to say that for any given data file it is equal likely that this file is any one of the four possible rhythm states. Although it is not true that 1/4 of all records are bigeminal or trigeminal, it is our feeling that one does not wish to bias the test against such rhythms. This essentially reflects a maximum likelihood philosophy as opposed to the use of unequal a priori probabilities. Of course the approach is quite flexible in that these initial probabilities can be chosen to reflect patient history.

The variances of measurement noise R_s, R_ℓ were set to 64,400, respectively for small, and large variational rhythms according to the statistical results given in Tables 4.3-4.6. The values for bigeminy (R_b) and trigeminy (R_t) should be the same and equal to that for the small variational rhythm, which was 64, according to the statistical results given in Tables 4.35 and 4.36. The initial error covariance matrix in all cases had equal diagonal elements, denoted by P_0 in the figures, with a nominal value of 1600 to reflect the possible large error in initial state estimate (see Equation (6.4)). All off-diagonal elements, P_{ij}, $i\neq j$, were set equal to each other with a value of 0 chosen to reflect the insignificant correlations

in the components of the error of the state estimate. The results of the multi-filter performance (as measured by the conditional probabilities) using this set of filter parameters are given in Figures 6.3-6.7. In these figures, all the data were clearly identified by the high a posteriori probabilities associated with the correct rhythm patterns.

For the two normal rhythms tested (Figures 6.3, 6.4), the a posteriori probability of each of the four possible rhythm states were approximately equal at k=1. Since at this point only one R-R interval was given, there was not enough information to determine anything about the data. However observe the behavior of the probabilities after 2nd data point, which had a value close to the first, was read in; because of the samll variation of this first two data points, the a posteriori probability for the small varitional rhythm became larger than the others. As more data points were available, the a posteriori probability of the small variational rhythm became even larger - i.e. we are more confident in our decision of identifying the correct rhythm state.

At k=1 in Figure 6.5, the a posteriori probability for large variational rhythm was larger than others. This is not surprising however, because of the fact that the filter initial state estimates were set at 200, which was way off the first data point (101), the large variational rhythm was favored more than others. Such transients due to initial conditions must be dealt with via an effective initialization

procedure, perhaps involving a preliminary scan of the first few R-R intervals. As more data became available, the probability of large variation started building up. However, because the variance of the R-R intervals at each time k up to k=7 were not large (see Table 4.6), the probability of small variational rhythm did not drop to the preset lower limit of 1% very fast, and thus made the detection of the large variational rhythm slower. Note also that a jump of the probability for bigeminy was seen at k=3. This was explained by the fact that the R-R interval sequence 101, 124, 99, could very well be a bigeminal pattern.

In Figure 6.6, a bigeminal data file #503, was tested. Again no diagnostic information was available at k=1, but at k=2, because the large separation of these two data points (which has a variance of 8192, see Table 4.9), only bigeminy and trigeminy were likely (the large variational rhythm does not have this much variation). In fact these two patterns have equal probabilities (since we need at least a third beat to distinguish between bigeminy and trigeminy). As the third interval (128) was read in, the bigeminal pattern begins to emerge, and this was indicated by the dramatic jump of the a posteriori probability for bigeminy from approximately 50% to over 90%. The preset upper limit of 97% was reached at the fourth beat.

For HUANPVCS (Figure 6.7), a sudden jump of the probability for large variation was observed at k=2; this was due to the variance (which was 1152, see Table 4.7) which made the large variational rhythm more favorable. At k=3, the only possible rhythm would be trigeminy, and this was clearly indicated by the 97% a posteriori probability in

Figure 6.7.

Next, two sets of tests were made by setting the variance of measurement noise for both bigeminy and trigeminy to 100, and 400, respectively. The motivation for these tests was that the a posteriori probability of bigeminy was quite high even in the case that the data file being tested was a normal rhythm (see Figures 6.3, and 6.4), which did not have any periodic bigeminal pattern. One possible reason for this was the equal noise variance, which was set at 64, for both bigeminy and small variation. Therefore we would like to increase the noise variance for both trigeminy and bigeminy; hopefully this would reduce the a posteriori probability of bigeminy and improve the detection performance in the case that the underlying rhythm pattern is small variation. Note also that it seems reasonable to expect larger fluctuations in bigeminy and trigeminy due to the instability of the ectopic foci. The resulting a posteriori probability plots for R_b=100 are given in Figures 6.8-6.12.

These results showed that the detection performances for the two normal rhythm data files, IN.5 and IN.30, were improved (Figures 6.8, 6.9) by the amount that the a posteriori probability of bigeminy was reduced, and the performances for the other three data files, namely, CUNATFIB, #503, and HUANPVCS were essentially unaffected (see Figures 6.10-6.12). However for R_b=400, although the performance for normal rhythm was further improved (see Figures 6.13,6.14), the performance of the other three were degraded as shown in Figures 6.15-6.17 (compared to Figures 6.10-6.12 respectively). Thus a noise variance of 100 was set for both bigeminy and trigeminy in the subsequent tests.

The diagonal elements of the initial error covariance matricies were next varied, while keeping them equal for all filter states. Two sets of tests were made, one with a smaller error covariance which was set at 64, and the other with larger value, which was set at 10,000. As these values increase, the filter gains also increase, reflecting the additional weighting to be given to the data relative to the a priori information. The resulting a posteriori probability plots for P_0=64 are shown in Figures 6.18-6.22. Both of the two normal rhythm data files were correctly identified (see Figures 6.18, 6.19); however their detection rate were much slower than those with the error covariance of 1600. The large initial a posteriori probability for large variation in Figure 6.19 was due to the small error covariance and the large deviation of the first data point from the given estimates of the mean of the R-R intervals. Thus we see that setting P(0) too small will make the filters quite sluggish (small gain) and will, in fact, accentuate unwanted transients.

For CUNATFIB (Figure 6.20), the large variational rhythm pattern was not clearly detected. For #503, and HUANPVCS (Figures 6.21,6.22), although the bigeminal and trigeminal pattern were detected, the performances were degraded. In all cases, except for CUNATFIB, the higher error covariance with value of 10,000 gave more rapid detection as shown in Figures 6.23, 6.24, 6.26, and 6.27. The detection performance of large variation (Figure 6.25) was degraded by this large initial error covariance (since the multifilter attributes the initial variation in the data to its large uncertainty in the estimate of x), and thus a compromise value of P_0=1600 appeared more suitable for

achieving best detection performance. (Note that if we used an initialization procedure based on the first few R-R intervals, we might be able to use a smaller initial covariance).

The effect of nonzero off-diagonal elements in error covariance matricies was studied, with all off-diagonal elements P_{ij}, $i \neq j$, set equal to each other, with a value of 20 chosen to reflect the possible small positive correlations in the components of the state estimate error. The results are given in Figures 6.28-6.32. By comparing these figures with those with a value of $P_{ij}=0$ (Figures 6.8-6.12), we see that a slightly better performance was obtained with $P_{ij}=0$.

The effect of varying the initial estimate of the mean R-R interval x_0 was studied next, with the resulting a posteriori probabilities given in Figures 6.33-6.42. For the two normal rhythms, the detection performance was essentially unaffected. However, trigeminy detection was best at $x_0=150$ (Figure 6.37), while large variation was best at $x_0=300$ (Figure 6.40). This is explained by the fact that the trigeminy value was close to the actual mean value (see Table 6.2). However, the large variation detection is degraded by a good a priori mean value estimate since this produces a small initial measurement residual.

We had tried to reduce the bigeminy and trigeminy a posteriori probabilities in the presence of normal rhythm by increasing the noise variance for both bigeminy and trigeminy from a value of 64 to 100, these probabilities were still quite high (see Figures 6.8 and 6.9).

In this case all components of the state estimates of both bigeminy and trigeminy are about the same, which would indicate that normal rhythm is present. A test was thus done incorporating the differences between bigeminy and trigeminy filter state components aid in the discrimination of normal rhythm. The results are shown in Figures 6.43-6.47. The detection performances for bigeminy and trigeminy were essentially unaffected. However the performance for the normal rhythms was improved with the use of state estimate information. Note that this problem stems from the fundamental indistinguisability of normal rhythm from bigeminy and trigeminy (equal component bigeminy and trigeminy look like a normal rhythm) and the above tests allow one to remove this difficulty.

One critical test of the multiple hypothesis testing algorithm is its ability to detect sudden switches of the underlying rhythm pattern. Six cases were selected for experimentation: (1) small variation (IN.5)→ large variation (CUNATFIB), (2) large variation (CUNATFIB)→ small variation (IN.5), (3) small variation (IN.5)→ bigeminy (#503), (4) bigeminy (#503)→ small variation (IN.5), (5) small variation (IN.5)→ trigeminy (HUANPVCS), (6) trigeminy (HUANPVCS)→ small variation (IN.5), and the results are shown in Figures 6.48-6.59. Filter parameters used were P_0=1600, P_{ij}=0, x_0=200, R_b=100. Both the non-reinitialization and reinitialization of the filter after detection of a switch of rhythm pattern were tested. In the filter reinitialization case, the gains and state estimate were reinitialized at the point where the switch was detected. An outlier test, $\gamma^2(k)/2V(k)$,

which is an effective test for distinguishing a piece of data from a particular ensemble, was used to detect rhythm switches. A rhythm switch is declared if $\gamma^2(k)/2V(k)>\varepsilon$, where ε is a positive valued threshold that represents the tolerance we are willing to accept before declaring a piece of data to be an outlier. It seems reasonable to assume that any data which has a deviation greater than two standard deviations will be an outlier. This gives the threshold ε a value of 2. For the data tested, this threshold value successfully detected all the rhythm switches. As seen in the figures, identification of rhythm switches was degraded without filter reinitialization, and fast and accurate with the reinitialization. Thus it is necessary to reinitialize the filter when a rhythm switch is detected.

Two other comments are necessary. First of all the use of this outlier test should be viewed as a temporary tool in detecting rhythm switches. As the results in the next chapter indicate, the GLR provides an excellent tool for the effective detection of sudden rhythm changes. Secondly, note the one example of a shift from large variation to small variation (Figure 6.51) involves a situation in which there is a large shift in the underlying mean value as well. This in fact makes detection much easier. If the two patterns had the same means, then an outlier test - which looks for a large deviation from the mean - would not work (since the shift is to a small variation rhythm at the same mean). This is a situation that merits study in the future.

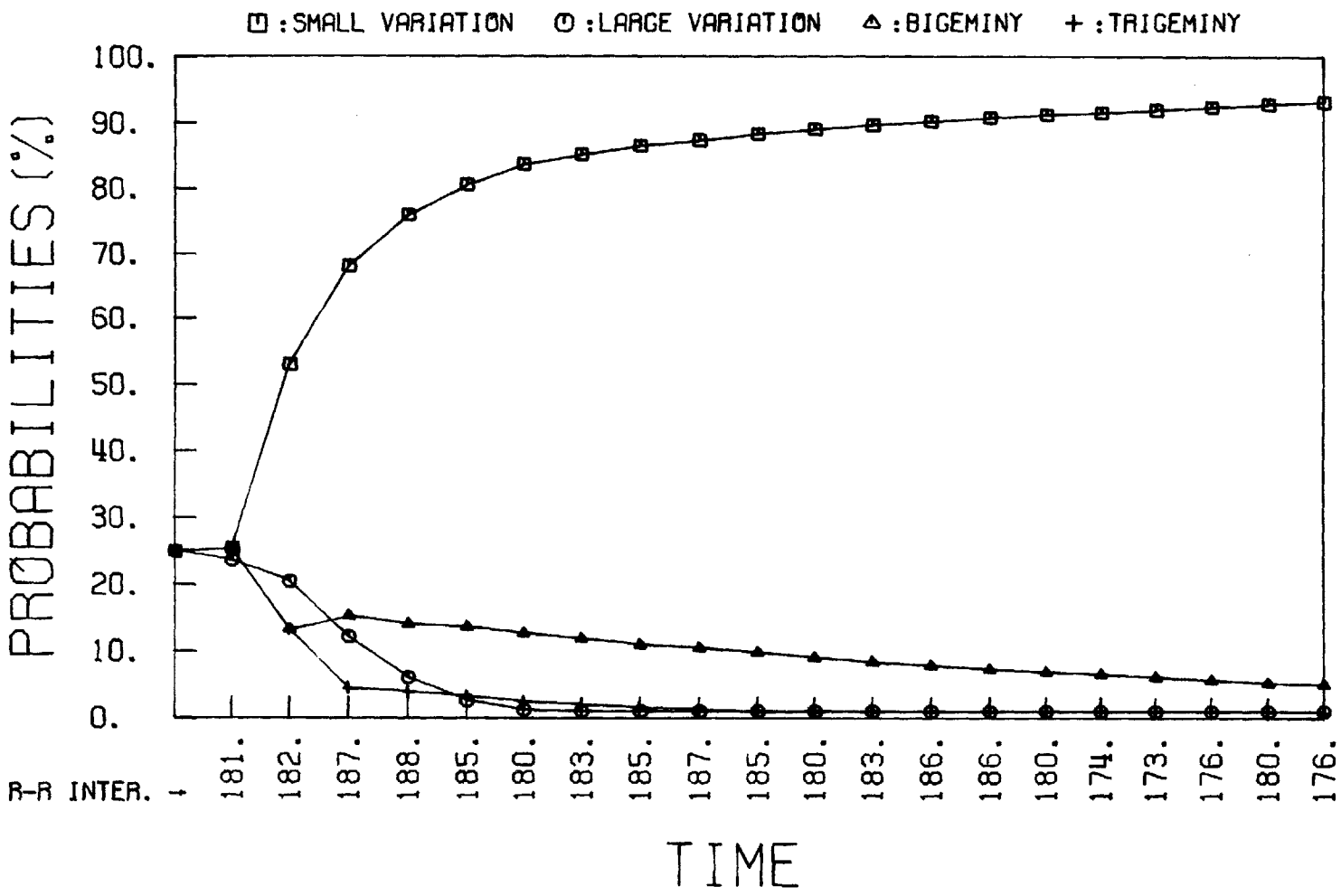

Figure 6.3 A Posteriori Probabilities of Data File IN.5 at P_0=1600, x_0=200, R_b=64

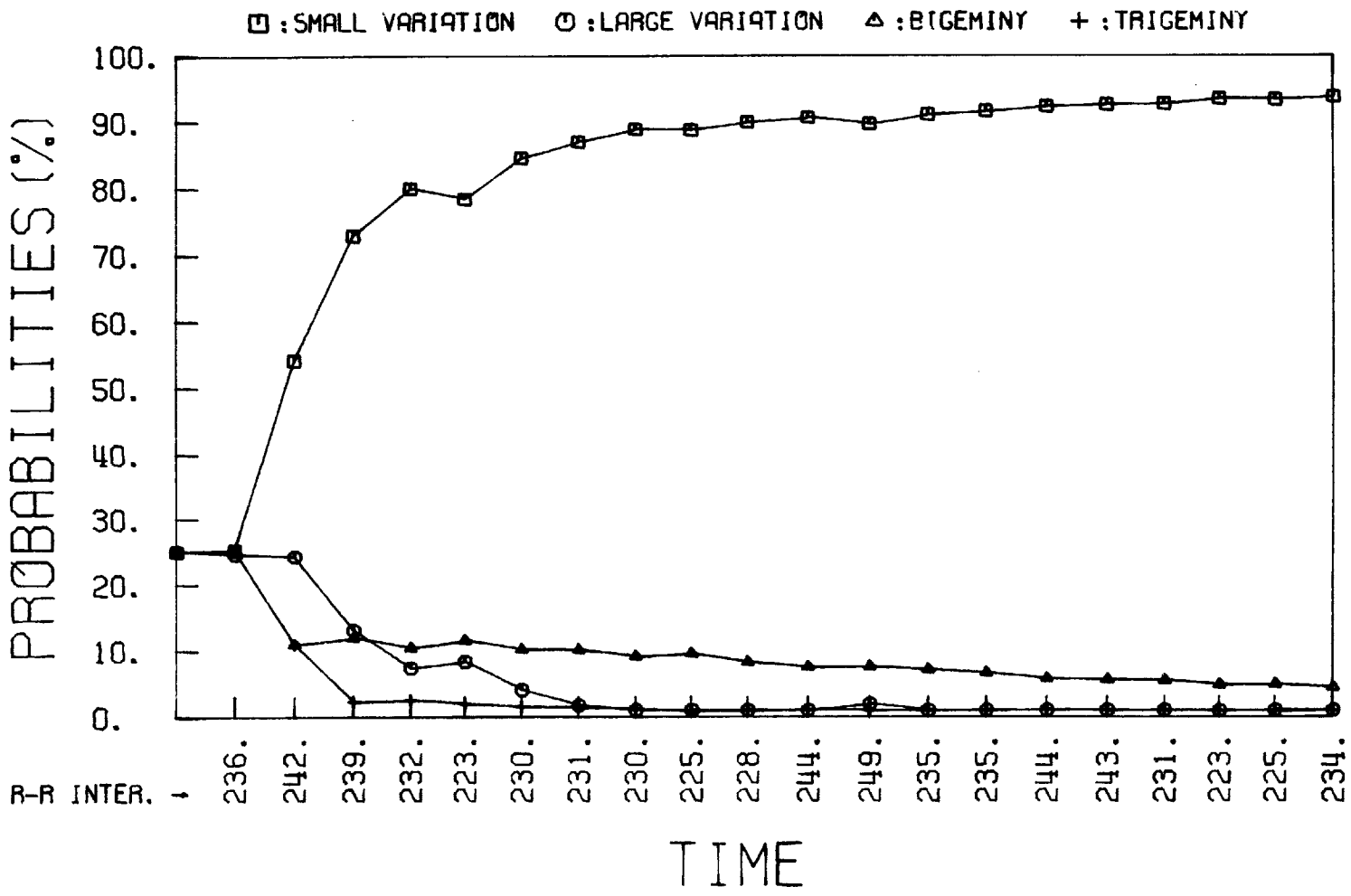

Figure 6.4 A Posteriori Probabilities of Data File IN.30 at P_0=1600, x_0=200, R_b=64

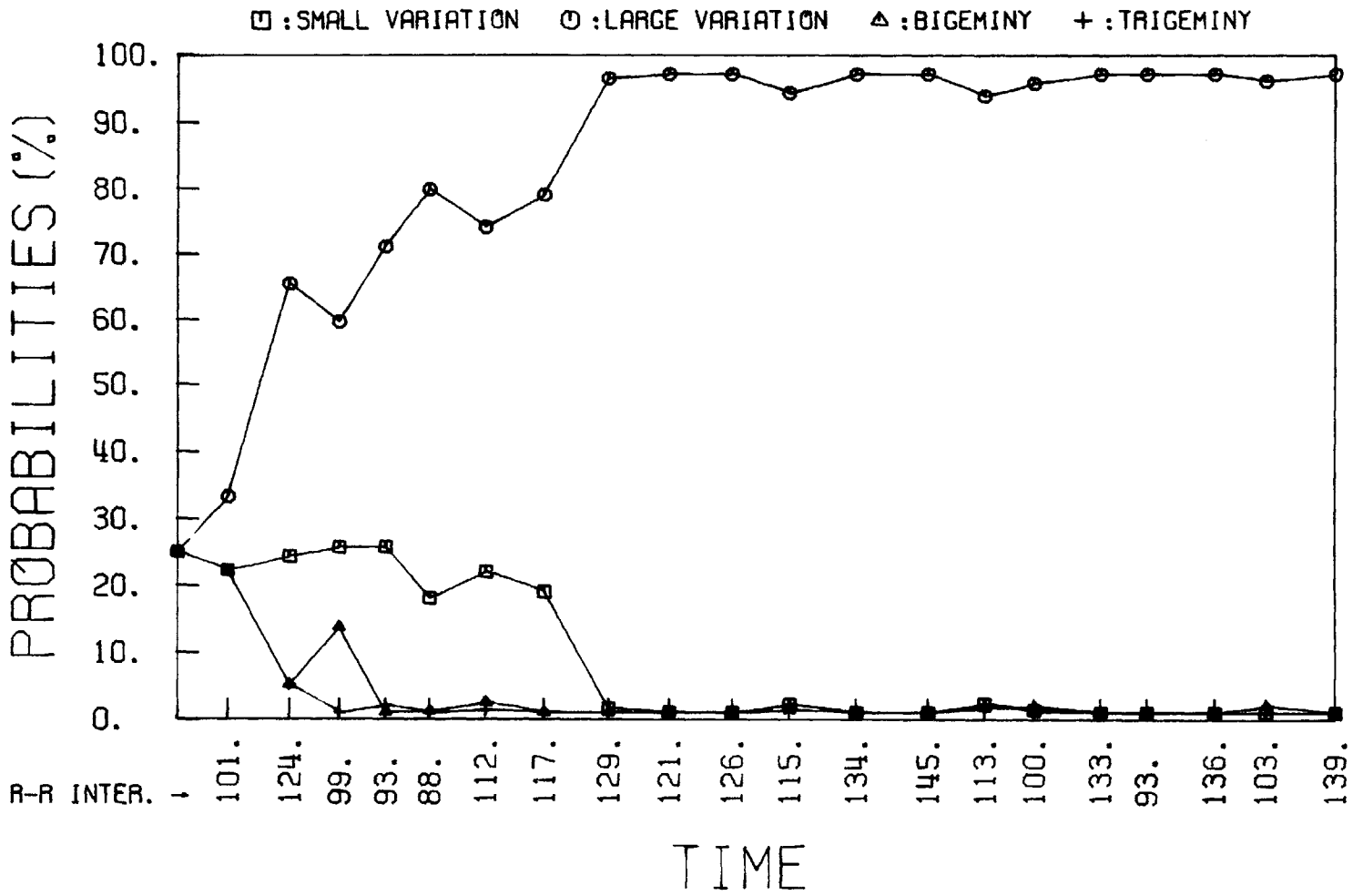

Figure 6.5 A Posteriori Probabilities of Data File CUNATFIB at P_0=1600, x_0=200, R_b=64

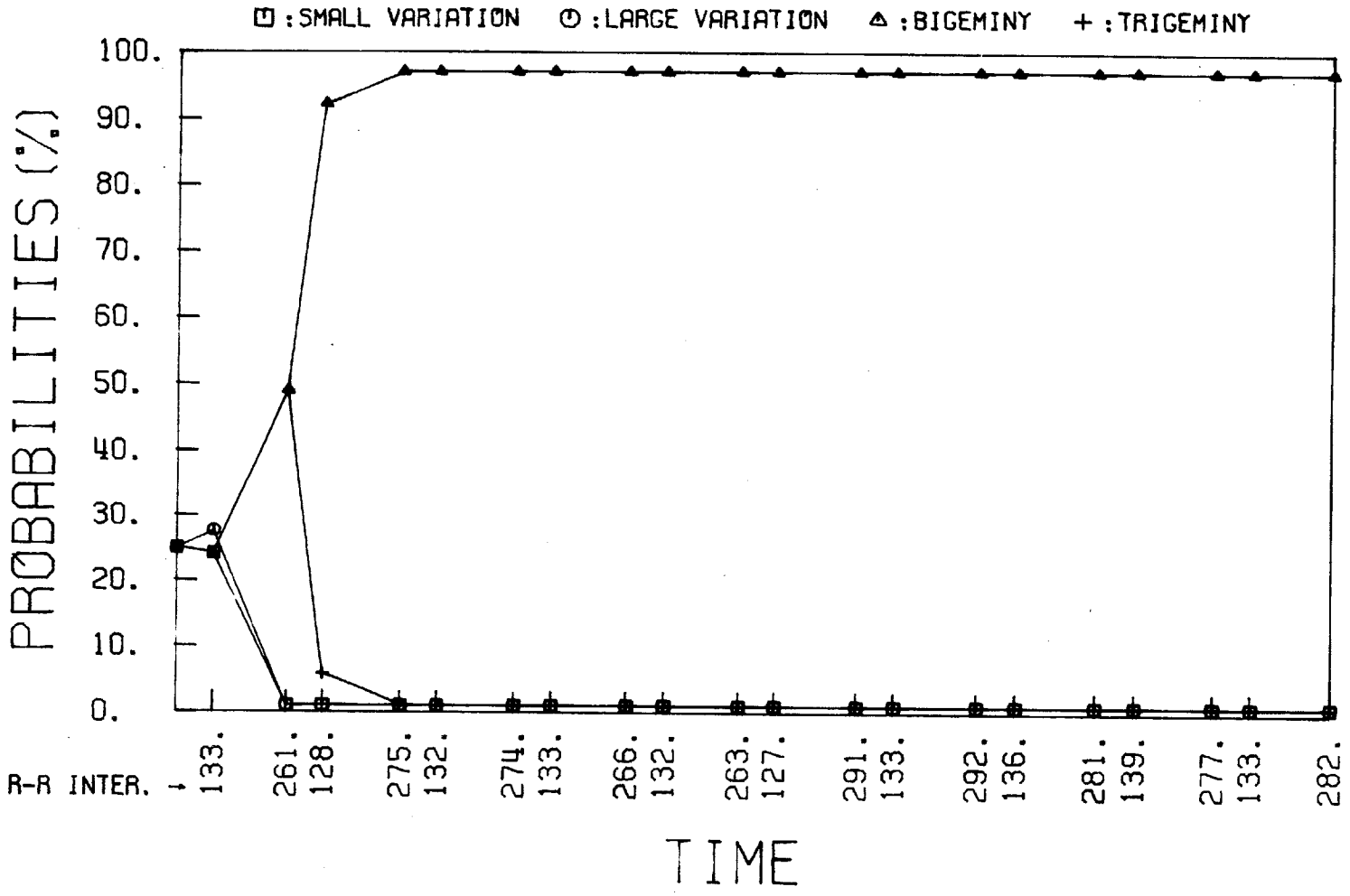

Figure 6.6 A Posteriori Probabilities of Data File #503 at P_0=1600, x_0=200, R_b=64

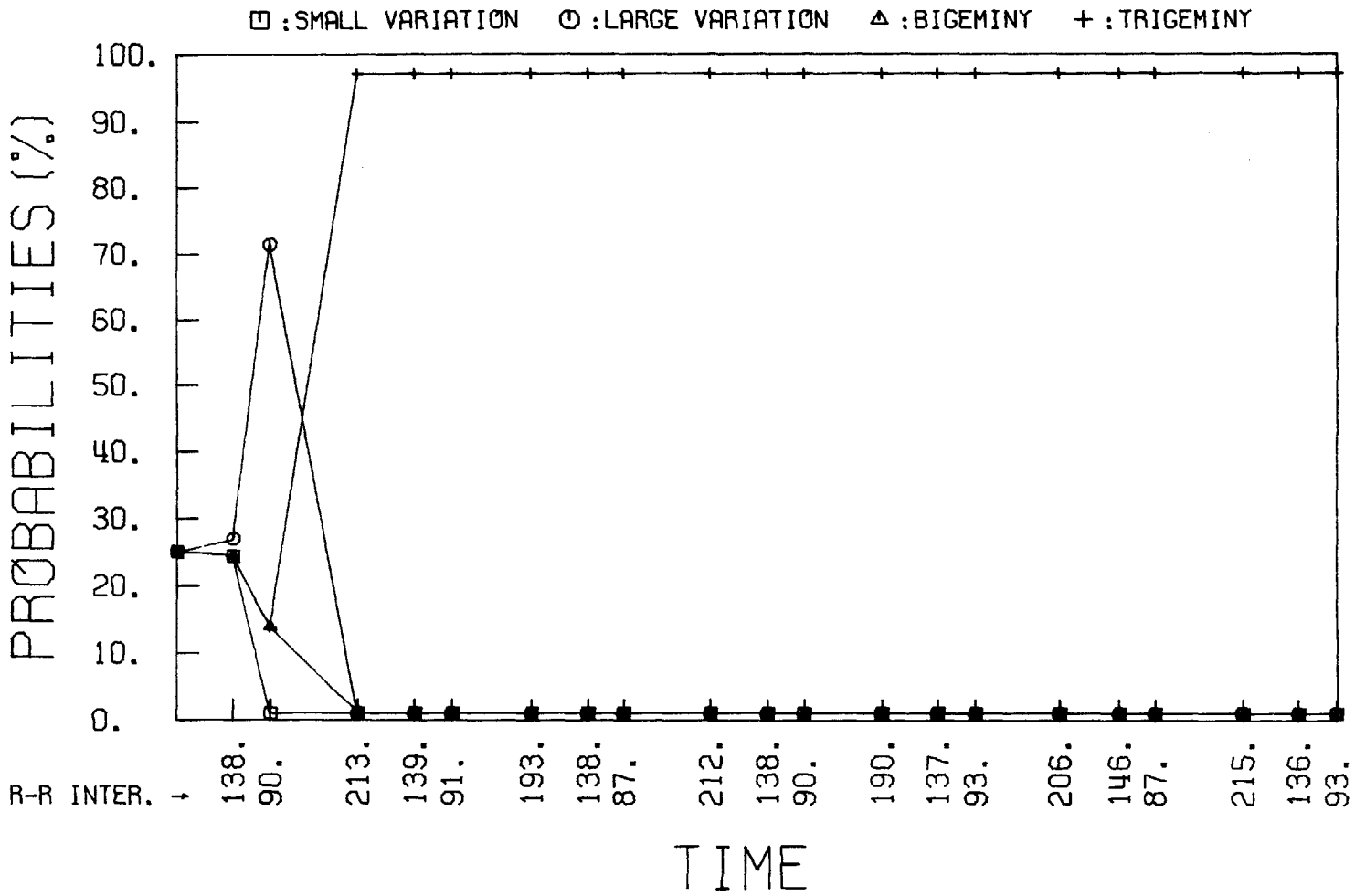

Figure 6.7 A Posteriori Probabilities of Data File HUANPVCS at P_0=1600, x_0=200, R_b=64

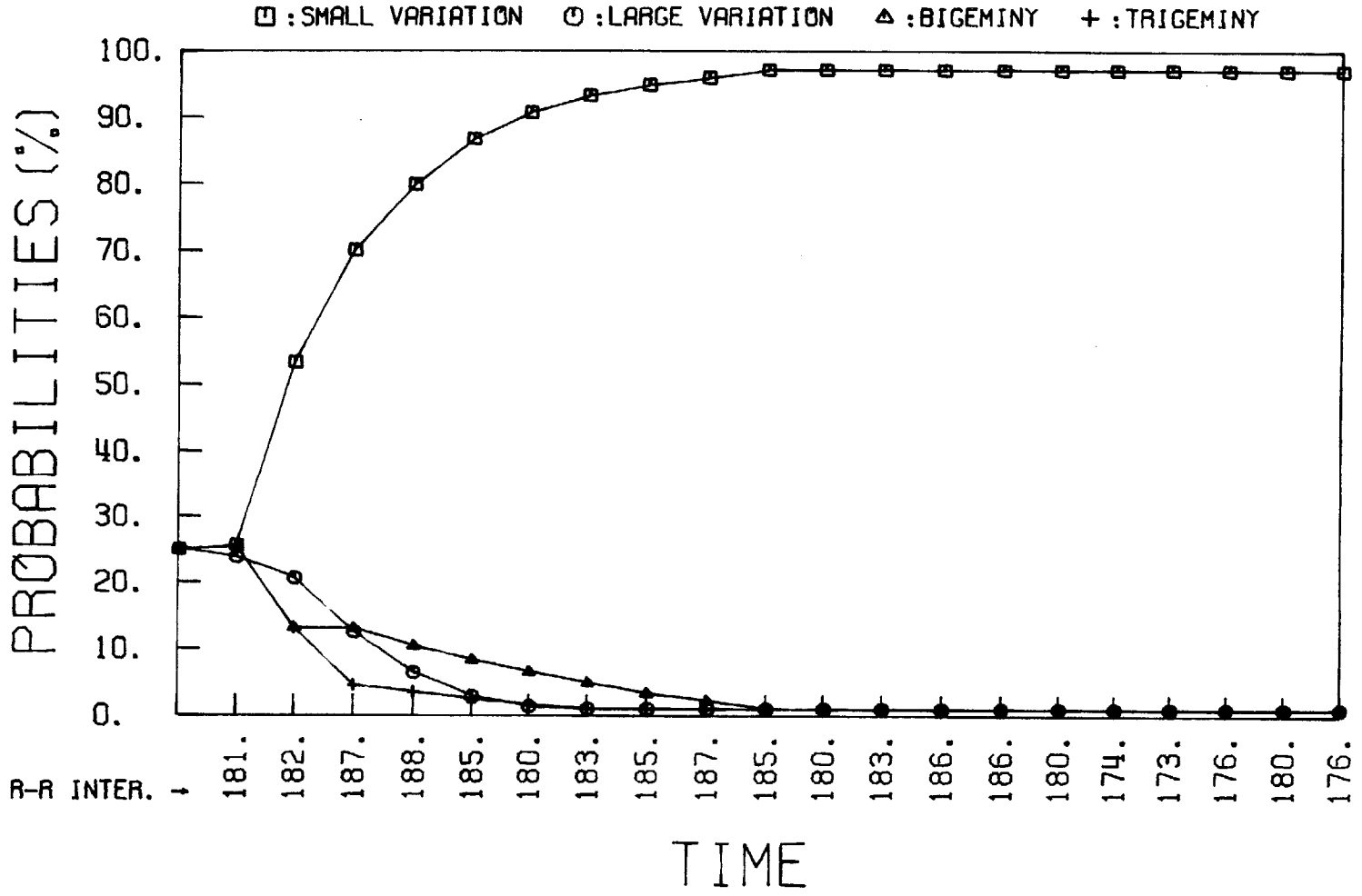

Figure 6.8 A Posteriori Probabilities of Data File IN.5 at P_0=1600, x_0=200, R_b=100

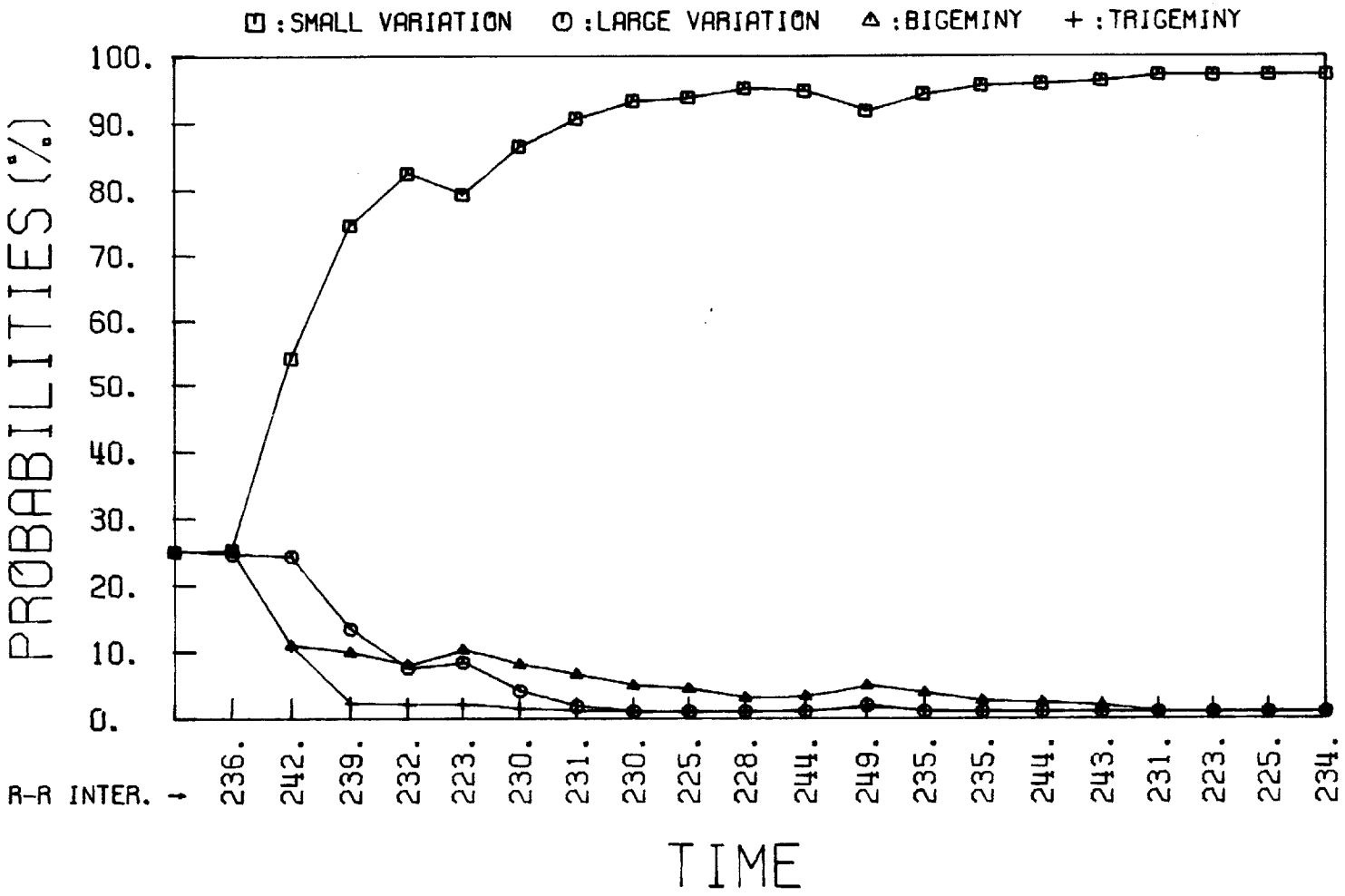

Figure 6.9 A Posteriori Probabilities of Data File IN.30 at P_0=1600, x_0=200, R_b=100

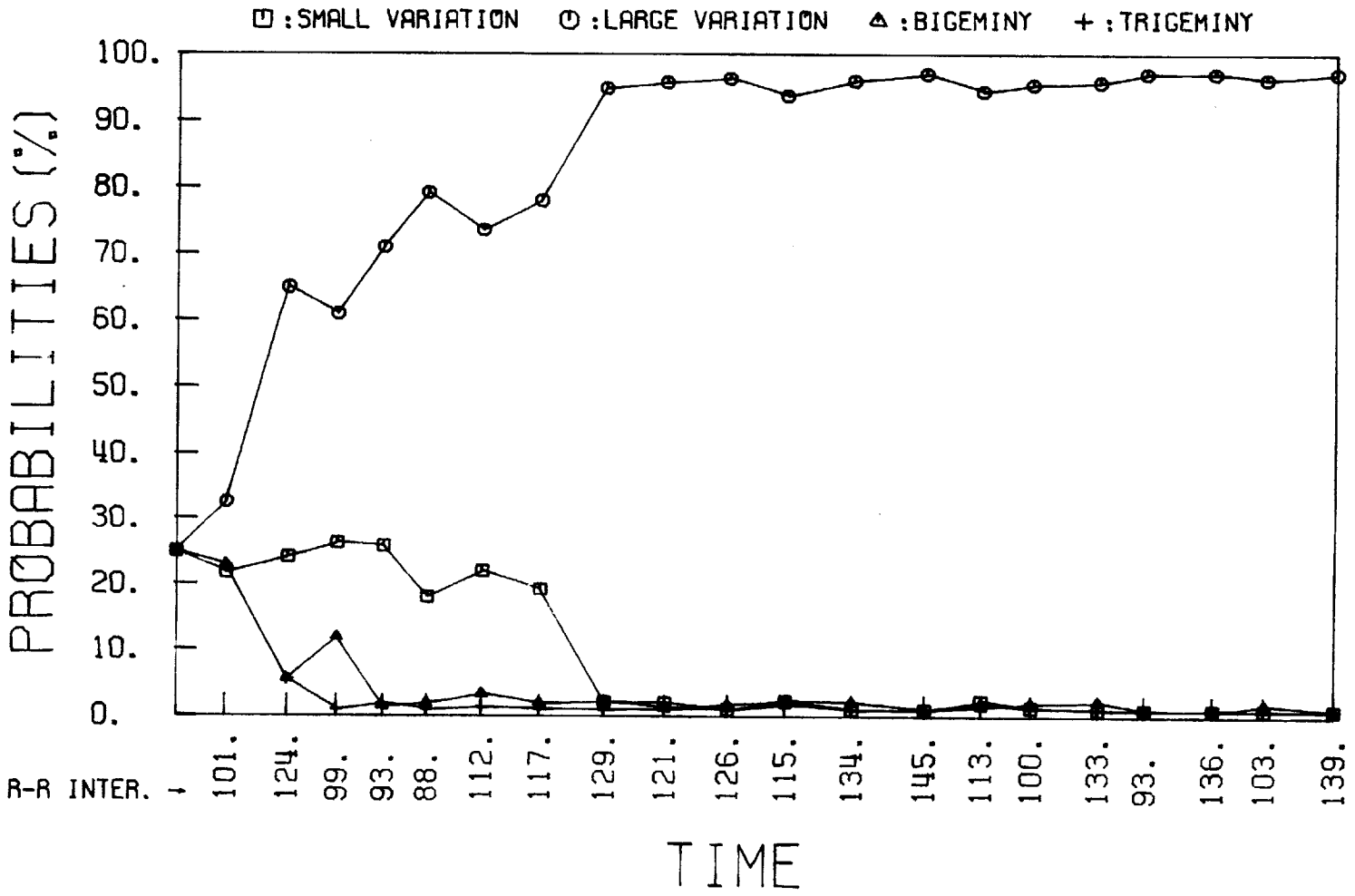

Figure 6.10 A Posteriori Probabilities of Data File CUNATFIB at P_0=1600, x_0=200, R_b=100

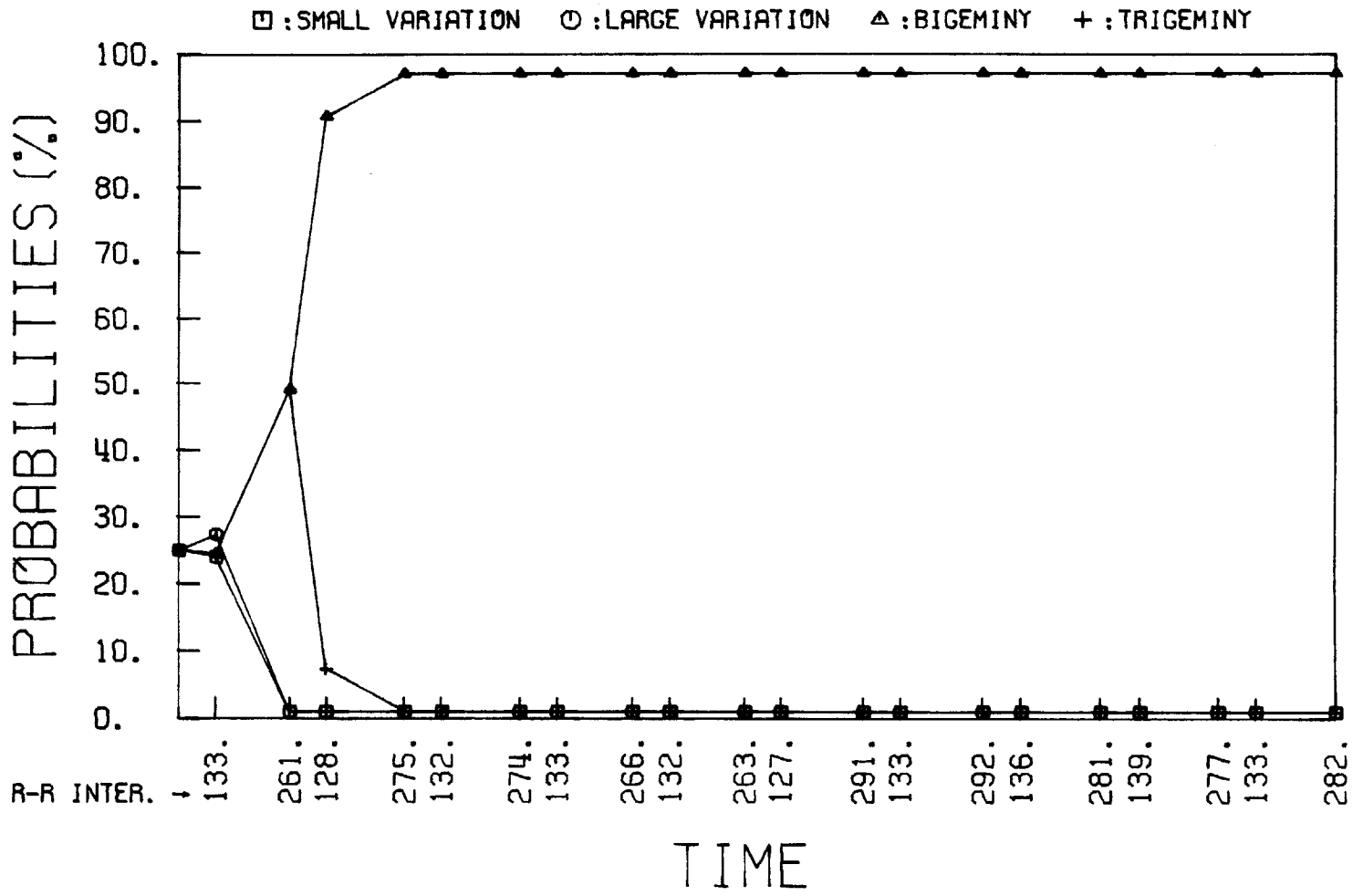

Figure 6.11 A Posteriori Probabilities of Data File #503 at P_0=1600, x_0=200, R_b=100

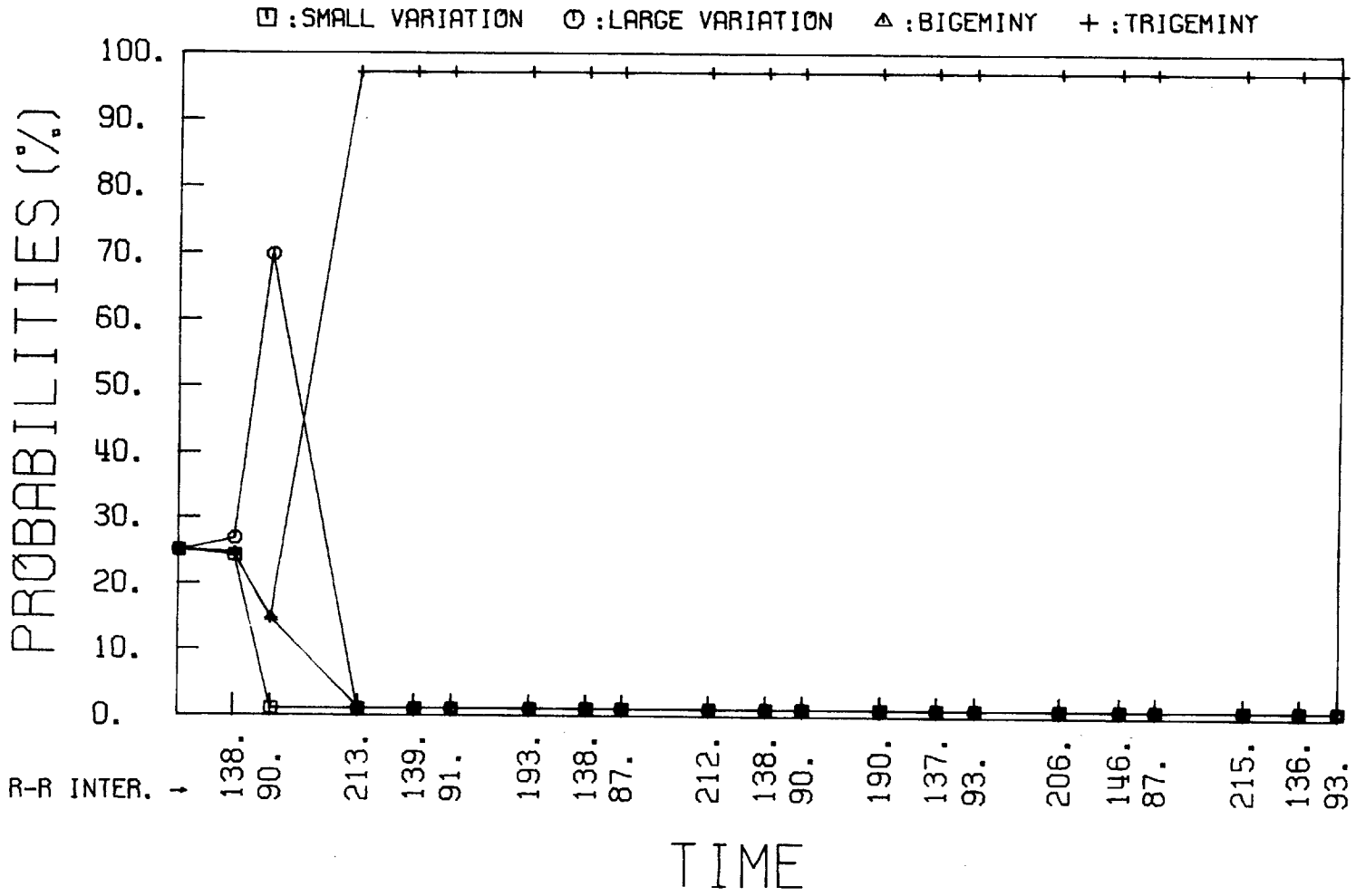

Figure 6.12 A Posteriori Probabilities of Data File HUANPVCS at P_0=1600, x_0=200, R_b=100

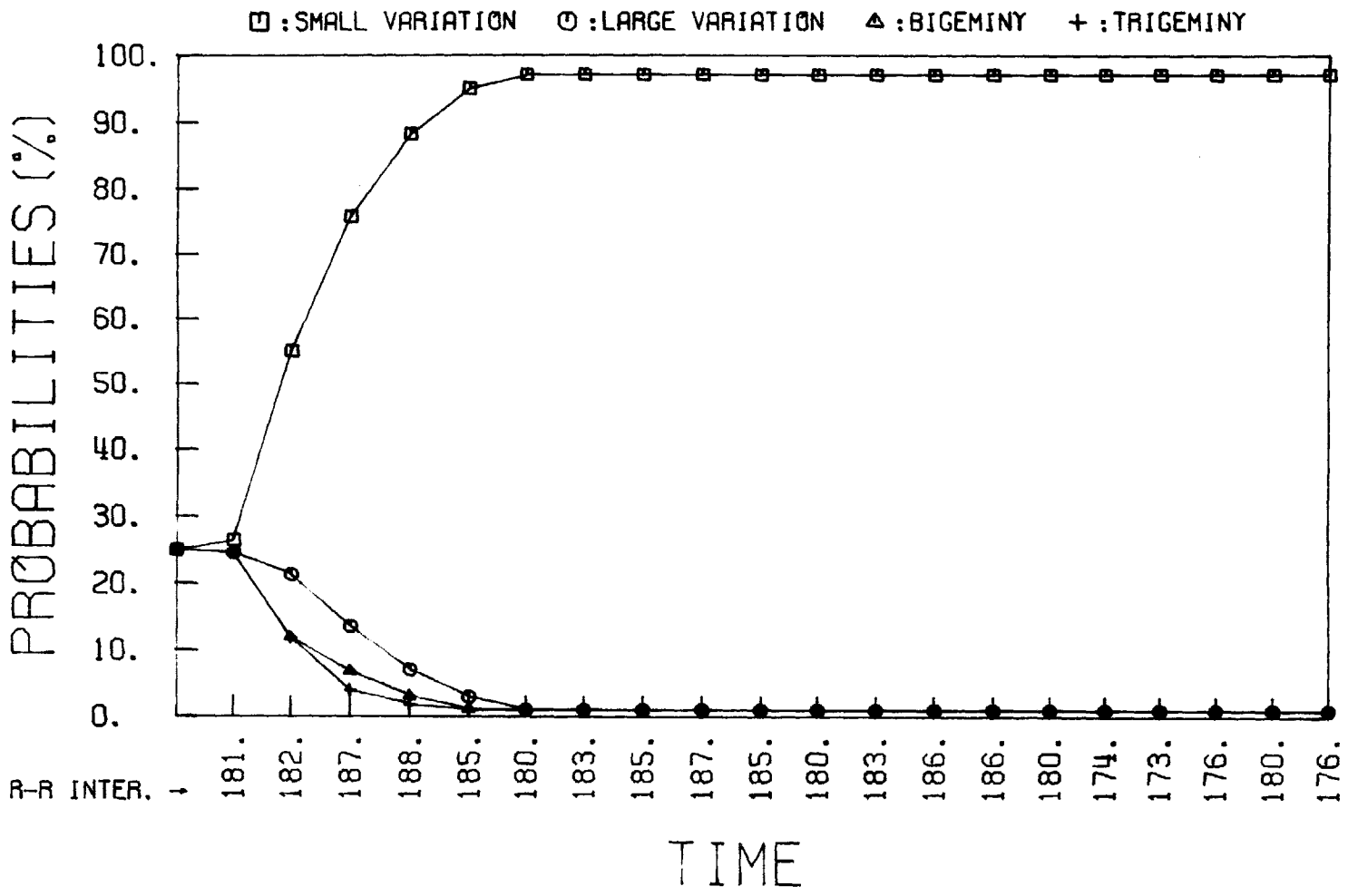

Figure 6.13 A Posteriori Probabilities of Data File IN.5 at P_0=1600, x_0=200, R_b=400.

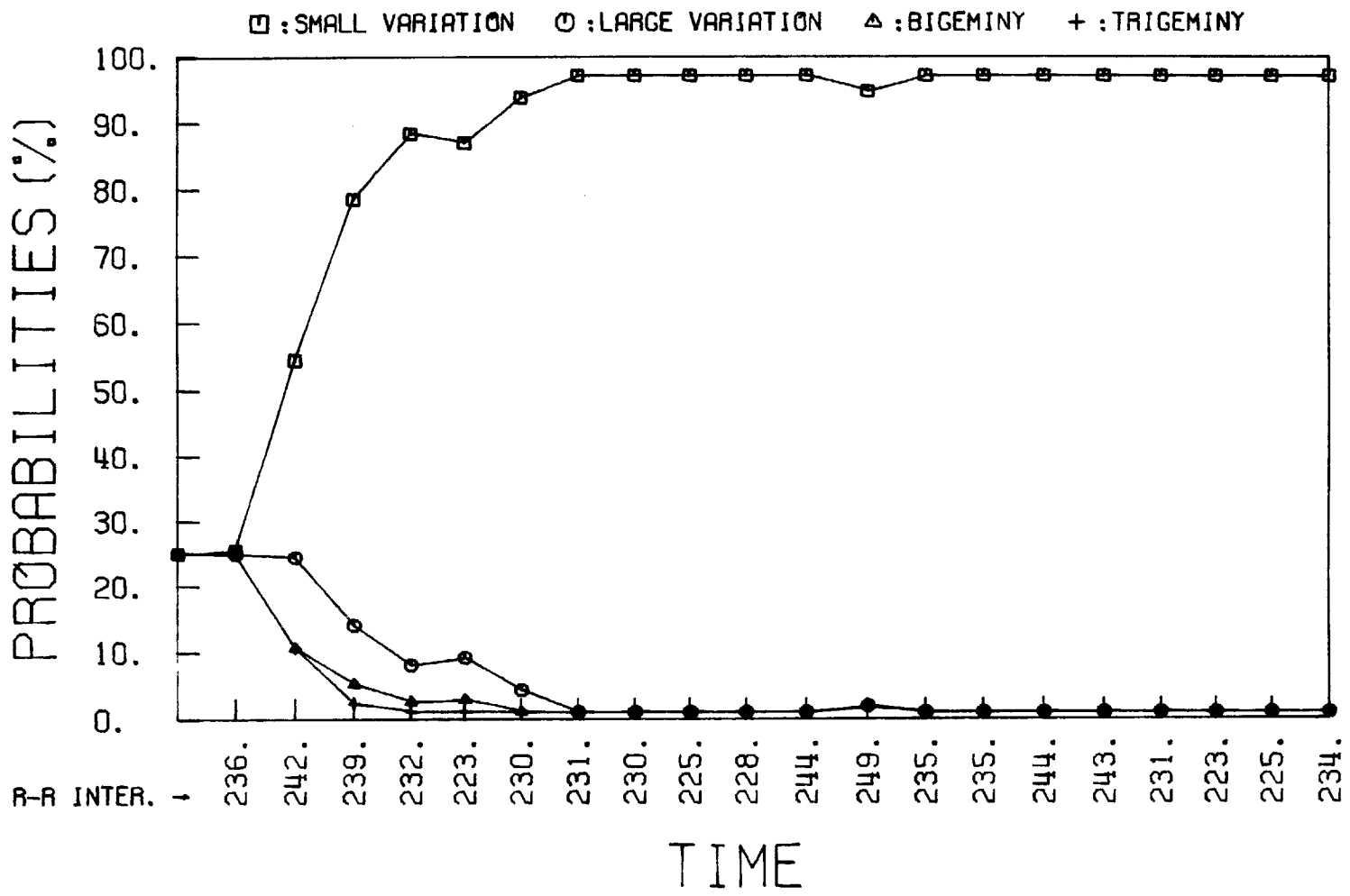

Figure 6.14 A Posteriori Probabilities of Data File IN.30 at P_0=1600, x_0=200, R_b=400

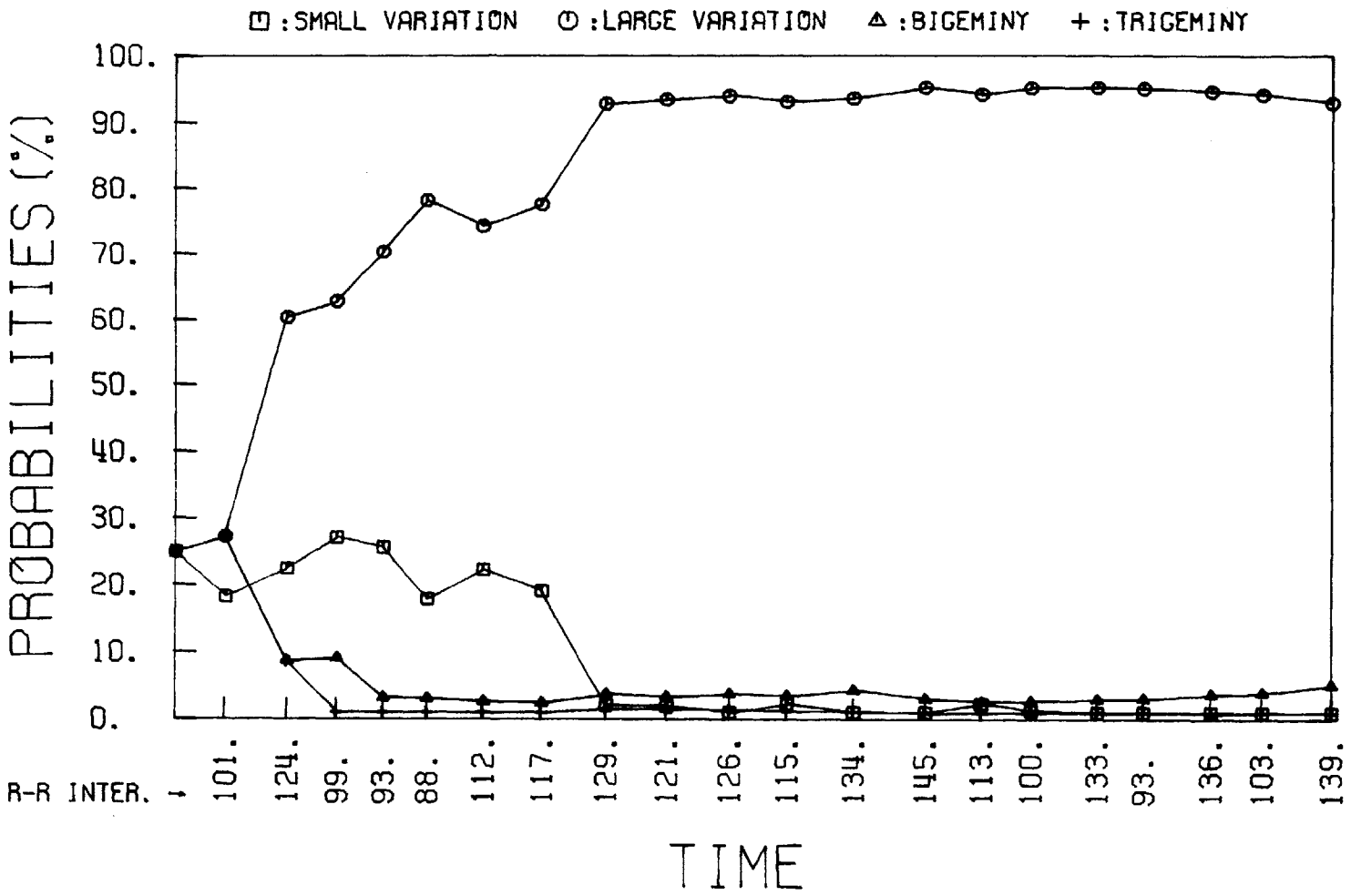

Figure 6.15 A Posteriori Probabilities of Data File CUNATFIB at P_0=1600, x_0=200, R_b=400

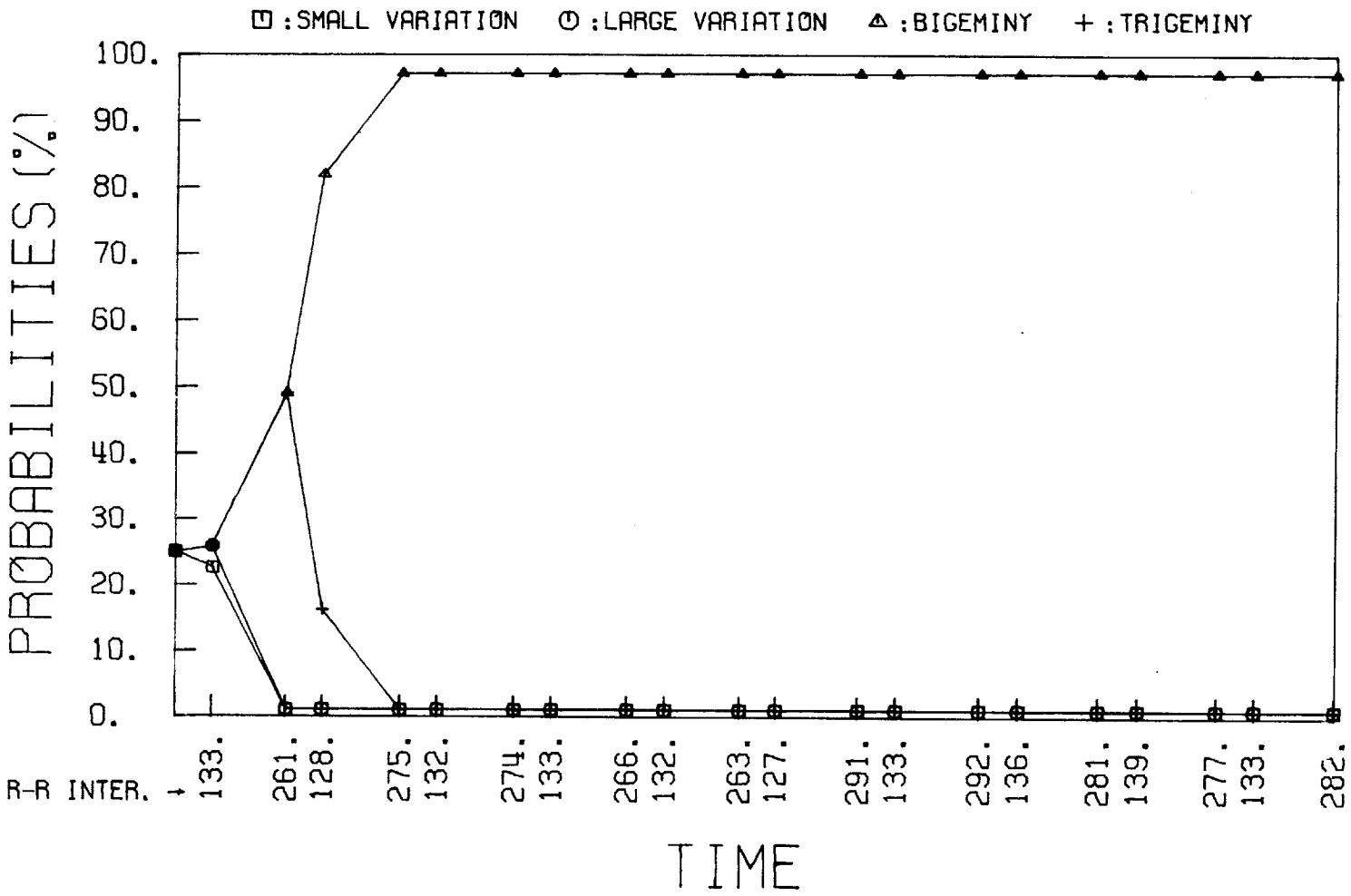

Figure 6.16 A Posteriori Probabilities of Data File #503 at P_0=1600, x_0=200, R_b=400

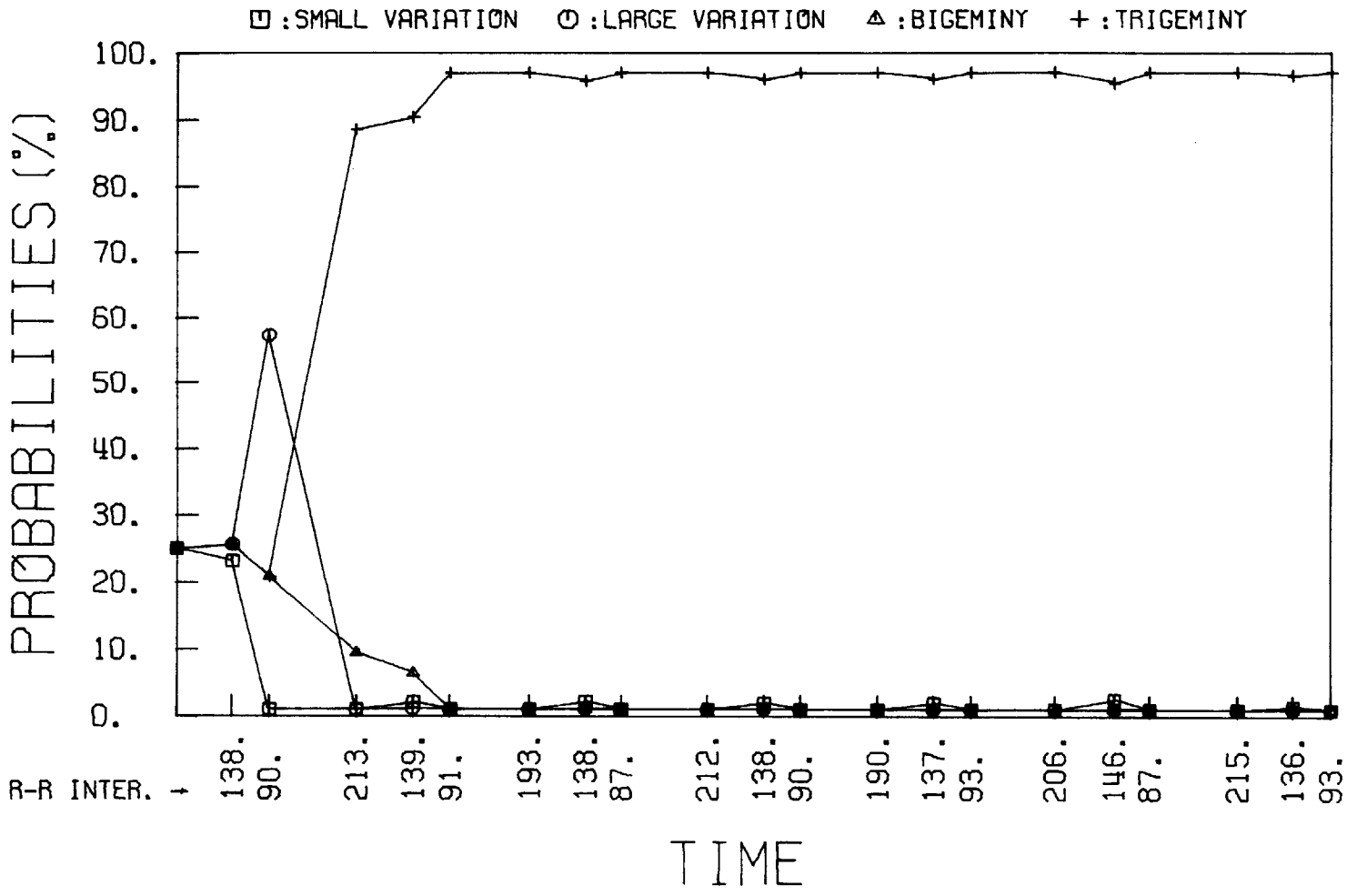

Figure 6.17 A Posteriori Probabilities of Data File HUANPVCS at P_0=1600, x_0=200, R_b=400

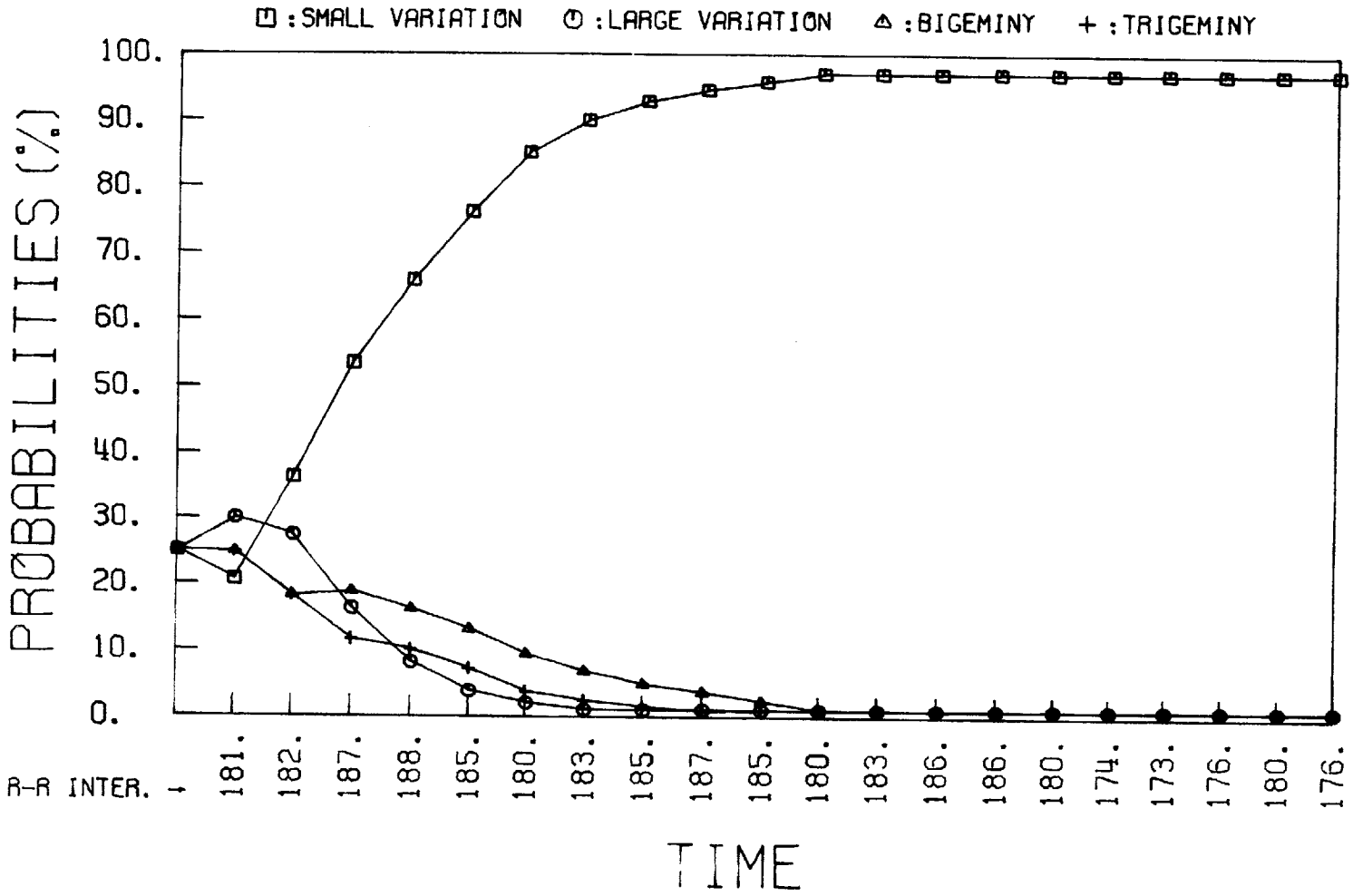

Figure 6.18 A Posteriori Probabilities of Data File IN.5 at P_0=64, x_0=200, R_b=100

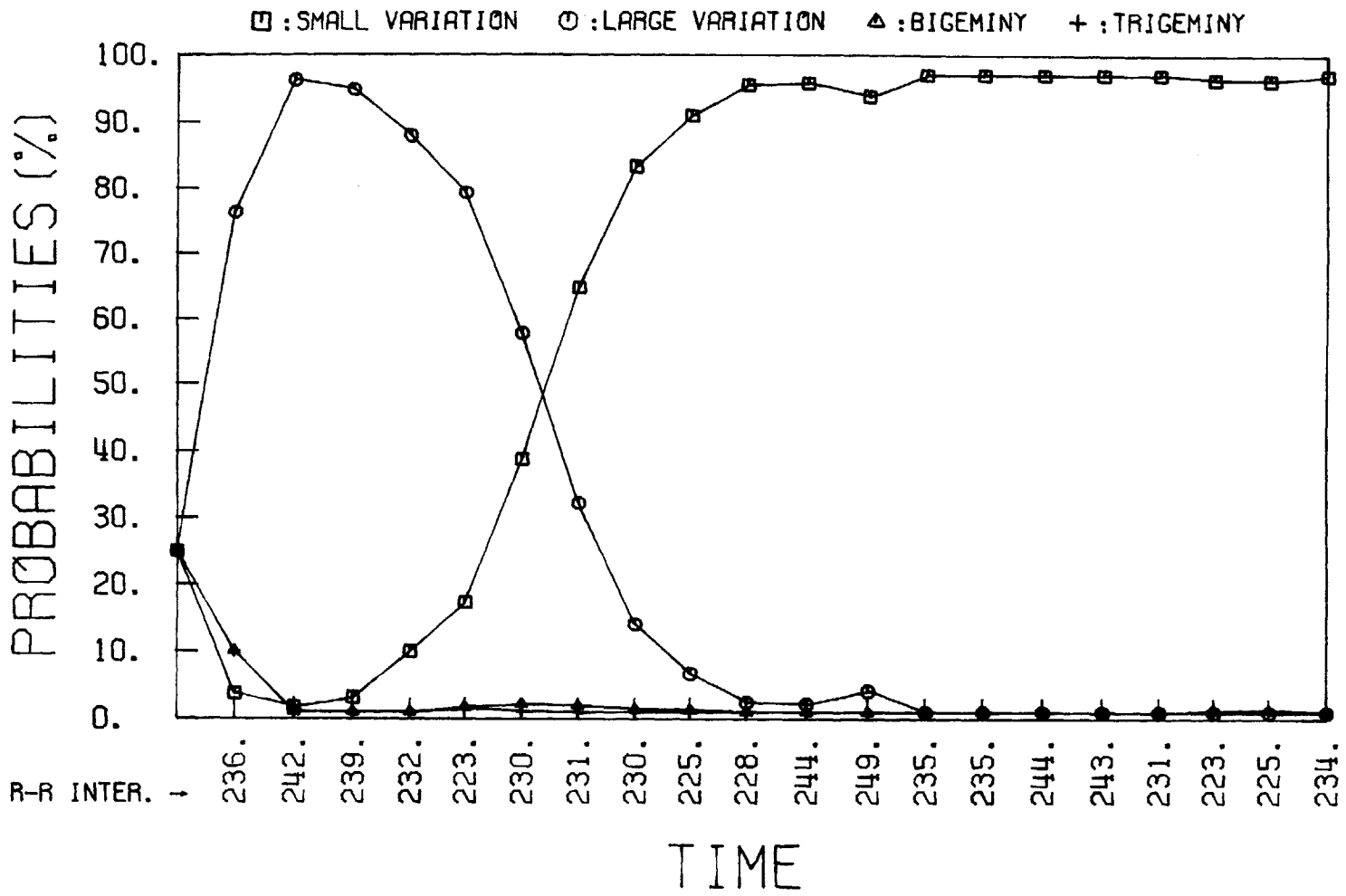

Figure 6.19 A Posteriori Probabilities of Data File IN.30 at P_0=64, x_0=200, R_b=100

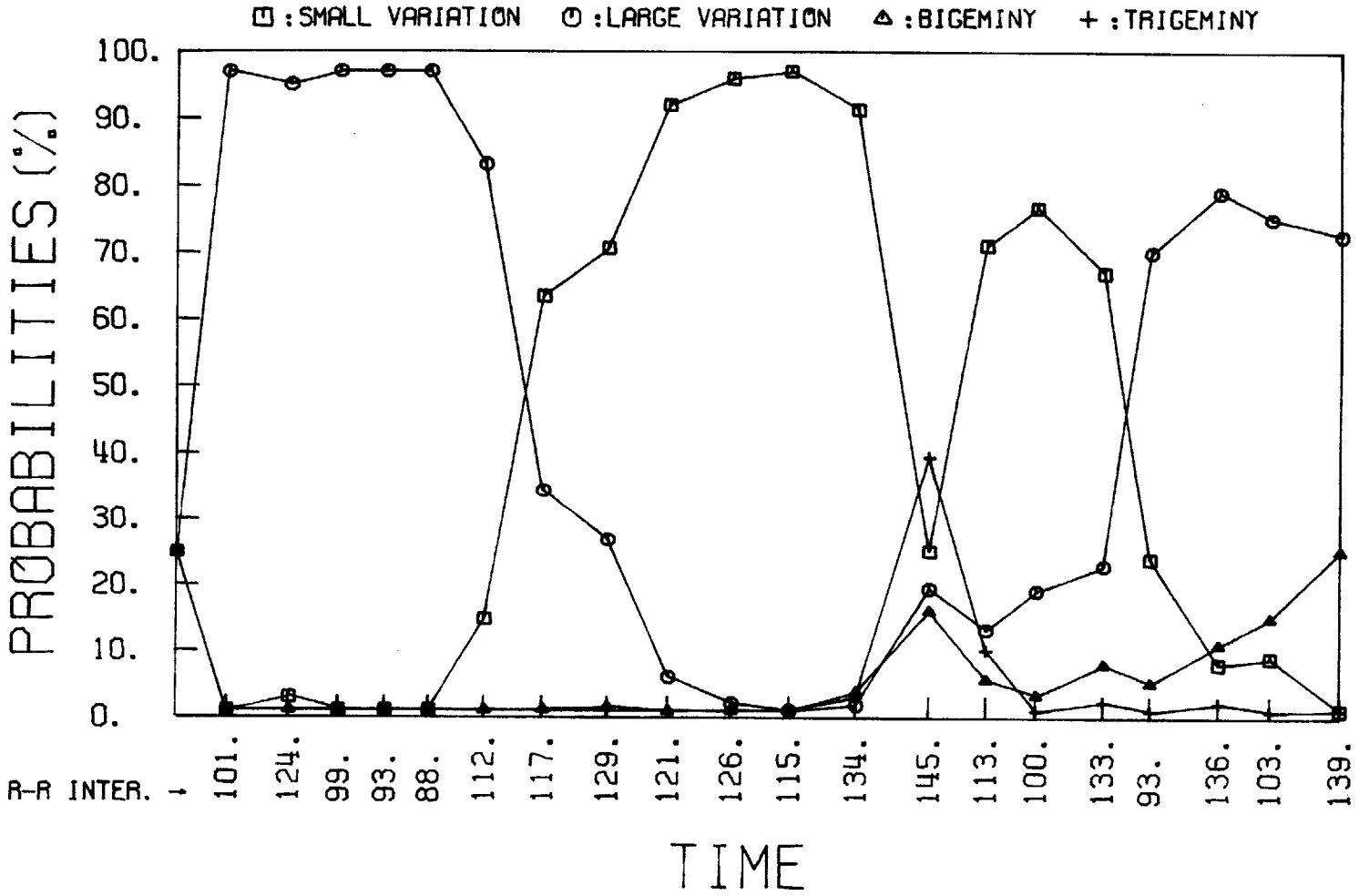

Figure 6.20 A Posteriori Probabilities of Data File CUNATFIB at P_0=64, x_0=200, R_b=100

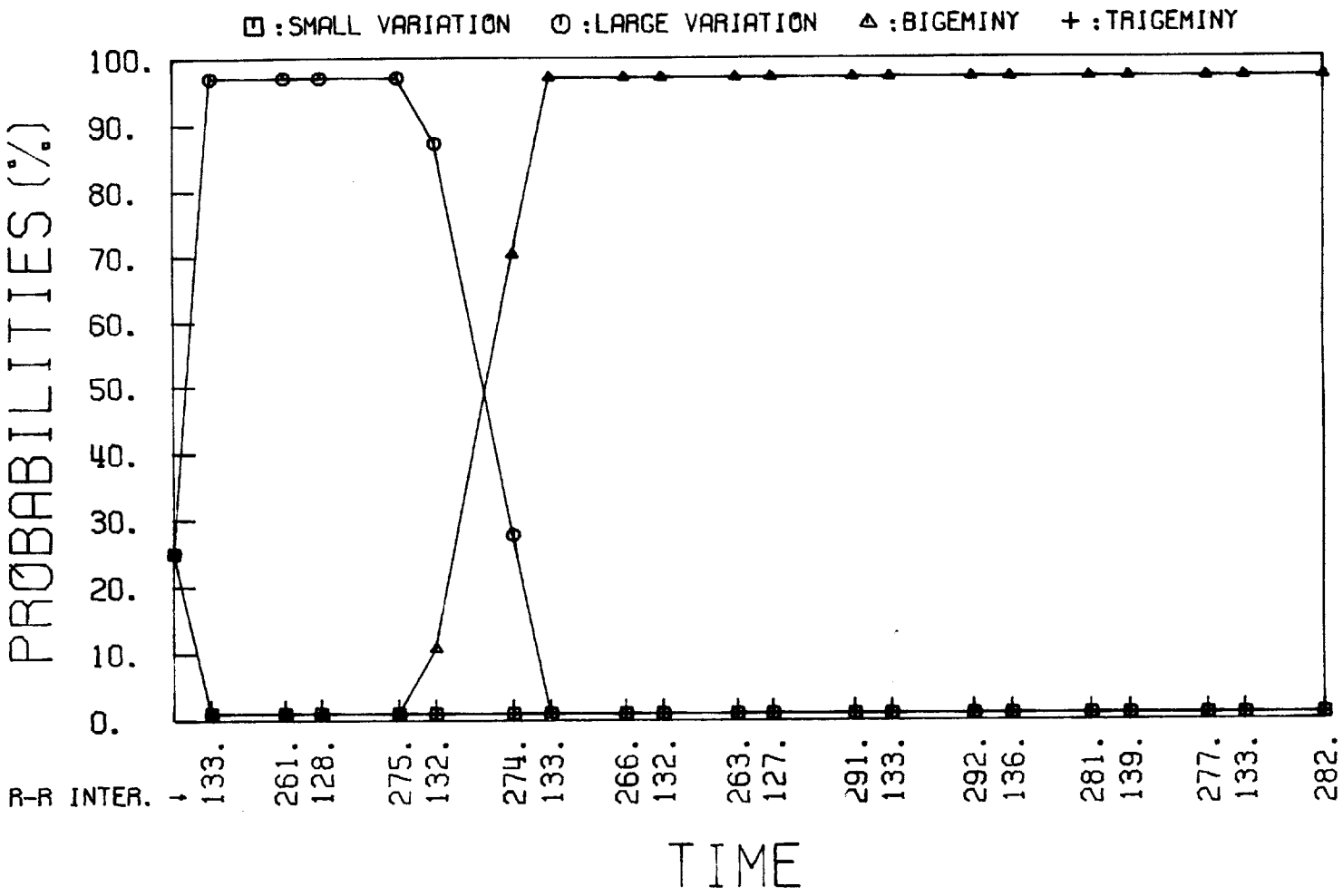

Figure 6.21 A Posteriori Probabilities of Data File #503 at P_0=64, x_0=200, R_b=100

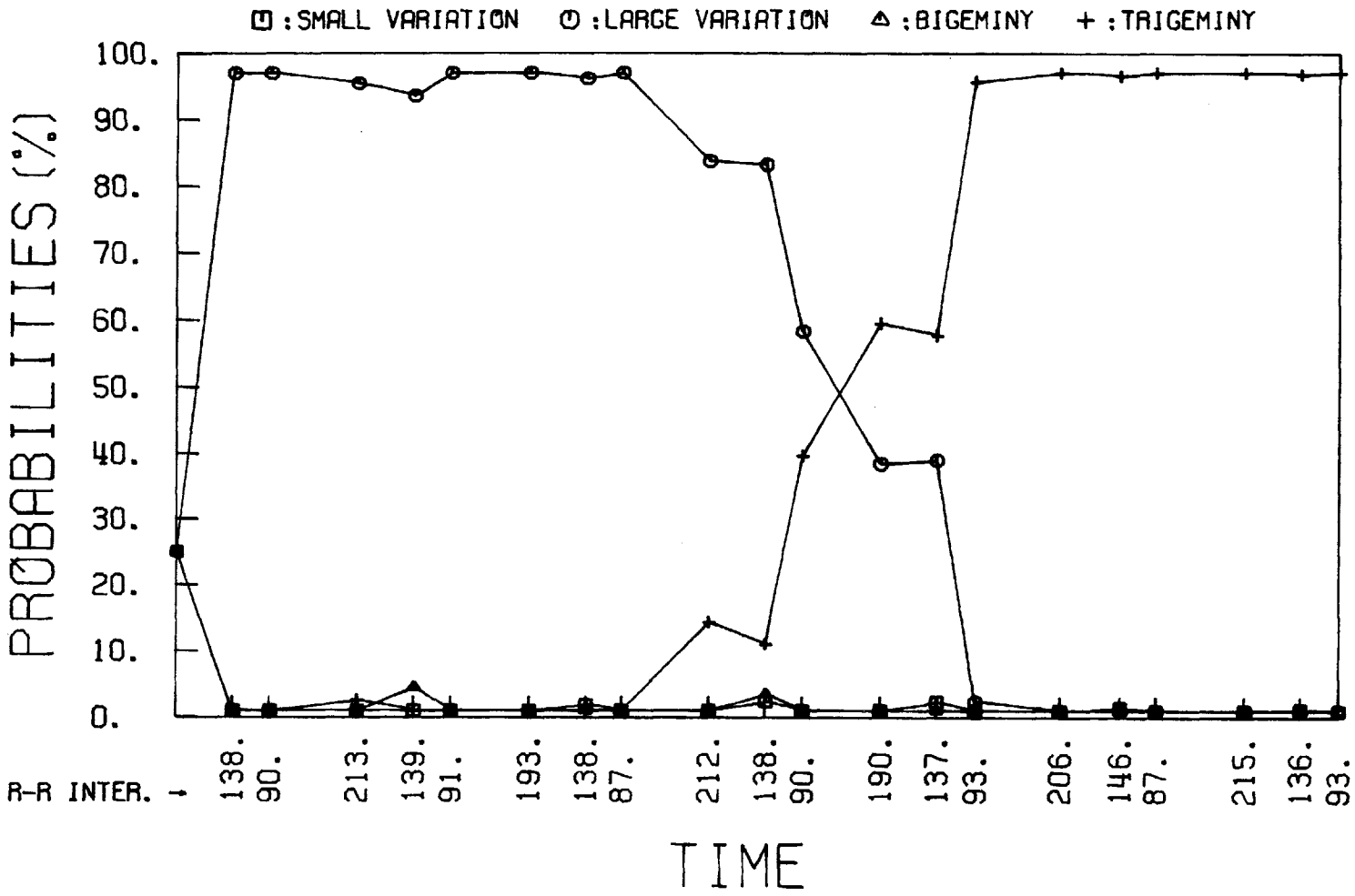

Figure 6.22 A Posteriori Probabilities of Data File HUANPVCS at P_0=64, x_0=200, R_b=100

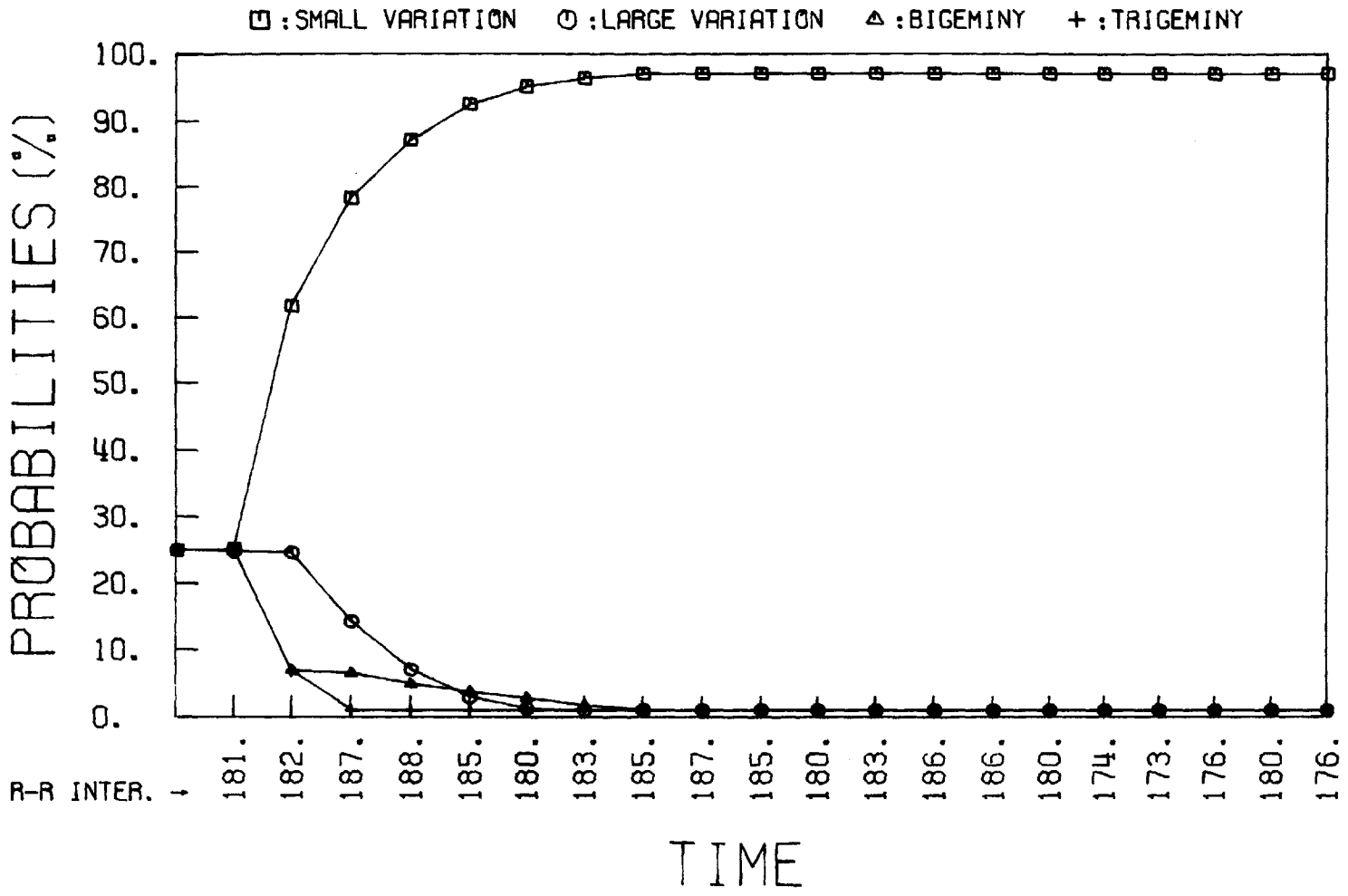

Figure 6.23 A Posteriori Probabilities of Data File IN.5 at P_0=10000, x_0=200, R_b=100

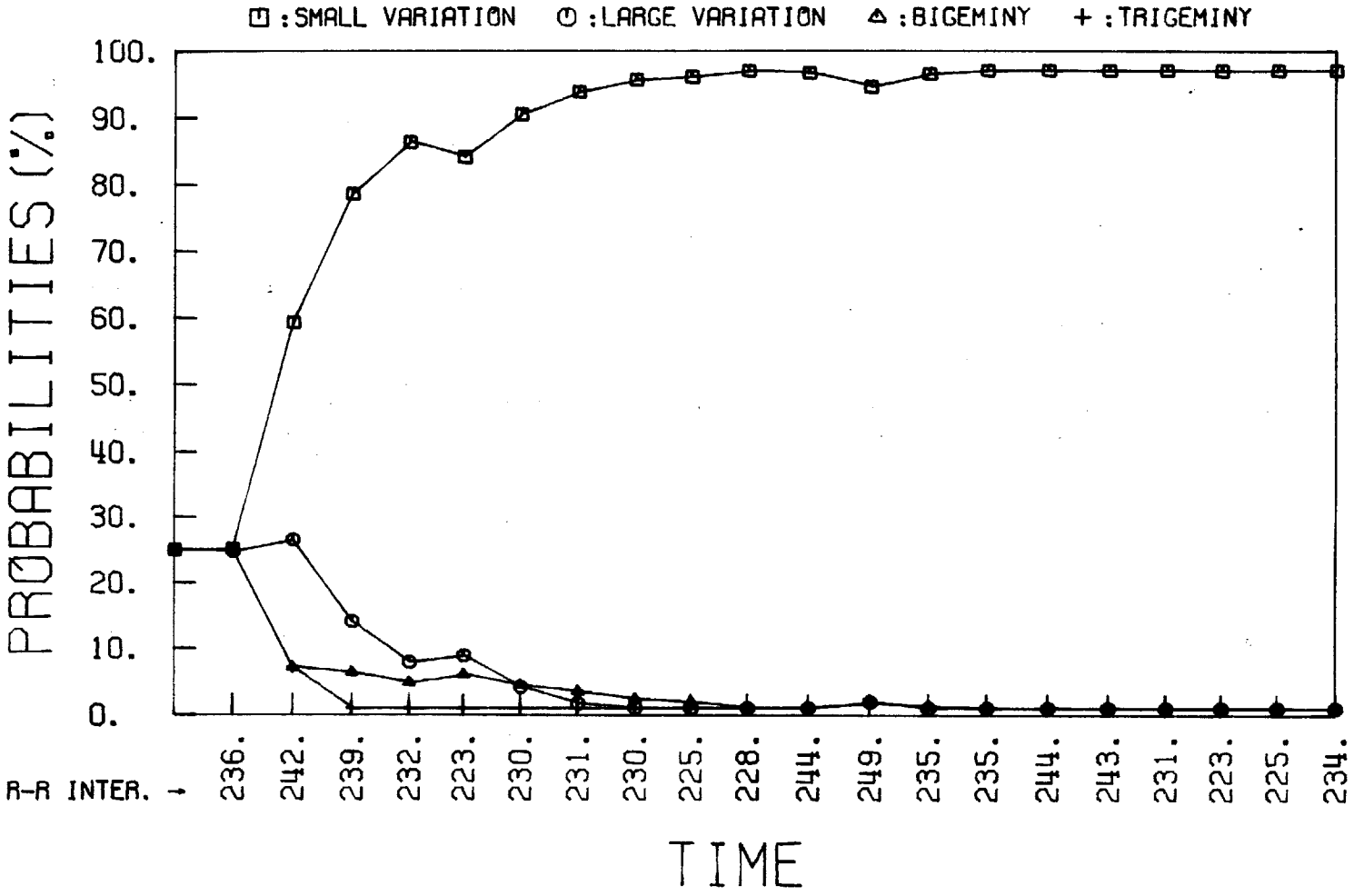

Figure 6.24 A Posteriori Probabilities of Data File IN.30 at P_0=10000, x_0=200, R_b=100

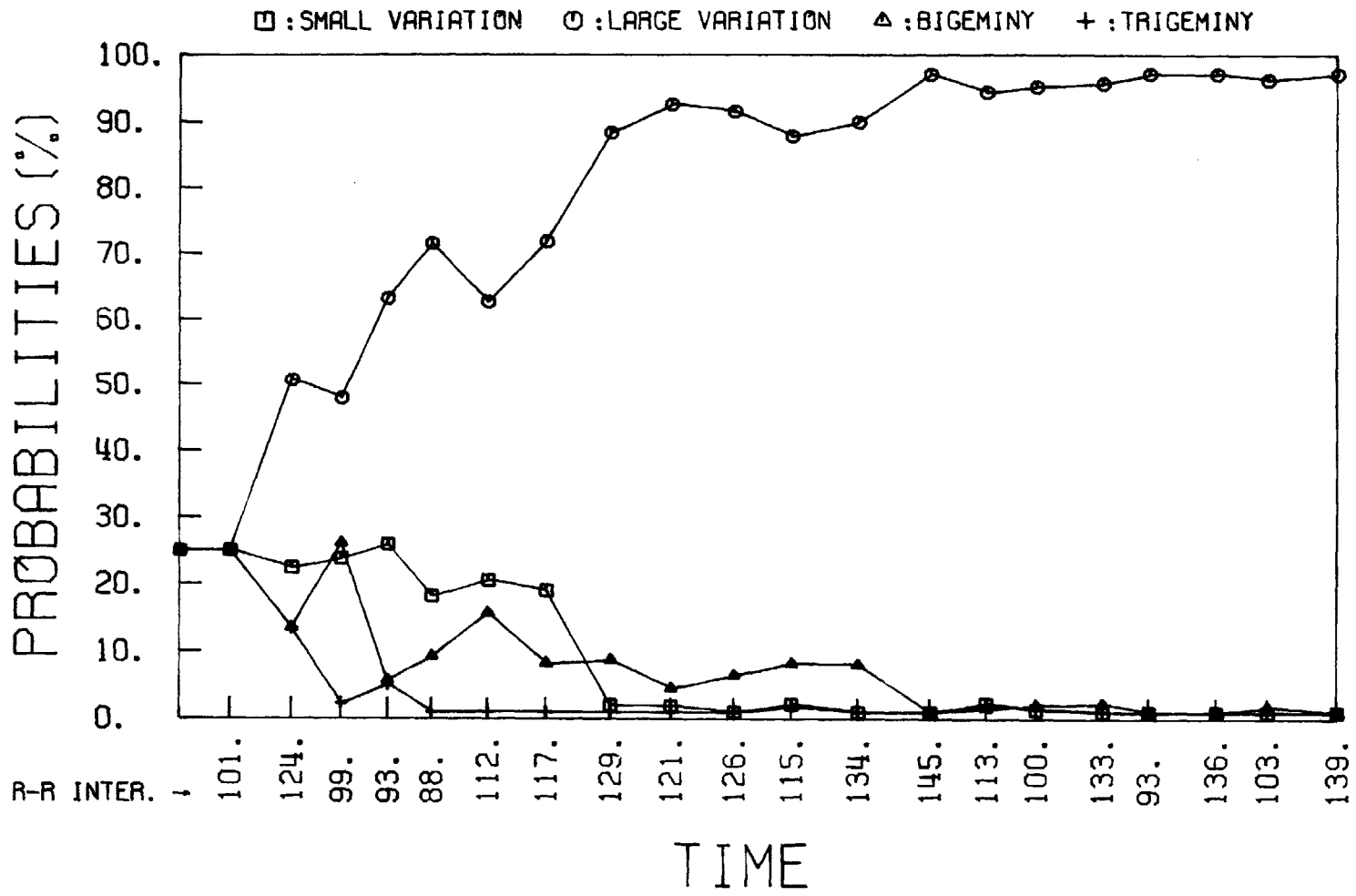

Figure 6.25 A Posteriori Probabilities of Data File CUNATFIB at P_0=10000, x_0=200, R_b=100

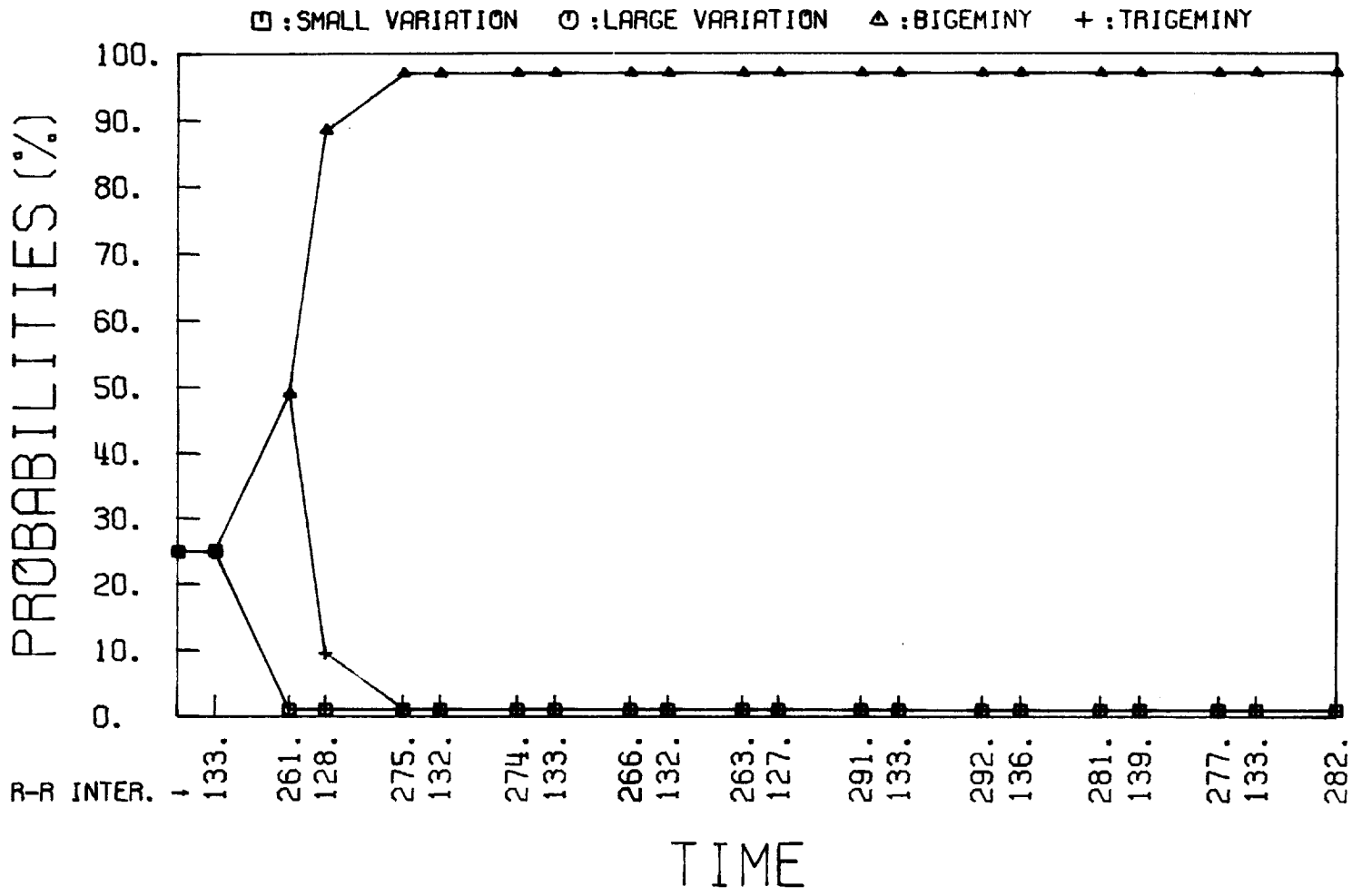

Figure 6.26 A Posteriori Probabilities of Data File #503 at P_0=10000, x_0=200, R_b=100

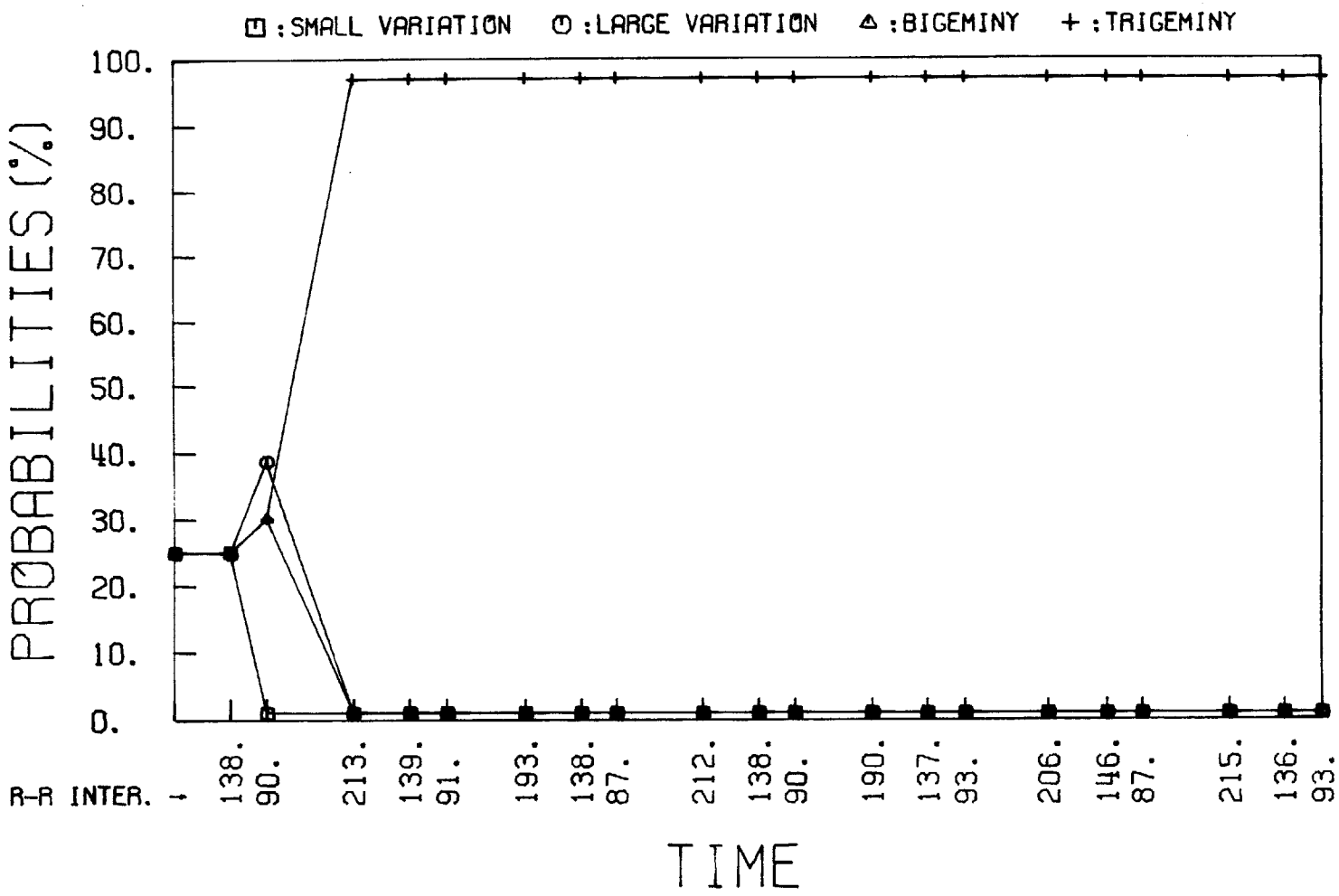

Figure 6.27 A Posteriori Probabilities of Data File HUANPVCS at P_0=10000, x_0=200, R_b=100

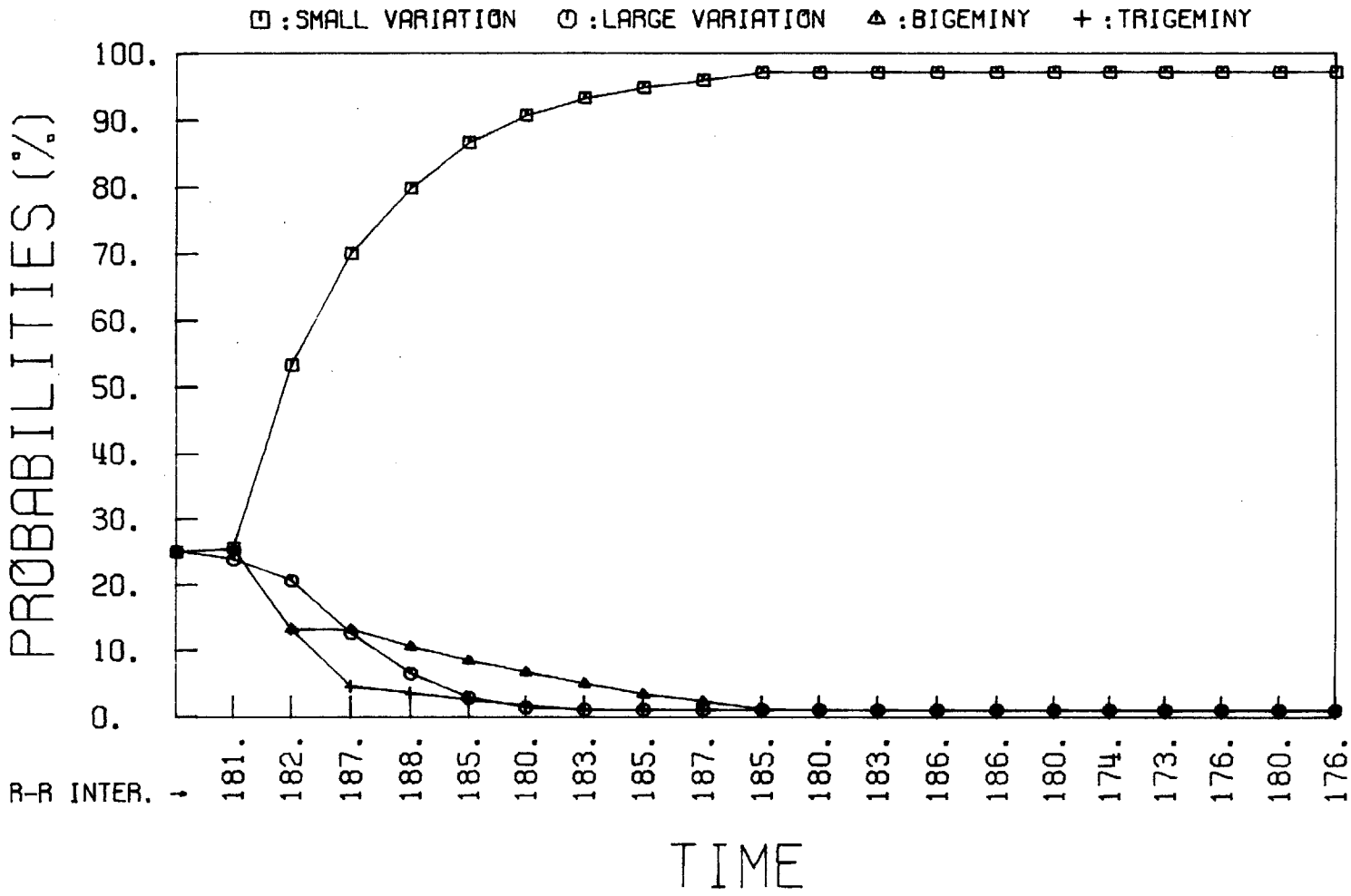

Figure 6.28 A Posteriori Probabilities of Data File IN.5 at P_0=1600, P_{ij}=20, x_0=200, R_b=100

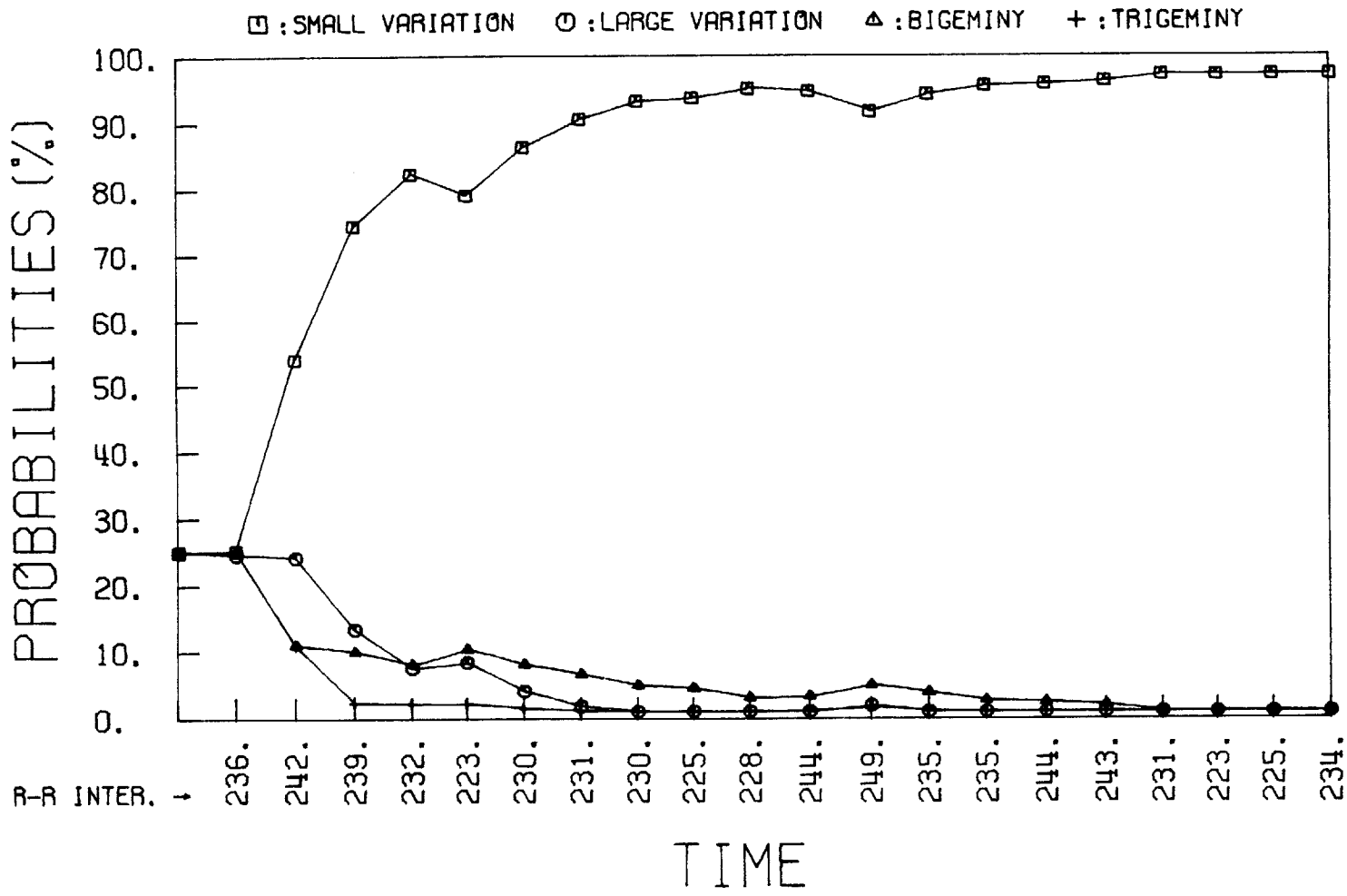

Figure 6.29 A Posteriori Probabilities of Data File IN.30 at P_0=1600, P_{ij}=20, x_0=200, R_b=100

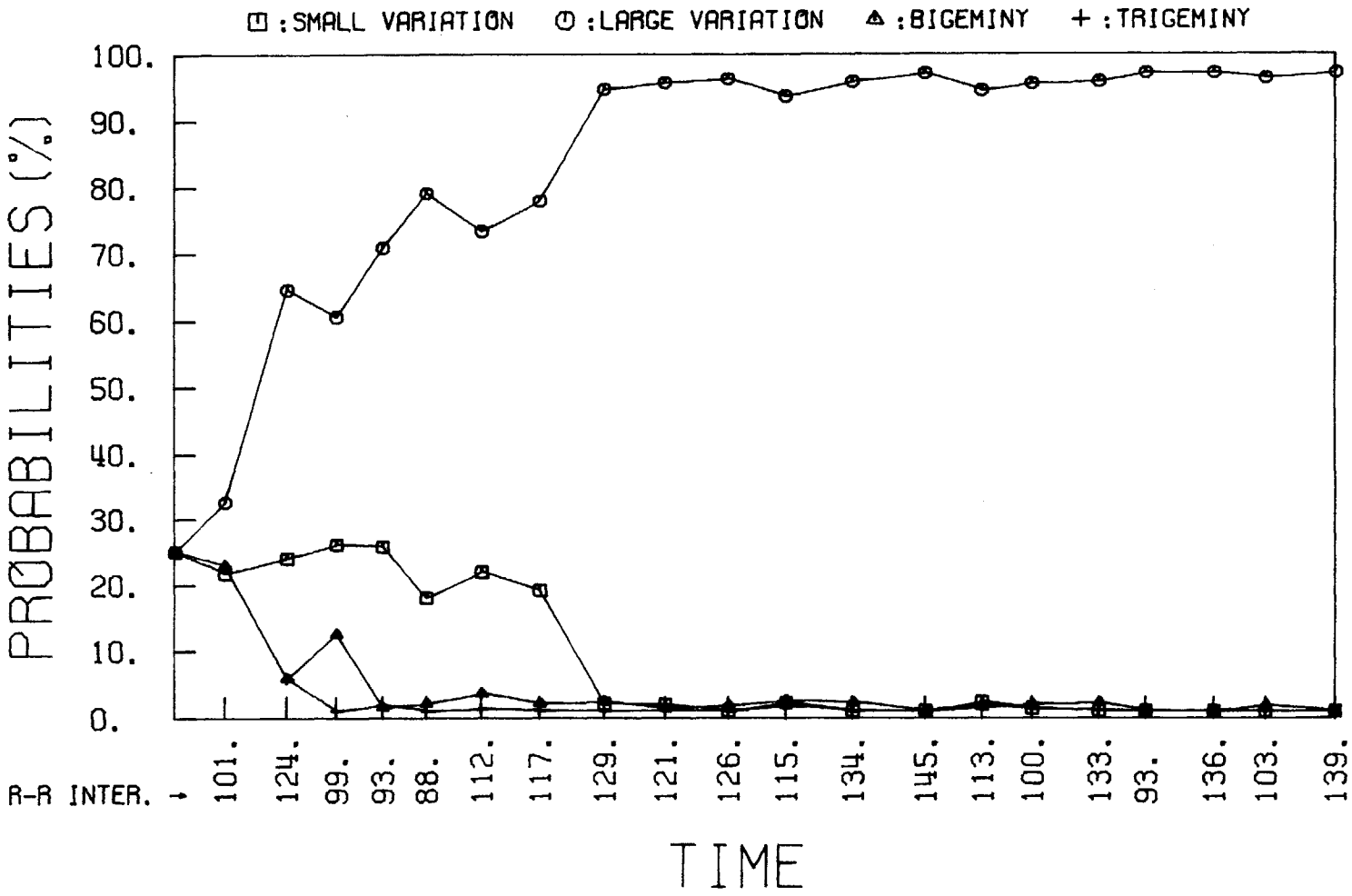

Figure 6.30 A Posteriori Probabilities of Data File CUNATFIB at P_0=1600, P_{ij}=20, x_0=200, R_b=100

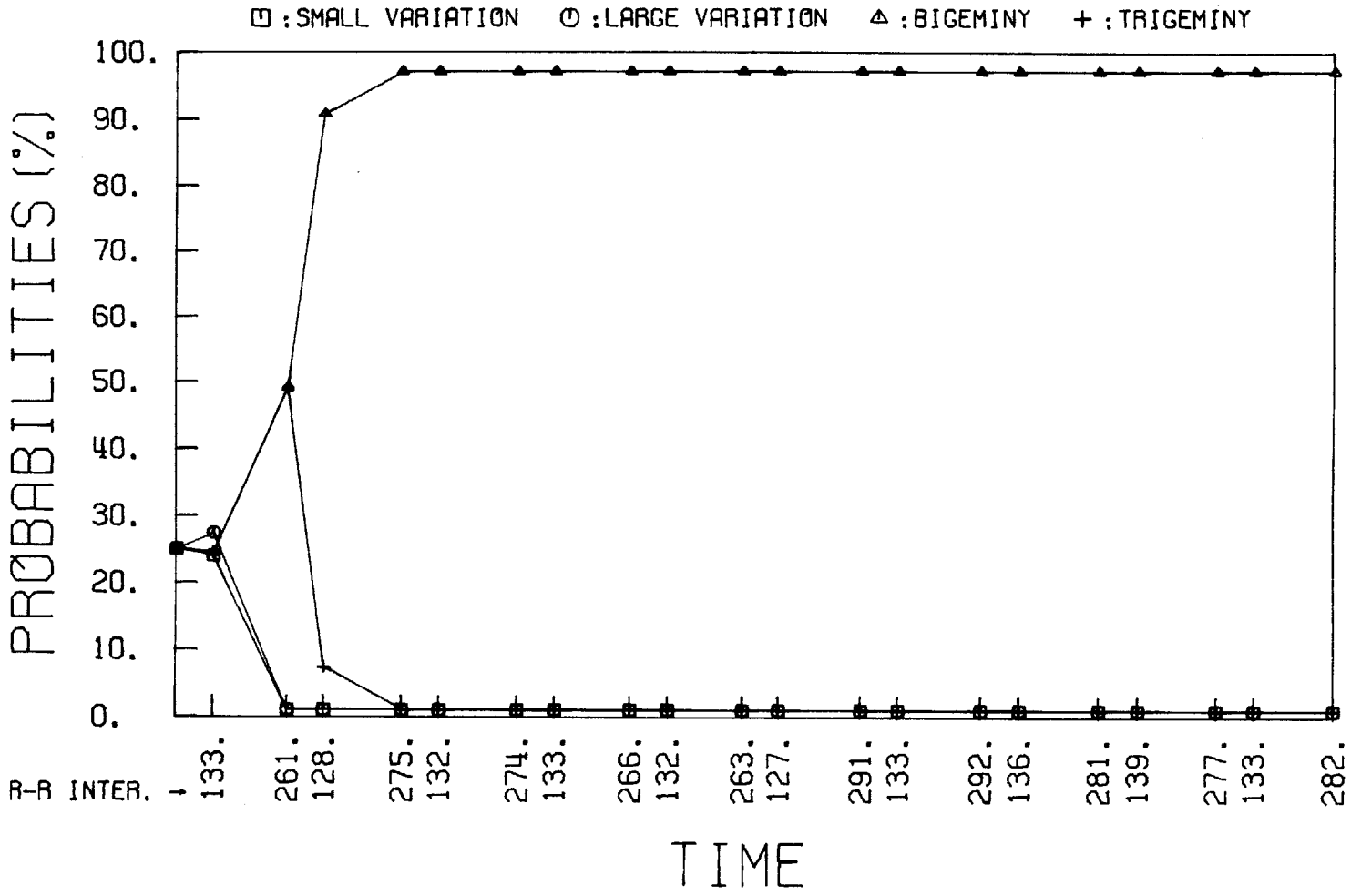

Figure 6.31 A Posteriori Probabilities of Data File #503 at P_0=1600, P_{ij}=20, x_0=200, R_b=100

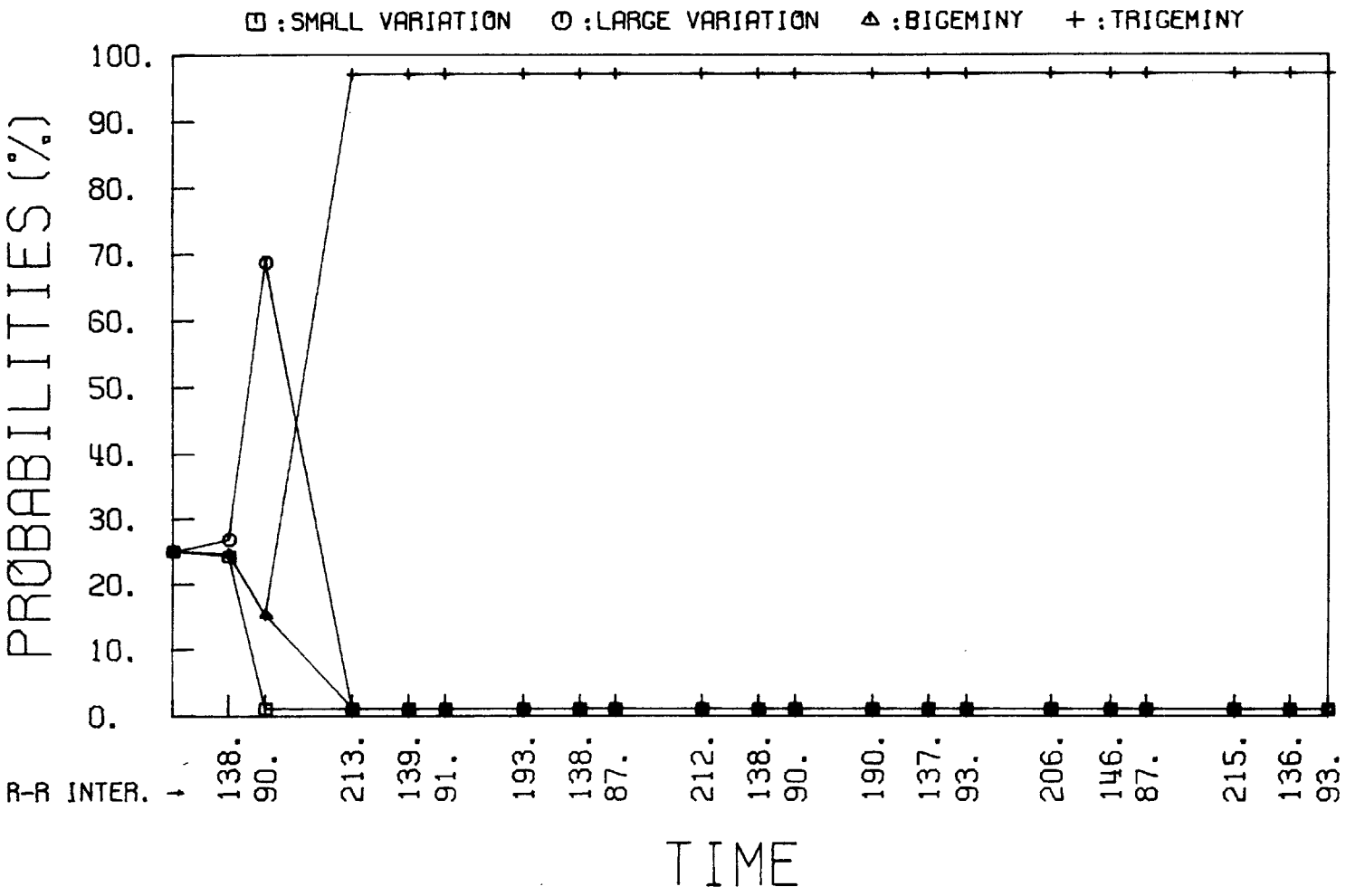

Figure 6.32 A Posteriori Probabilities of Data File HUANPVCS at P_0=1600, P_{ij}=20, x_0=200, R_b=100

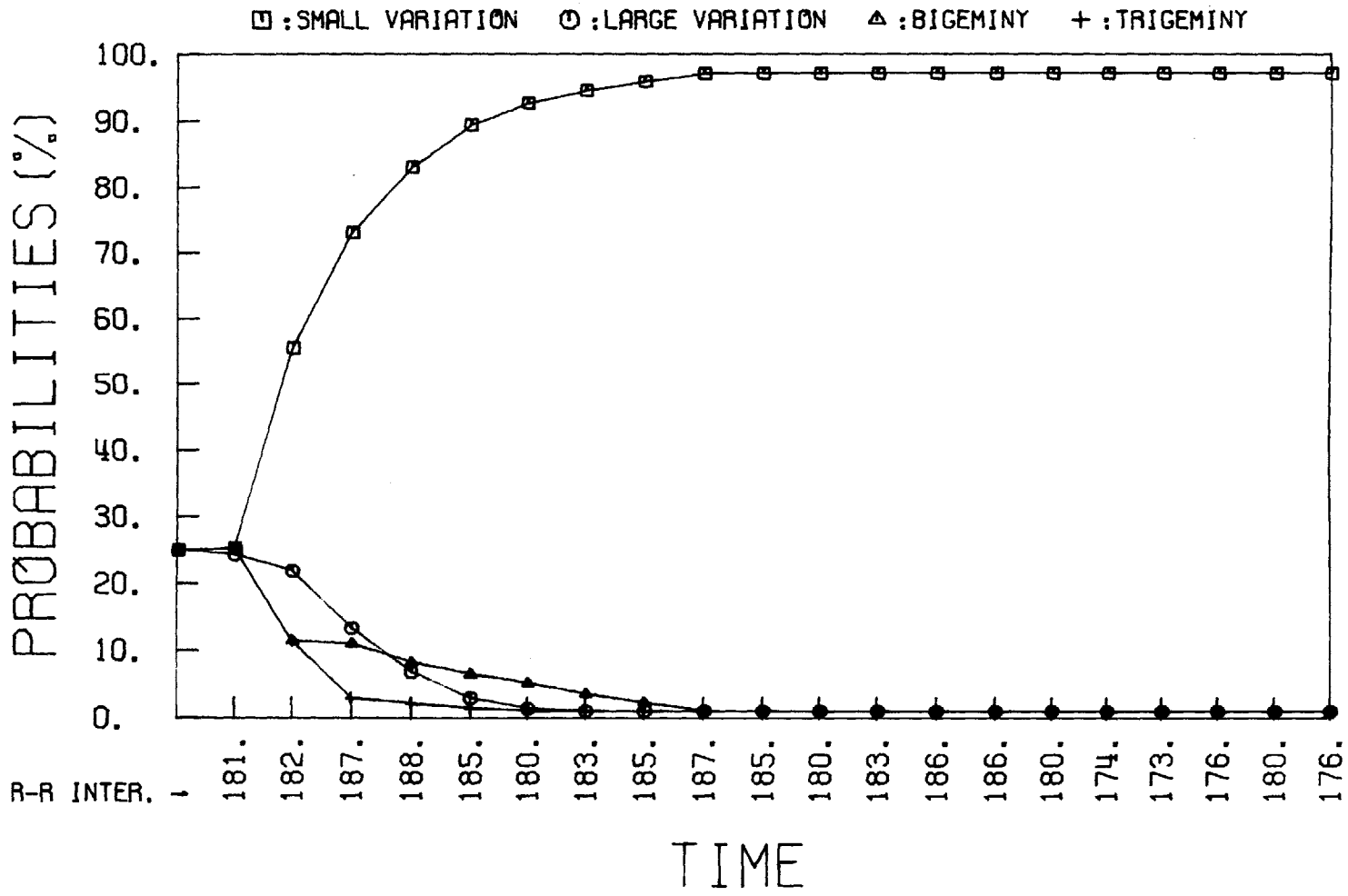

Figure 6.33 A Posteriori Probabilities of Data File IN.5 at P_0=1600, x_0=150, R_b=100

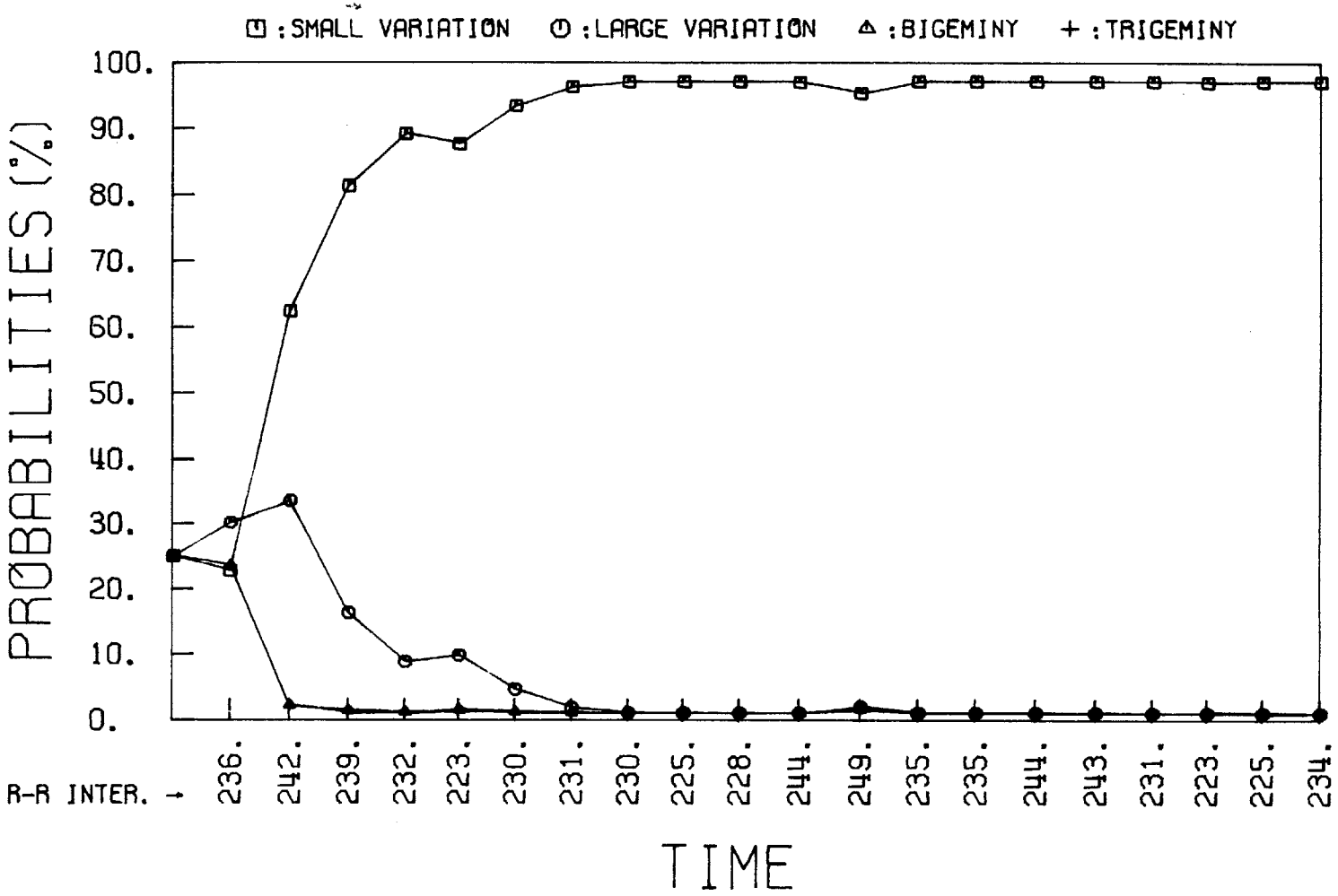

Figure 6.34 A Posteriori Probabilities of Data File IN.30 at P_0=1600, x_0=150, R_b=100

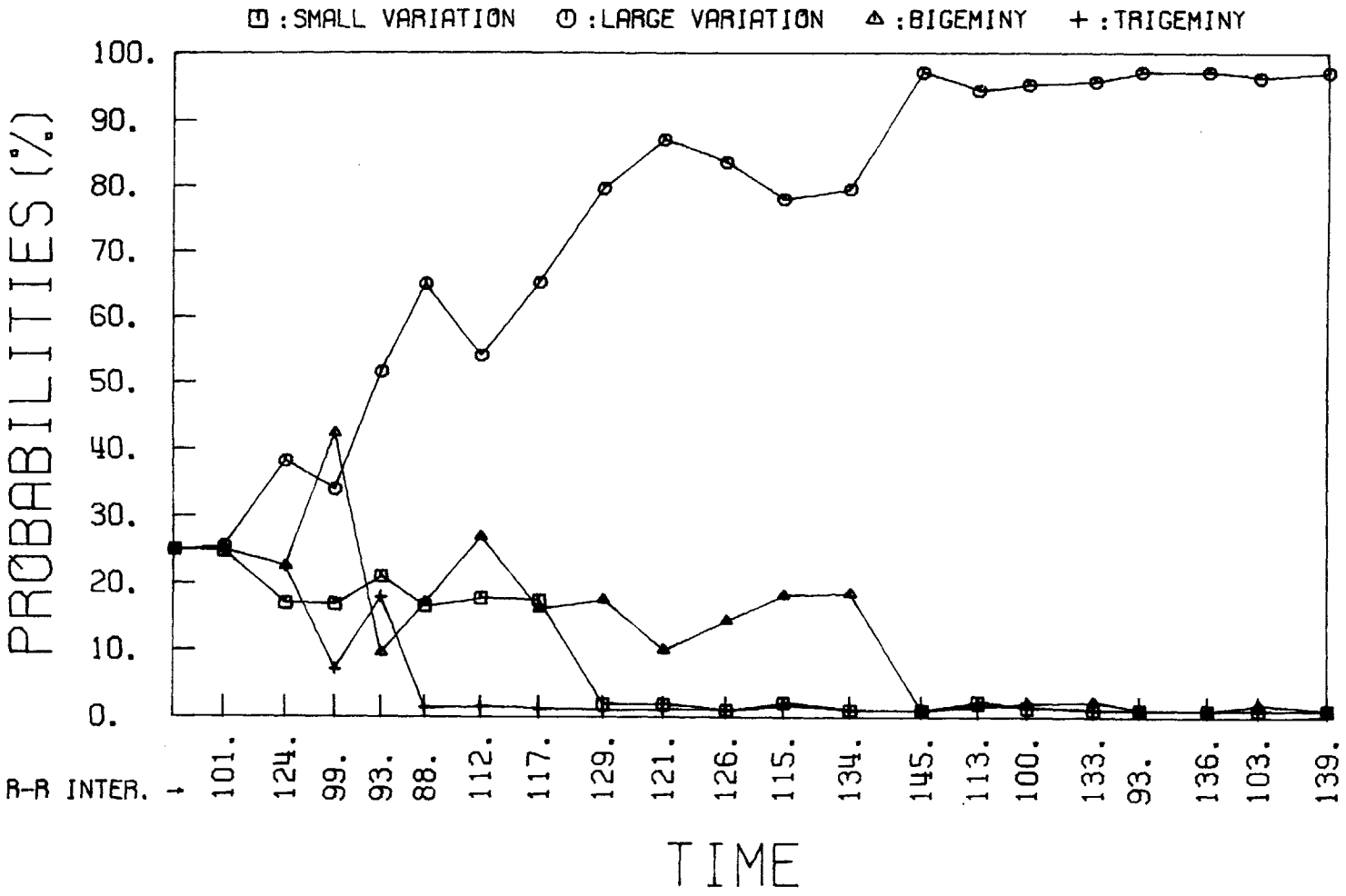

Figure 6.35 A Posteriori Probabilities of Data File CUNATFIB at P_0=1600, x_0=150, R_b=100

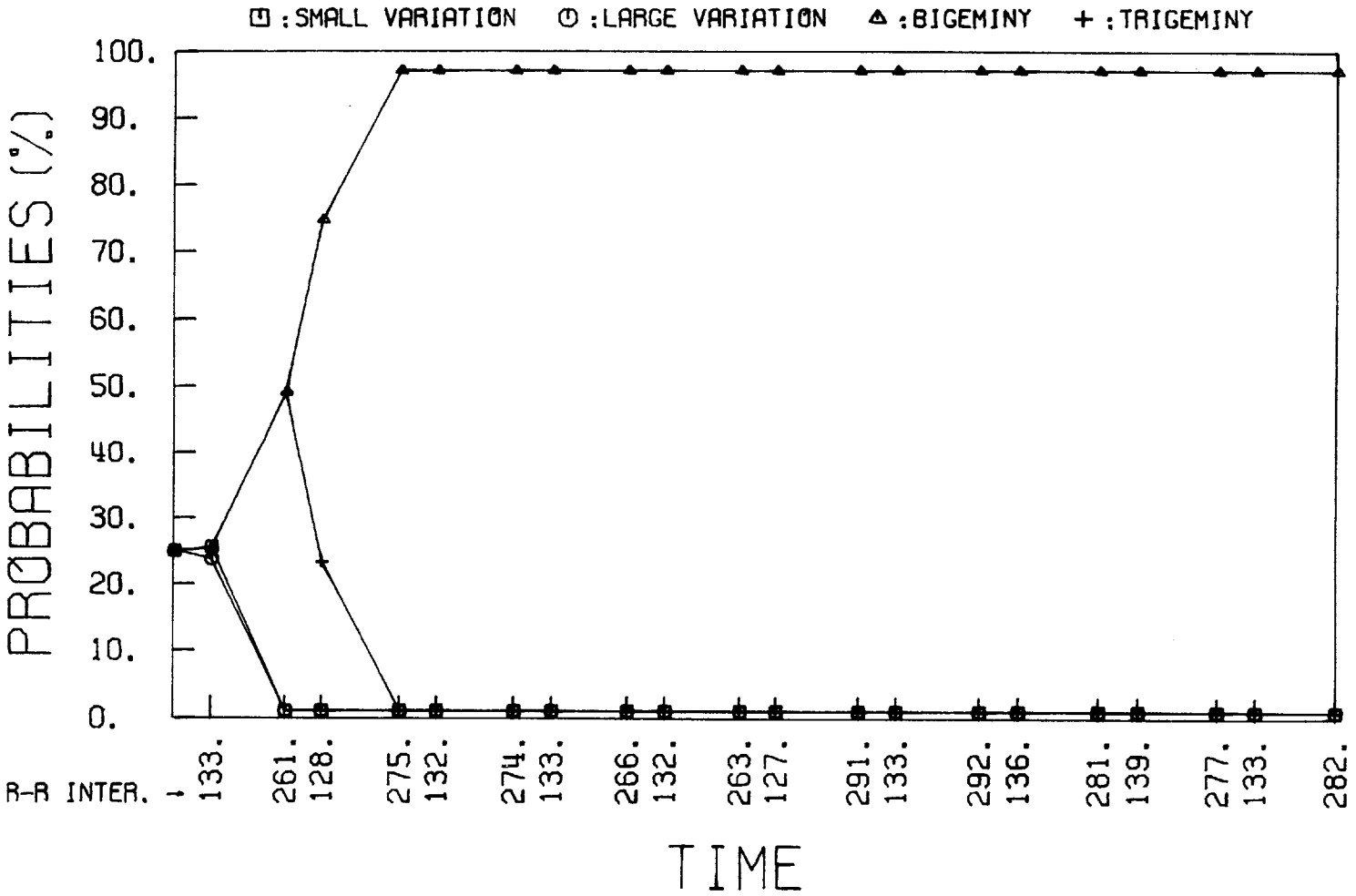

Figure 6.36 A Posteriori Probabilities of Data File #503 at P_0=1600, x_0=150, R_b=100

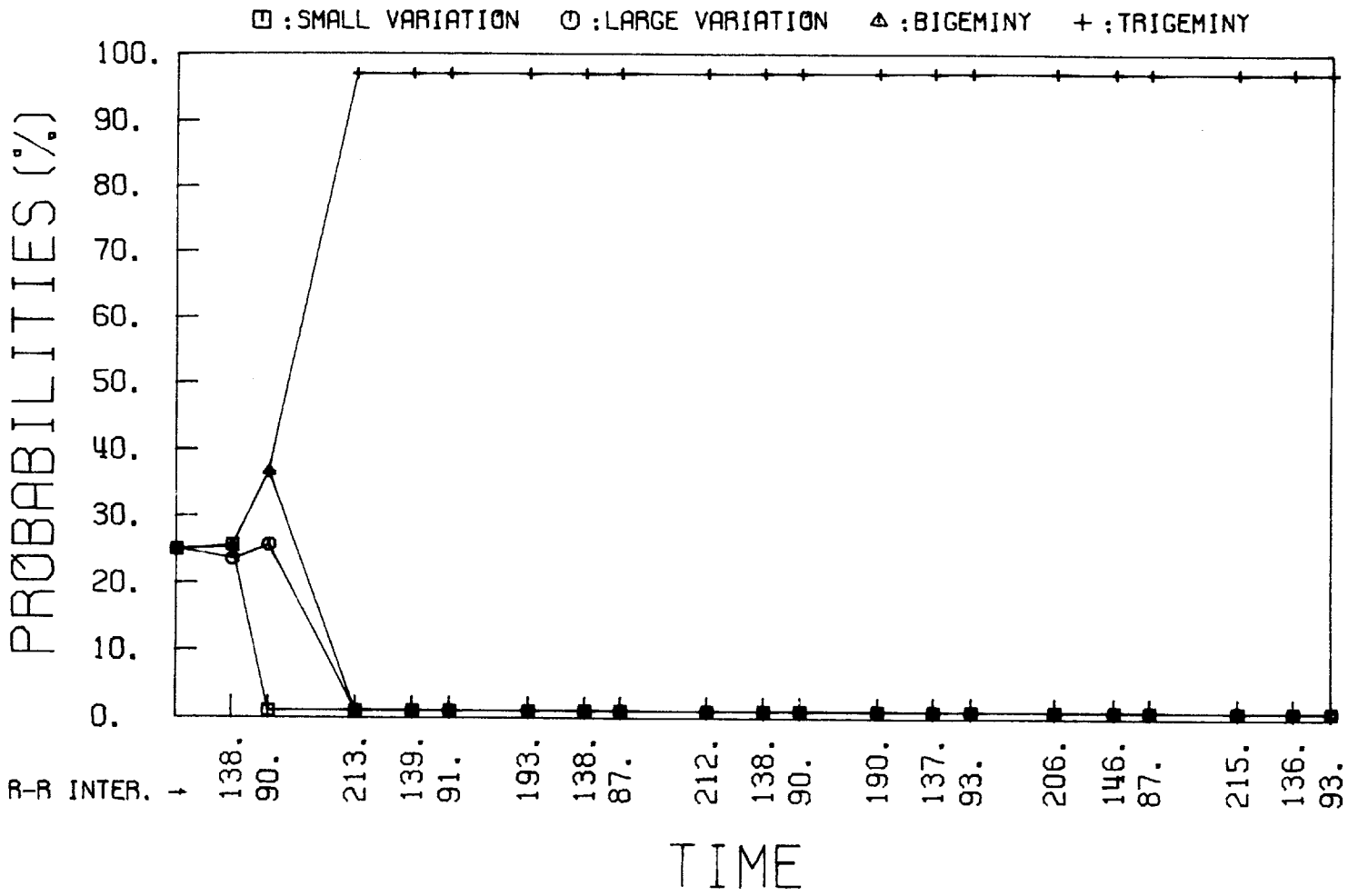

Figure 6.37 A Posteriori Probabilities of Data File HUANPVCS at P_0=1600, x_0=150, R_b=100

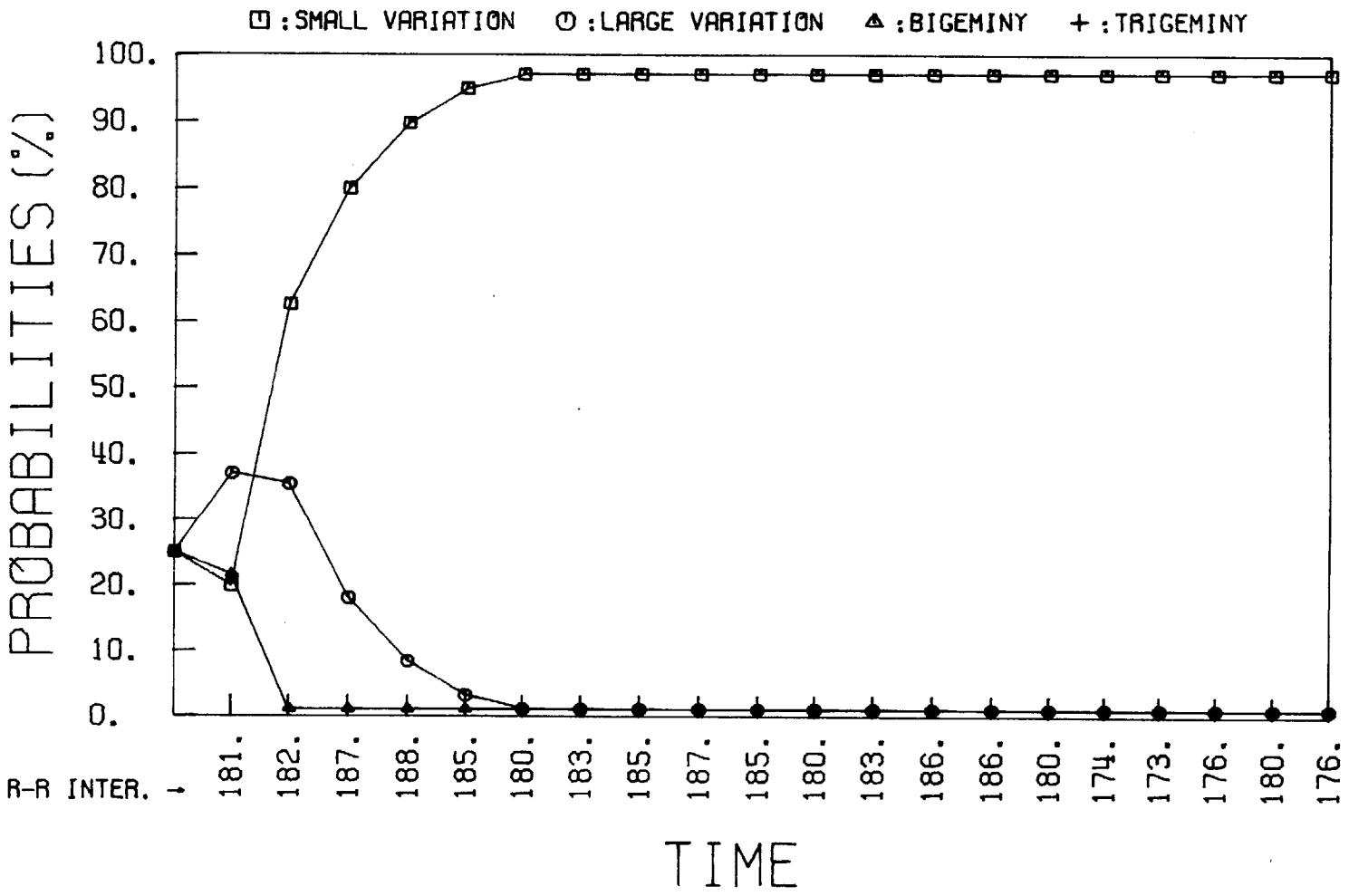

Figure 6.38 A Posteriori Probabilities of Data File IN.5 at P_0=1600, x_0=300, R_b=100

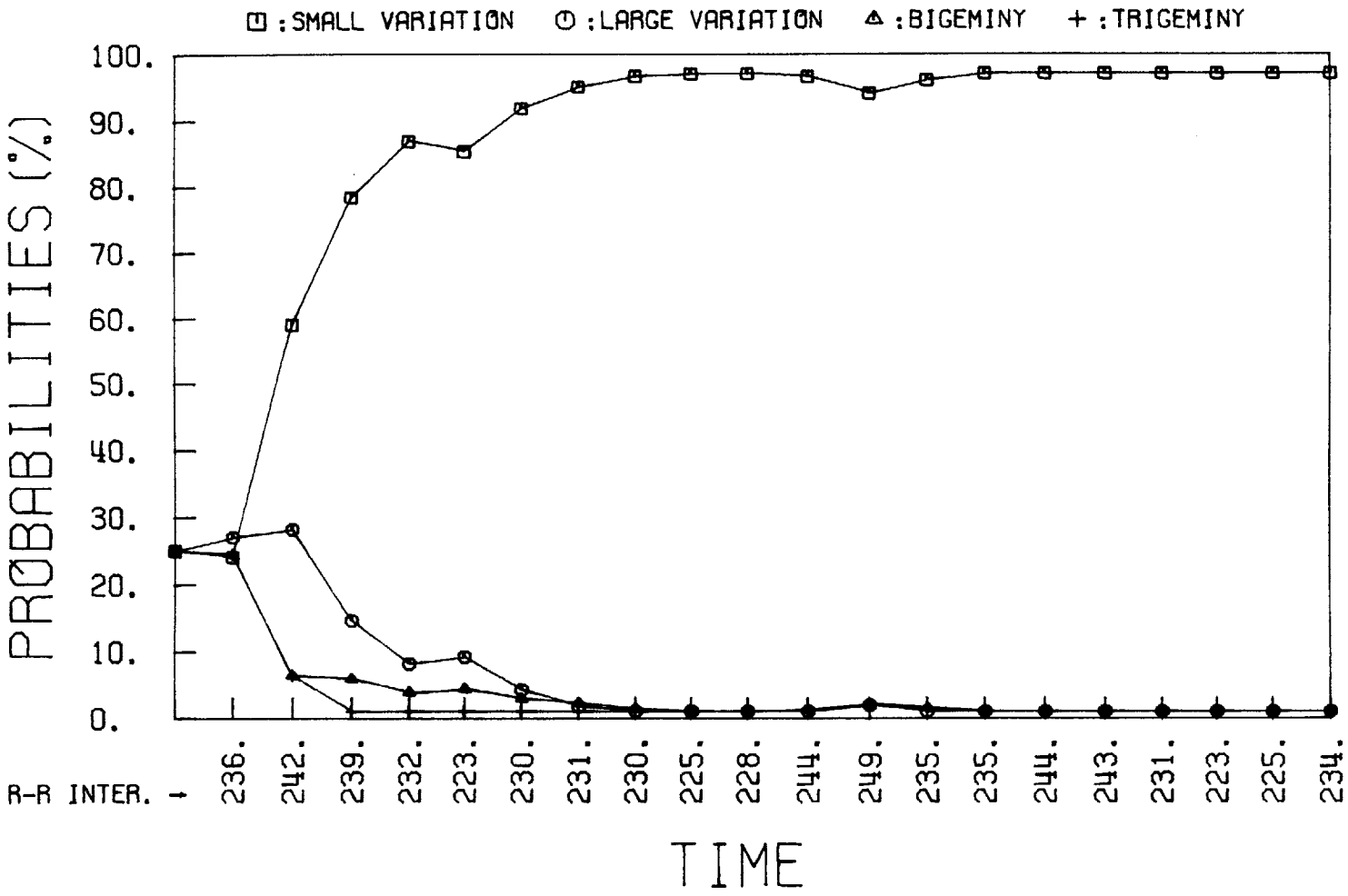

Figure 6.39 A Posteriori Probabilities of Data File IN.30 at P_0=1600, x_0=300, R_b=100

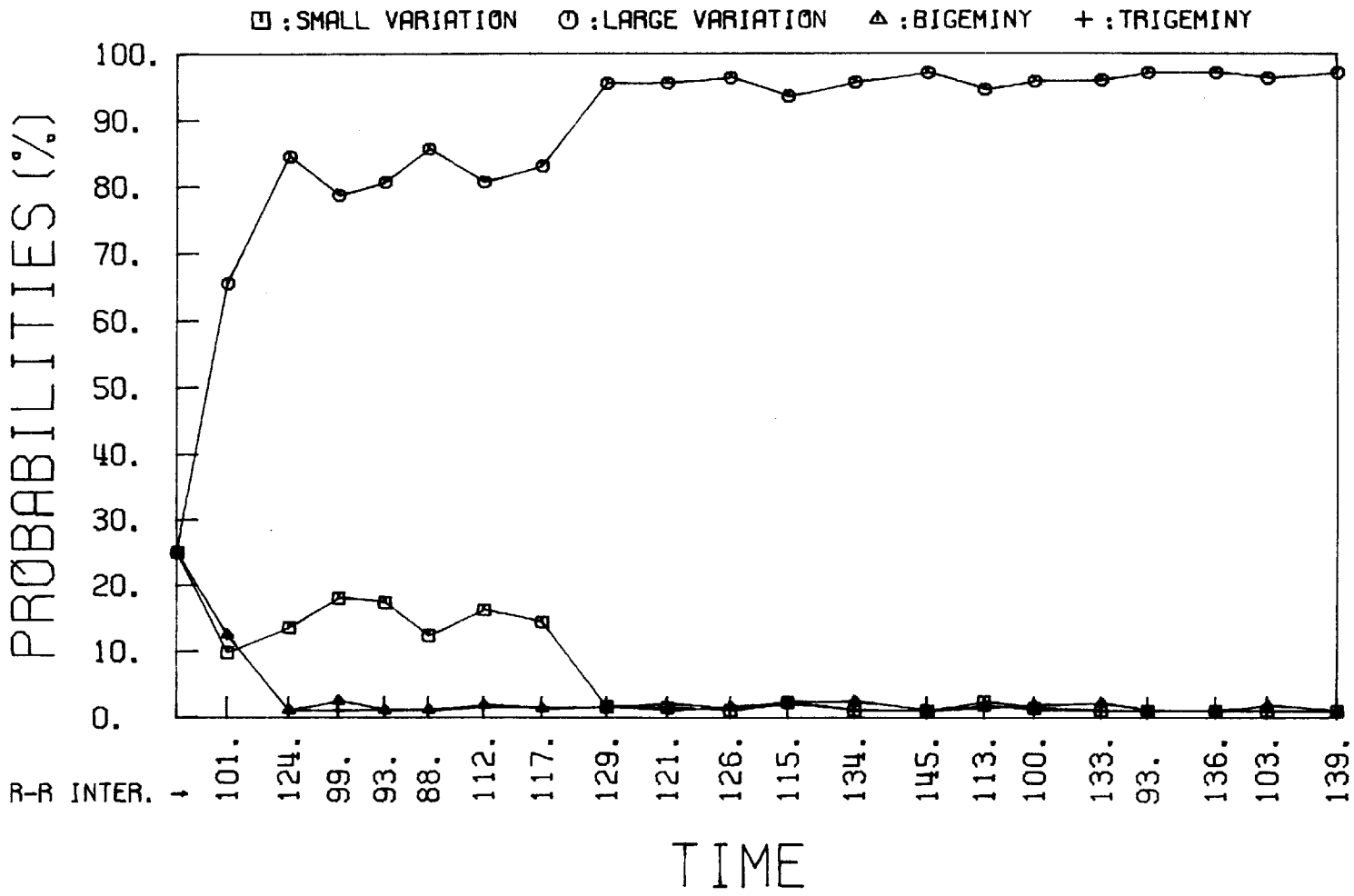

Figure 6.40 A Posteriori Probabilities of Data File CUNATFIB at P_0=1600, x_0=300, R_b=100

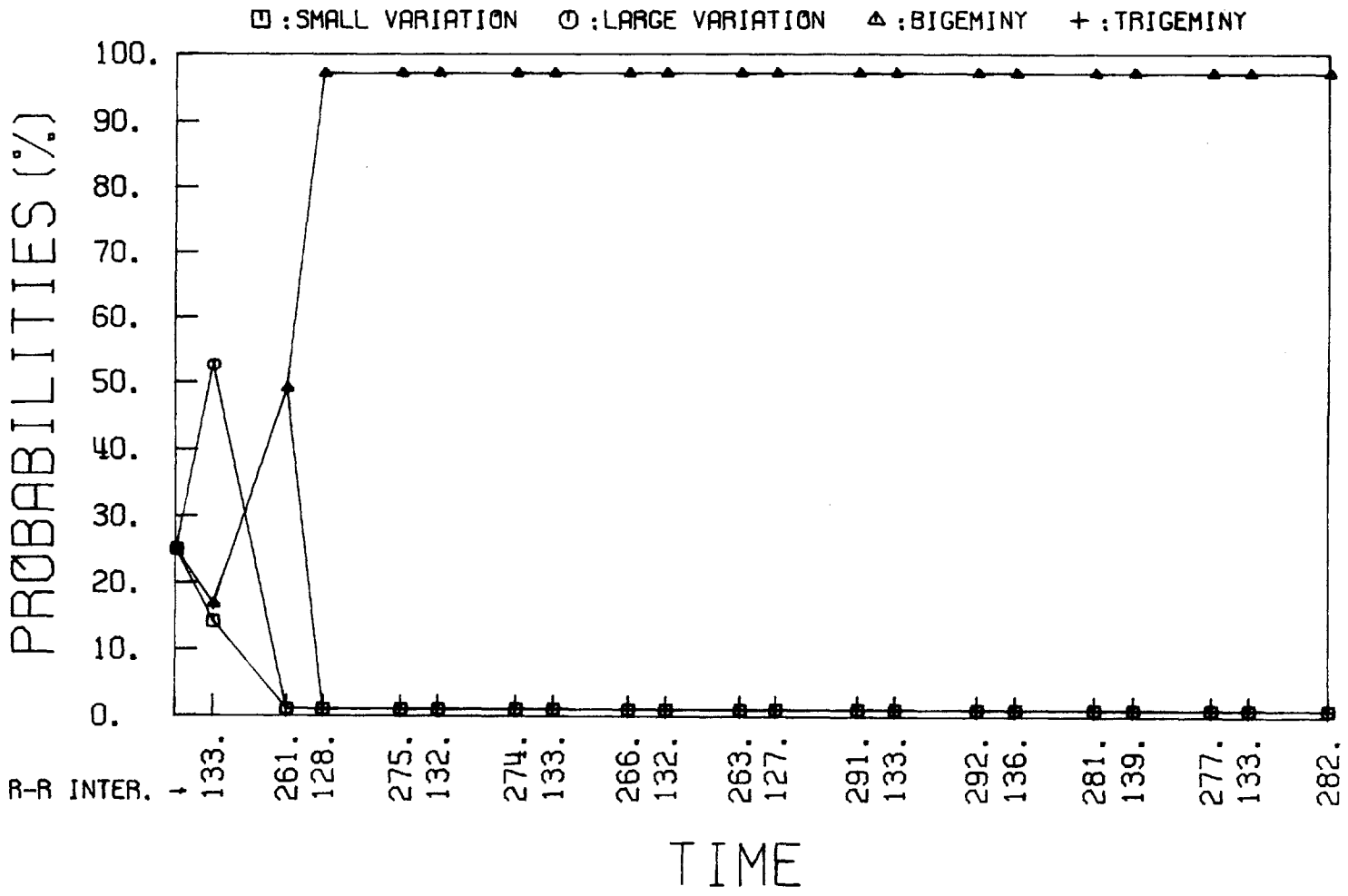

Figure 6.41 A Posteriori Probabilities of Data File #503 at P_0=1600, x_0=300, R_b=100

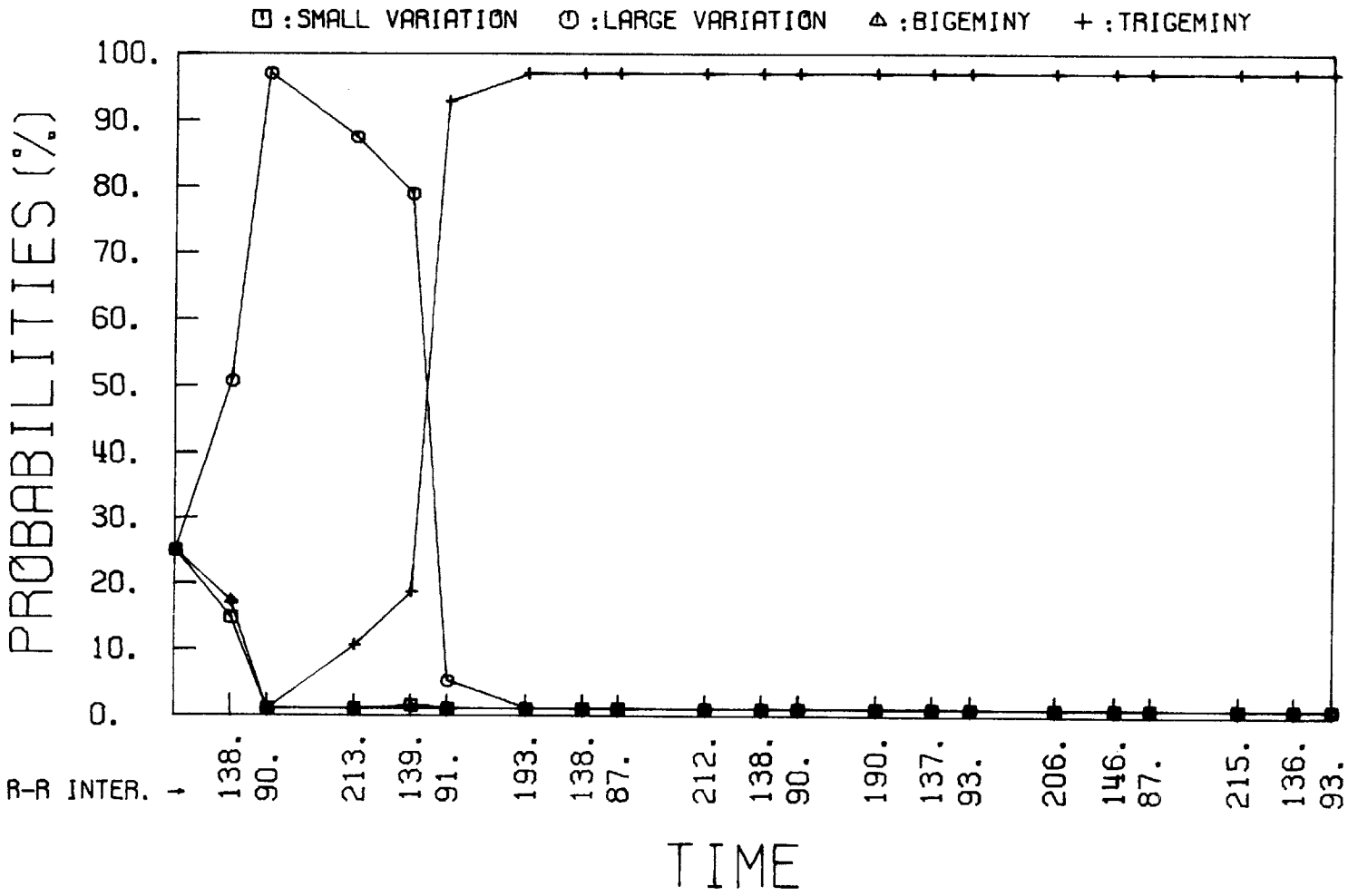

Figure 6.42 A Posteriori Probabilities of Data File HUANPVCS at P_0=1600, x_0=300, R_b=100

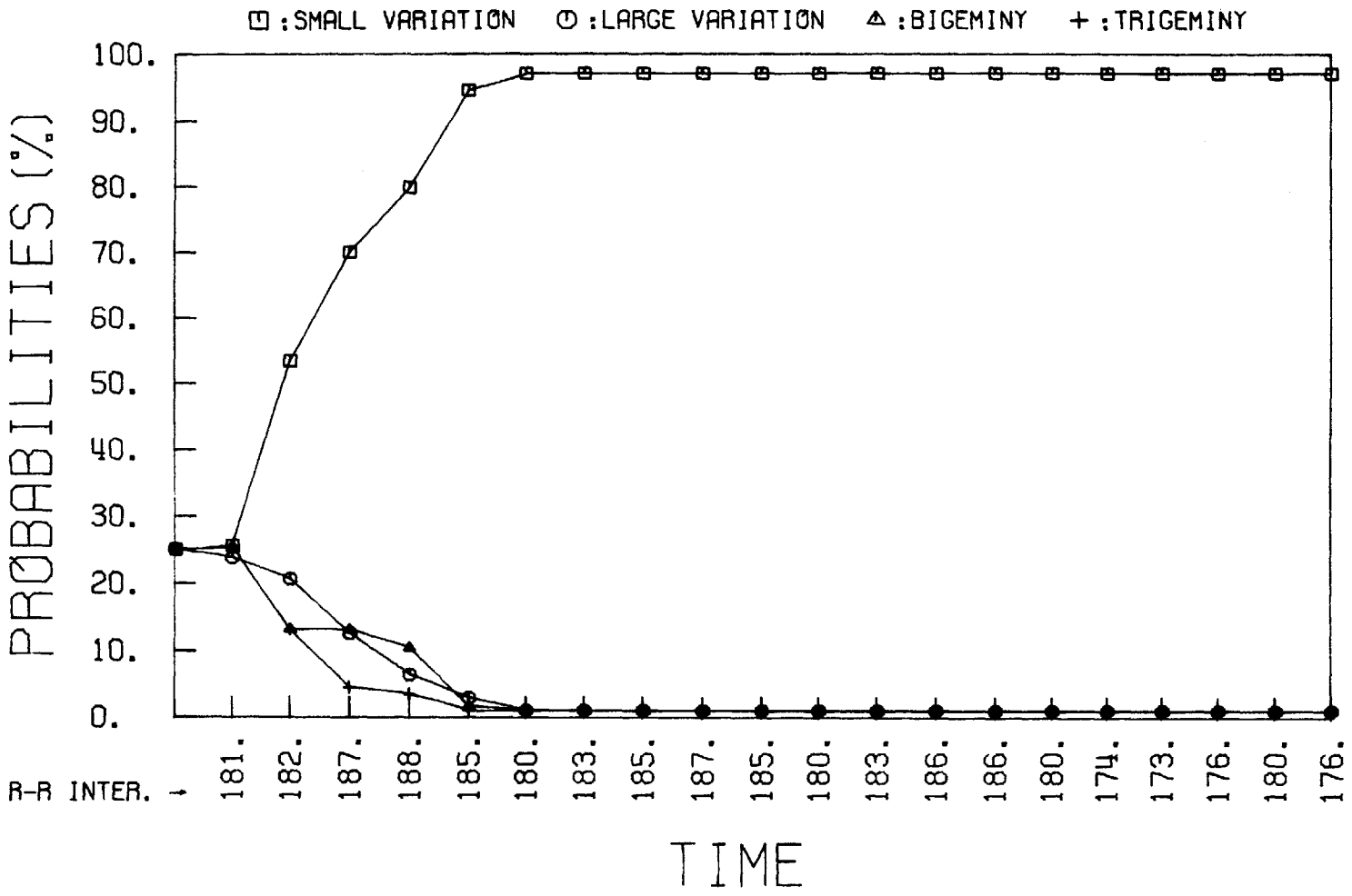

Figure 6.43 A Posteriori Probabilities of Data File IN.5 at P_0=1600, x_0=200, R_b=100

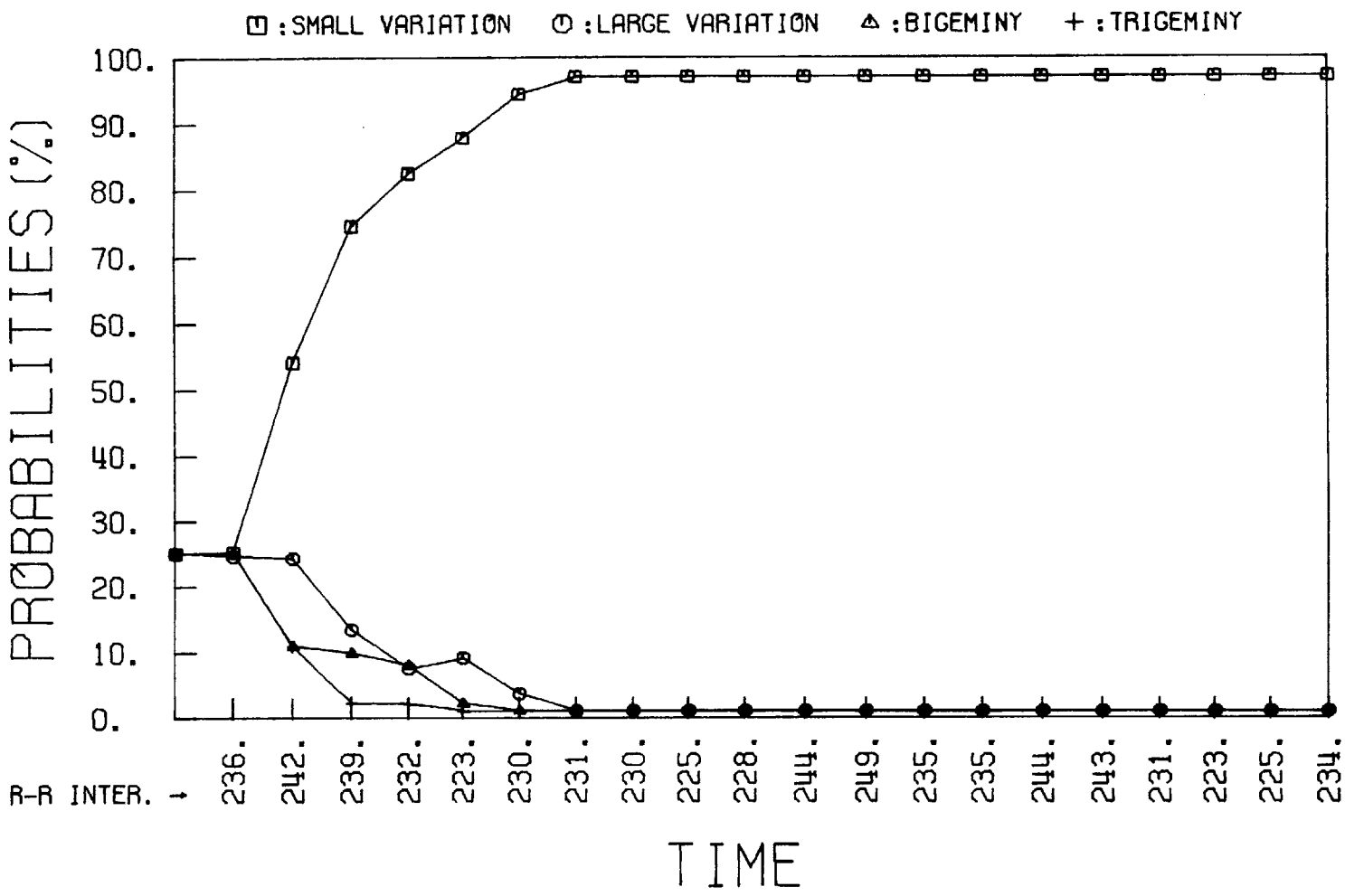

Figure 6.44 A Posteriori Probabilities of Data File IN.30 at P_0=1600, x_0=200, R_b=100

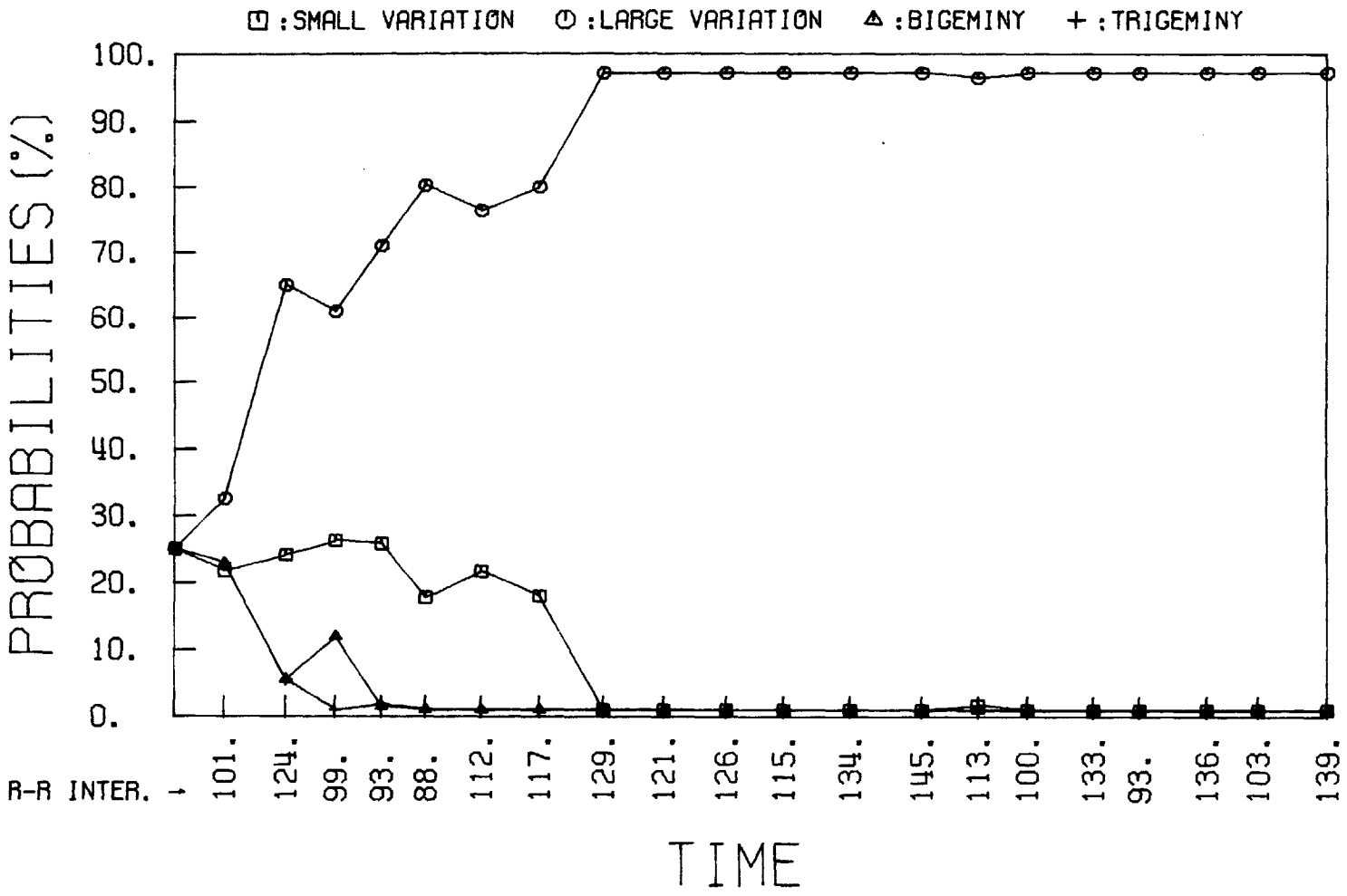

Figure 6.45 A Posteriori Probabilities of Data File CUNATFIB at P_0=1600, x_0=200, R_b=100

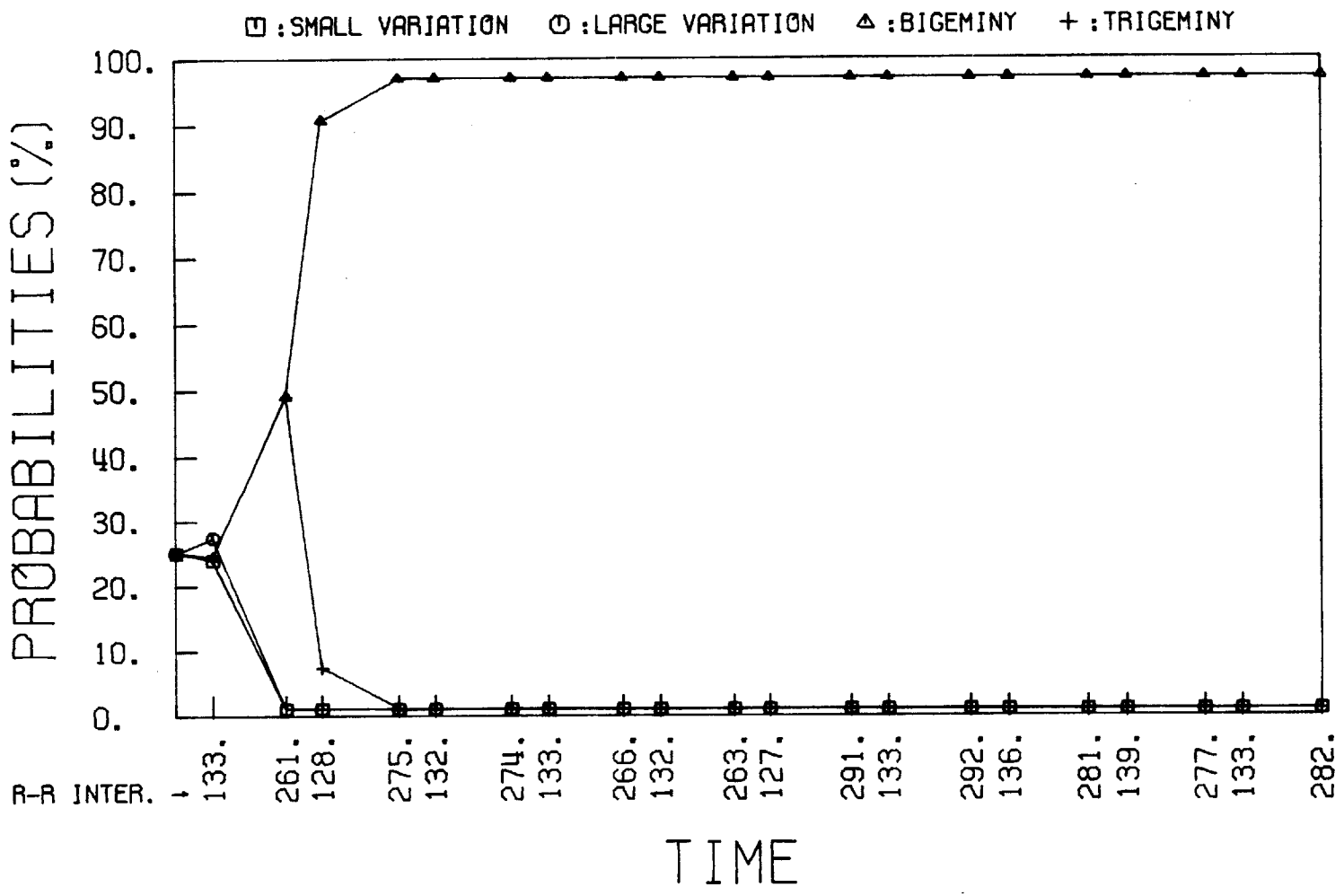

Figure 6.46 A Posteriori Probabilities of Data File #503 at P_0=1600, x_0=200, R_b=100

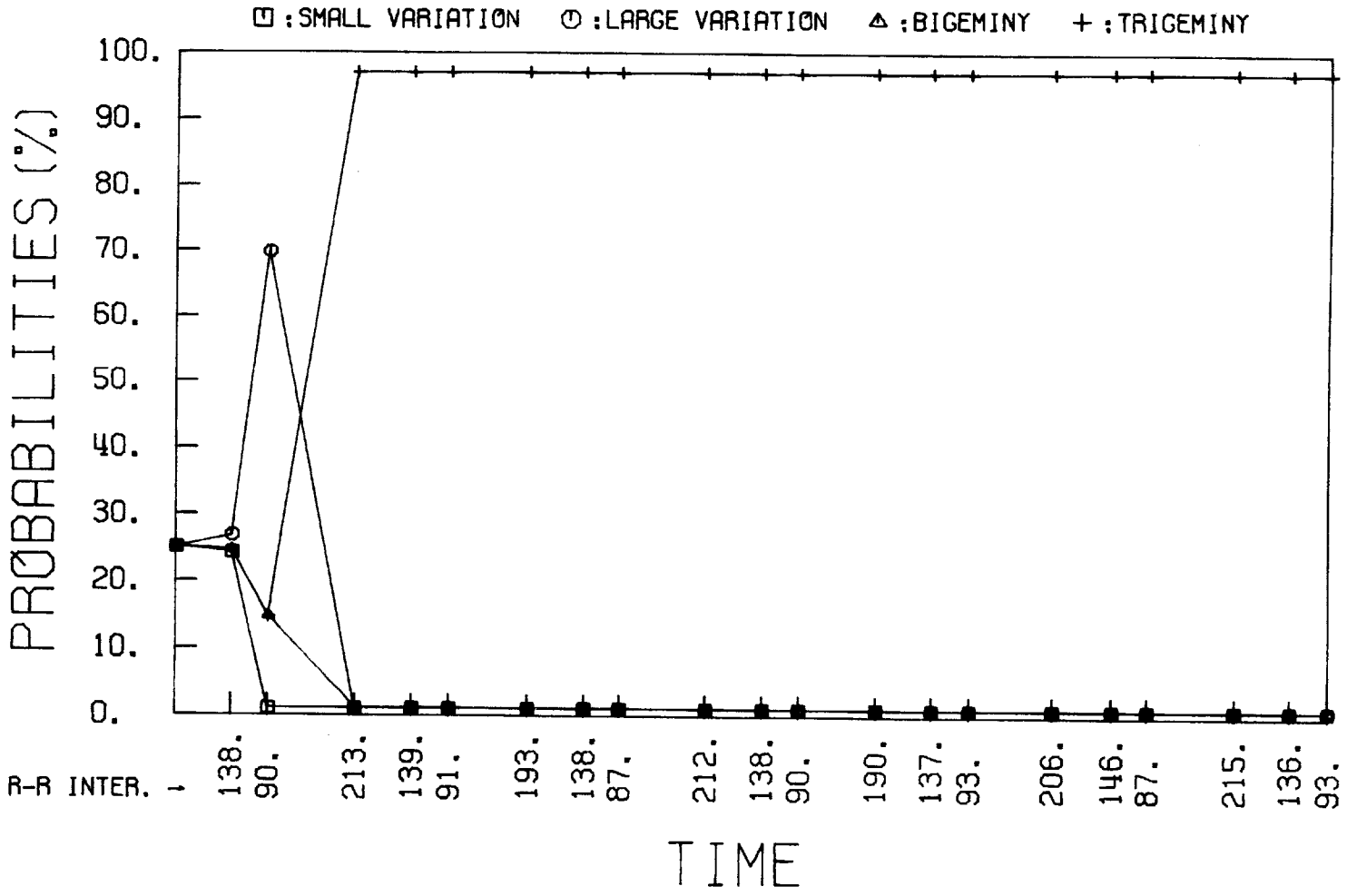

Figure 6.47 A Posteriori Probabilities of Data File HUANPVCS at P_0=1600, x_0=200, R_b=100

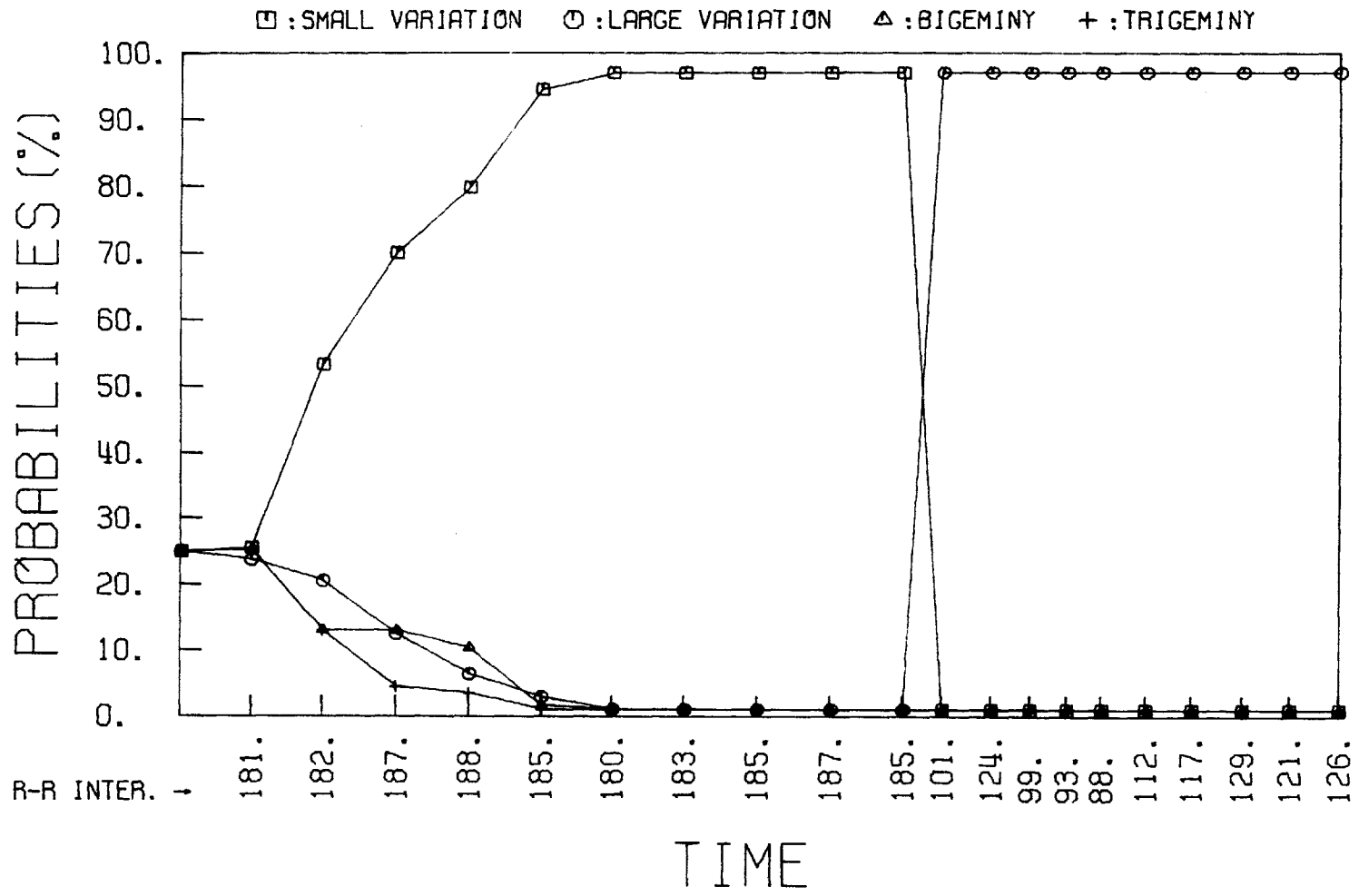

Figure 6.48 A Posteriori Probabilities of IN.5 → CUNATFIB Without Reinitialization of the Filter Parameters

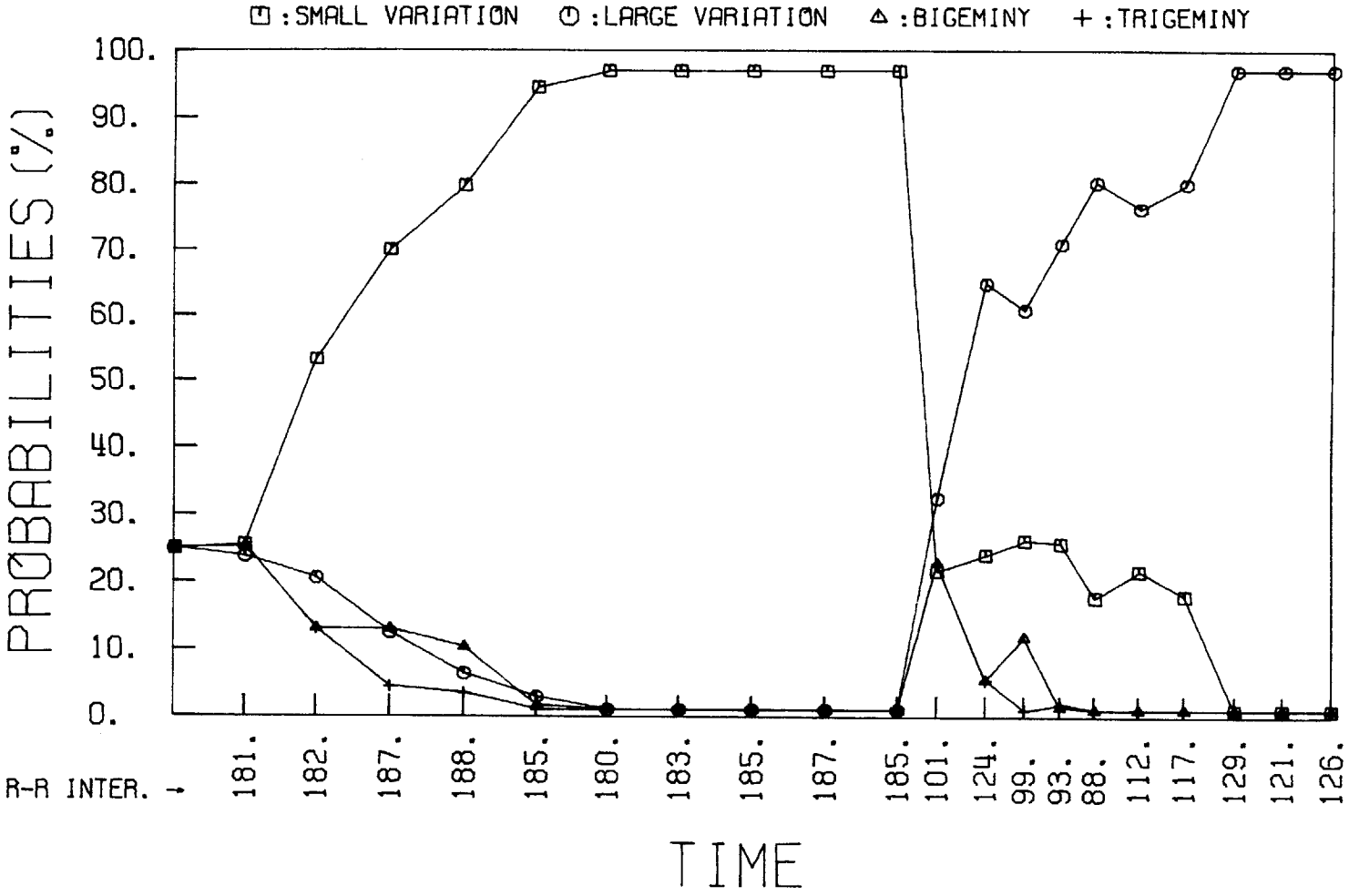

Figure 6.49 A Posteriori Probabilities of IN.5 → CUNATFIB With Reinitialization of the Filter Parameters

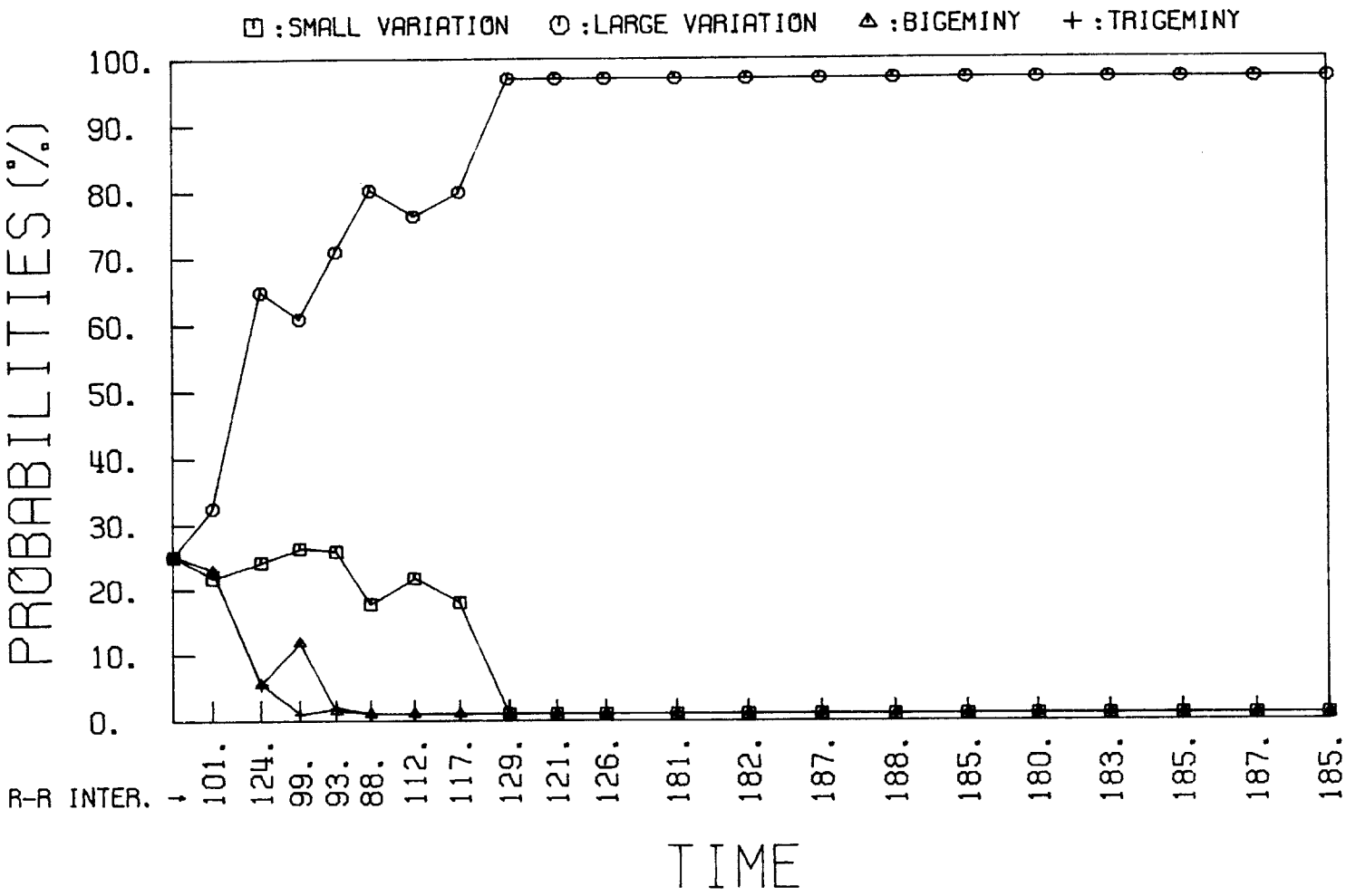

Figure 6.50 A Posteriori Probabilities of CUNATFIB → IN.5 Without Reinitialization of the Filter Parameters

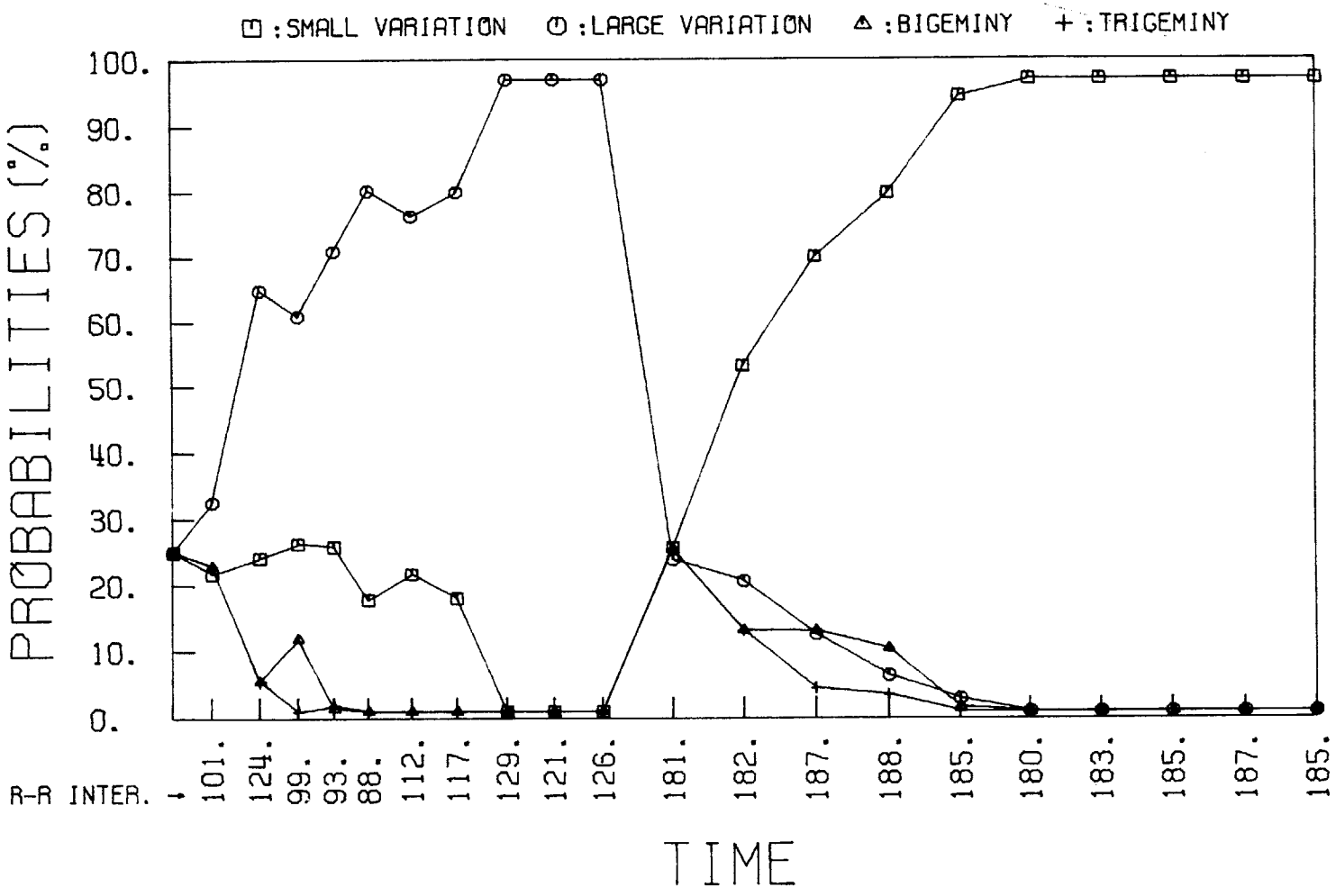

Figure 6.51 A Posteriori Probabilities of CUNATFIB → IN.5 With Reinitialization of the Filter Parameters

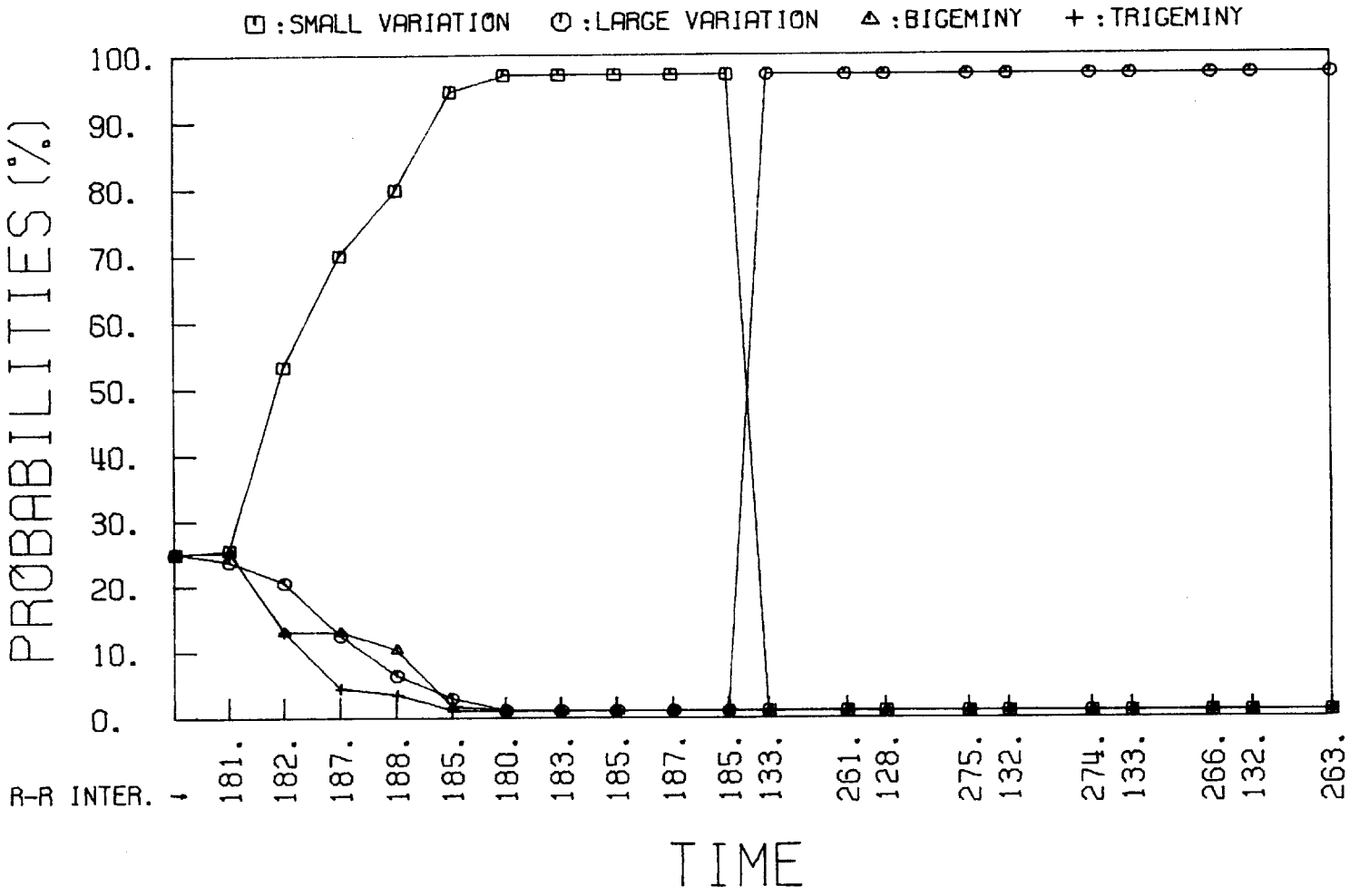

Figure 6.52 A Posteriori Probabilities of IN.5 → #503 Without Reinitialization of the Filter Parameters

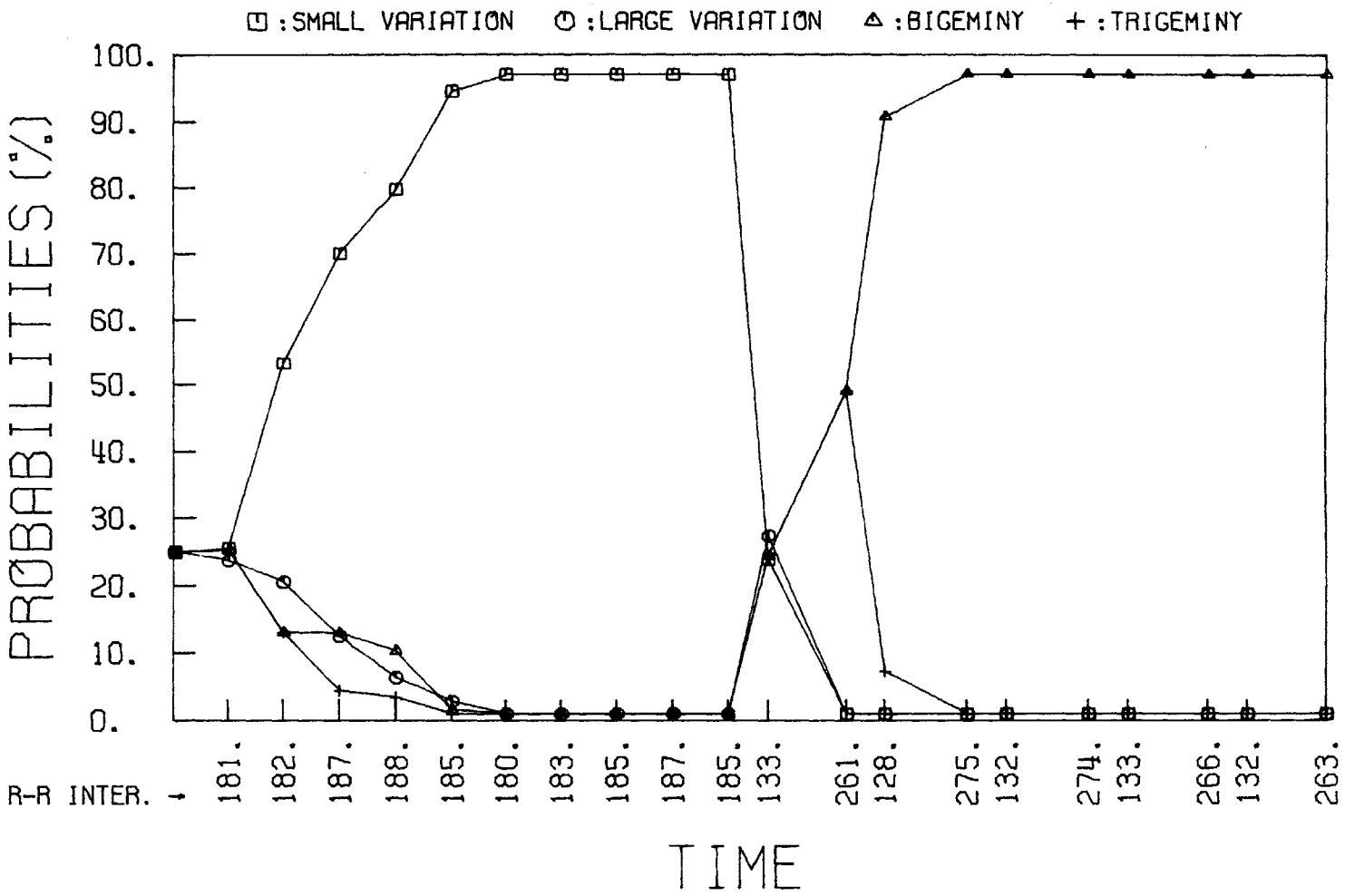

Figure 6.53 A Posteriori Probabilities of IN.5 → #503 With Reinitialization of the Filter Parameters

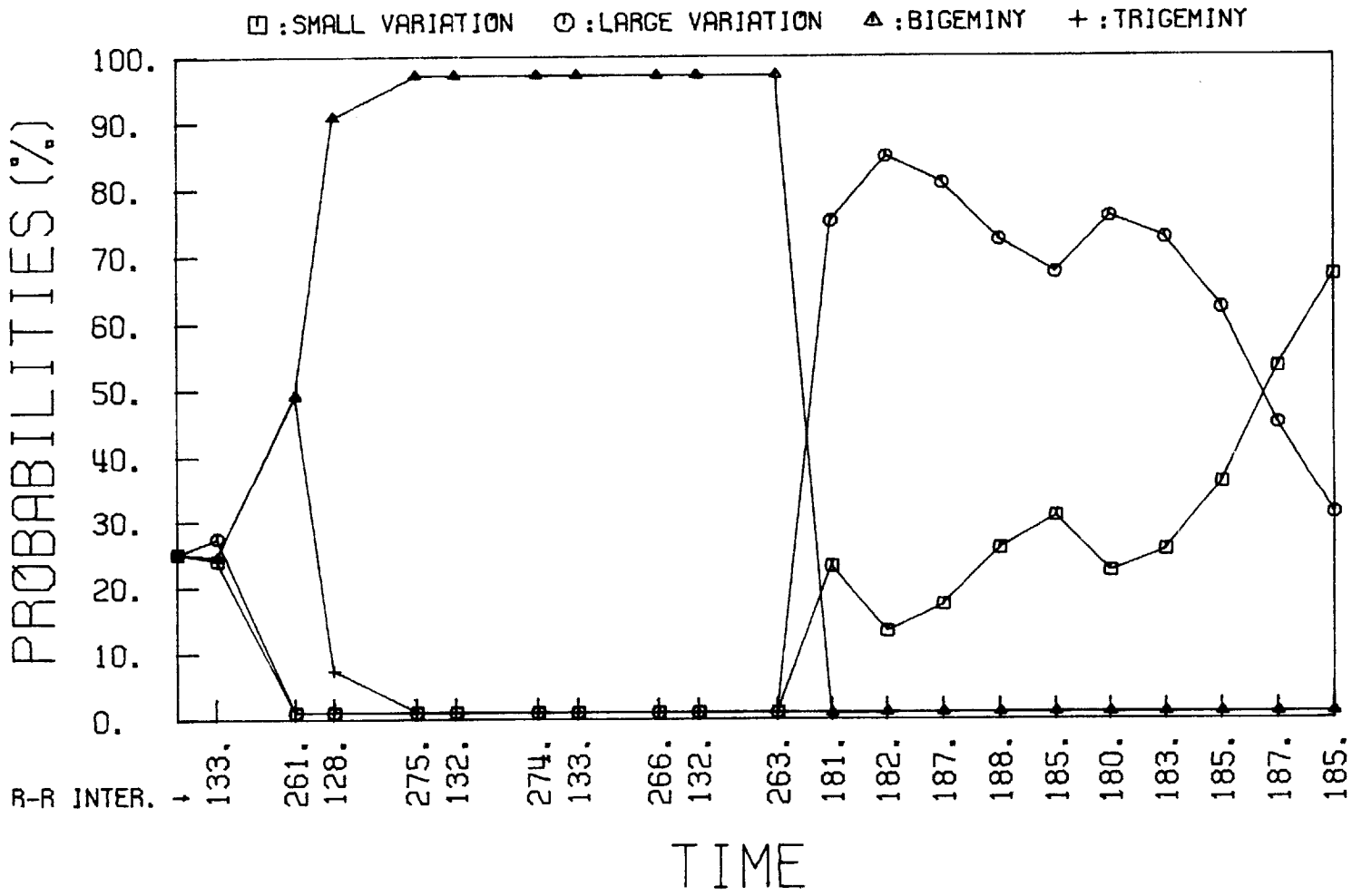

Figure 6.54 A Posteriori Probabilities of #503 → IN.5 Without Reinitialization of Filter Parameters

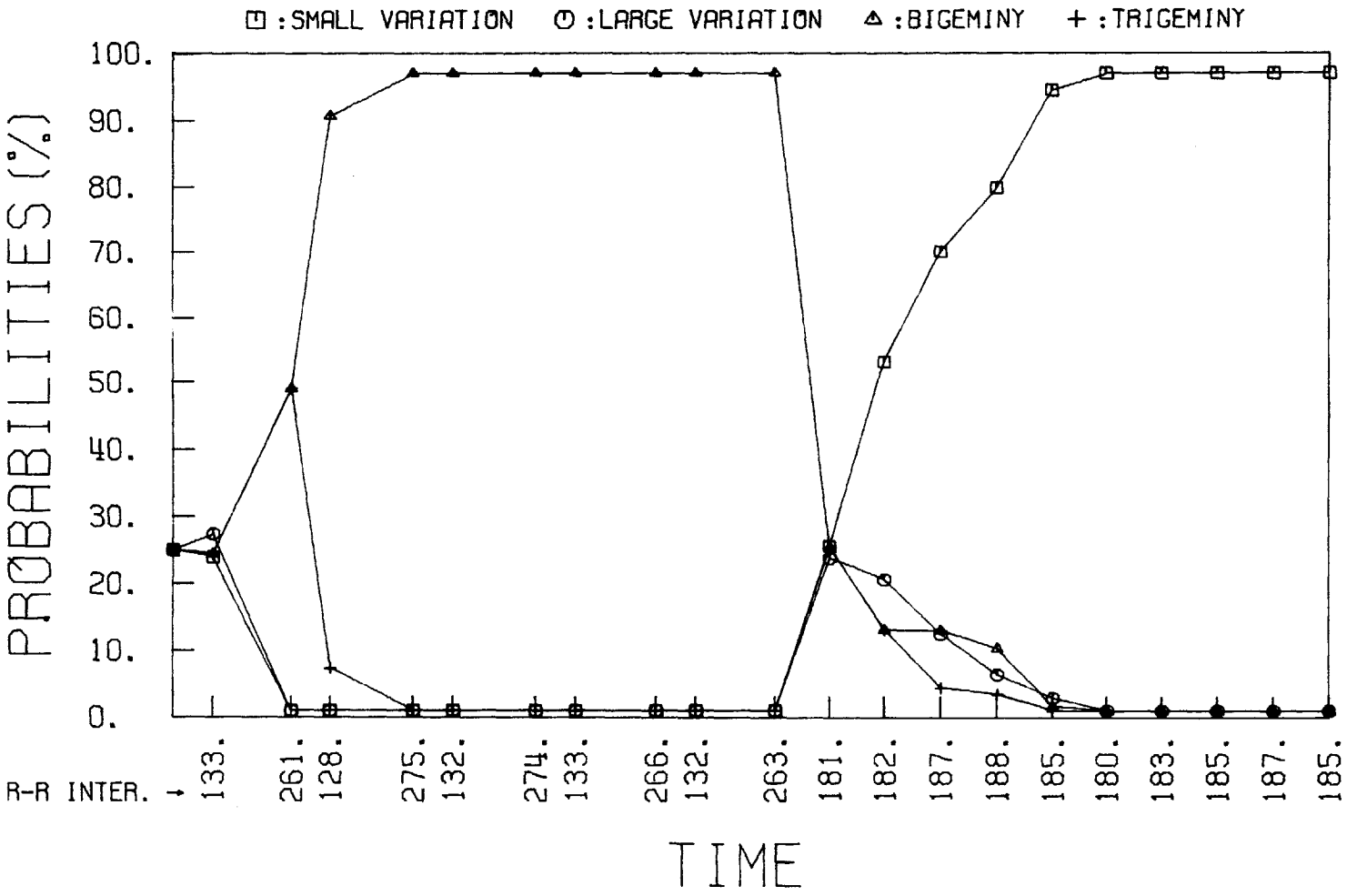

Figure 6.55 A Posteriori Probabilities of #503 → IN.5 With Reinitialization of the Filter Parameters

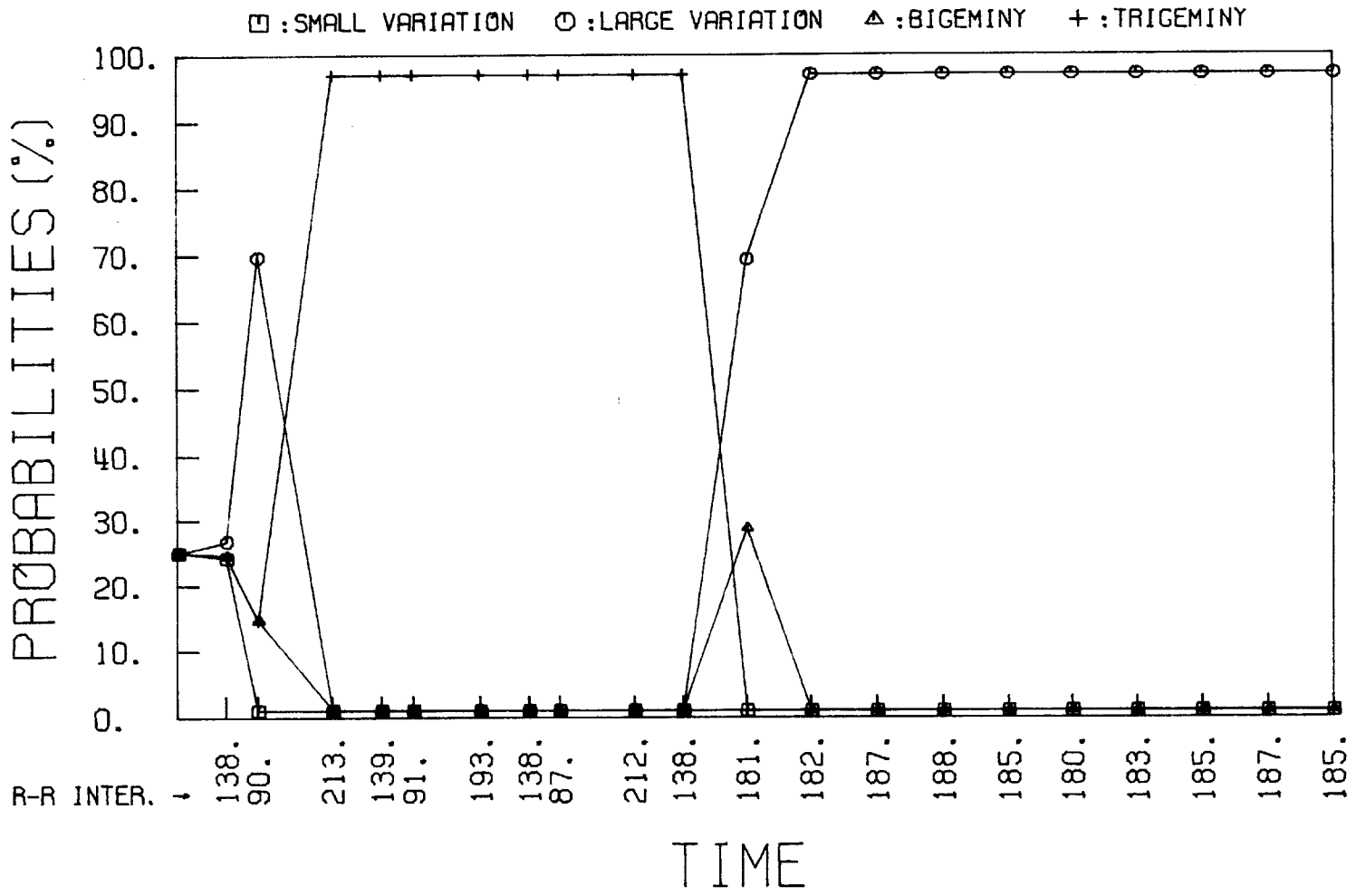

Figure 6.56 A Posteriori Probabilities of IN.5 → HUANPVCS Without Reinitialization of the Filter Parameters

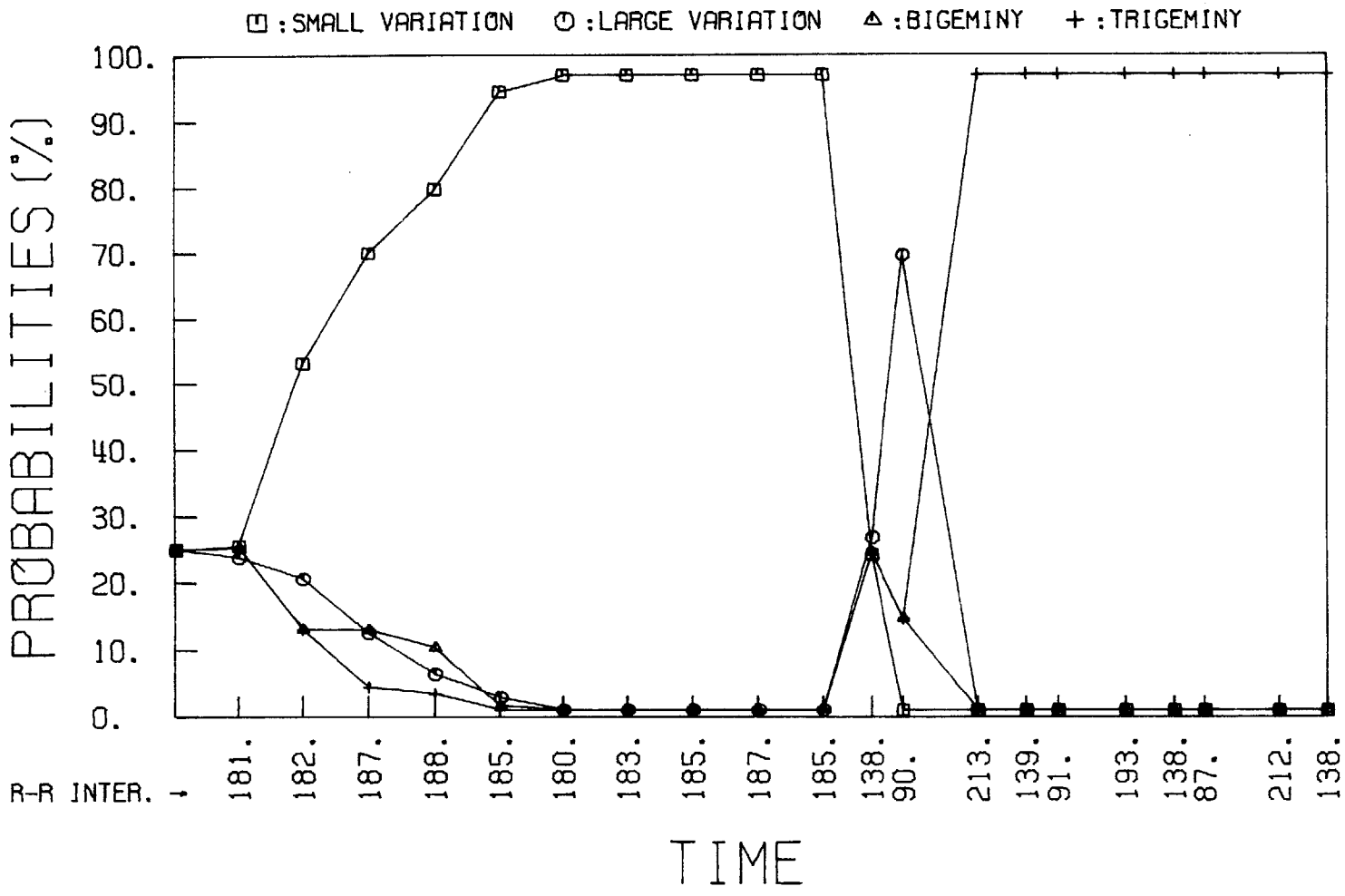

Figure 6.57 A Posteriori Probabilities of IN.5 → HUANPVCS With Reinitialization of the Filter Parameters

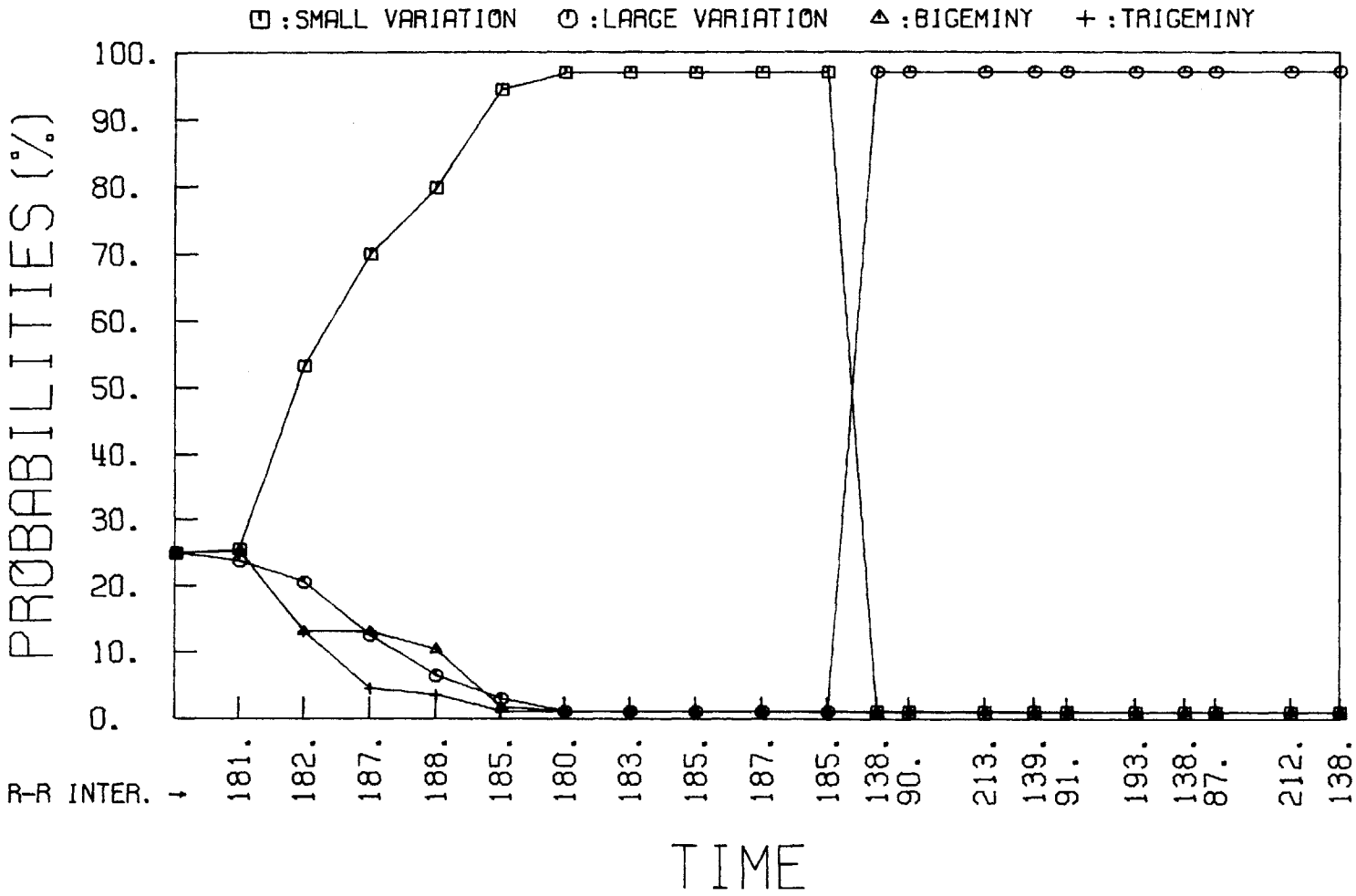

Figure 6.58 A Posteriori Probabilities of HUANPVCS → IN.5 Without Reinitialization of the Filter Parameters

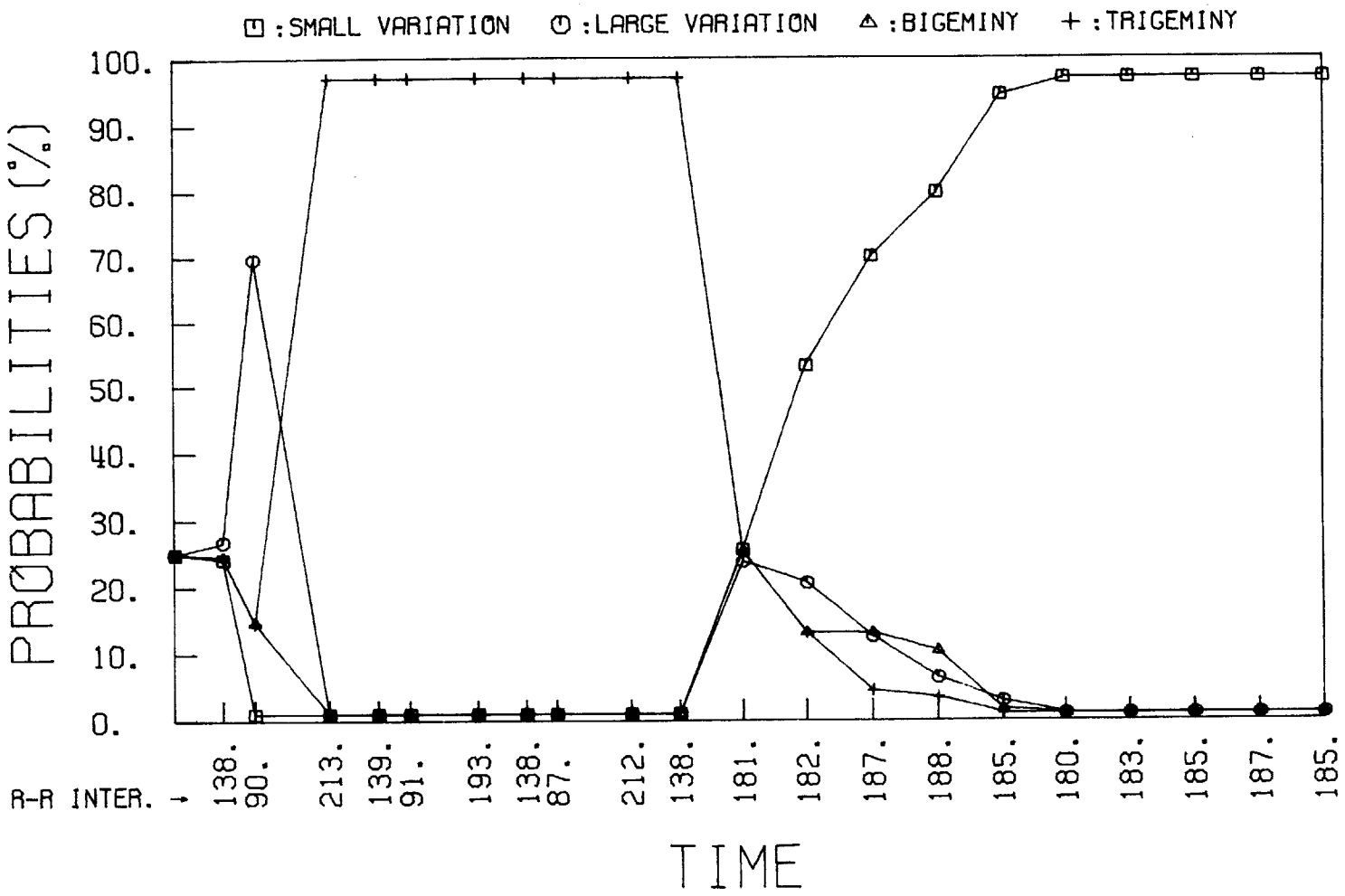

Figure 6.59 A Posteriori Probabilities of HUANPVCS → IN.5 With Reinitialization of the Filter Parameters

CHAPTER 7

DETECTION AND CLASSIFICATION OF TRANSIENT RHYTHMS

7.1 Generalized Likelihood Ratio Technique

In Chapter 5, we have developed dynamical models for several transient arrhythmia classes. We now would like to consider the problem of detection and identification for this class of arrhythmias. All the dynamical models for these arrhythmia classes can be written in a general form

$$x(k) = x(k-1) + F(k,\theta)\nu \tag{7.1}$$

$$y(k) = x(k) + v(k) \tag{7.2}$$

where $x(k)$ is the state of the system, and $y(k)$ is the measurement of the state, which is corrupted by a white Gaussian noise $v(k)$. The term $F(k,\theta)\nu$ in the process equation, Equation (7.1), represents the transient effect, where θ is an unknown time where this transient event commences and ν is the unknown strength of this change. $F(k,\theta)$ is a function of both k and θ. Refering to Equations (7.1) and (7.2), $F(k,\theta)$ for the transient arrhythmia classes modeled in Chapter 5 are then given as follows:

(1) normal rhythm jump

$$F(k,\theta) = \delta_{\theta,k}$$

(2) non-compensatory beat

$$F(k,\theta) = \delta_{\theta,k} - \delta_{\theta,k-1}$$

(3) compensatory beat

$$F(k,\theta) = \delta_{\theta,k} - 2\delta_{\theta,k-1} + \delta_{\theta,k-2}$$

(4) double non-compensatory beat

$$F(k,\theta) = \delta_{\theta,k} - \delta_{\theta,k-2}$$

Therefore a satisfactory method of detection and identification for this class of problems should not only be able to detect these abrupt changes, but also be able to estimate the time, θ, where this change occurs, and, ν, the strength of this abrupt change. Our design of the detection and estimation of this class of problems is based on the Generalized Likelihood Ratio (GLR) technique [42]. This GLR approach will detect the abrupt changes and also give a maximum likelihood estimate of ν and θ.

The philosophy of our approach based on the GLR method is described in the following. The GLR equations for a jump model have been derived previously in [43]. However, in this study a more general derivation of these equations is given in Section 7.2. For each dynamical model developed in Chapter 5, there is associated with it a $F(k,\theta)\nu$ term. We first construct a Kalman filter based on this dynamical model neglecting this term. The measurement residual sequence, $\gamma(k)$, and the associated variances, $V(k)$, from the Kalman filter are then used as the input to a GLR detector. In this case, if there is no abrupt change of the R-R interval sequence, the statistics of $\gamma(k)$ are those computed based on the Kalman filter neglecting the $F(k,\theta)\nu$ term. Otherwise, $\gamma(k)$ contains a bias term, which is proportional to ν. The proportionality matrix $G(k,\theta)$, called the rhythm signature, can be computed from the $\gamma(k)$, $V(k)$ and $F(k,\theta)$. We can then perform a maximum likelihood estimation procedure to determine the most likely values of θ and ν, and then

determine the generalized likelihood ratio $\ell(k,\theta)$ for the abrupt change. This GLR detection system is shown in Figure 7.1. Here y(k) is the actual R-R interval sequence.

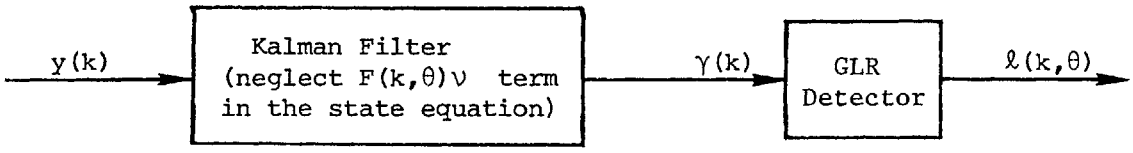

Figure 7.1 The GLR Detector

Since the transient events are always viewed, from the cardiologists' stand point, with respect to an underlying regular rhythm, the Kalman filter to be used in the GLR detector is designed based on a regular rhythm dynamical model. Since, we have no a priori information as to which of the arrhythmia classes described in Chapter 3 will occur, a bank of GLR detectors in parallel is built. Each member of this bank of detectors corresponds to one of the possible arrhythmia classes we wish to detect. In other words, we hypothesize several possible arrhythmia classes and wish to determine which is the correct one. This transient rhythm detection configuration is shown in Figure 7.2.

In use, the generalized log-likelihood ratio, $\ell(k,\theta)$, corresponding to the correct model should be a monotonically increasing function of k; i.e., we should become more confident that this is the correct model as more data becomes avaliable. Thus, a correlation test on

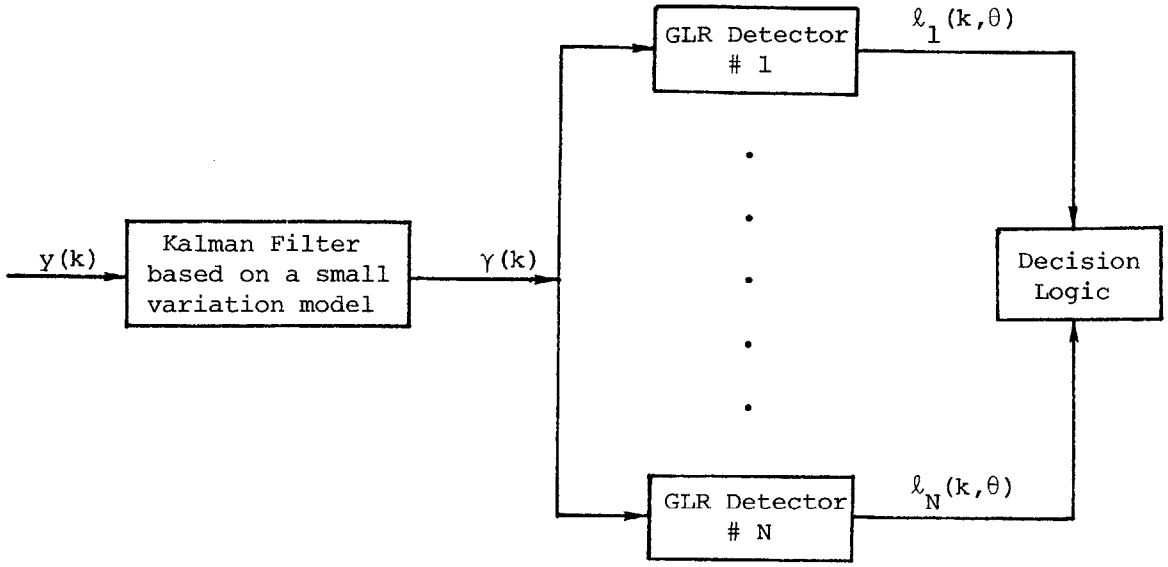

Figure 7.2 The Transient Rhythm Detection Configuration

$\ell_i(k,\theta)$ for varying k, and a monotone increasing test on $\ell_i(k,\theta)$ for increasing k should be able to identify the correct arrhythmia classes (see experimental results in Section 7.4).

7.2 Derivation of GLR Equations

7.2.1 Derivation of Rhythm Signatures

Consider a general discrete-time dynamical system of the following form:

$$x(k) = \Phi(k,k-1)x(k-1) + \Gamma(k)w(k) + F(k,\theta)\nu \tag{7.3}$$

$$y(k) = H(k)x(k) + v(k) \tag{7.4}$$

where $x(k) \in R^n$ is the state, with initial condition $x(0)$ being a gaussian random variable with mean $\hat{x}(0)$ and covariance $P(0)$, and $\{w(k)\}$ is an m-dimensional white Gaussian sequence with statistics

$$E[w(k)]=0 \tag{7.5}$$

$$E[w(k)w^T(j)]=Q(k)\delta_{kj} \tag{7.6}$$

$y(k) \in R^p$ is the observation, and $\{v(k)\}$ is a p-dimensional white Gaussian sequence with statistics

$$E[v(k)]=0 \tag{7.7}$$

$$E[v(k)v^T(j)]=R(k)\delta_{kj} \tag{7.8}$$

In addition,

$$E[w(k)v^T(j)]=0 \tag{7.9}$$

$$E[w(k)x^T(0)]=0 \tag{7.10}$$

$$E[v(k)x^T(0)]=0 \tag{7.11}$$

The term $F(k,\theta)\nu$ represents the abrupt changes defined in Section 7.1, where ν is an unknown shift and θ is the unknown time at which this shift occurs.

The problem of determining whether there is an abrupt change or not is equivalent to a decision problem with the following two hypotheses:

H_0: No abrupt change up to the present time (i.e., $\theta > k$)

H_1: An abrupt change has occurred ($\theta \leq k$)

Under hypothesis H_0, the Kalman-Bucy filter for the system [(7.3)-(7.4)] is implemented:

$$\hat{x}(k|k-1) = \Phi(k,k-1)\hat{x}(k-1|k-1) \tag{7.12}$$

$$\hat{x}(k|k) = \hat{x}(k|k-1) + M(k)\gamma(k) \tag{7.13}$$

where $\gamma(k)$ is the measurement residual

$$\gamma(k) = y(k) - H(k)\hat{x}(k|k-1) \tag{7.14}$$

with statistics

$$E[\gamma(k)]=0 \tag{7.15}$$

$$E[\gamma(k)\gamma^T(j)] = V(k)\delta_{kj} \tag{7.16}$$

and $\hat{x}(i|j)$ is the estimate of $x(i)$ given observations $y(1),y(2),\ldots,y(j)$ under hypothesis H_0, and $M(k)$ is the filter gain. The associated error covariance matrix, $P(i|j)$, is computed according to the following recursive relations:

$$P(k|k-1) = \Phi(k,k-1)P(k-1|k-1)\Phi^T(k,k-1) + \Gamma(k)Q(k)\Gamma^T(k) \tag{7.17}$$

$$V(k) = H(k)P(k|k-1)H^T(k) + R(k) \tag{7.18}$$

$$M(k) = P(k|k-1)H^T(k)V^{-1}(k) \tag{7.19}$$

$$P(k|k) = P(k|k-1) - M(k)H(k)P(k|k-1) \tag{7-20}$$

with initial condition $P(0|0) = P(0)$.

Using Equations (7.3),(7.4) and (7.12) through (7.20) we can derive an expression for the measurement residual $\gamma(k)$ that explicitly involves θ and ν; i.e., we wish to compute the effect of the $F(k,\theta)\nu$ term on the state estimates and measurement residuals.

Let us first define the error of the estimate as the difference between the estimated state and true state

$$e(k|k) = \hat{x}(k|k) - x(k) \tag{7.21}$$

and

$$e(k|k-1) = \hat{x}(k|k-1) - x(k) \tag{7.22}$$

Substituting Equations (7.3) and (7.12) into Equation (7.22), we have

$$\begin{aligned} e(k|k-1) &= \Phi(k,k-1)\hat{x}(k-1|k-1) - \Phi(k,k-1)x(k-1) \\ &\quad - \Gamma(k)w(k) - F(k,\theta)\nu \\ &= \Phi(k,k-1)[\hat{x}(k-1|k-1) - x(k-1)] \\ &\quad - \Gamma(k)w(k) - F(k,\theta)\nu \end{aligned} \tag{7.23}$$

Using Equation (7.21), Equation (7.23) becomes

$$\begin{aligned} e(k|k-1) &= \Phi(k,k-1)e(k-1|k-1) - \Gamma(k)w(k) \\ &\quad - F(k,\theta)\nu \end{aligned} \tag{7.24}$$

From Equation (7.14), the measurement residual is given as

$$\gamma(k) = y(k) - H(k)\hat{x}(k|k-1) \tag{7.25}$$

Using Equation (7.4) in Equation (7.25), we get

$$\gamma(k) = H(k)x(k) + v(k) - H(k)\hat{x}(k|k-1)$$

$$= - H(k)[\hat{x}(k|k-1) - x(k)] + v(k) \tag{7.26}$$

By Equation (7.22), this is just

$$\gamma(k) = - H(k)e(k|k-1) + v(k) \tag{7.27}$$

Substituting Equation (7.13) into Equation (7.21), we obtain

$$e(k|k) = \hat{x}(k|k-1) + M(k)\gamma(k) - x(k)$$

$$= [\hat{x}(k|k-1) - x(k)] + M(k)\gamma(k)$$

$$= e(k|k-1) + M(k)\gamma(k) \tag{7.28}$$

Under hypothesis H_0, which assumes no abrupt change up to the present time, Equations (7.24),(7.27) and (7.28) become, upon setting $\nu=0$:

$$e^o(k|k-1) = \Phi(k,k-1)e^o(k-1|k-1) - \Gamma(k)w(k) \tag{7.29}$$

$$\gamma^o(k) = -H(k)e^o(k|k-1) + v(k) \tag{7.30}$$

and

$$e^o(k|k) = e^o(k|k-1) + M(k)\gamma^o(k) \tag{7.31}$$

Here, the superscript "o" is used to indicate the estimation error and measurement residual under the hypothesis H_0.

Now we define the difference between $e(k|k-1)$ and $e^{o}(k|k-1)$ as

$$e^{o}(k|k-1) - e(k|k-1) = B(k,\theta)\nu \tag{7.32}$$

where $B(k,\theta)$ is a function of both k and θ. Note that there is no difference between $e(k|k-1)$ and $e^{o}(k|k-1)$, unless some abrupt changes occur. Thus, we require

$$B(k,\theta)=0 \qquad k<\theta \tag{7.33}$$

Using Equations (7.24) and (7.29) in Equation (7.32), we have

$$\Phi(k,k-1)[e^{o}(k-1|k-1) - e(k-1|k-1)] + F(k,\theta)\nu$$
$$= B(k,\theta)\nu \tag{7.34}$$

Substituting Equations (7.28) and (7.31) into Equation (7.34), we get

$$B(k,\theta)\nu = \Phi(k,k-1)[e^{o}(k-1|k-2) - e(k-1|k-2) + M(k-1)\gamma^{o}(k-1) - M(k-1)\gamma(k-1)]$$
$$+ F(k,\theta)\nu$$
$$= \Phi(k,k-1)[B(k-1,\theta)\nu + M(k-1)(\gamma^{o}(k-1) - \gamma(k-1))] + F(k,\theta)\nu \tag{7.35}$$

Using Equations (7.27) and (7.30) for $\gamma(k-1)$ and $\gamma^{o}(k-1)$, respectively, we have

$$B(k,\theta)\nu = \Phi(k,k-1)[B(k-1,\theta)\nu - M(k-1)H(k-1)B(k-1,\theta)\nu]$$
$$+ F(k,\theta)\nu$$
$$= \Phi(k,k-1)[I-M(k-1)H(k-1)]B(k-1,\theta)\nu$$
$$+ F(k,\theta)\nu \tag{7.36}$$

or, since this must be satisfied for all ν:

$$B(k,\theta) = \Phi(k,k-1)[I-M(k-1)H(k-1)]B(k-1,\theta) + F(k,\theta) \tag{7.37}$$

From Equation (7.33) we have $B(k-1,\theta)=0$ for $k=\theta$; therefore, we have

$$B(\theta,\theta) = F(\theta,\theta) \tag{7.38}$$

We can also define a relationship between $\gamma(k)$ and $\gamma^{o}(k)$ similar to the one we defined for $e(k|k-1)$ and $e^{o}(k|k-1)$ as follows

$$\gamma(k) = \gamma^{o}(k) + G(k,\theta)\nu \tag{7.39}$$

where $\gamma^{o}(k)$ is the measurement residual under hypothesis H_0 (no abrupt changes up to present time k). The $G(k,\theta)\nu$ term is the effect of $F(k,\theta)\nu$ term on the measurement residual, and $G(k,\theta)$ is a function of both k and θ. For the same reason, we also have

$$G(k,\theta)=0 \qquad k<\theta \tag{7.40}$$

Substituting Equations (7.27) and (7.30) into Equation (7.39), we obtain

$$\begin{aligned} G(k,\theta)\nu &= -H(k)[e(k|k-1) - e^{o}(k|k-1)] \\ &= H(k)B(k,\theta)\nu \end{aligned} \tag{7.41}$$

or,

$$G(k,\theta) = H(k)B(k,\theta) \tag{7.42}$$

From Equation (7.38), we have, as the initial condition

$$G(\theta,\theta) = H(\theta)B(\theta,\theta)$$
$$= H(\theta)F(\theta,\theta) \tag{7.43}$$

Using Equations (7.37),(7.38) and (7.42), we can compute $G(k,\theta)$ for all k and θ. The values of $G(k,\theta)$ are all zero for θ greater than k, as given by Equation (7.40). Therefore for a given k, we need only to compute $G(k,\theta)$ for θ less than or equal to k. For θ less than k $B(k,\theta)$ can be calculated using Equation (7.37), while for θ equal to k, $B(k,\theta)$ is given by Equation (7.38). Once $B(k,\theta)$ is computed, $G(k,\theta)$ are then given by Equation (7.42).

7.2.2 Derivation of Likelihood Ratios and Jump Estimates

Now the problem of determing whether or not there is an abrupt change is equivalent to a decision problem based on the observations $\gamma(k)$, with the following two hypotheses:

$$H_0: \quad \gamma(k) = \gamma^o(k)$$

$$H_1: \quad \gamma(k) = \gamma^o(k) + G(k,\theta)\nu$$

where $\gamma^o(k)$ is the measurement residual assume no abrupt changes occur, and is a zero-mean white sequence with covariance V(k).

Here we have two hypotheses with two unknown parameters θ and ν. If θ and ν are random variables with known probability density functions, then the decision rule can be formulated easily by using a likelihood ratio test. But in our case, θ is the time at which the abrupt change occurs and ν is the strength of this abrupt change. They are not random variables but rather are two unknown quantities.

Therefore a generalized likelihood ratio test technique [42] will be utilized to formulate the decision rule. The procedure of this generalized likelihood ratio test is first to estimate both θ and ν as functions of k assuming that hypothesis H_1 is true, and then use these estimates $\hat{\theta}(k)$ and $\hat{\nu}(k)$ in a likelihood ratio test as if they were correct. The estimates of θ and ν are done using a maximum likelihood estimate as follows:

$$\frac{\partial}{\partial\theta(k)}\left[P(\gamma(1),\ldots,\gamma(k)\,|\,H_1,\theta(k),\hat{\nu}(k))\right]=0 \qquad \theta(k)=\hat{\theta}(k) \tag{7.44}$$

and

$$\frac{\partial}{\partial\nu(k)}\left[P(\gamma(1),\ldots,\gamma(k)\,|\,H_1,\hat{\theta}(k),\nu(k))\right]=0 \qquad \nu(k)=\hat{\nu}(k) \tag{7.45}$$

where $P(\gamma(1),\ldots,\gamma(k)\,|\,H_1,\theta,\nu)$ is the joint probability density function of $\gamma(1),\ldots,\gamma(k)$ conditioned on θ,ν and under hypothesis H_1. Since the measurement residual $\gamma(i)$ are Gaussian, this conditional probability density function is

$$P(\gamma(i)\,|\,H_1,\theta(k),\nu(k)) = (2\pi|V(i)|)^{-1/2}\exp\left[-\frac{1}{2}(\gamma(i)-G(i,\theta(k))\nu(k))^T V^{-1}(i)(\gamma(i)-G(i,\theta(k))\nu(k))\right] \tag{7.46}$$

We have assumed $\gamma(i)$ is a scalaer here. The extension to vector case is straightforward.

Because the $\gamma(i)$ are statistically independent, the joint probability density function of $\gamma(1),\ldots,\gamma(k)$ is simply the product of the individual probability densities. Thus

$$P(\gamma(1),\ldots,\gamma(k)\,|\,H_1,\theta(k),\nu(k)) = \prod_{i=1}^{k} P(\gamma(i)\,|\,H_1,\theta(k),\nu(k)) \tag{7.47}$$

or, upon some simplifications:

$$P(\gamma(1),\ldots,\gamma(k)\,|\,H_1,\theta(k),\nu(k)) = \left[\prod_{i=1}^{k} \frac{1}{\sqrt{2\pi|V(i)|}}\right] \cdot \exp\left[-\frac{1}{2}\sum_{i=1}^{k}(\gamma(i)-G(i,\theta(k))\nu(k))^T V^{-1}(i)(\gamma(i)-G(i,\theta(k))\nu(k))\right] \tag{7.48}$$

Having computed the maximum likelihood estimates $\hat{\theta}(k)$, $\hat{\nu}(k)$, the generalized likelihood ratio, denoted by $\Lambda(k)$, is given as:

$$\Lambda(k) = \frac{P(\gamma(1),\ldots,\gamma(k)\,|\,H_1,\hat{\theta}(k),\hat{\nu}(k))}{P(\gamma(1),\ldots,\gamma(k)\,|\,H_0)} \tag{7.49}$$

where $P(\gamma(1),\ldots,\gamma(k)\,|\,H_0)$ is the conditional probability density function of $\gamma(1),\ldots,\gamma(k)$ assuming H_0 is true, and is given as:

$$P(\gamma(1),\ldots,\gamma(k)\,|\,H_0) = \left[\prod_{i=1}^{k} \frac{1}{2\pi|V(i)|}\right] \exp\left[-\frac{1}{2}\sum_{i=1}^{k}\gamma^T(i)V^{-1}(i)\gamma(i)\right] \tag{7.50}$$

The decision rule for selecting either H_0 or H_1 is

$$\Lambda(k) \underset{H_0}{\overset{H_1}{\gtrless}} \eta \tag{7.51}$$

where η is the threshold. Since the natural logarithm is a monotonic function, the decision rule is equivalent to, upon taking logarithm on both sides of Equation (7.51):

$$\ell n\ \Lambda(k) \underset{H_0}{\overset{H_1}{\gtrless}} \ell n\eta \tag{7.52}$$

Now, we would like to compute $\hat{\nu}(k)$ using Equations (7.45) and (7.48). Substituting Equation (7.48) into Equation (7.45), we have

$$\frac{\partial}{\partial \nu(k)} \left[\prod_{i=1}^{k} \frac{1}{\sqrt{2\pi |V(i)|}} \right] \exp \left[-\frac{1}{2} \sum_{i=1}^{k} (\gamma(i)-G(i,\hat{\theta}(k))\nu(k))^T \cdot \right.$$
$$\left. \cdot V^{-1}(i)(\gamma(i)-G(i,\hat{\theta}(k))\nu(k) \right] = 0$$
$$\nu(k)=\hat{\nu}(k) \tag{7.53}$$

or, equivalently,

$$\frac{\partial}{\partial \nu(k)} \left[\sum_{i=1}^{k} (\gamma(i)-G(i,\hat{\theta}(k))\nu(k))^T V^{-1}(i)(\gamma(i)-G(i,\hat{\theta}(k))\nu(k)) \right] = 0$$
$$\nu(k)=\hat{\nu}(k) \tag{7.54}$$

writing out the product term in the bracket, we have

$$\frac{\partial}{\partial \nu(k)} \sum_{i=1}^{k} \Big[\gamma^T(i)V^{-1}(i)\gamma(i) - \gamma^T(i)V^{-1}(i)G(i,\hat{\theta}(k))\nu(k)$$

$$- \nu^T(k)G^T(i,\hat{\theta}(k))V^{-1}(i)\gamma(i) + \nu^T(k)G^T(i,\hat{\theta}(k))V^{-1}(i) \cdot$$

$$\cdot G(i,\hat{\theta}(k))\nu(k) \Big] = 0 \Big|_{\nu(k)=\hat{\nu}(k)} \tag{7.55}$$

The first term is independent of $\nu(k)$, and the second and third terms are equal, because they are scalers and $V(i) = V^T(i)$. Thus we have

$$\frac{\partial}{\partial \nu(k)} \sum_{i=1}^{k} \Big[-2\gamma^T(i)V^{-1}(i)G(i,\hat{\theta}(k))\nu(k)$$

$$+ \nu^T(k)G^T(i,\hat{\theta}(k))V^{-1}(i)G(i,\hat{\theta}(k))\nu(k) \Big] = 0 \Big|_{\nu(k)=\hat{\nu}(k)} \tag{7.56}$$

upon differentiating with respect to $\nu(k)$, we have

$$-2 \sum_{i=1}^{k} \gamma^T(i)V^{-1}(i)G(i,\hat{\theta}(k)) + 2 \sum_{i=1}^{k} \hat{\nu}^T(k)G^T(i,\hat{\theta}(k))V^{-1}(i) \cdot$$

$$G(i,\hat{\theta}(k))=0 \tag{7.57}$$

or

$$\hat{\nu}^T(k) \left[\sum_{i=1}^{k} G^T(i,\hat{\theta}(k))V^{-1}(i)G(i,\hat{\theta}(k)) \right] =$$

$$\sum_{i=1}^{k} \gamma^T(i)V^{-1}(i)G(i,\hat{\theta}(k)) \tag{7.58}$$

therefore (assuming the indicated inverse exist:)

$$\hat{\nu}(k) = \left[\sum_{i=1}^{k} G^T(i,\hat{\theta}(k)) V^{-1}(i) G(i,\hat{\theta}(k)) \right]^{-1} \cdot \left[\sum_{i=1}^{k} G^T(i,\hat{\theta}(k)) V^{-1}(i) \gamma(i) \right] \tag{7.59}$$

If we define

$$C(k,\theta(k)) = \sum_{i=1}^{k} G^T(i,\theta(k)) V^{-1}(i) G(i,\theta(k)) \tag{7.60}$$

and

$$D(k,\theta(k)) = \sum_{i=1}^{k} G^T(i,\theta(k)) V^{-1}(i) \gamma(i) \tag{7.61}$$

then Equation (7.59) becomes

$$\hat{\nu}(k) = C^{-1}(k,\hat{\theta}(k)) D(k,\hat{\theta}(k)) \tag{7.62}$$

The maximum likelihood estimate of $\hat{\theta}(k)$ is that value of $\theta(k)$ at which the conditional probability density function $P(\gamma(1),\ldots,\gamma(k)|H_1,\theta(k),\hat{\nu}(k))$, which is given in Equation (7.48), is a maximum. Thus, we have

$$\hat{\theta}(k) = \arg \max_{\theta(k)} P(\gamma(1),\ldots,\gamma(k)|H_1,\theta(k),\hat{\nu}(k)) \tag{7.63}$$

which is equivalent to

$$\hat{\theta}(k) = \arg \min_{\theta(k)} \sum_{i=1}^{k} (\gamma(i)-G(i,\theta(k))\hat{\nu}(k))^T V^{-1}(i)(\gamma(i)-G(i,\theta(k))\hat{\nu}(k)) \tag{7.64}$$

or, upon some simplifications

$$\hat{\theta}(k) = \arg \min_{\theta(k)} \sum_{i=1}^{k} \left[-2\gamma^T(i)V^{-1}(i)G(i,\theta(k))\hat{\nu}(k) + \hat{\nu}^T(k)G^T(i,\theta(k))V^{-1}(i)G(i,\theta(k))\hat{\nu}(k) \right] \tag{7.65}$$

Using Equations (7.60) through (7.62) in Equation (7.65), we have

$$\hat{\theta}(k) = \arg \min_{\theta(k)} \left[-2D^T(k,\theta(k))C^{-1}(k,\theta(k))D(k,\theta(k)) + D^T(k,\theta(k))C^{-1^T}(k,\theta(k))C(k,\theta(k))C^{-1}(k,\theta(k))D(k,\theta(k)) \right] \tag{7.66}$$

or

$$\hat{\theta}(k) = \arg \max_{\theta(k)} \left[D^T(k,\theta(k))C^{-1}(k,\theta(k))D(k,\theta(k)) \right] \tag{7.67}$$

Once the maximum likelihood estimates $\hat{\theta}(k)$ and $\hat{\nu}(k)$ are computed, we can then use Equations (7.48) through (7.50) to compute the generalized likelihood ratio. Upon canceling common terms, we obtain

$$\Lambda(k) = \frac{\exp\left[-\frac{1}{2} \sum_{i=1}^{k} ((\gamma(i)-G(i,\hat{\theta}(k))\hat{\nu}(k))^T V^{-1}(i)(\gamma(i)-G(i,\hat{\theta}(k))\hat{\nu}(k)) \right]}{\exp\left[-\frac{1}{2} \sum_{i=1}^{k} \gamma^T(i)V^{-1}(i)\gamma(i) \right]} \tag{7.68}$$

taking the logarithm, and after some simplifications, we have

$$\ell n\Lambda(k) = -\frac{1}{2}\sum_{i=1}^{k}\Big[-2\gamma^T(i)V^{-1}(i)G(i,\hat{\theta}(k))\hat{\nu}(k) + \hat{\nu}^T(k)G^T(i,\hat{\theta}(k))V^{-1}(i)G(i,\hat{\theta}(k))\hat{\nu}(k)\Big] \tag{7.69}$$

Using Equations (7.60) through (7.62), we have

$$\ell n\Lambda(k) = \frac{1}{2} D^T(k,\hat{\theta}(k))C^{-1}(k,\hat{\theta}(k))D(k,\hat{\theta}(k)) \tag{7.70}$$

Using Equation (7.52), thus the generalized likelihood ratio test is

$$\ell n\Lambda(k) = \frac{1}{2} D^T(k,\hat{\theta}(k))C^{-1}(k,\hat{\theta}(k))D(k,\hat{\theta}(k)) \underset{H_0}{\overset{H_1}{\gtrless}} \ell n\eta \tag{7.71}$$

or

$$\ell(k,\hat{\theta}(k)) = D^T(k,\hat{\theta}(k))C^{-1}(k,\hat{\theta}(k))D(k,\hat{\theta}(k)) \underset{H_0}{\overset{H_1}{\gtrless}} 2\ell n\eta = \varepsilon \tag{7.72}$$

Equation (7.67) can be rewritten as

$$\hat{\theta}(k) = \arg \max_{\theta(k)} [\ell(k,\theta)] \tag{7.73}$$

where

$$\ell(k,\theta) = D^T(k,\theta(k))C^{-1}(k,\theta(k))D(k,\theta(k)) \tag{7.74}$$

Finally, a summary of the computation algorithm for this generalized likelihood ratio test is given as follows:

(1) $G(k,\theta)$ are computed first for all $\theta \leq k$, using the following equations

$$B(\theta,\theta) = F(\theta,\theta) \tag{7.75}$$

$$B(k,\theta) = \Phi(k,k-1)[I-M(k-1)H(k-1)]B(k-1,\theta) + F(k,\theta) \tag{7.76}$$

and

$$G(k,\theta) = H(k)B(k,\theta) \tag{7.77}$$

(2) Compute $C(k,\theta(k))$ and $D(k,\theta(k))$ for all $\theta \leq k$ from

$$C(k,\theta(k)) = \sum_{i=1}^{k} G^T(i,\theta(k))V^{-1}(i)G(i,\theta(k)) \tag{7.78}$$

$$D(k,\theta(k)) = \sum_{i=1}^{k} G^T(i,\theta(k))V^{-1}(i)\gamma(i) \tag{7.79}$$

(3) Estimates $\hat{\nu}(k)$ and $\hat{\theta}(k)$ are then given as

$$\hat{\theta}(k) = \arg \max_{\theta(k)} [\ell(k,\theta)] \tag{7.80}$$

where

$$\ell(k,\theta) = D^T(k,\theta(k))C^{-1}(k,\theta(k))D(k,\theta(k)) \tag{7.81}$$

and

$$\hat{\nu}(k) = C^{-1}(k,\hat{\theta}(k))D(k,\hat{\theta}(k)) \tag{7.82}$$

(4) The decision rule for selecting either H_1 or H_0 is

$$\ell(k,\hat{\theta}(k)) \underset{H_0}{\overset{H_1}{\gtrless}} \varepsilon \tag{7.83}$$

where the threshold ε can be adjusted to achieve acceptable performance.

7.3 Additional Considerations for GLR Computations

7.3.1 GLR Window Width

From Section 7.1, we see that the basic GLR configuration (Figure 7.2) requires the computation of the likelihood ratios $\ell_i(k,\theta)$, where the index i refers to the transient event being looked for (rhythm jump, compensatory beat, non-compensatory beat, and double non-compensatory beat), k is the number of the latest R-R interval to be processed by the system, and θ is the number of the R-R interval at which the hypothesized transient event began. Because of the causal nature of the processing, $\theta \leq k$. From Equations 7.75-7.81, we see that the required computations of the number of the likelihood ratios grows linearly with time k. Because of the fact that for each k, we must, in principle, evaluate $\ell_i(k,\theta)$ for all θ which are less than or equal to k. One possible way of avoiding this computation problem is using a "data window" which requires only a fixed number of likelihood ratios computations. Specifically, for a GLR "data window" width of N, we only need to evaluate $\ell_i(k,\theta)$ for the N most recent values of θ (i.e., $k-N+1 \leq \theta \leq k$).

It is clear that using a finite "data window", a great reduction in the required number of likelihood ratios to be evaluated is

achieve. The basic philosophy here is that if we have not detected an transient event over the given window, it is very likely that the event is not there, so why keep searching for it? Another advantage of using finite data window is that a better detection performance for multiple transient events can be achieved. In many records one may have several transient events. On the other hand, the GLR is designed to looking for a single transient event. Therefore, if one has a very wide window (or if one calculates all of the $\ell_i(k,\theta)$ for $\theta=1,2,\ldots,k$), it may become very difficult to separate these transient events. On the other hand using a narrow window, we can isolate events which are spaced at points wider than the window width. However, we do not want to make the GLR window too narrow because of the following facts:

(1) Suppose we are looking for an event at time θ. As we incorporate more and more data (i.e., as we take data at time θ, $\theta+1$, $\theta+2,\ldots,$), we are more likely to obtain an accurate picture of what happened at time θ. This is because by waiting to look at several data points, we essentially make the filter noncausal and are performing smoothing which inherently increases the accuracy of the test.

(2) Several of the transient events we are looking for can not be distinguished until we have seen several data points. For example, we need at least 3 R-R intervals in order to distinguish a double non-compensatory beat

from a jump to tachycardia, at least 2 to distinguish between a compensatory and non-compensatory event, etc.

Motivated by these considerations, a GLR window width of 5 is chosen in order to provide a reasonable tradeoff between computation, multiple event isolation, and the question of smoothing and event distinguishability.

7.3.2 Filter Initialization

Another problem with the GLR technique as described so far is the detection of transient events that occur at the start of a record. The difficulty is that the filter, which is trying to estimate the average R-R interval, initially has no data on which to base its estimate. Therefore, a great deal of weighting is placed on the first few R-R intervals. The consequence of this is that the filter tends to "follow" the first few intervals, and the GLR detector, which is looking at the filter behavior in order to determine if a transient event has occured, will be fooled. Of course, as we smooth the data by processing more and more data points, the GLR will, in principle, be able to determine that it is the first beat that is the problem, but for short record lengths or for narrow GLR windows, one may not be able to obtain enough smoothing in this manner.

Therefore a filter initialization is needed for providing for more initial smoothing. One possible method is to compute an average over the first several R-R intervals and use this average to initialize the filter, along with a smaller initial error covariance. We then

start the filter from the beginning of the record. The smaller initial covariance implies a smaller filter gain, which means that the filter will not "follow" the data as much initially. This will speed up the correct GLR response. However, there is one problem with this initialization method. If the first several R-R intervals to be averaged are extremely erratic, the average we will provide may not aid things very well. For example, one extremely long R-R interval can greatly effect the average.

Motivated by the problem of one aberrant interval causing a problem in computing an initial average, we propose the following initialization scheme:

Step (1): Search the first 5 beats and find the first two consecutive intervals $y(k)$ and $y(k+1)$ that are sufficiently close in length

$$|y(k) - y(k+1)| < \beta$$

Step (2): Set the initial filter estimate equal to their average

$$\hat{x}(0) = \frac{y(k) + y(k+1)}{2}$$

and set the initial covariance $P(0)$ to 1/2 of the noise covariance associated with the measurement of a normal R-R interval. This reflects accurately the variance associated with an estimate of a random variable obtained by averaging two samples.

Step (3): If none of the first 5 beats are less than β apart, the initial filter estimate is set equal to the average of the first 5 beats and set P(0) at a lower value.

For the actual runs described in the next section, we have taken β=20 and P(0)=32.

7.4 Experiments and Results

The generalized likelihood ratio detection system described in Section 7.1 was tested on a wide variety of actual data. The objective of this test was to determine whether the generalized likelihood ratio testing algorithm described in the previous section could detect and classify the presence of the transient rhythms, described in Chapter 5, in the R-R interval data files being tested. A summary of the R-R interval data used in the tests is given in Table 7.1. Three R-R interval sequences were used as rhythm jump data. The first was a shift from IN.5 to IN.30 at θ=6, and represents a sudden increase in heart rate from approximately 81 beats/min to 64 beats/min. This was formed artificially by putting the first five R-R intervals from data file IN.30 after the first five of those from IN.5 (see Tables 4.3, 4.5). The second R-R interval sequence was a shift from IN.30 to IN.5 at θ=6 and represents a sudden decrease in heart rate. The third one was the R-R interval sequence of data file #476 (see Table 4.14), which was indicative of a gradual slowing of the heart rate from approximately 85 beats/min to 45 beats/min.

For the non-compensatory beat model, three R-R interval sequences were tested. The first (second) sequence was obtained using a single,

Beat Number	Data Type and R-R Intervals					
	Rhythm Jump			Non-Compensatory Beat		
	IN.5→ IN.30	IN.30→ IN.5	#476	IN.30 (300at θ=6)	IN.30 (140at θ=6)	#463
1	181	236	171	236	236	211
2	182	242	180	242	242	192
3	187	239	174	239	239	203
4	188	232	175	232	232	344
5	185	223	186	223	223	197
6	236	181	202	300	140	190
7	242	182	203	230	230	198
8	239	187	216	231	231	328
9	232	188	233	230	230	213
10	223	185	256	225	225	209
11			302			366
12			299			215
13			323			209
14			333			
15			337			

Table 7.1(a) R-R Interval Data Used in Testing The Generalized Likelihood Ratio Detection System.

artificial beat 300 (140), inserted after θ=5 in IN.30, represents possibly an SA block, dropped beat, or sinus arrest (premature contraction). This gave ν a value of about +65 (-95). Here ν is the size of the jump due to the non-compensatory beat (see Chapter 5). The third sequence was the R-R interval sequence of data file #463. This file includes three lengthened beats at θ=4, 8 and 11. A segment of

Beat Number	Data Type and R-R Intervals		
	Compensatory Beat	Double Non-Compensatory Beat	
	HARNETPVCS	#492-1	#534-1
1	159	247	252
2	165	238	193
3	163	110	191
4	157	137	201
5	160	244	201
6	105	258	211
7	229	259	96
8	155	254	80
9	162		249
10	154		

Table 7.1(b) R-R Interval Data Used in Testing The Generalized Likelihood Ratio Detection System.

the R-R interval sequence, N=14 to N=23, in data file HARNETPVCS (Table 4.10) was selected as compensatory data. This data contained a single compensatory PVC at θ=6. For the double non-compensatory data, two files, #492-1 and #534-1, (see Table 7.1), were tested. In #492-1, the normal rhythm was interrupted by one atrial premature contraction at θ=3, resulting in two consective shortened R-R intervals. In #534-1, there is a PVC in the first beat, and there are two ventricular complexes, indicative of a rate of more than 150 beats/min (if there were only a single focus) at θ=7,8.

Using the R-R interval data given in Table 7.1, a series of tests were made. First the GLR detection system was tested using a full GLR

window width, i.e., the window width was equal to the total number of R-R intervals contained in a file being tested. In addition, the filter reinitialization procedure described in the previous section was not utilized; rather, the initial R-R interval estimate was set to 200, and the initial error covariance was set to 1600 as suggested in Section 6.4. The next set of tests was made using a small sliding window of length 5 for the GLR detection system without using the filter reinitialization procedure given in Section 7.3. In the cases where the transient events occur at the very beginning of a record, the detection performance of the GLR system were degraded due to the high initial filter gains. This problem was resolved by using the filter reinitialization procedure given in Section 7.3. All the test results are shown in Figures 7.1-7.7.72. In the figures, the likelihood ratio $\ell(k,\theta)$ of each of the four possible transient rhythms, namely, rhythm jump, non-compensatory beat, compensatory beat, and double non-compensatory beat, is plotted vs. time. The time is not explicitly given; rather, the locations of the R wave are shown, denoted by the vertical lines along the abscissa, and the R-R intervals are also given along the time axis. Also shown in the figures are the values of the best jump estimates, $\hat{\nu}(k,\theta)$, which are computed at the local maxima of the likelihood ratios $\ell(k,\theta)$.

The results for a sudden normal rhythm shift from IN.5 to IN.30 at $\theta=6$ are shown in Figures 7.1-7.5. The jumped GLR likelihoods are shown in Figure 7.1. For $k\leq 5$, the likelihoods are small indicating that no transient event has occurred. However, for $k\geq 6$, a strong peak

of the likelihood is observed at $\theta=6$. Furthermore, $\ell(k,6)$ increases monotonically with k, indicating that the likelihood of a rhythm shift at $\theta=6$ increases as more data is available. This behavior is clearly indicative of a rhythm shift occurring at $\theta=6$. The likelihood for the other GLR detectors, namely, non-compensatory, compensatory, and double non-compensatory, are given in Figures 7.2-7.4. Note that in each of these cases a jump of the likelihood is observed at k=6. However, in each case $\ell(k,6)$ is seen to decrease as more data is available, indicating that none of these transient events is present. The data of Figures 7.1-7.4 are summarized in Figure 7.5, which shows the maximum of $\ell(k,\theta)$ over all θ plotted vs. k. For $k\leq 5$, the likelihood of each possible transient events is small, indicating that no ectopic change has occurred. However at k=6, the likelihoods for all models increase as the lengthened R-R interval 236 is obtained. This is what we expected, because any one of the four possible transient events can start with a single, lengthened (or shortened) R-R interval. Therefore with the data available up to k=6, there is no way to determine which one of the four ectopic events is present. This is indicated by the equal likelihoods for all models at k=6. As the next data point 242, which is another lengthened R-R interval, becomes available, the only possible transient rhythm models which can describe this data pattern are rhythm jump, and double non-compensatory beat; and there is no way to distinguish between these two. This is indicated by the decreases of the compensatory and non-compensatory likelihoods, and the increases of the jump and double non-compensatory likelihoods. As one more

lengthened R-R interval, 239, is obtained, only the rhythm jump model can match this data sequence, which is indicated as a high likelihood for jumped GLR at k=8. As more data becomes available, the likelihood of the jump GLR increases monotonically and is never lower than any of the likelihoods for the other GLR detectors. Furthermore, the confidence that a jump has actually occurred increases as more data is obtained.

Next, a sudden shift in normal rhythm from IN.30 to IN.5 was tested to demonstrate the detection capability of the GLR detection system to a shift from a lower heart rate to a higher heart rate. The resulting likelihood plots are shown in Figures 7.6-7.10. In this case a similar detection performance is achieved, and the detection of a rhythm jump at θ=6 is accomplished as seen in Figures 7.6, 7.10.

The next rhythm data tested was file #476, which has a gradual slowing heart rate from about 85 beats/min to 45 beats/min. The likelihood ratios are shown in Figures 7.11-7.15. A jump is strongly identified in Figure 7.11. The width of the likelihood peaks indicates that a gradual jump is taking place, which is consistent with gradual slowing. The summary plot of Figures 7.15 shows that a jump is clearly identified, however the exact location of this jump is not so obviously determined due to the characteristic of a gradual slowing R-R interval sequence.

Next, several tests were made using the non-compensatory data given in Table 7.1. The results of a non-compensatory beat of (1) 300(ν= +65), and (2) 140(ν= -95) at θ=6 are shown in Figures 7.16-7.20, and 7.21-7.25, respectively. In each case, detection of the

non-compensatory beat at $\theta=6$ was accomplished as seen in Figures 7.17, 7.20 and Figure 7.22, 7.25. However the confidence that a non-compensatory beat has actually occurred in the second case is much greater than that of the first, this is due to the high value of $|\nu|(=95)$, which means a higher signal/noise ratio, in the former case. The results for file #463, which contains three lengthened R-R intervals at $\theta=4,8$, and 11, are given in Figures 7.26-7.30. In Figure 7.27 three non-compensatory beats are clearly detected at $\theta=4,8$, and 11, as desired. Since the GLR system is designed assuming that only one transient event occurs within the window, it is rather encouraging that multiple transient events can be detected within the same window. (here of length 13). However, since multiple transient events occur within the window, the summary plot of Figure 7.30 suggests little information on the detection and classification of the ectopic events. In such cases one may wish to track all of the local maxima of the likelihood ratios separately, or we may want to use a very short GLR window, in which case we will detect and classify each separate event as it occurs and will be able to avoid the difficulties of multiple events within a window. Success with such a technique will be discussed shortly.

The next test was made using the compensatory R-R interval data given in Table 7.1. This data sequence contains a single compensatory PVC at $\theta=6$. The results are shown in Figures 7.31-7.35 and demonstrate that detection of the compensatory PVC is accomplished easily (see Figures 7.33, 7.35). Since the effect of the PVC on the innovations is negligible after the compensatory pause, the likelihood for

the compensatory GLR remains essentially constant for $K \geq 7$ (i.e., there is no more information in the filter output concerning this event, since the lengthened and shortened R-R intervals effectively average out in the filter).

Next, two tests were made to evaluate the detection performance of the double non-compensatory GLR detector. First, we studied file #492-1, which has an interpolated beat at $\theta=3$, resulting in two consecutive shortened R-R intervals at $\theta=3,4$. The resulting likelihood plots are given in Figures 7.36-7.40, and the two consective shortened beats are clearly identified. Note that the model for this arrhythmia, described in Chapter 5, specifies that the R-R interval jump is constant over two successive R-R intervals. Here we have demonstrated that our GLR detector system can detect quite easily a double non-compensatory beat with unequal lengthes (hence demonstrating its robustness). Next, file #534-1 was studied. This file contains a single PVC in the first beat ($\theta=1$ - i.e. we only have the compensatory pause part), and two ventricular complexes at $\theta=7,8$. The results are shown in Figures 7.41-7.45. The two shortened beats are clearly identified as double non-compensatory beat at $\theta=7$; however, the PVC in the first beat is either missed or weakly detected in Figure 7.42. This is basically an initialization problem.

Note that the window width in Figures 7.26-7.30 is 13 and that three transient events occur within the window. In Figures 7.41-7.45, we have a window width of 9, and two transient events occur within the window. The philosophy of design for the GLR detection system is based on the occurrence of a single transient event within the

window. In addition, it is not feasible to use a window of length equal to the total number of R-R intervals contained in a record. Thus, a "sliding window" GLR detection system of length 5 was studied. This value was selected since the effect of a transient rhythm persists over no more than three beats, and therefore a window width of at least three is necessary, but should be not so large that there is a high probability that more than one transient event will occur within the window. The results for file #463, #534-1, using the sliding window GLR detector, are shown in Figures 7.46-7.54, and Figures 7.55-7.59, respectively. In the figures, the value of T in the captions denotes the beat number at the far left side of the window, and the window moves, in successive plots, to the right over the data. For file #463, the first lengthened beat at θ=4 is clearly identified as a non-compensatory beat in Figure 7.46, and, as more data becomes available, as in the subsequent plots showed (Figures 7.47,7.48), we are more confident in our detection of this ectopic event. The second ectopic beat, which occurs at θ=8, is detected as seen in Figures 7.50 and 7.51. The third lengthened beat at θ=11 is also clearly identified in Figures 7.53 and 7.54. For file #534-1, either a non-compensatory beat at θ=1 or a rhythm jump occurs at θ=2 is detected, recall that in Figures 7.41-7.50 where a full window width was used, we were not be able to detect this ectopic beat. After the first beat passed the window, the peaked likelihoods of the jumped GLR detector indicate a rhythm jump as seen in Figure 7.56. The two successive shortened beats at θ=7,8 are detected and identified as a double non-compensatory beat at θ=7 as we wished (Figure 7.59).

Using the normal filter reinitialization procedure given in Section 7.3, data file #534-1 was tested again, with the initial R-R interval estimate set to 192 and the initial error covariance set to 32. The results are shown in Figures 7.60-7.64. It can be seen by comparing Figure 7.55 and 7.60 that filter reinitialization gives significantly improved detection performance, which is indicated by the much sharper peak of the likelihoods for non-compensatory GLR detector in Figure 7.60. Recall, this first R-R interval was the compensatory pause asociated with a PVC; since we do not have the preceding shortened interval available, we can not diagnose this as compensatory and hence classify it as non-compensatory. Clearly a scheme that uses this approach in conjunction with wave shape information would be able to do a better job of classification, but we can expect no more from R-R data alone. This behavior holds true as the window moves over the data. However as k becomes larger, the filter gain without reinitialization is approximately the same as that used with reinitialization and there will be little difference in the likelihood ratios. This behavior is clearly indicated by the approximately identical results in Figures 7.57-7.59 and Figures 7.62-7.64.

Finally, file #492-1 was tested using the sliding window with and without reinitialization. The reinitialization condition used was $x_o = 242.5$ and $P_o = 32$. The results are shown in Figures 7.65-7.68 for the non reinitialization run, and in Figures 7.69-7.72 for the reinitialization run. By comparing these results, we conclude that a much better detection performance can be achieved by using a sliding window GLR detector with filter reinitialization.

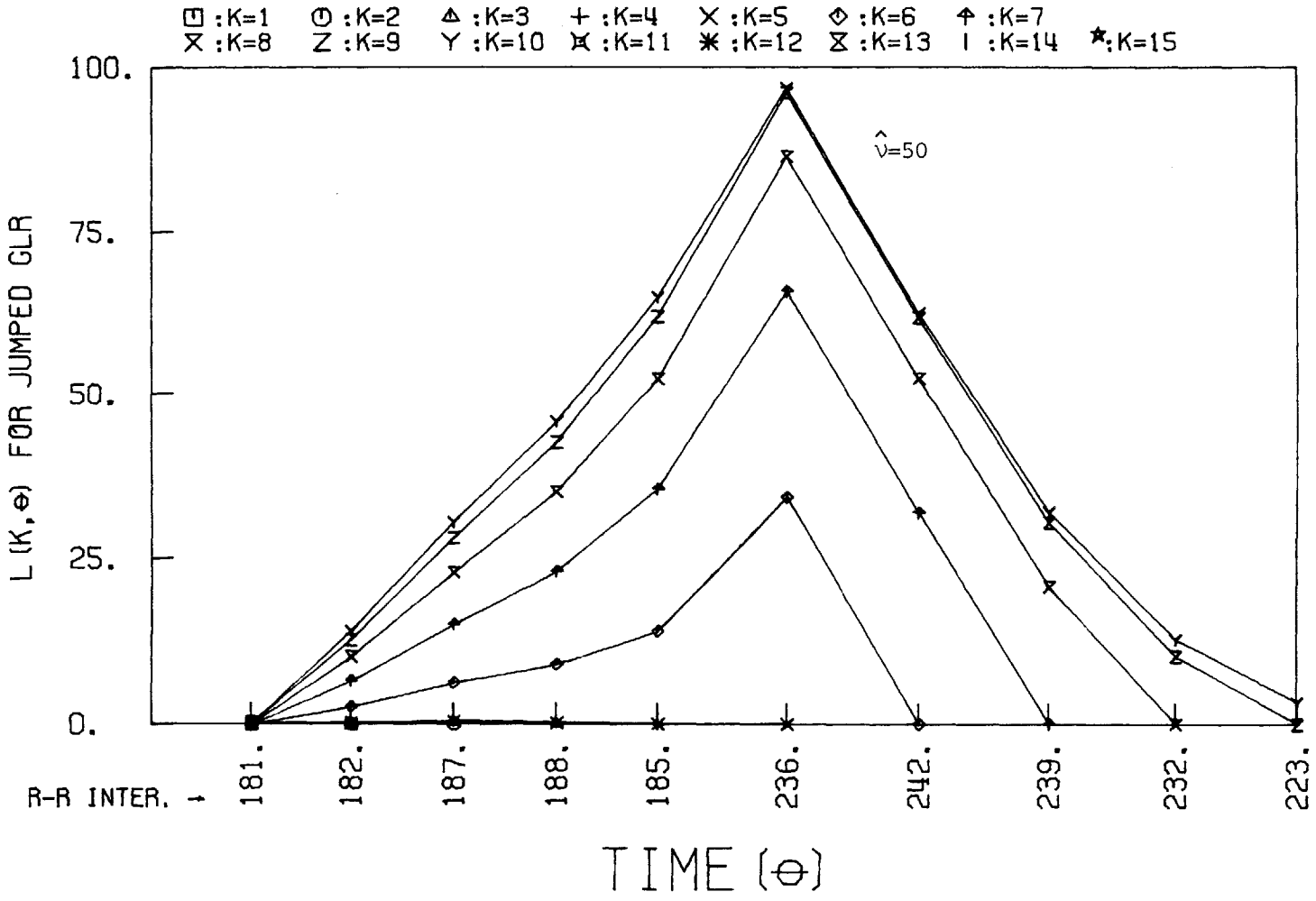

Figure 7.1 Jumped GLR for Rhythm Jump (IN.5 → IN.30)

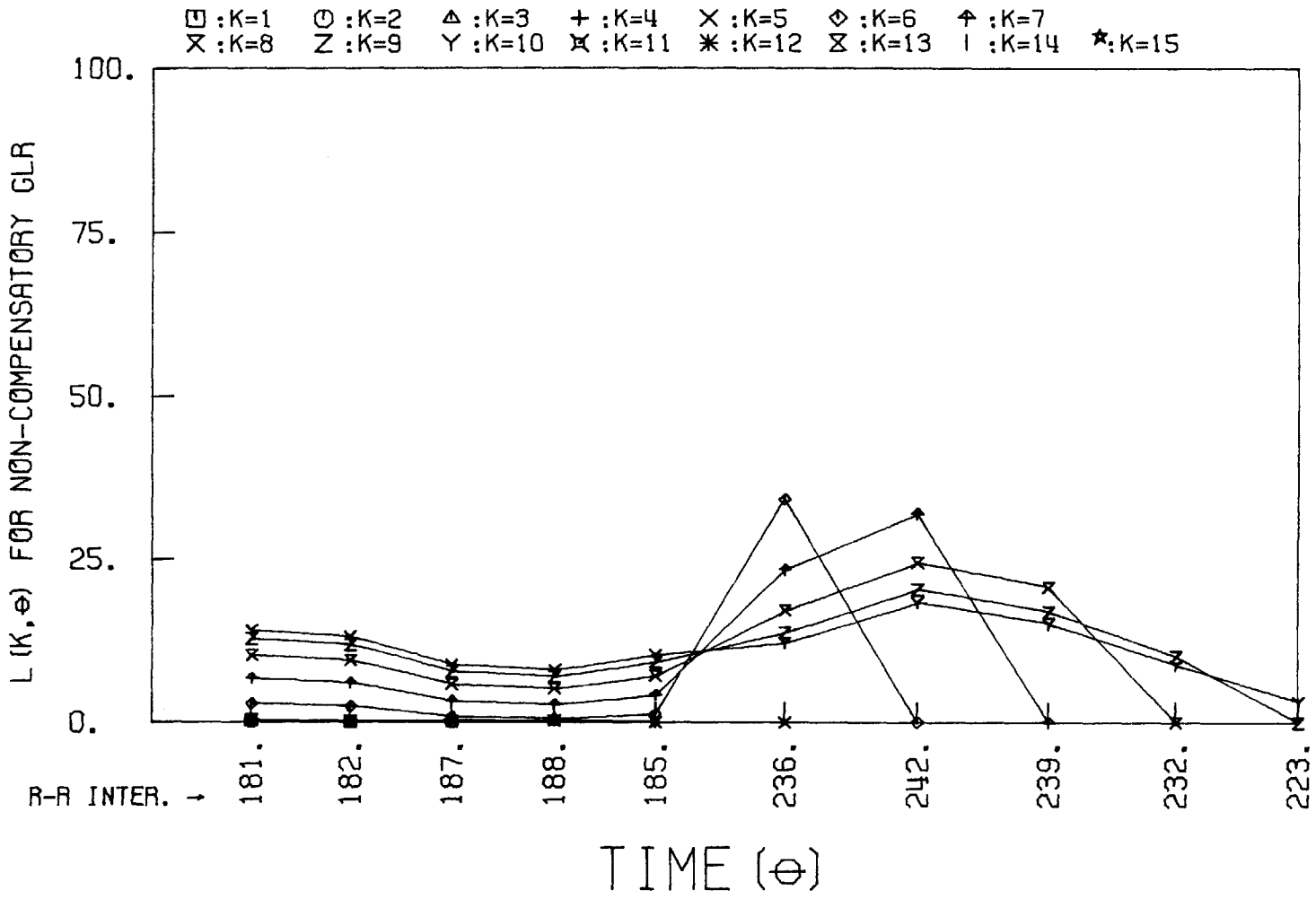

Figure 7.2 Non-Compensatory GLR for Rhythm Jump (IN.5 → IN.30)

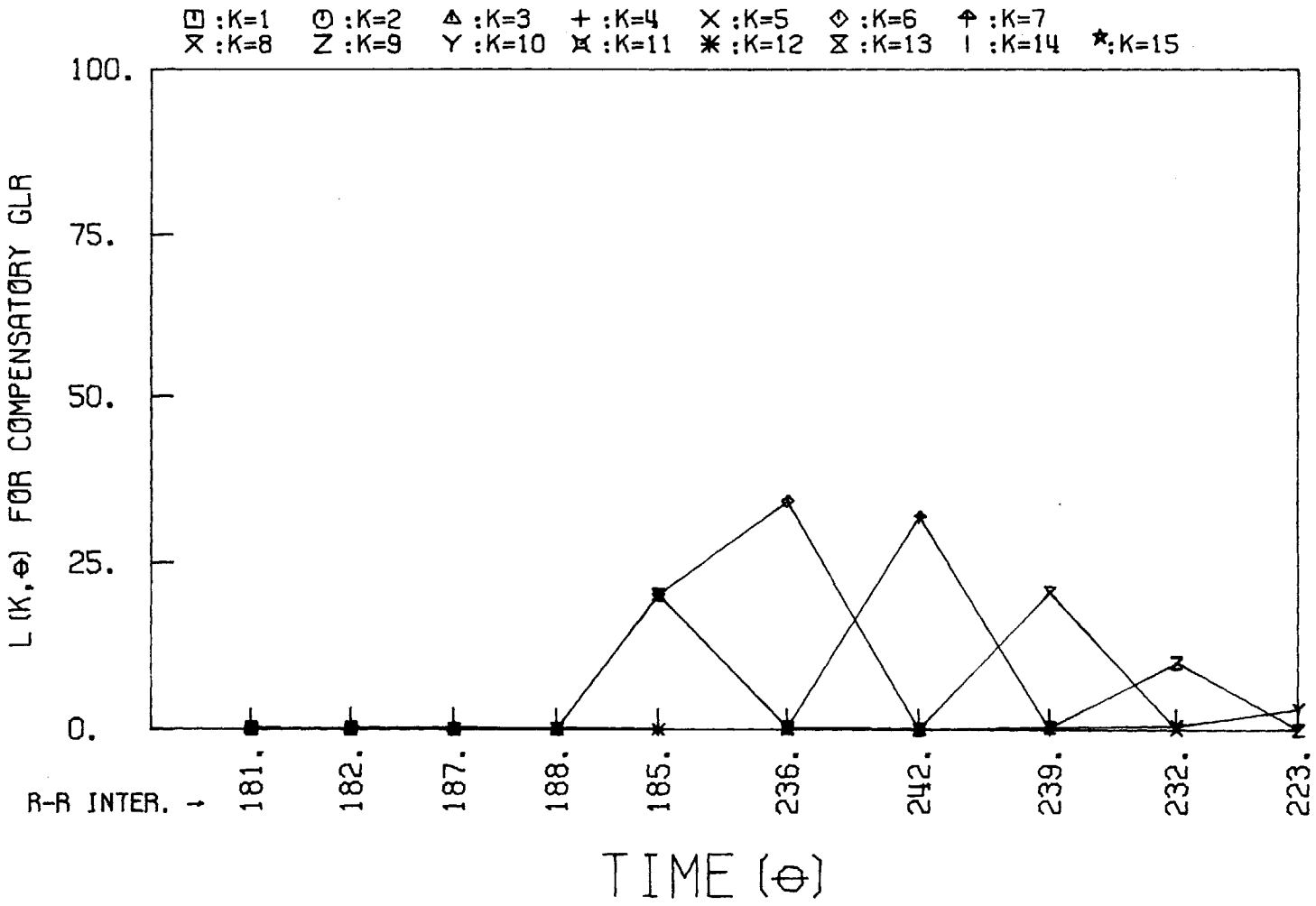

Figure 7.3 Compensatory GLR for Rhythm Jump (IN.5 → IN.30)

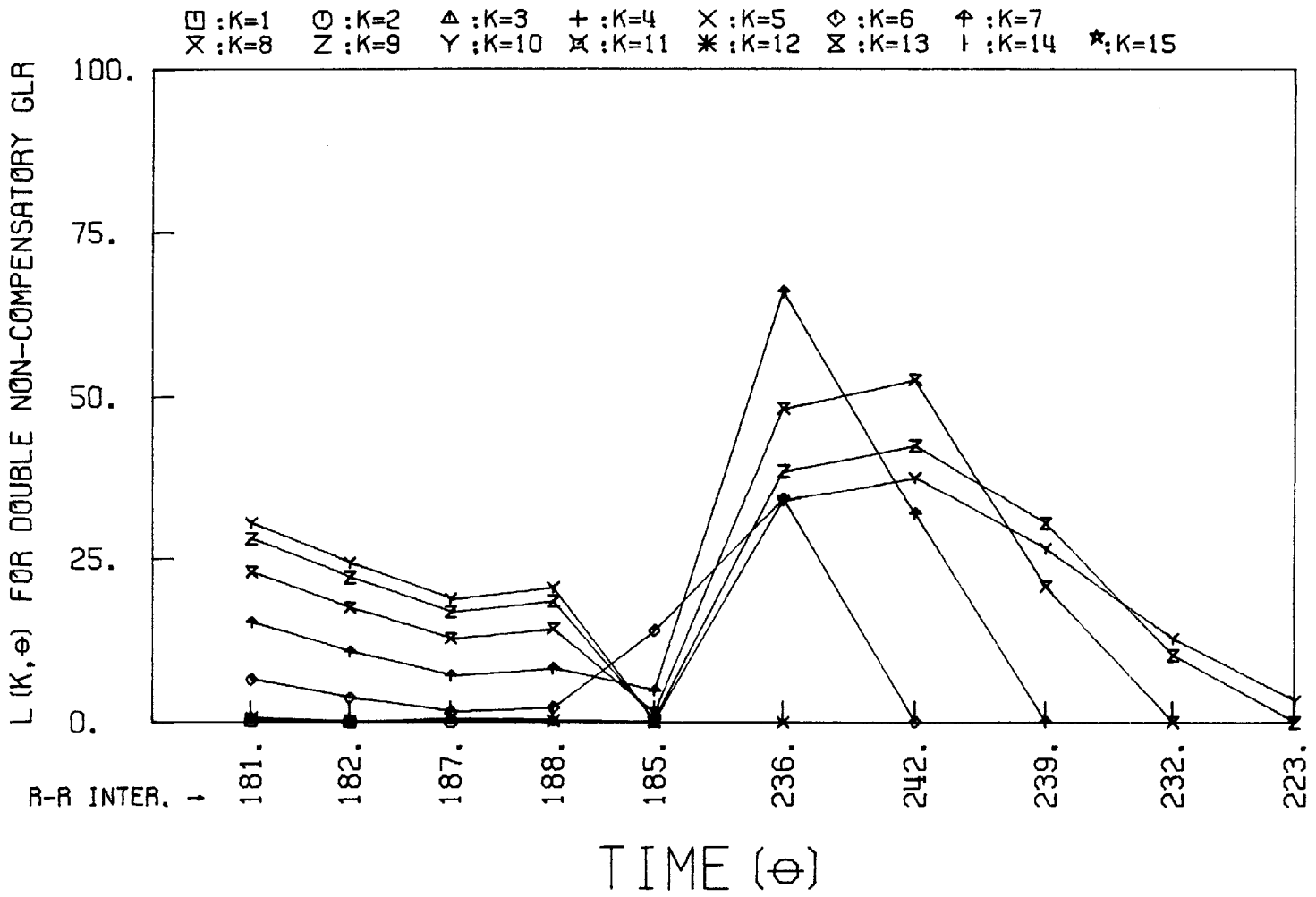

Figure 7.4 Double Non-Compensatory GLR for Rhythm Jump (IN.5 → IN.30).

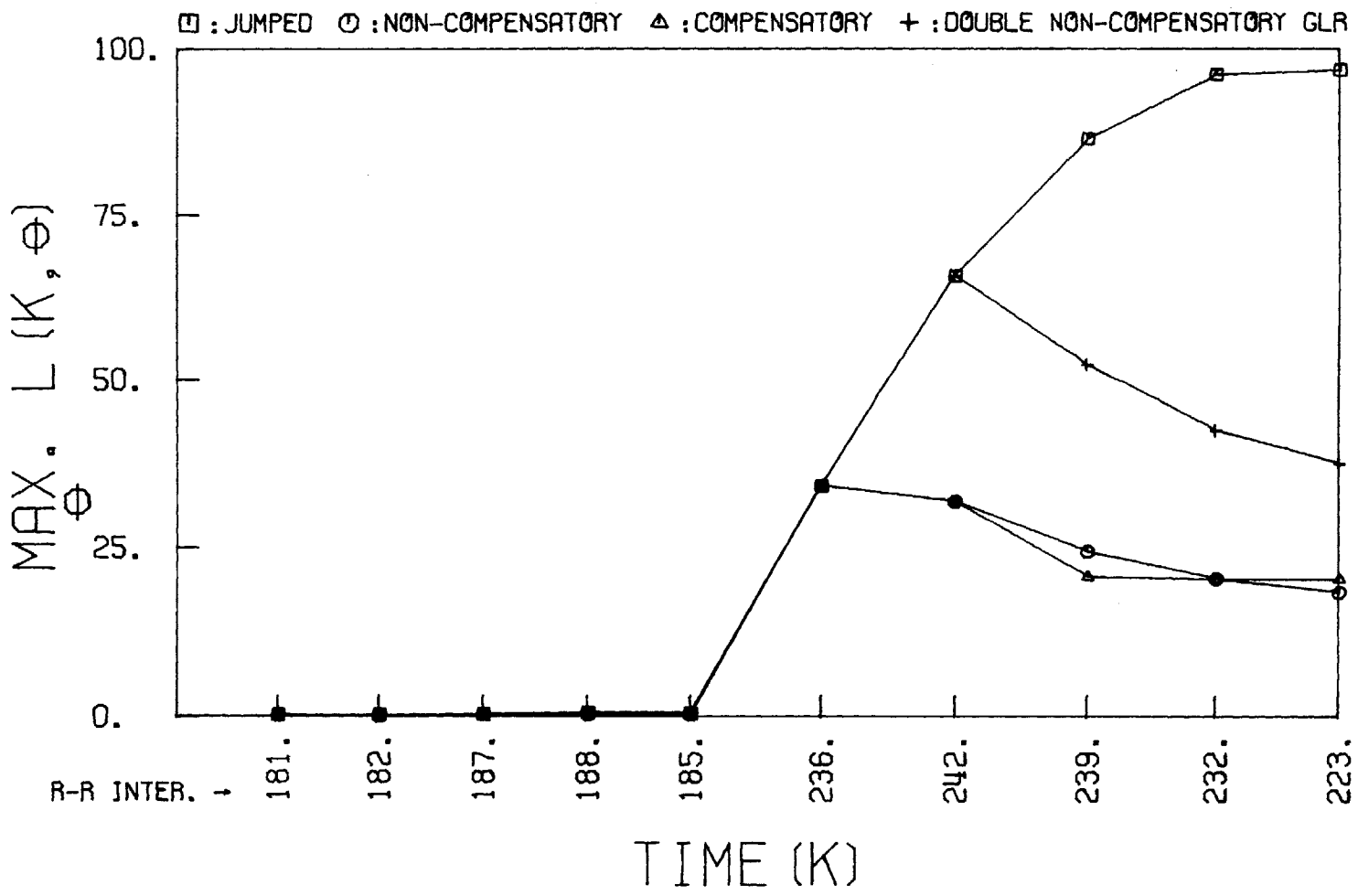

Figure 7.5 GLR Comparisons for Rhythm Jump (IN.5 → IN.30).

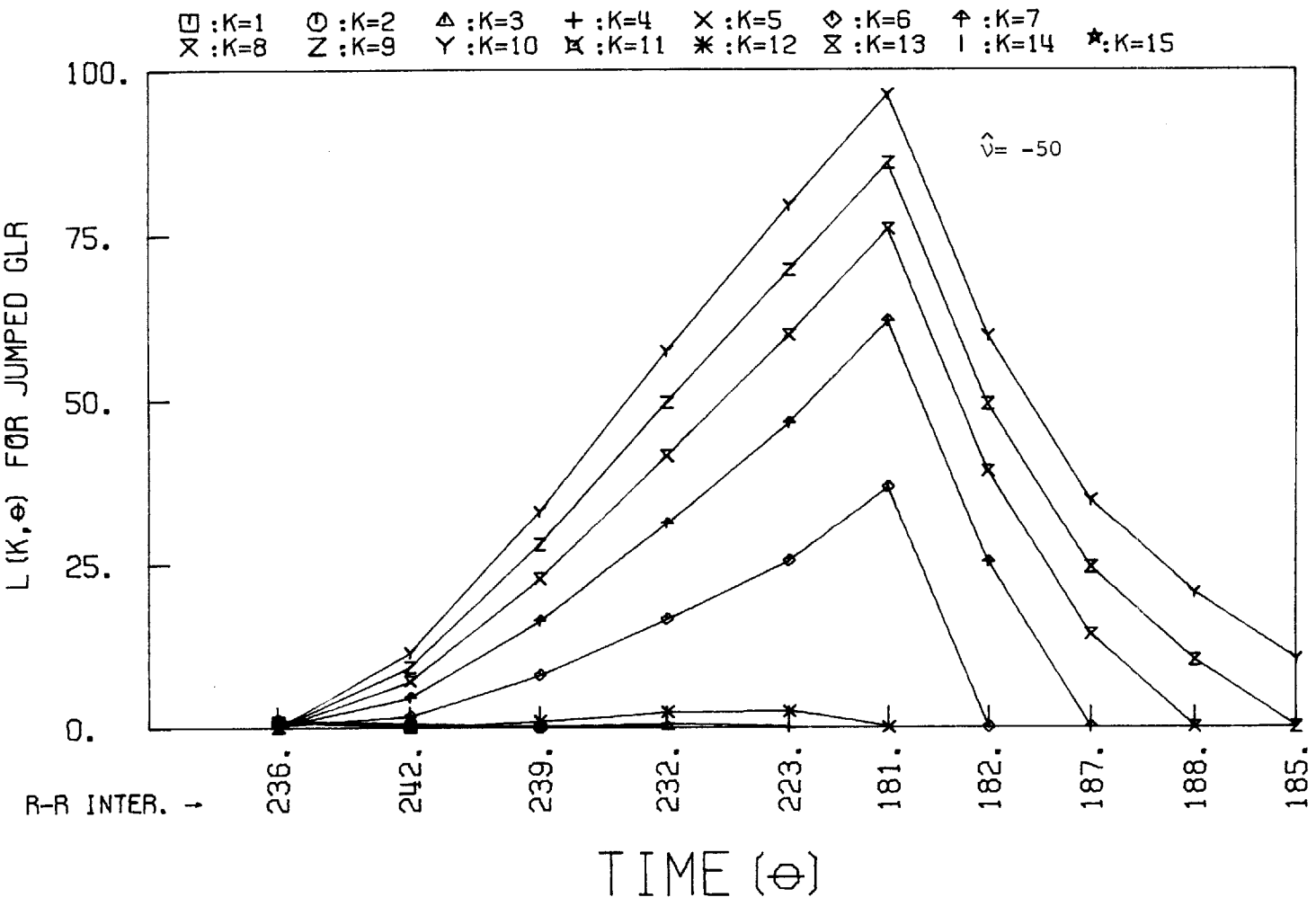

Figure 7.6 Jumped GLR for Rhythm Jump (IN.30 → IN.5)

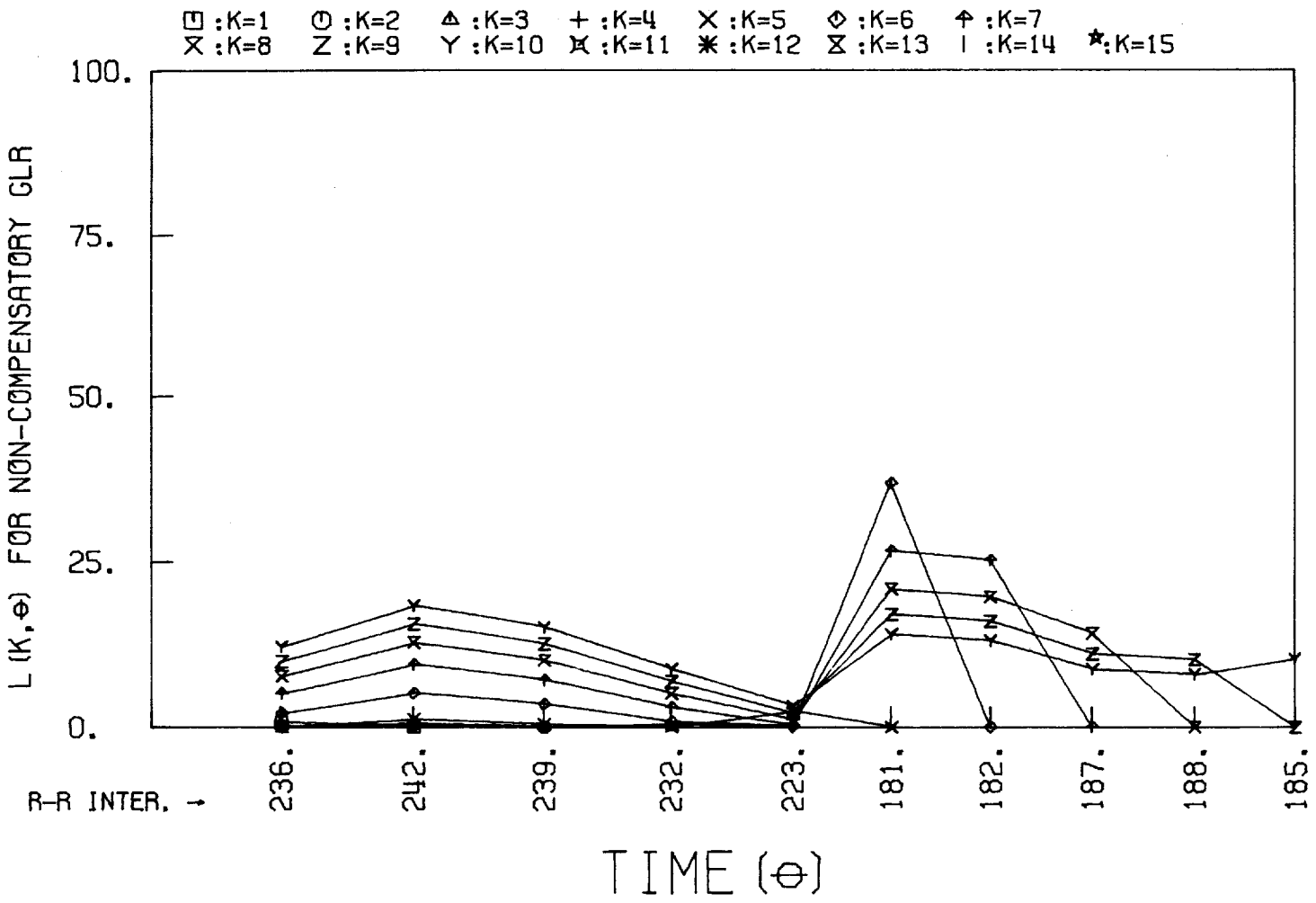

Figure 7.7. Non-Compensatory GLR for Rhythm Jump (IN.30 → IN.5)

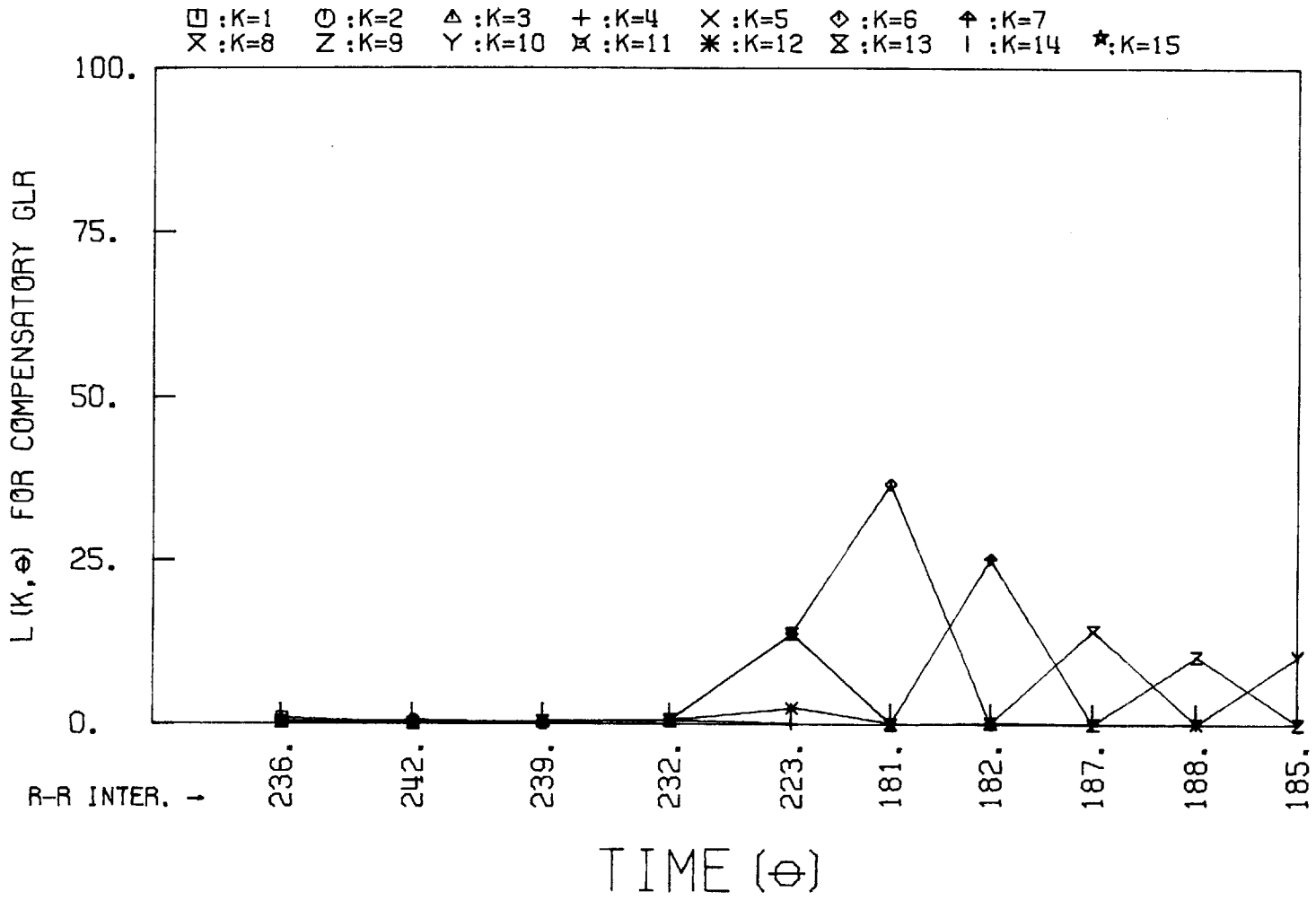

Figure 7.8 Compensatory GLR for Rhythm Jump (IN.30 → IN.5).

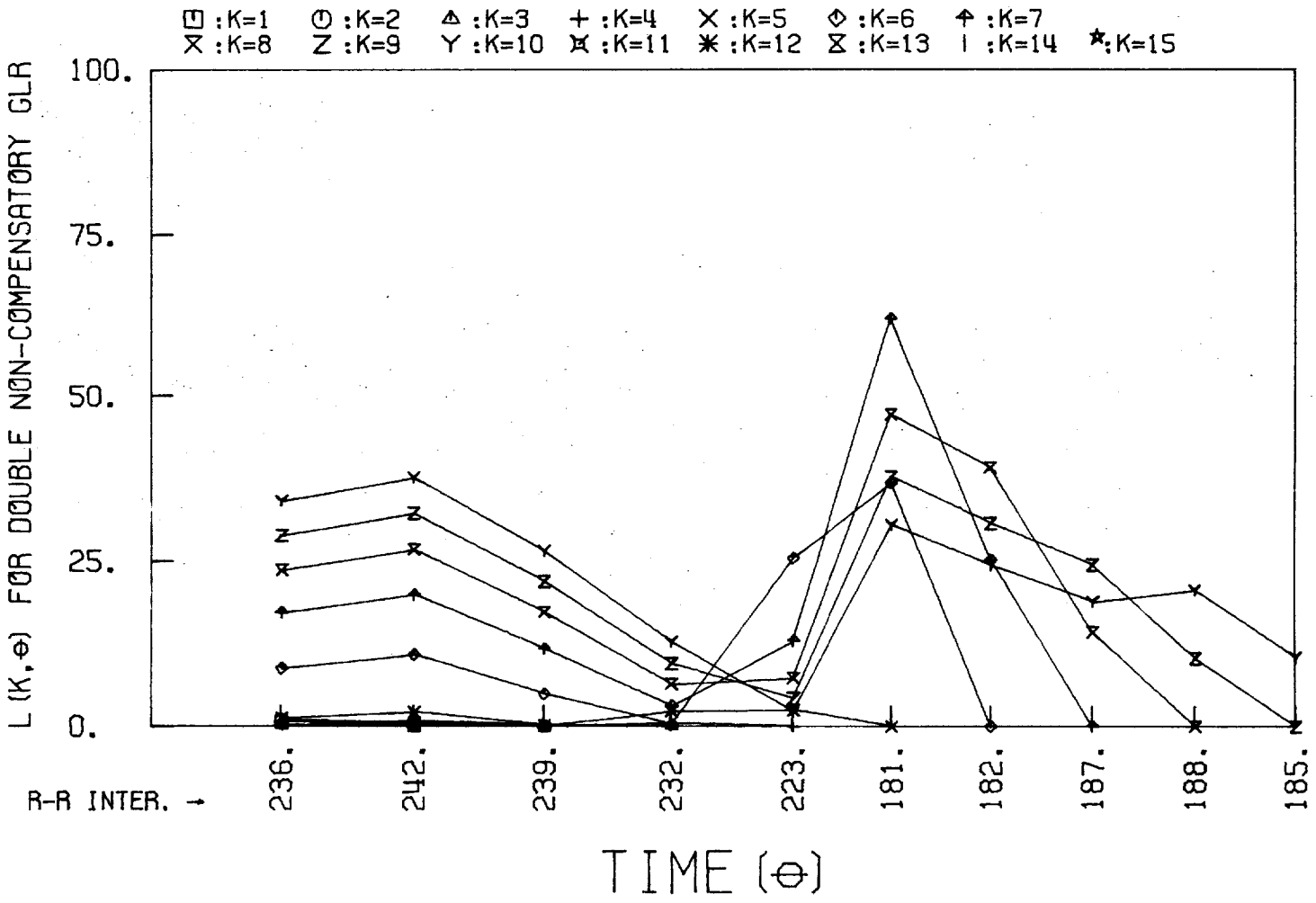

Figure 7.9 **Double Non-Compensatory GLR for Rhythm Jump (IN.30 → IN.5)**

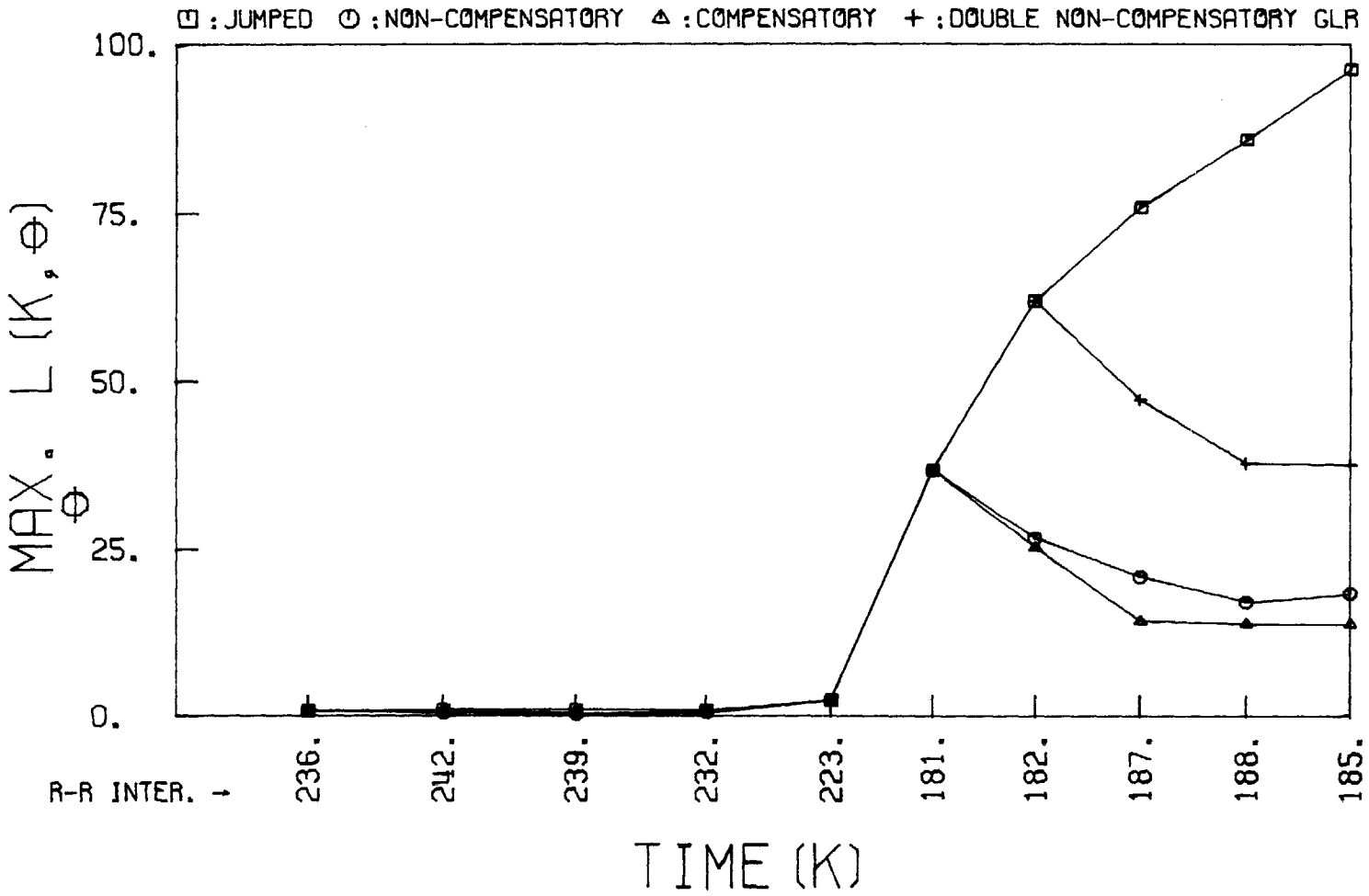

Figure 7.10 GLR Comparisons for Rhythm Jump (IN.30 → IN.5)

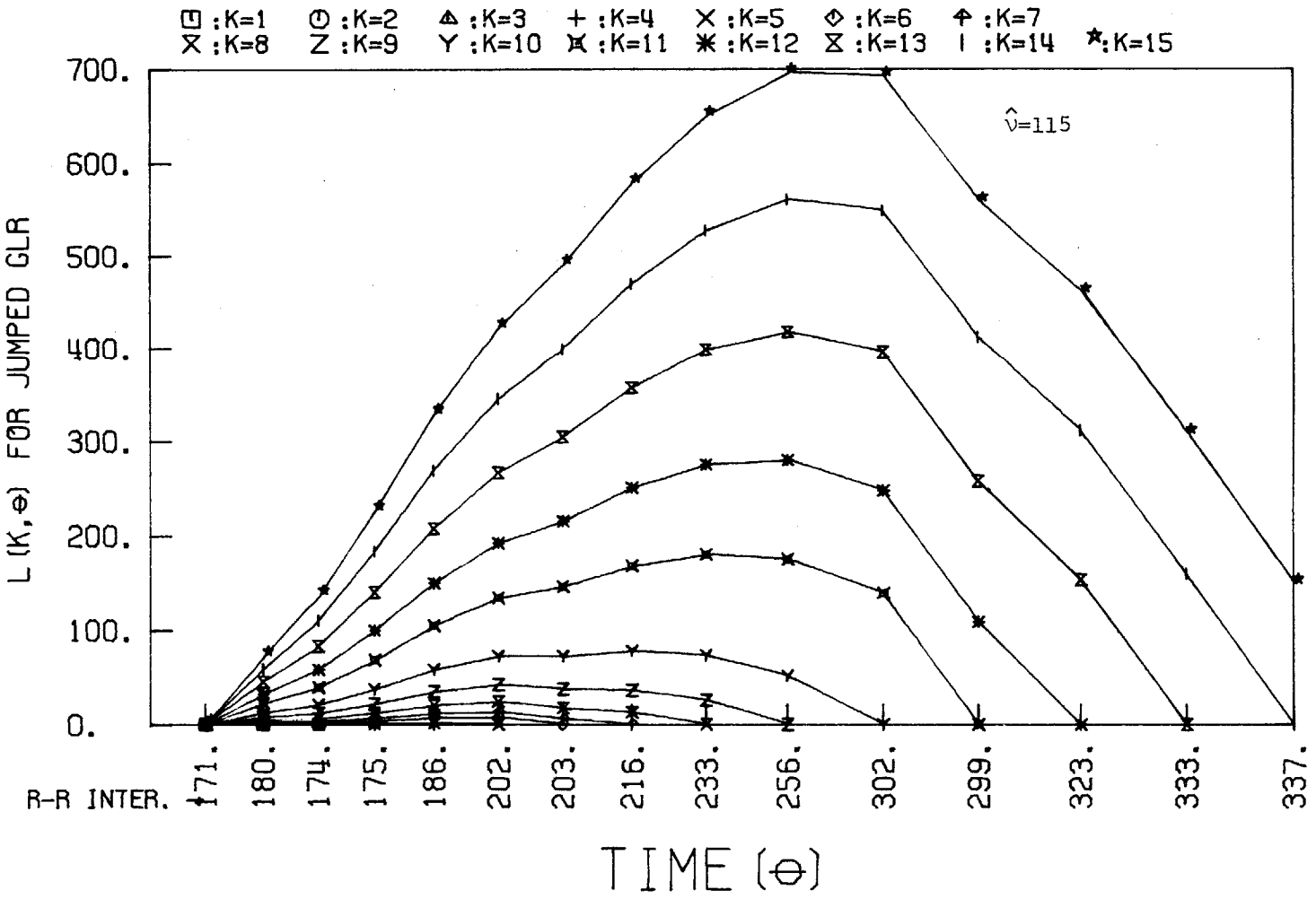

Figure 7.11 Jumped GLR for Data Fiel #476

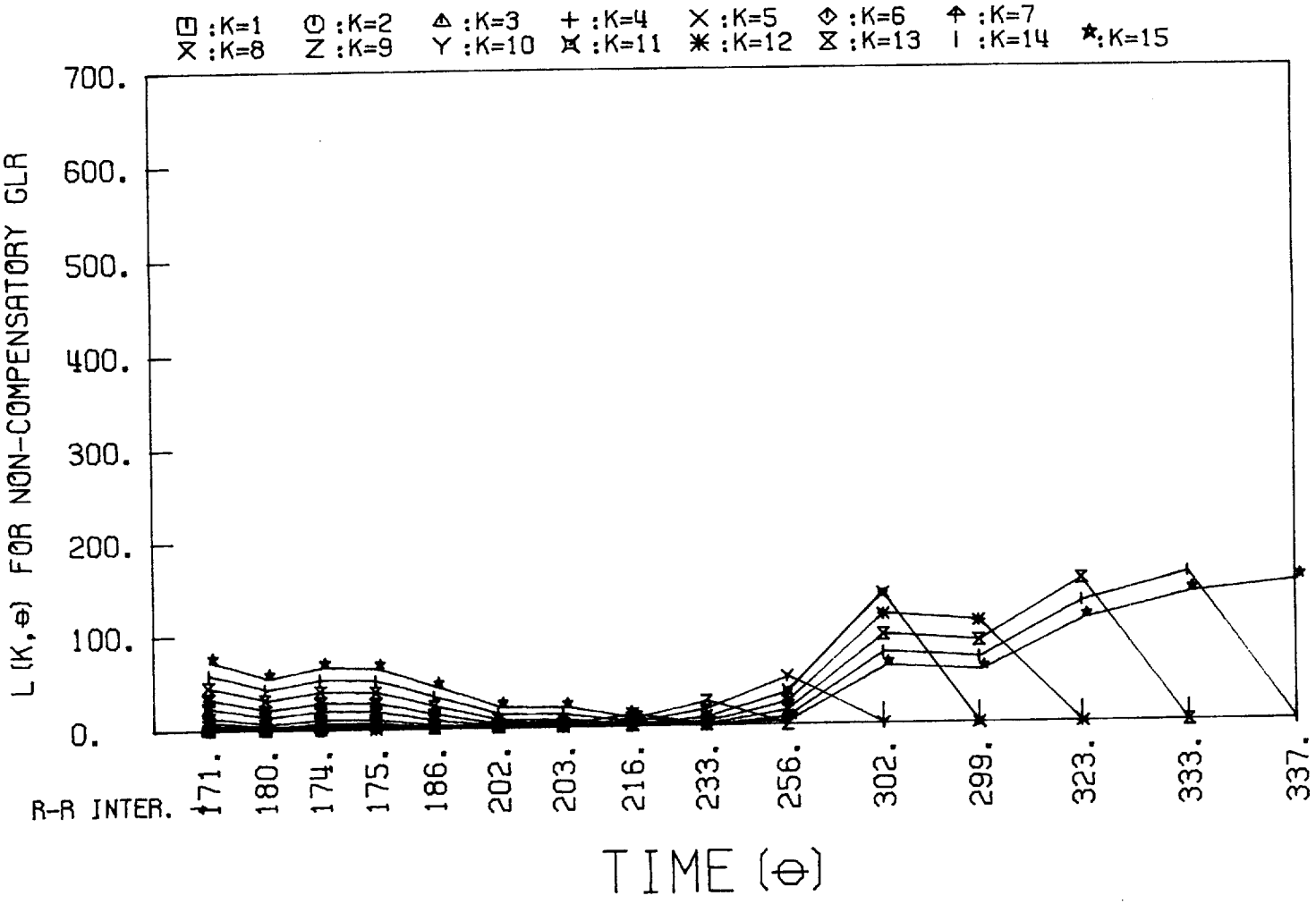

Figure 7.12 Non-Compensatory GLR for Data File #476

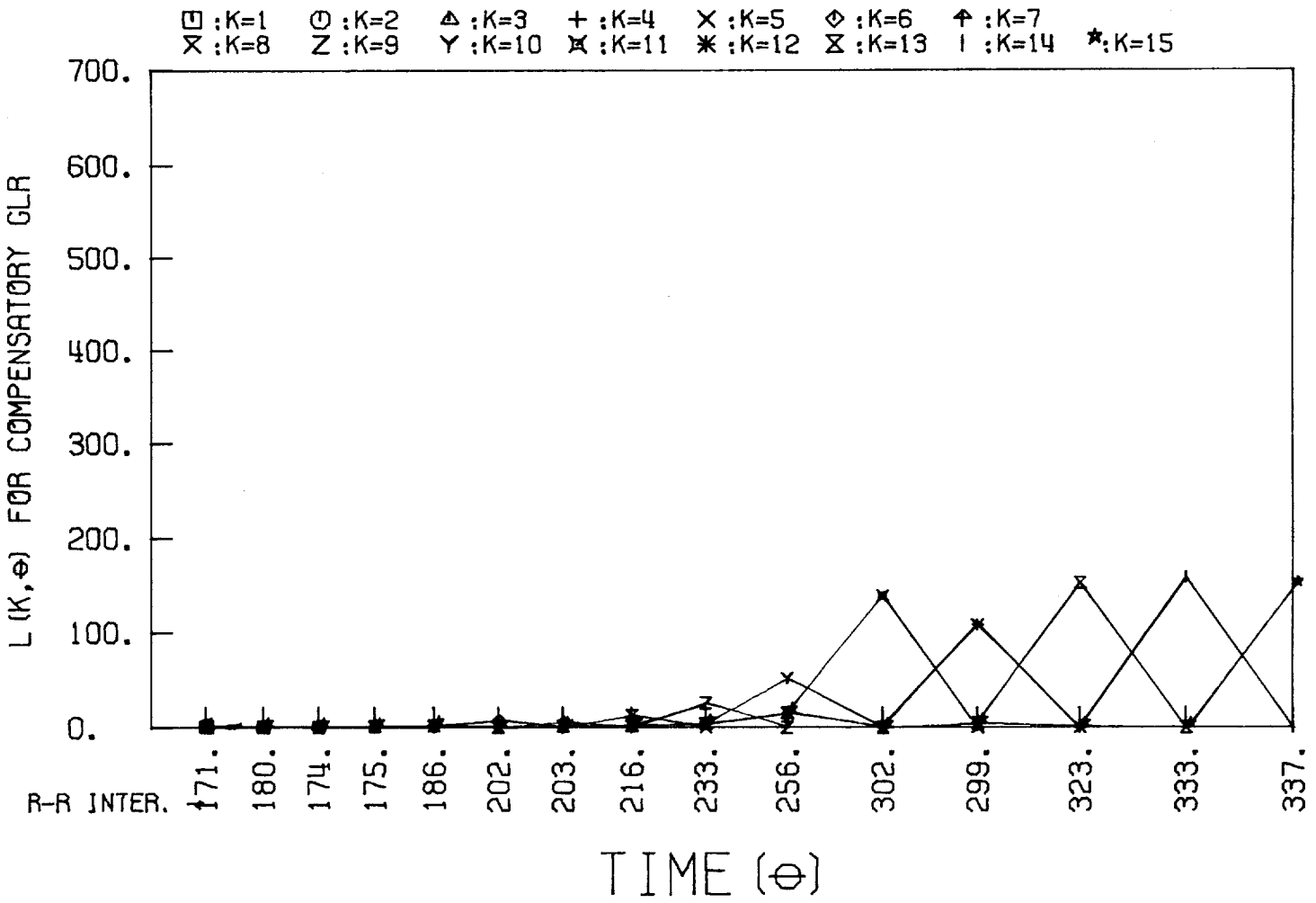

Figure 7.13 Compensatory GLR for Data File #476

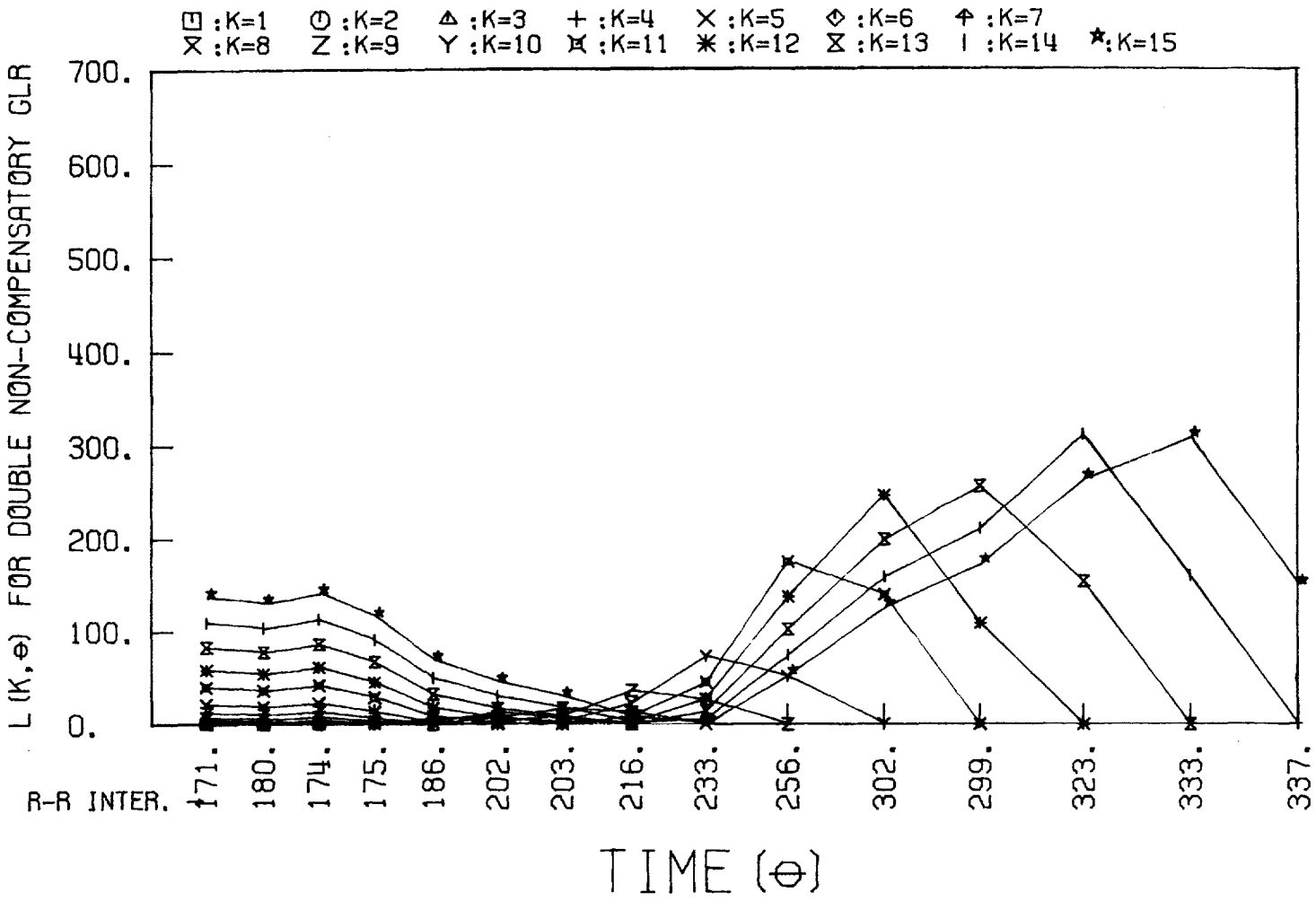

Figure 7.14 Double Non-Compensatory GLR for Data File #476

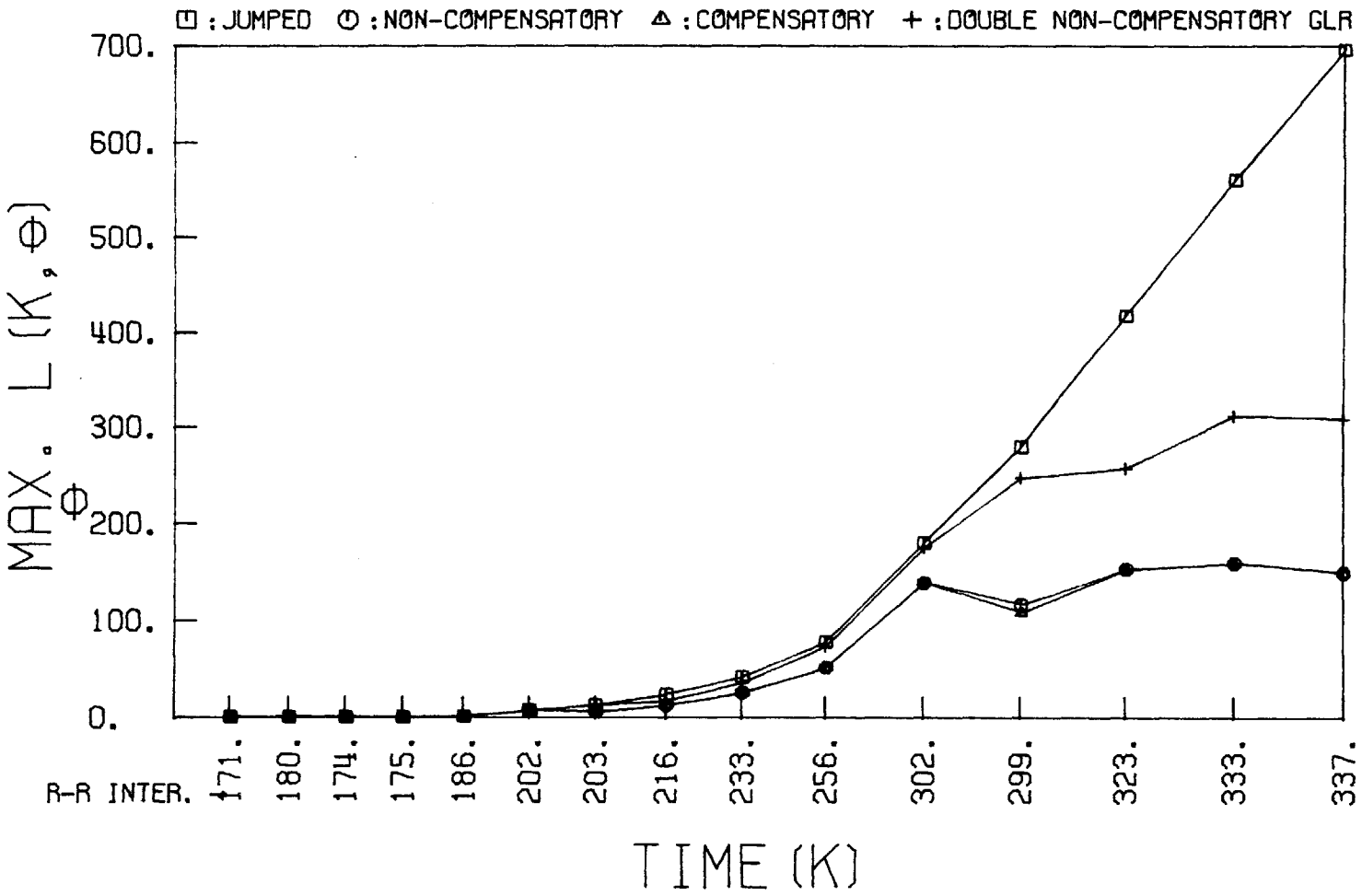

Figure 7.15 GLR Comparisons for Data File #476

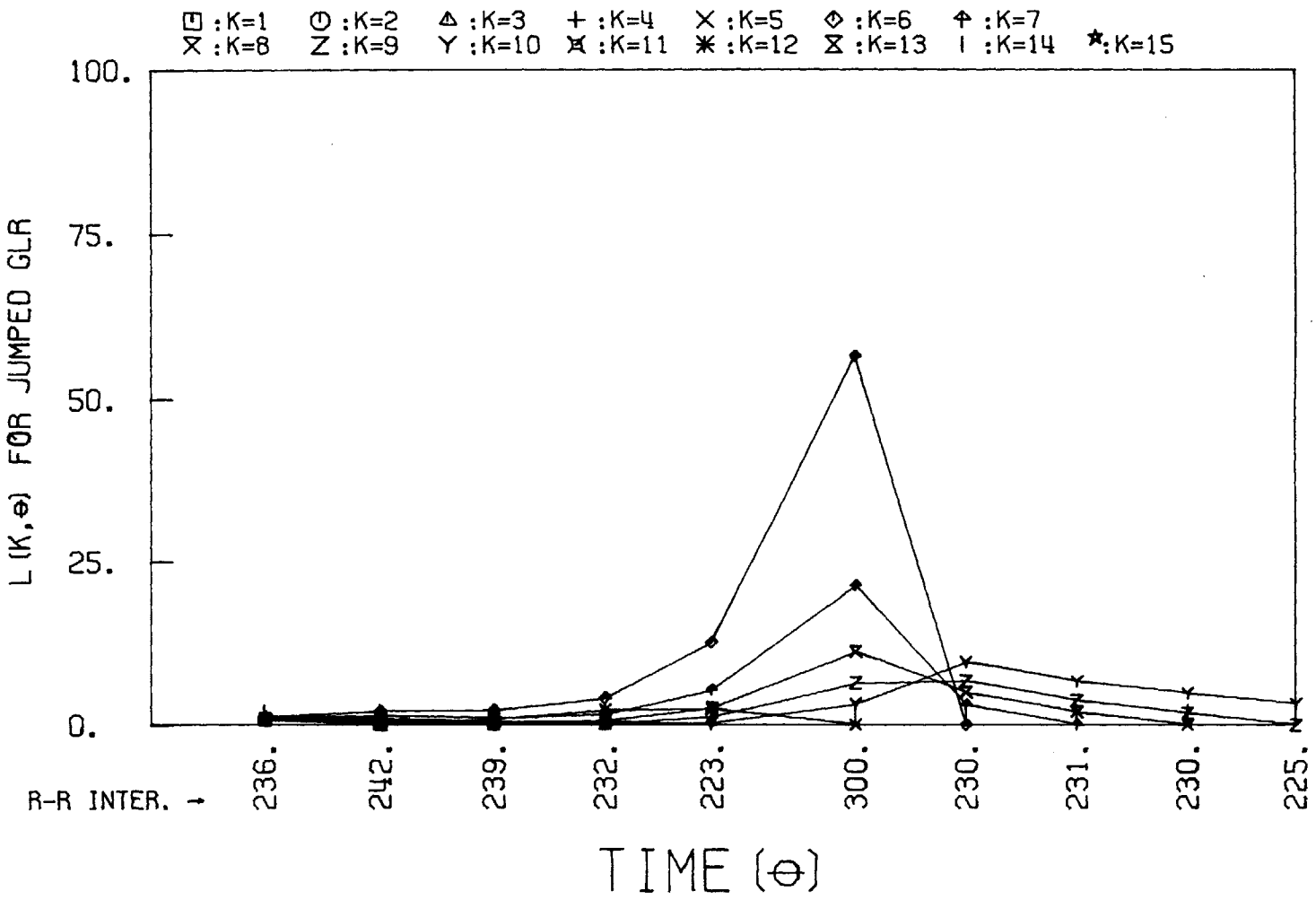

Figure 7.16 Jumped GLR for Non-Compensatory Beat (300).

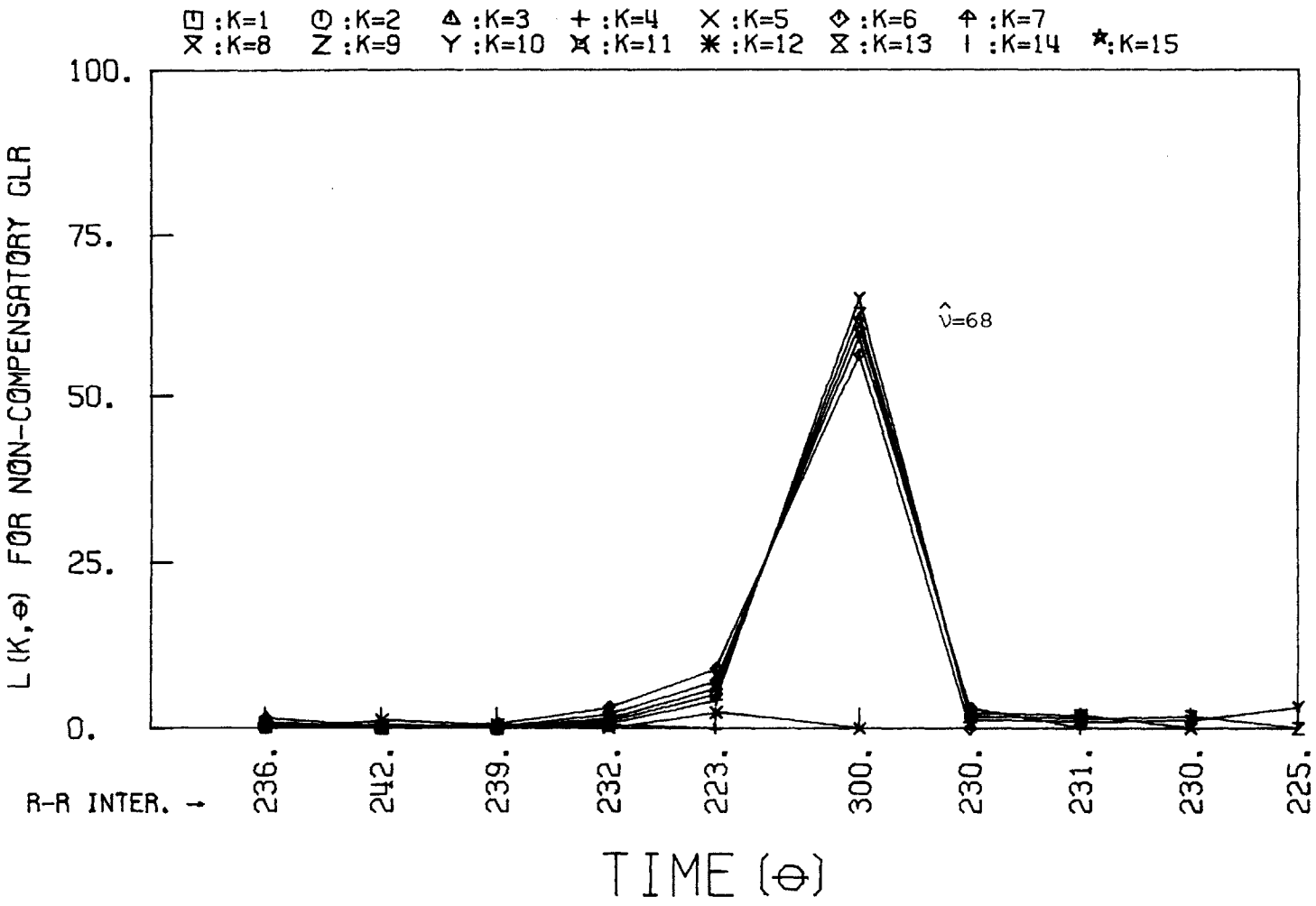

Figure 7.17 Non-Compensatory GLR for Non-Compensatory Beat (300)

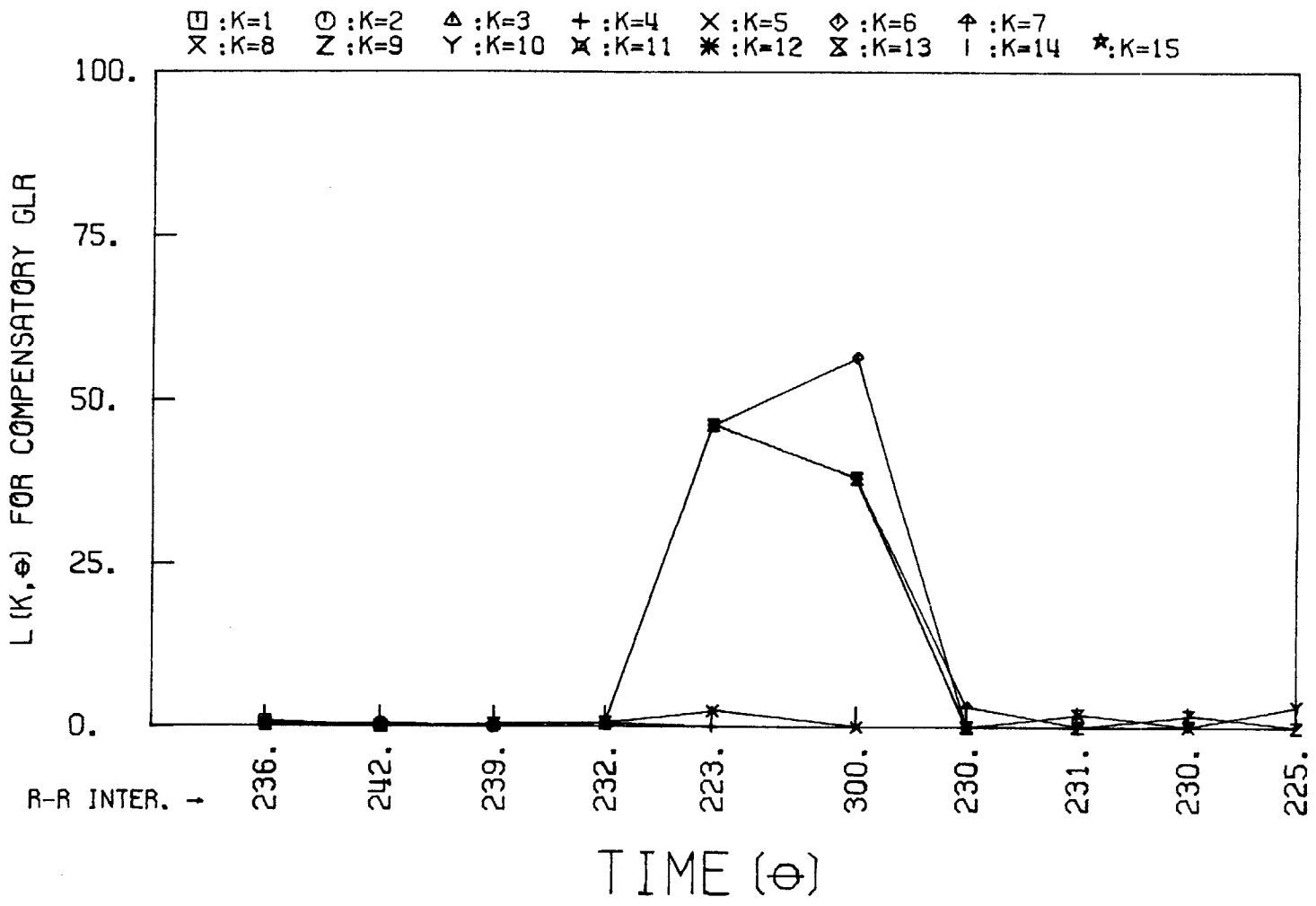

Figure 7.18 Compensatory GLR for Non-Compensatory Beat (300)

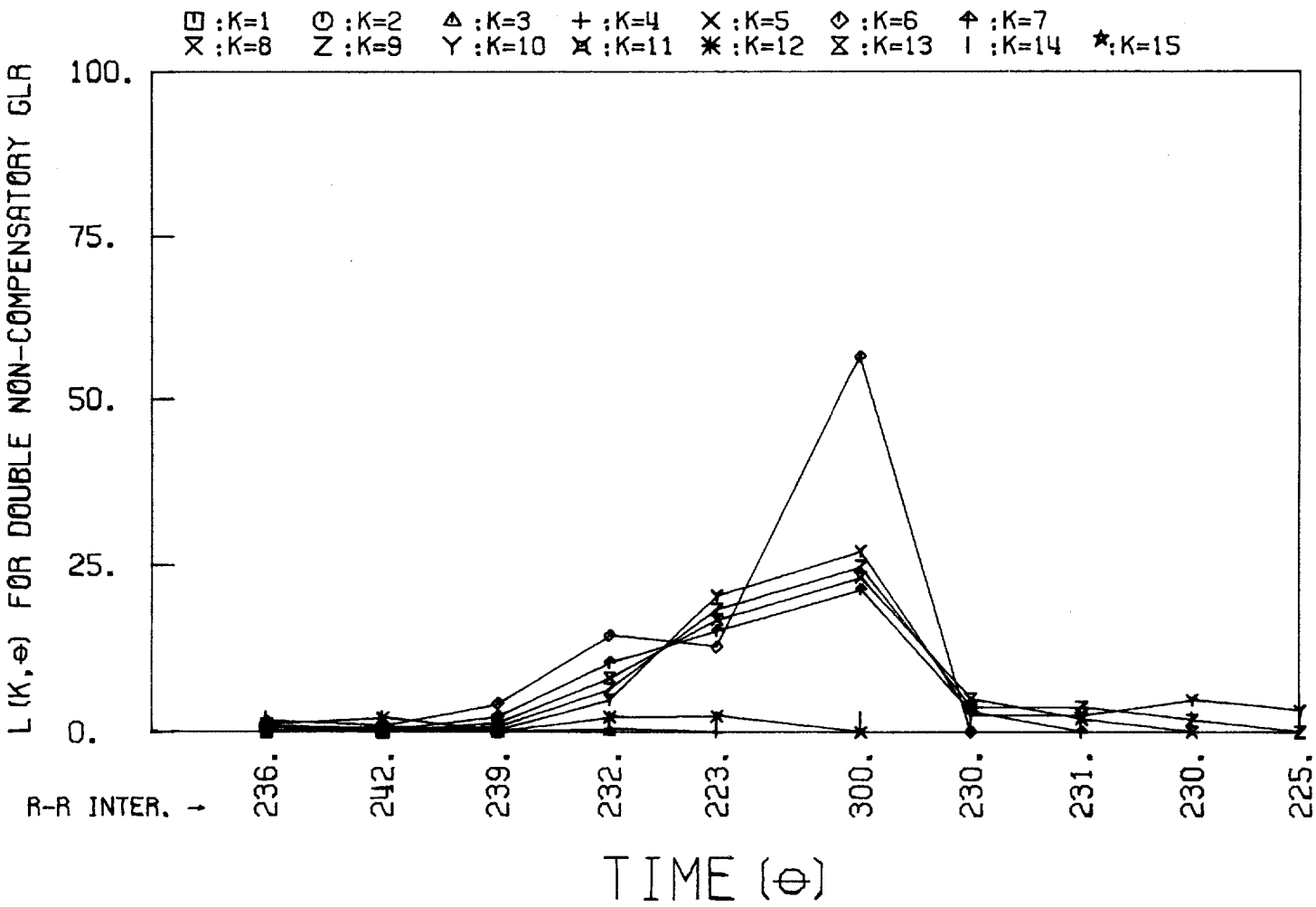

Figure 7.19 Double Non-Compensatory GLR for Non-Compensatory Beat (300)

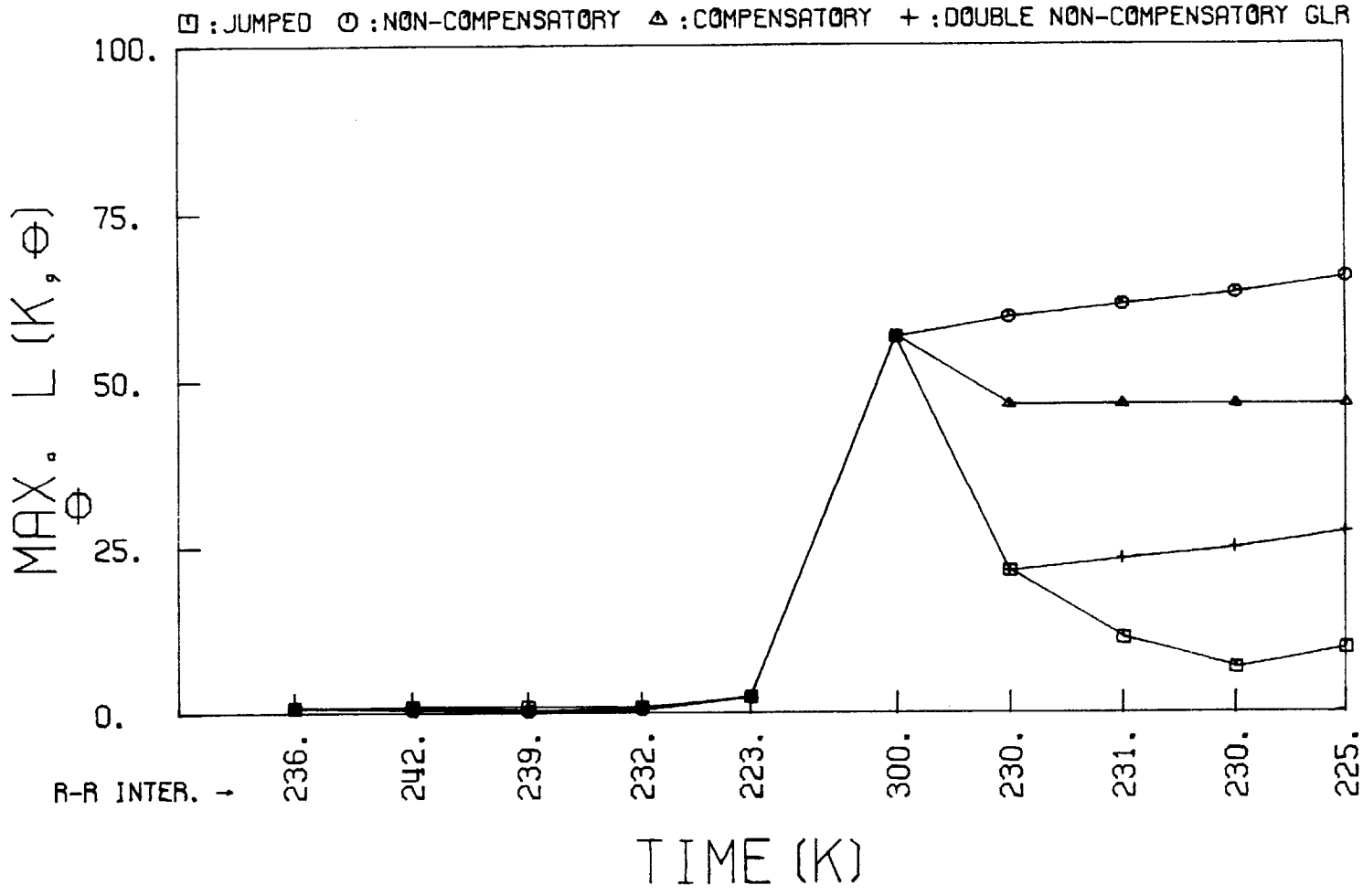

Figure 7.20 GLR Comparisons for Non-Compensatory Beat (300)

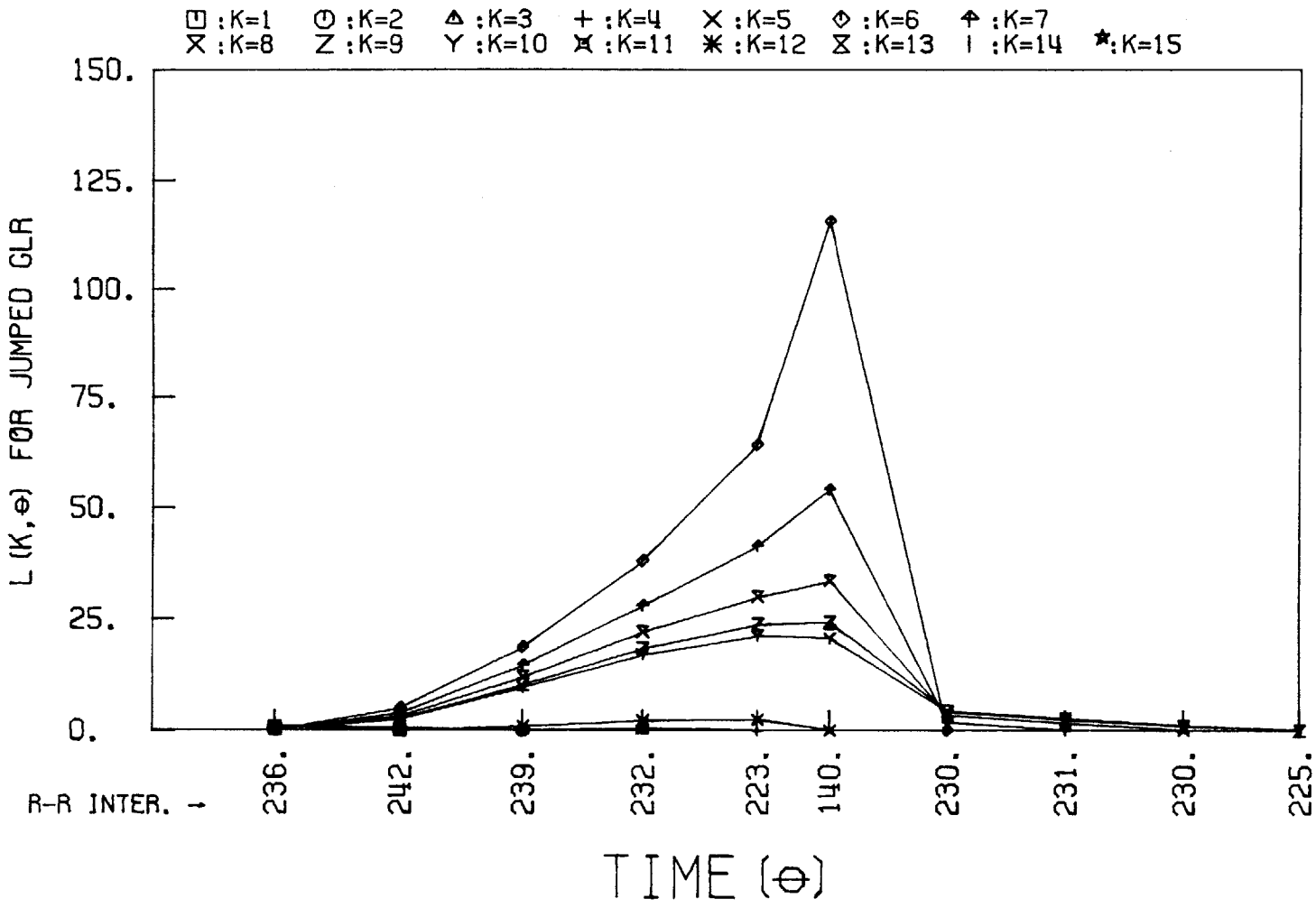

Figure 7.21 Jumped GLR for Non-Compensatory Beat (140)

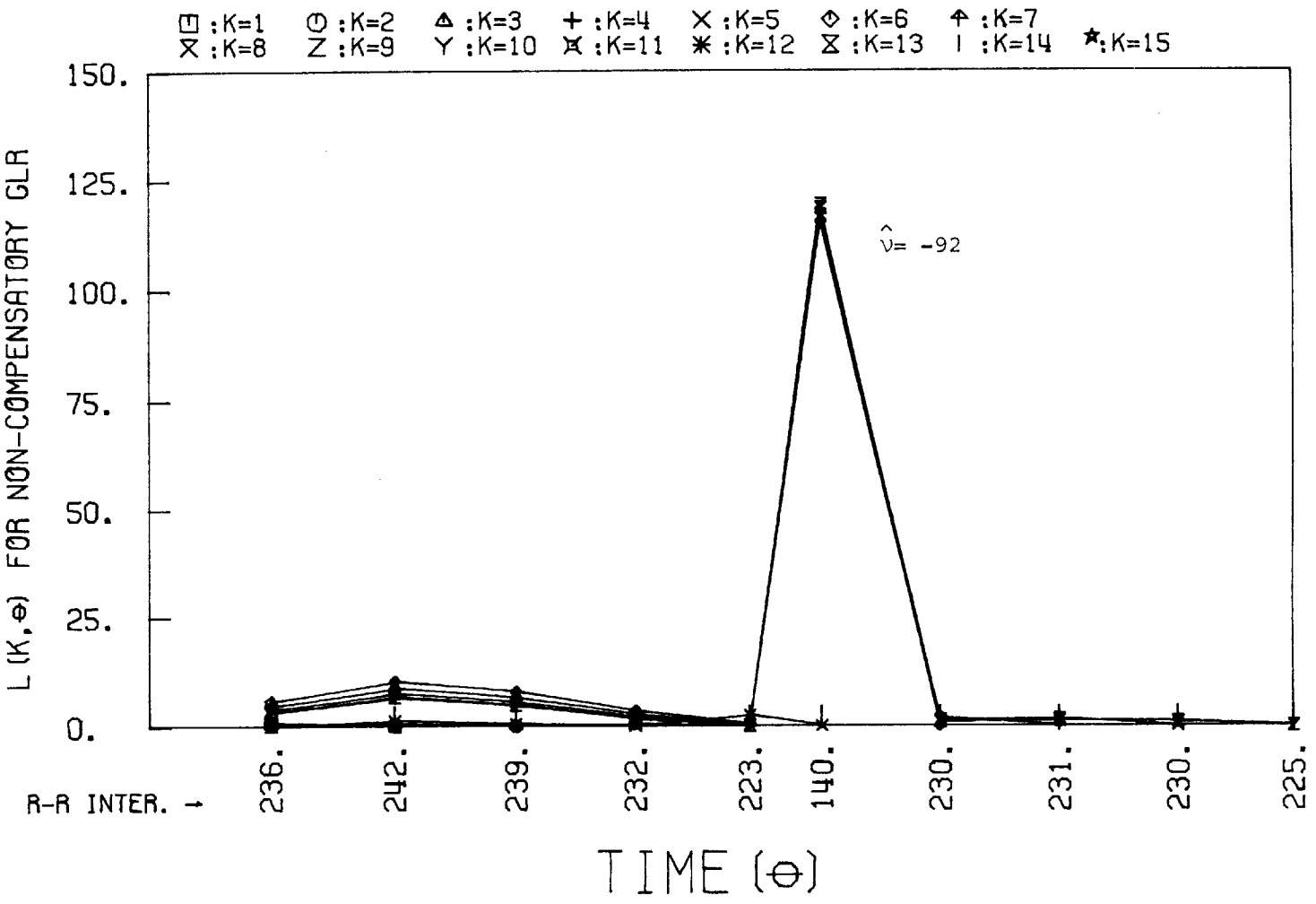

Figure 7.22 Non-Compensatory GLR for Non-Compensatory Beat (140)

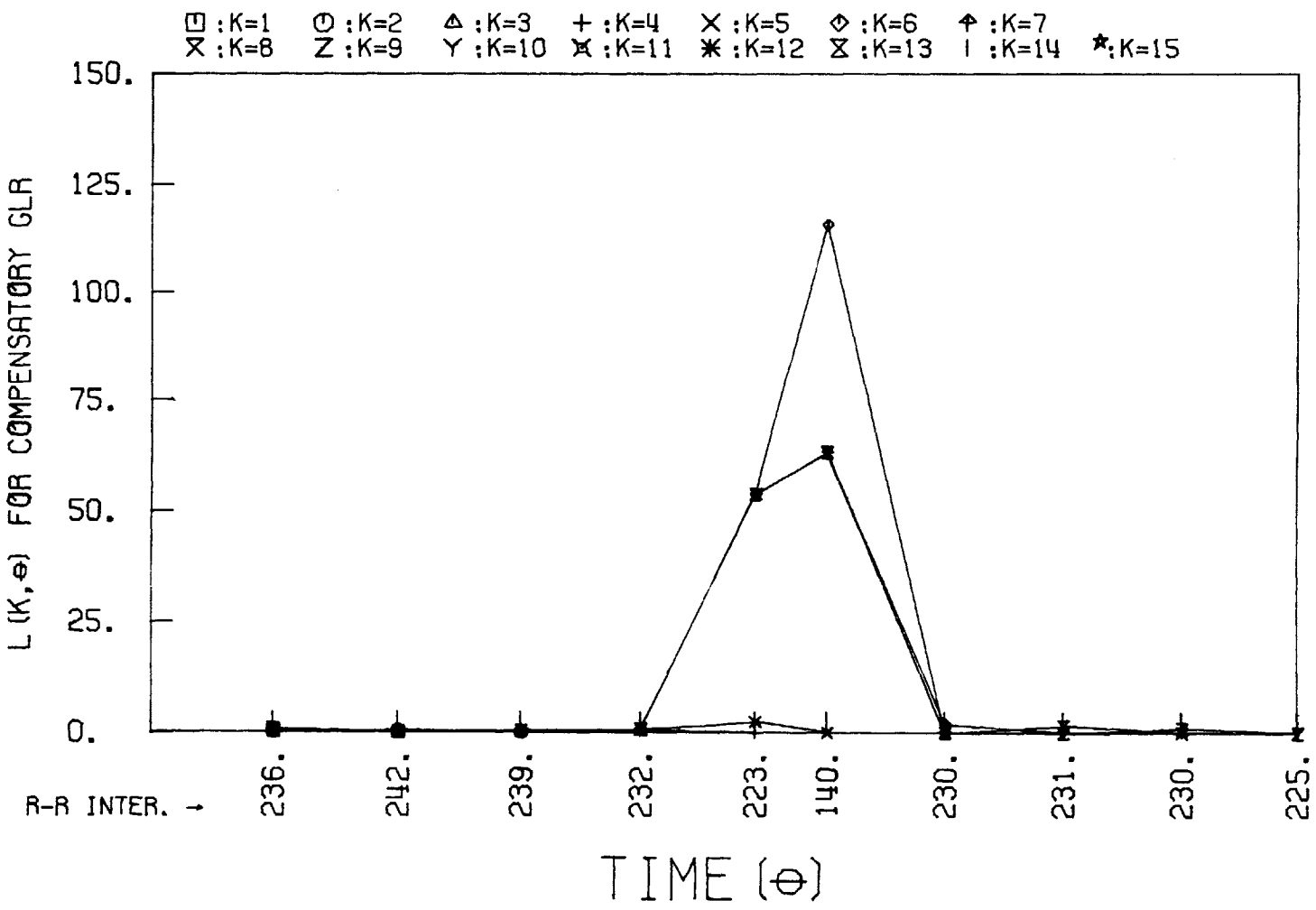

Figure 7.23 Compensatory GLR for Non-Compensatory Beat (140).

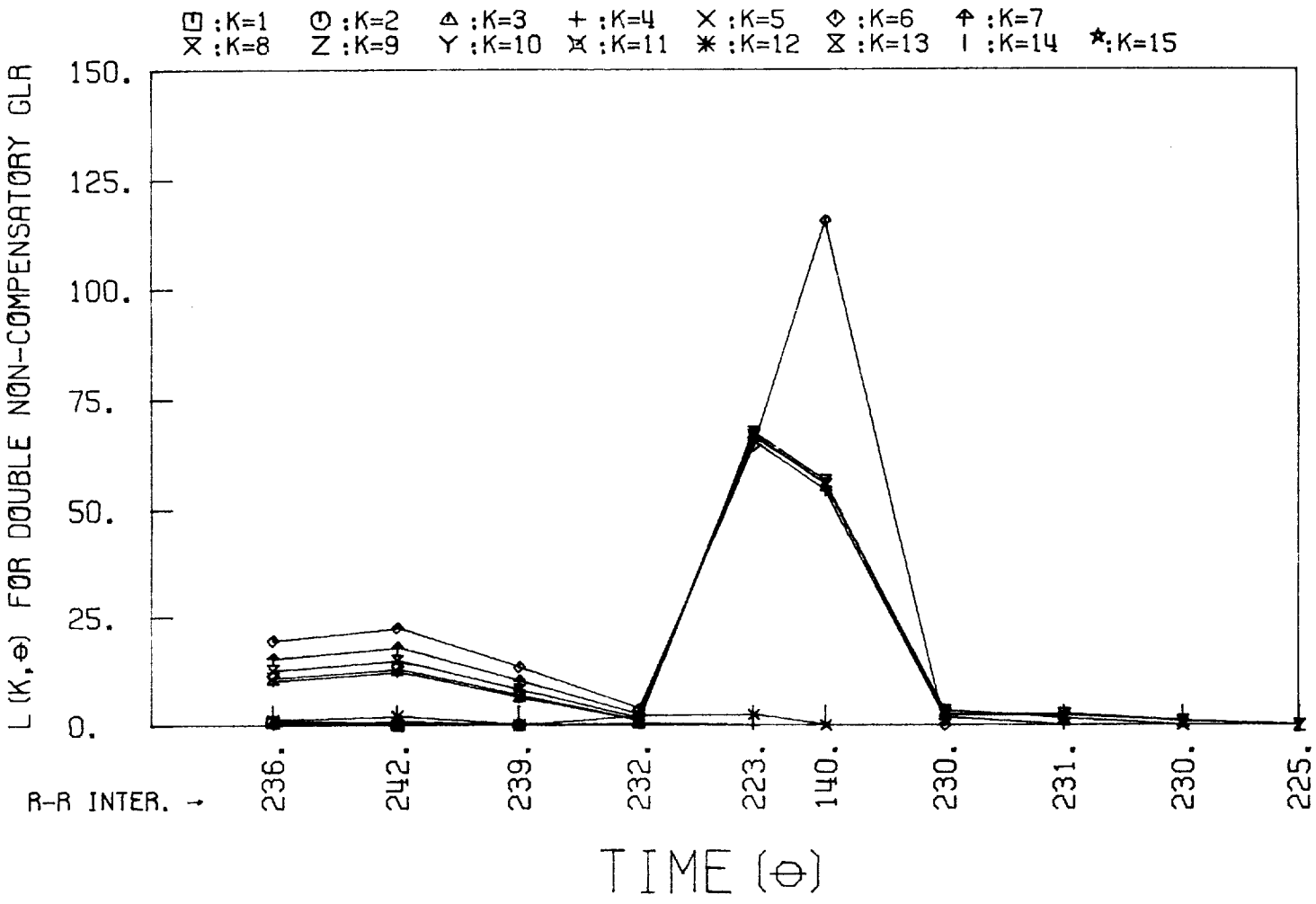

Figure 7.24 Double Non-Compensatory GLR for Non-Compensatory Beat (140)

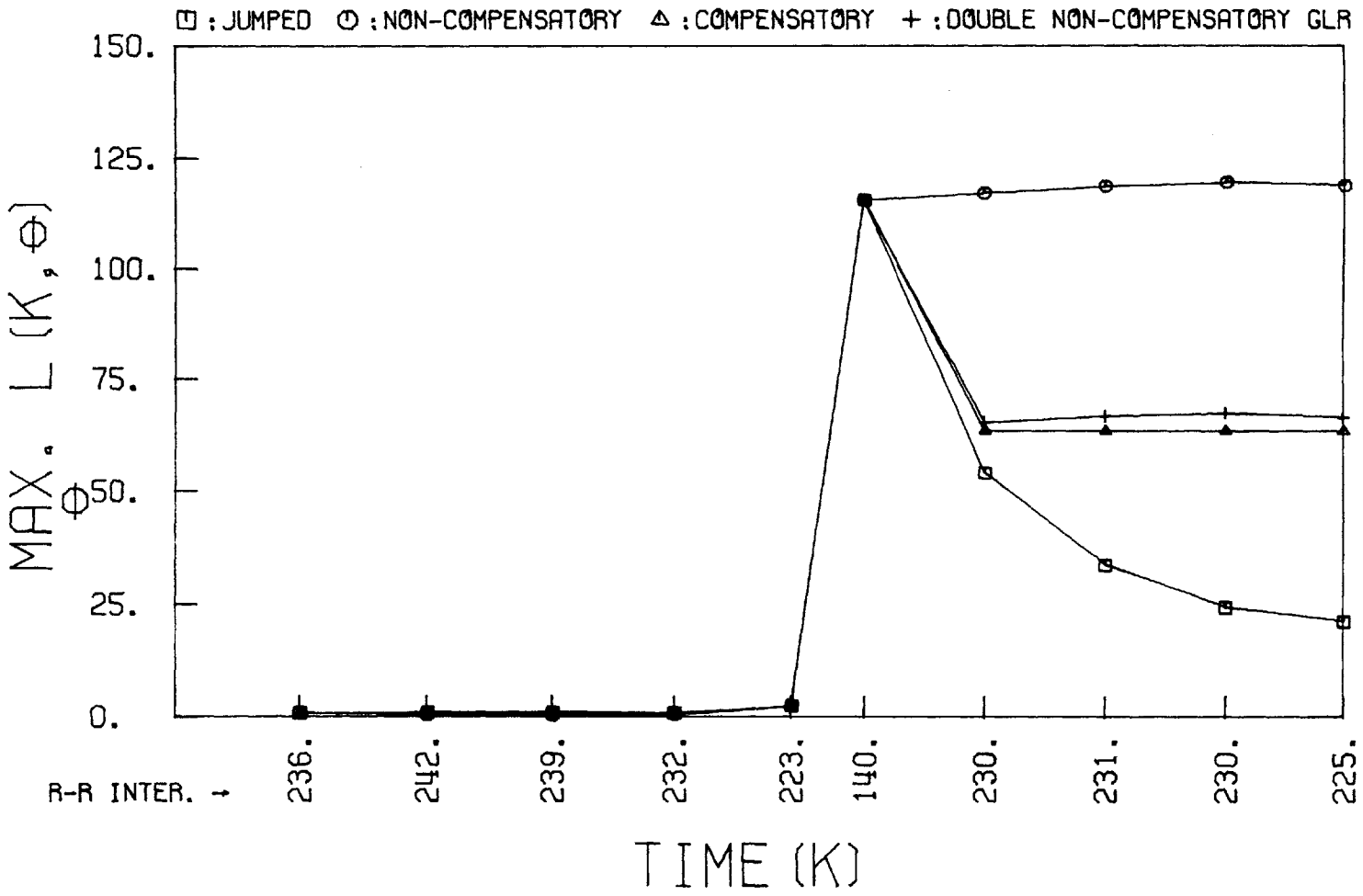

Figure 7.25 GLR Comparisons for Non-Compensatory Beat (140).

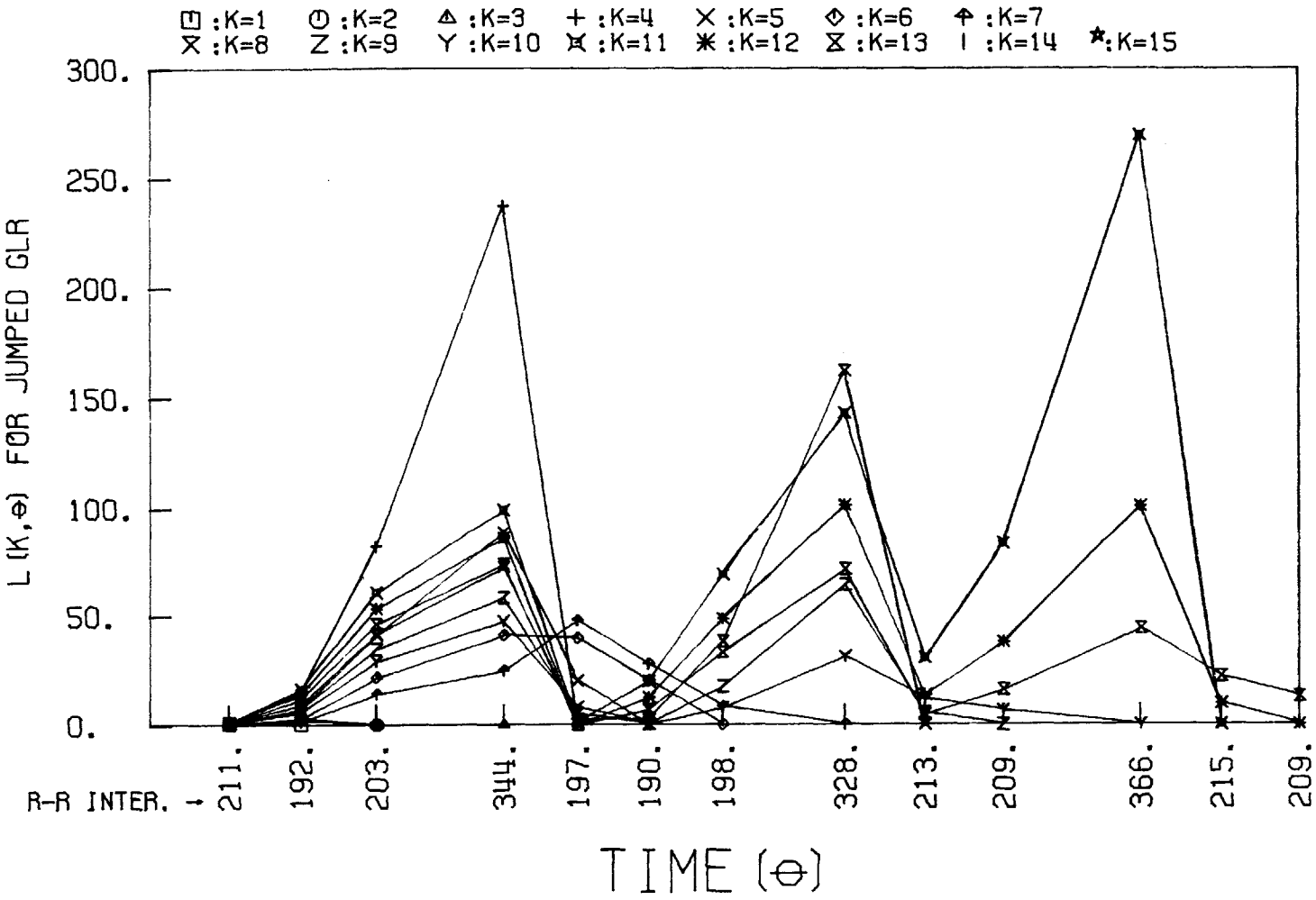

Figure 7.26 Jumped GLR for Data File #463.

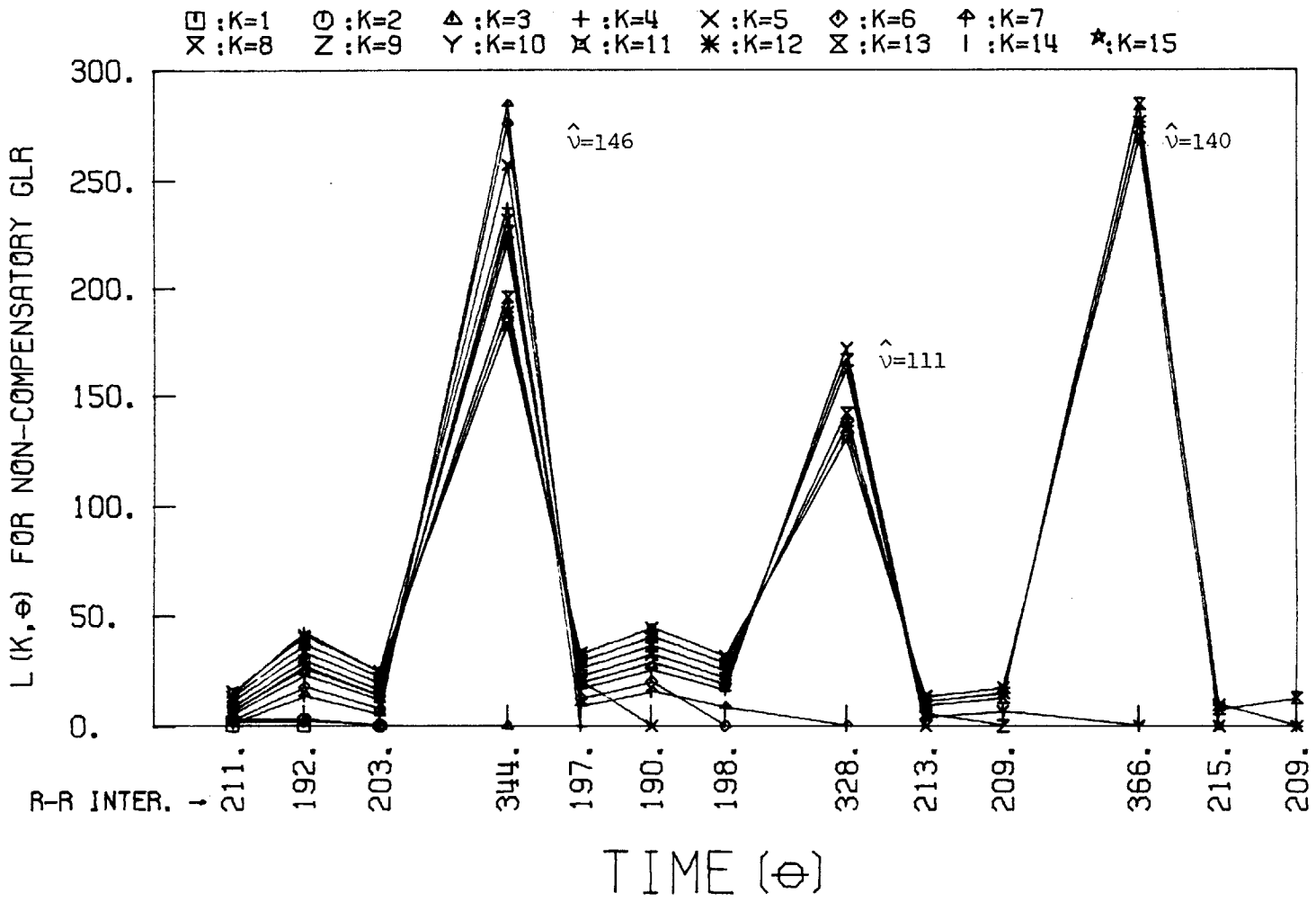

Figure 7.27 Non-Compensatory GLR for Data File #463

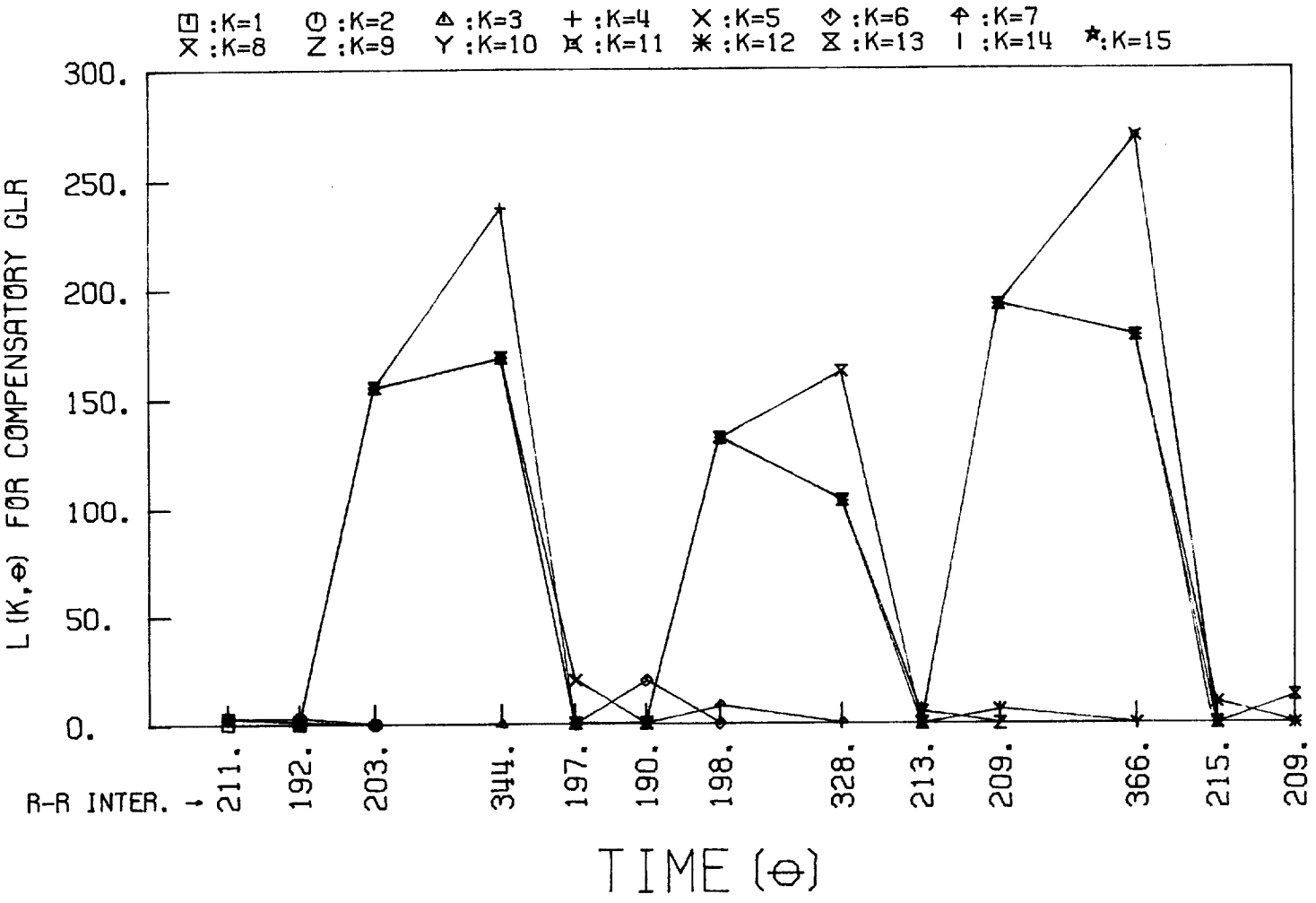

Figure 7.28 Compensatory GLR for Data File #463

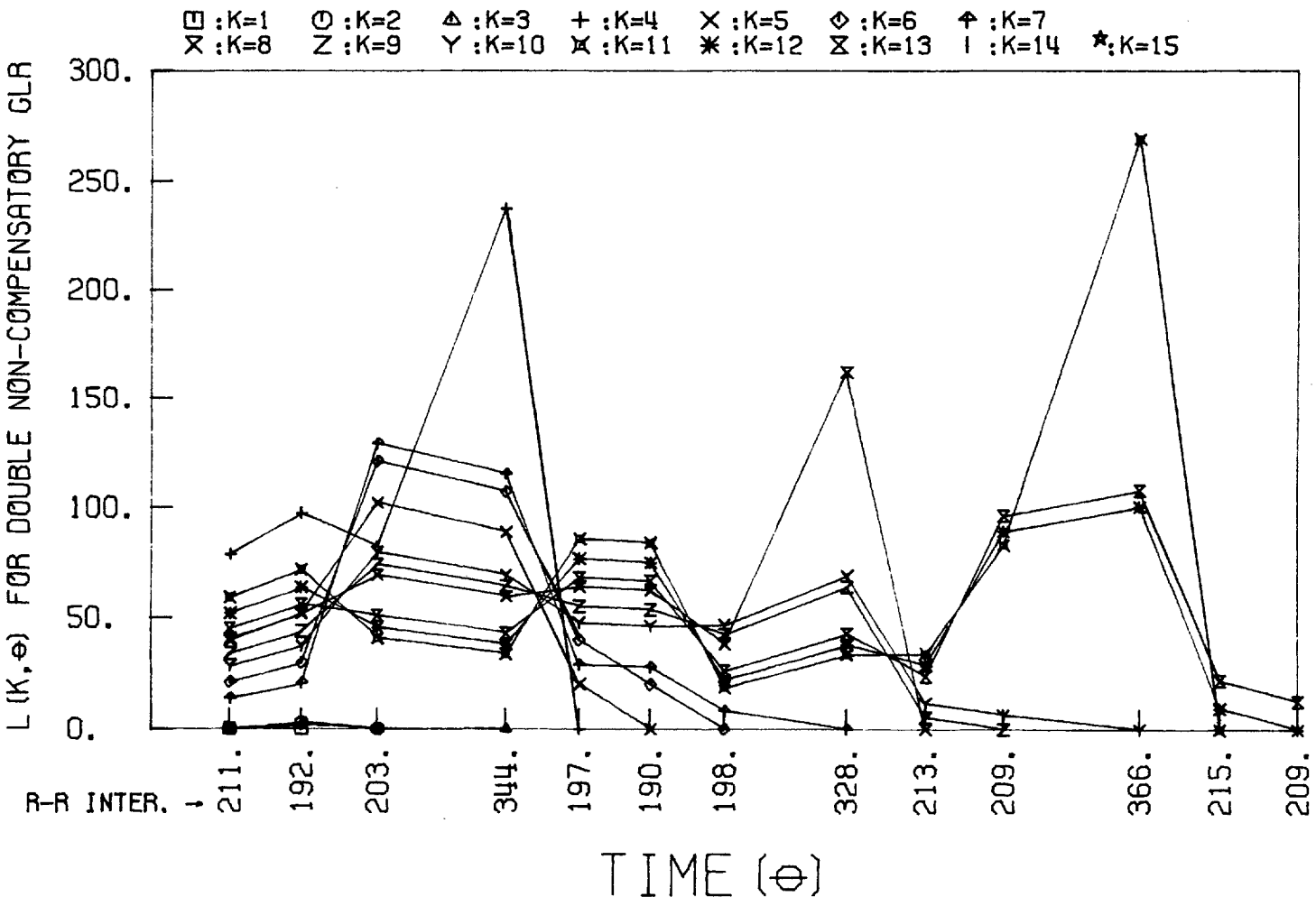

Figure 7.29 Double Non-Compensatory GLR for Data File #463

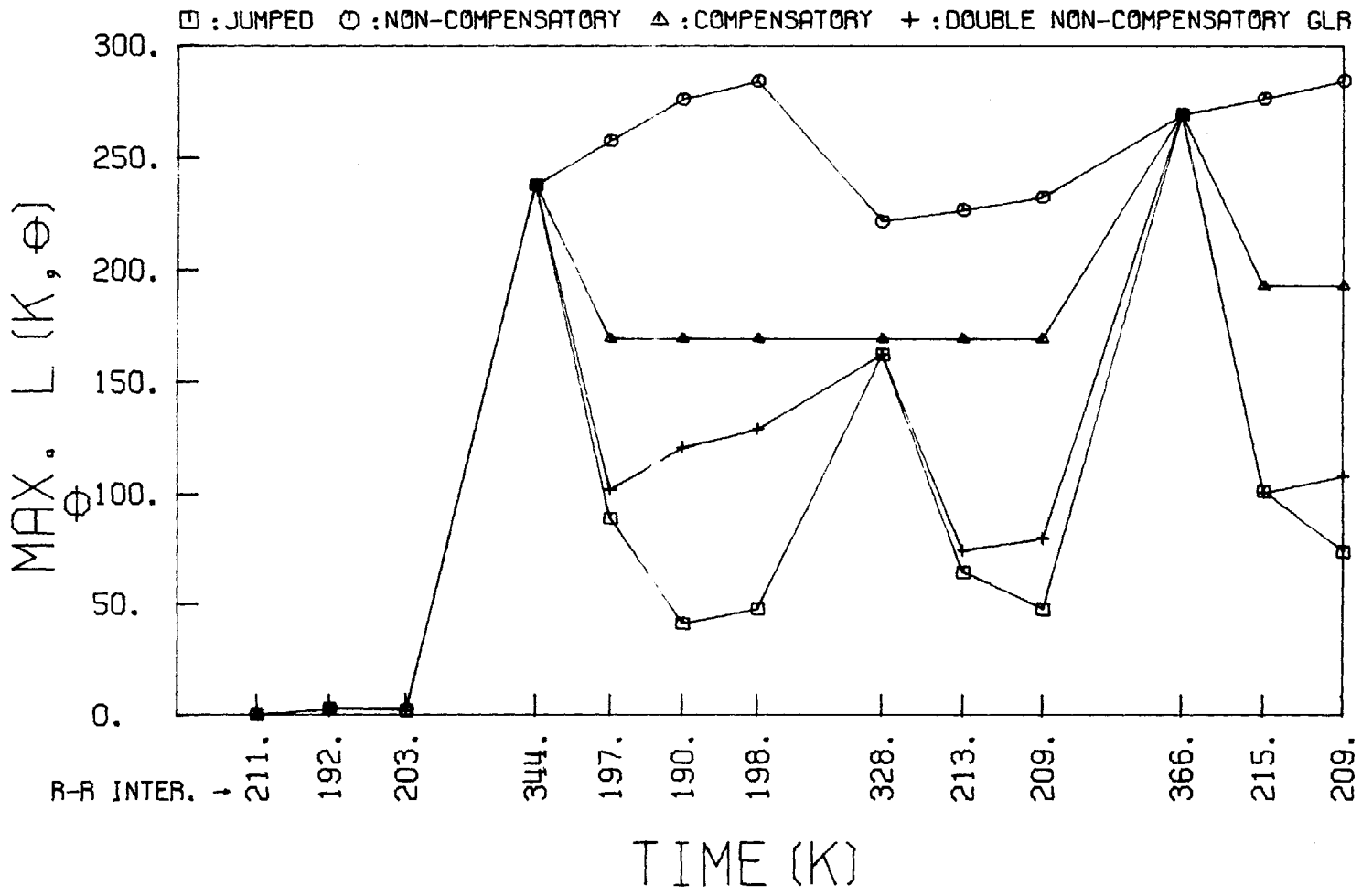

Figure 7.30 GLR Comparisons for Data File #463

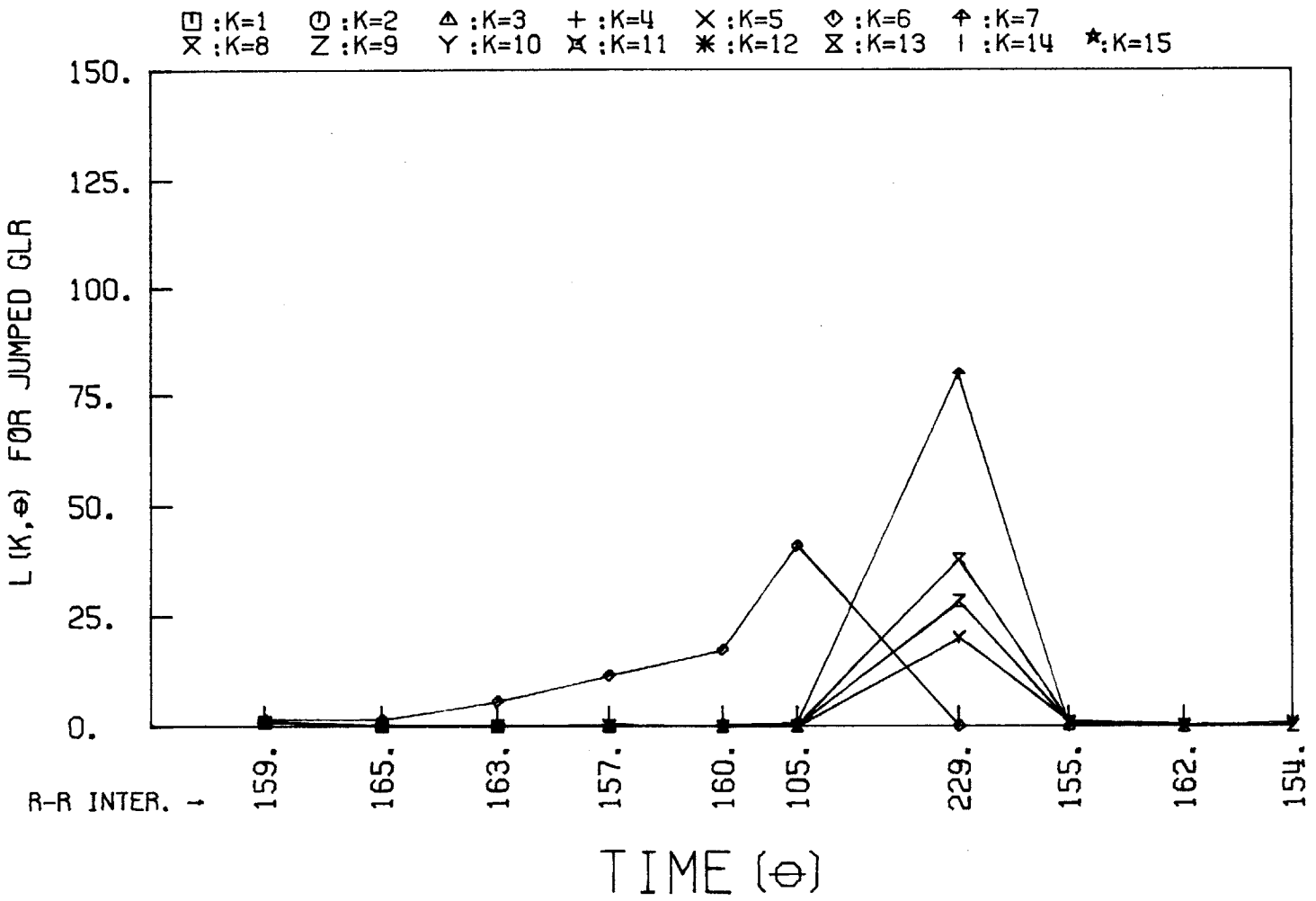

Figure 7.31 Jumped GLR for Data File HARNETPVCS

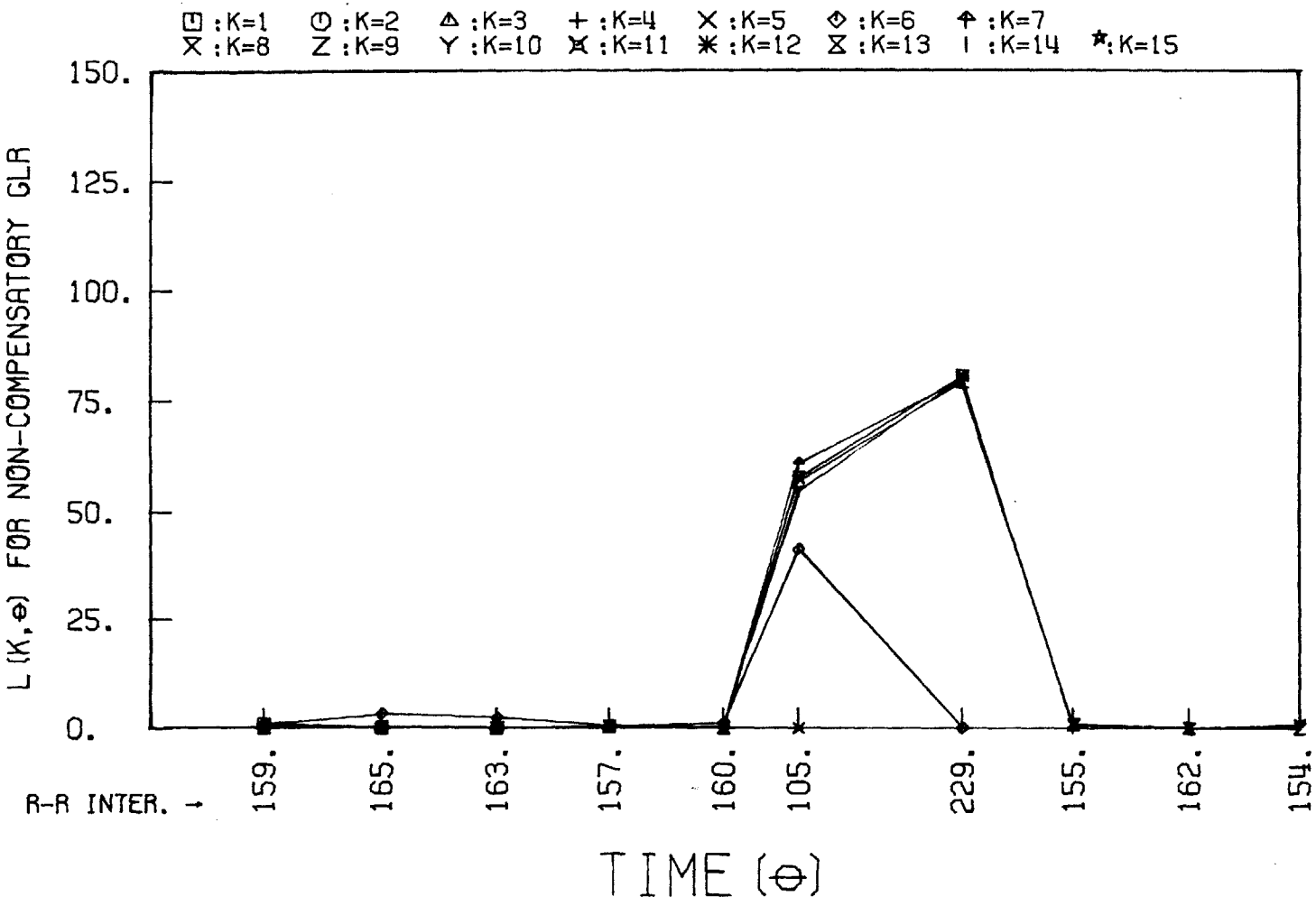

Figure 7.32 Non-Compensatory GLR for Data File HARNETPVCS

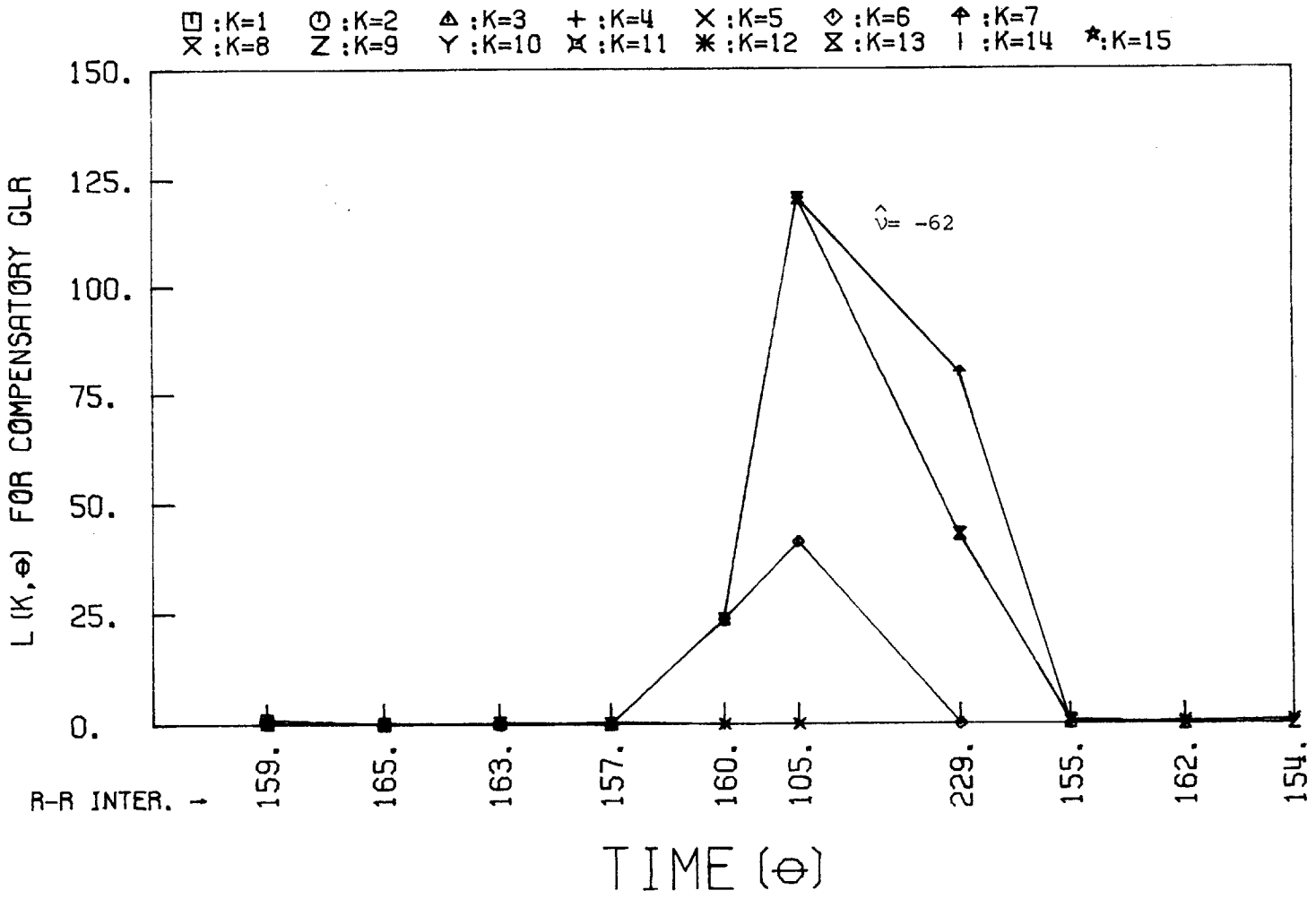

Figure 7.33 Compensatory GLR for Data File HARNETPVCS

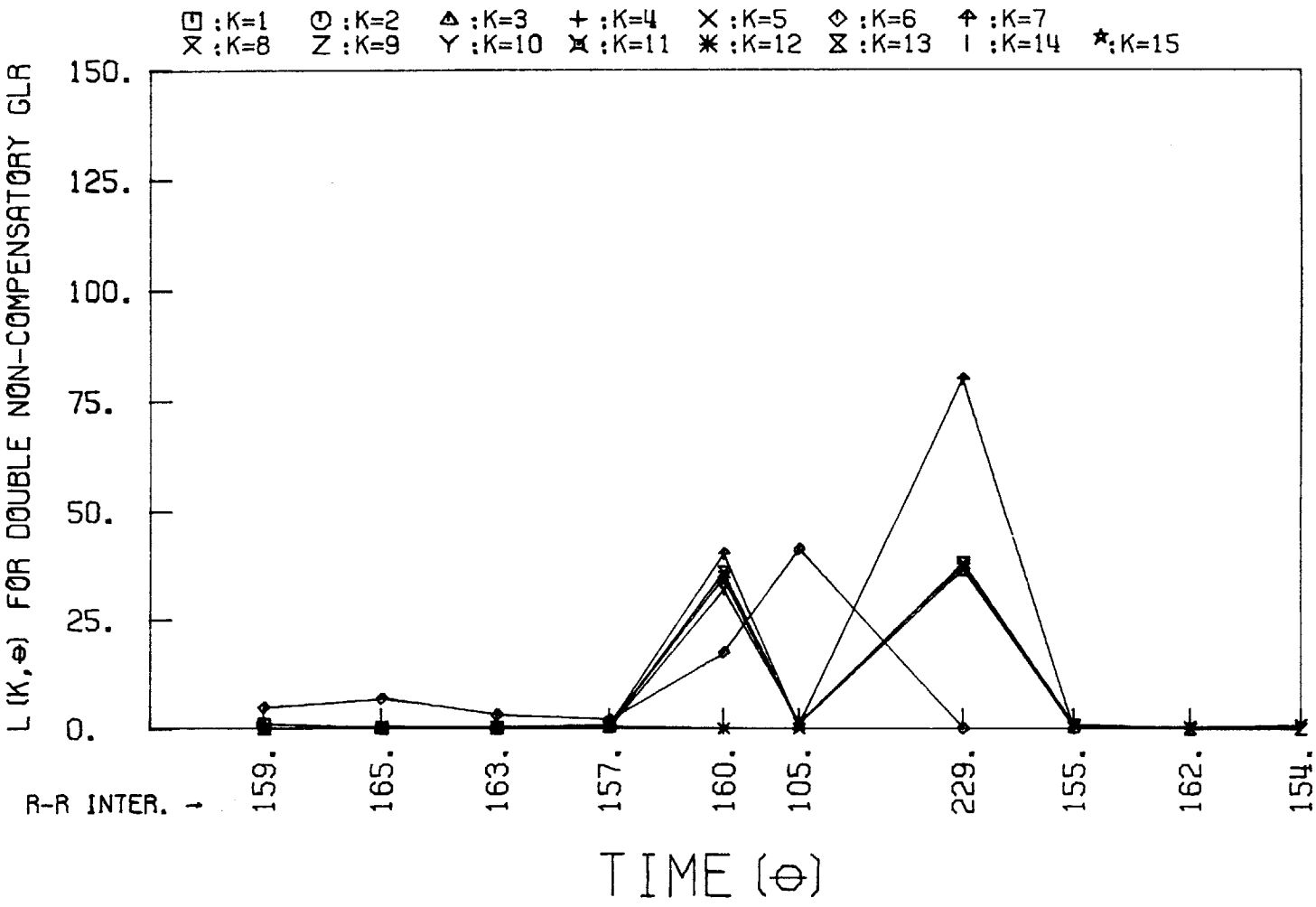

Figure 7.34 Double Non-Compensatory GLR for Data File HARNETPVCS

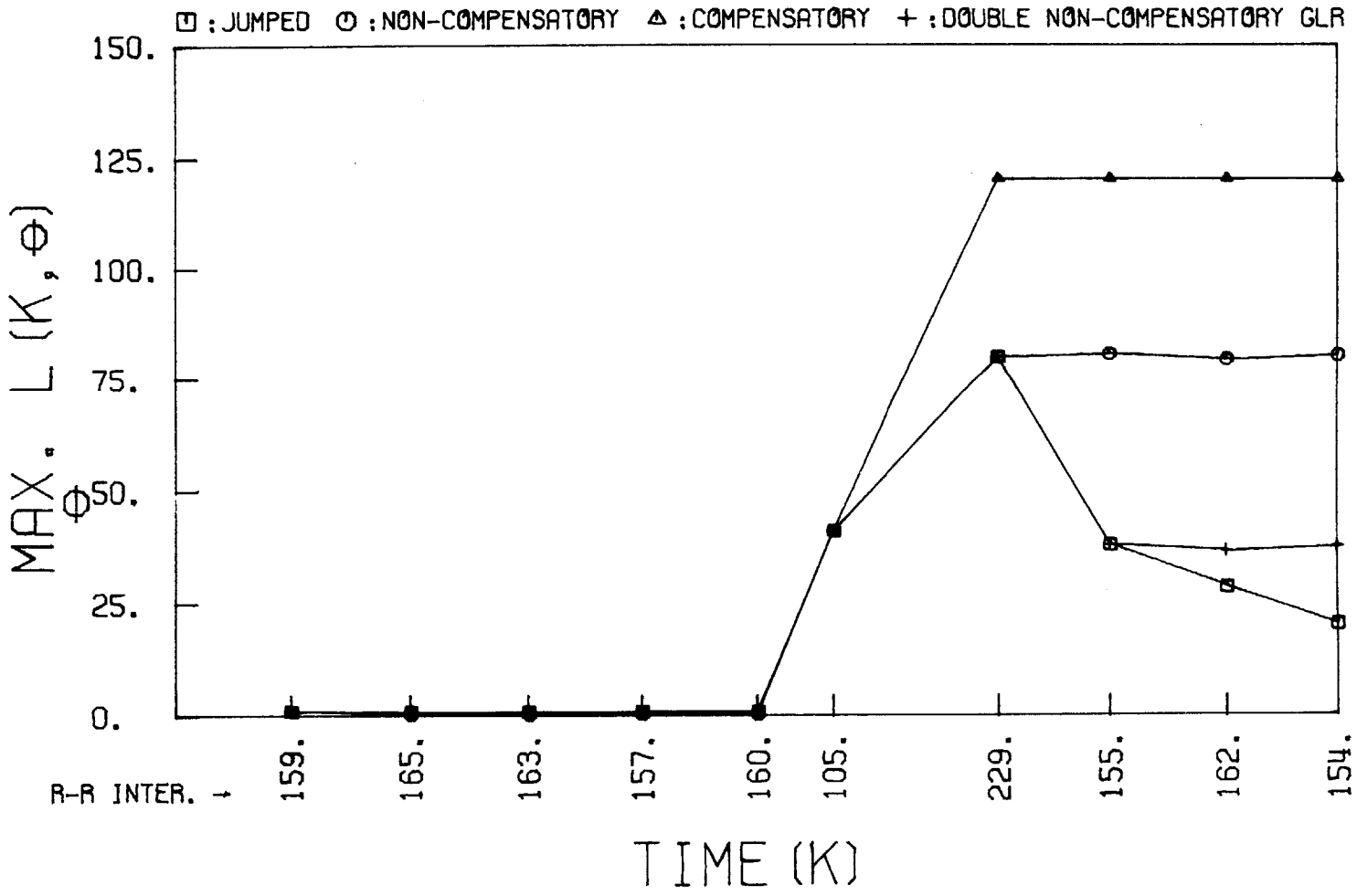

Figure 7.35 GLR Comparisons for Data File HARNETPVCS

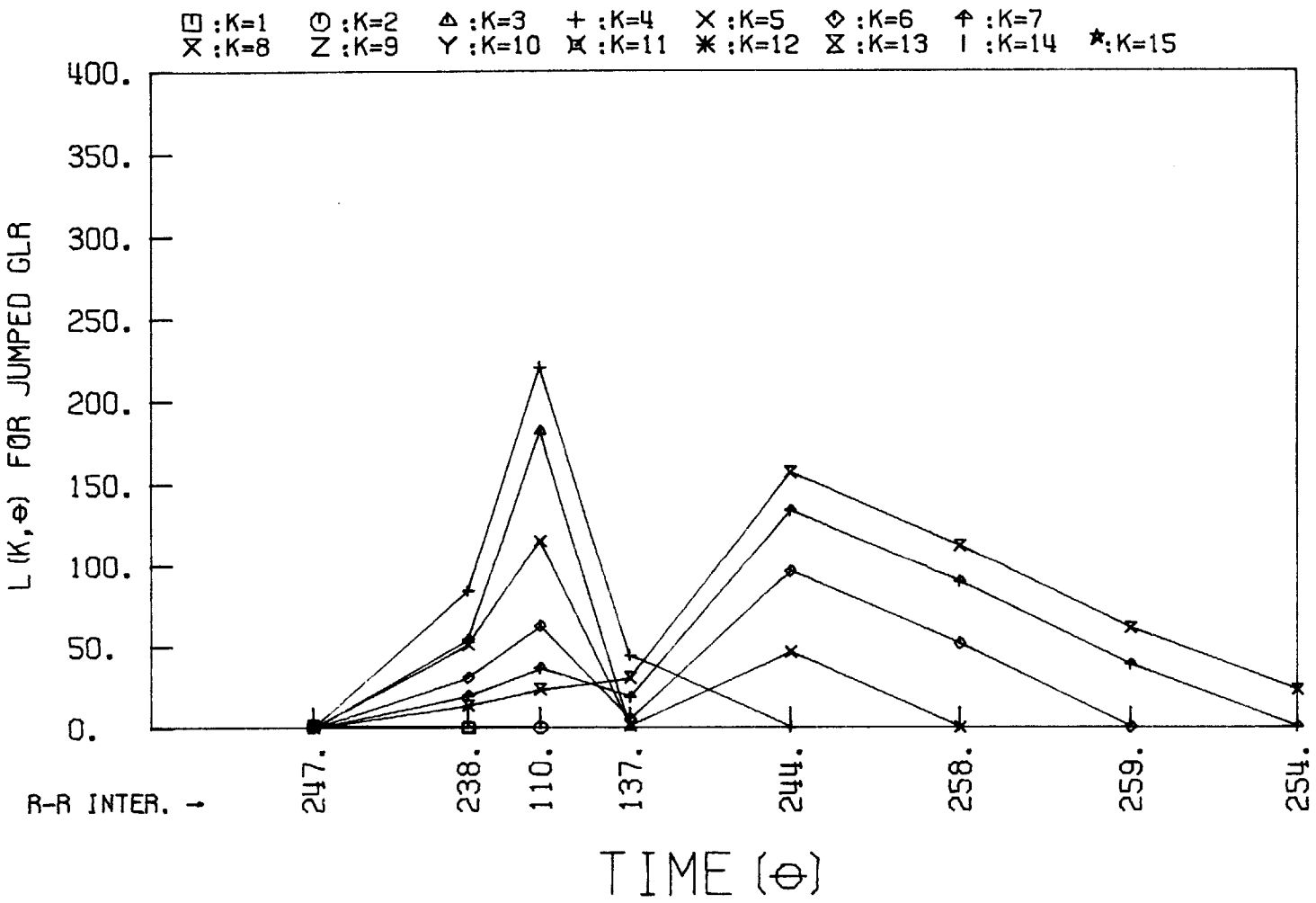

Figure 7.36 Jumped GLR for Data File #492-1

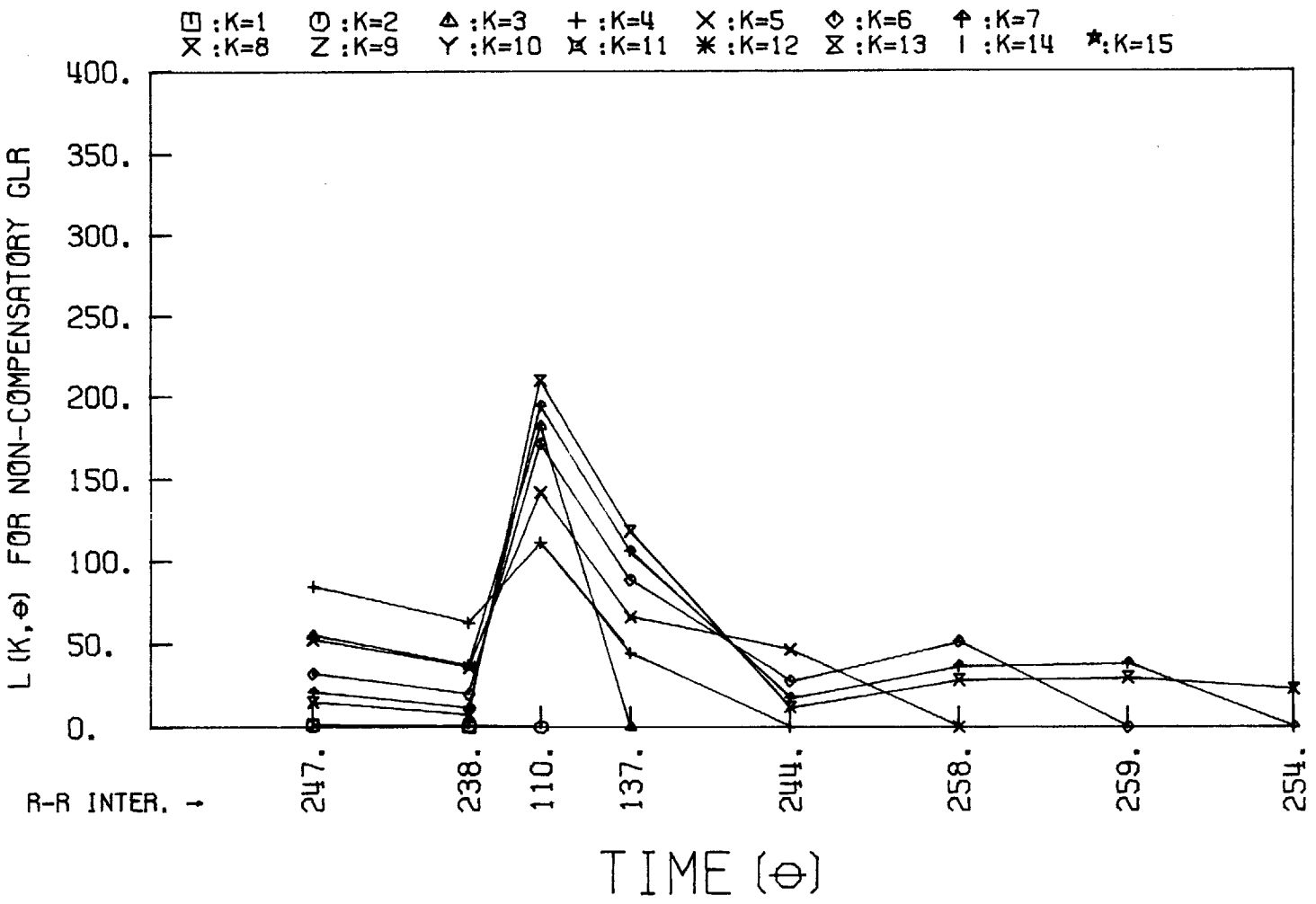

Figure 7.37 Non-Compensatory GLR for Data File #492-1

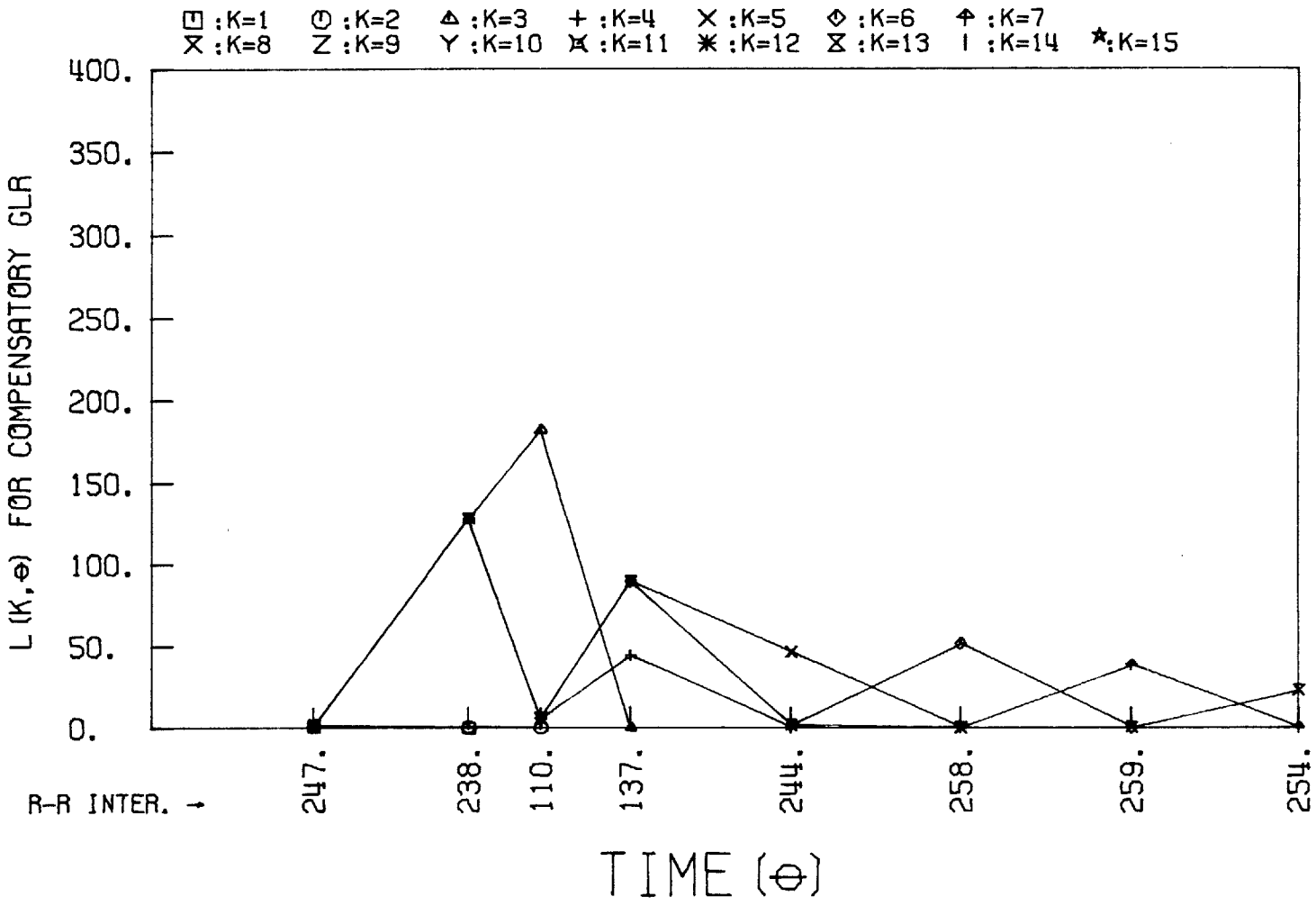

Figure 7.38 Compensatory GLR for Data File #492-1

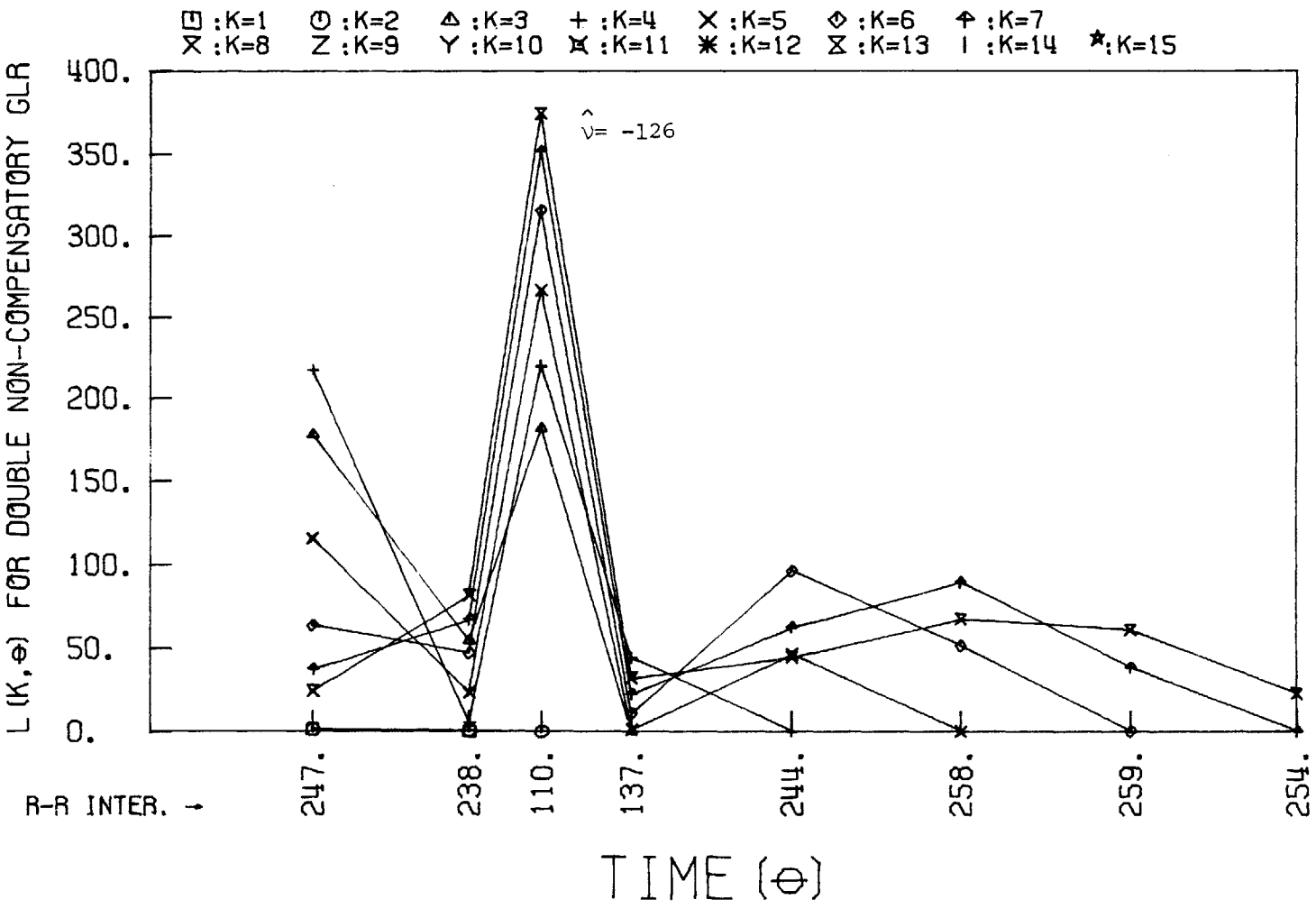

Figure 7.39 Double Non-Compensatory GLR for Data File #492-1

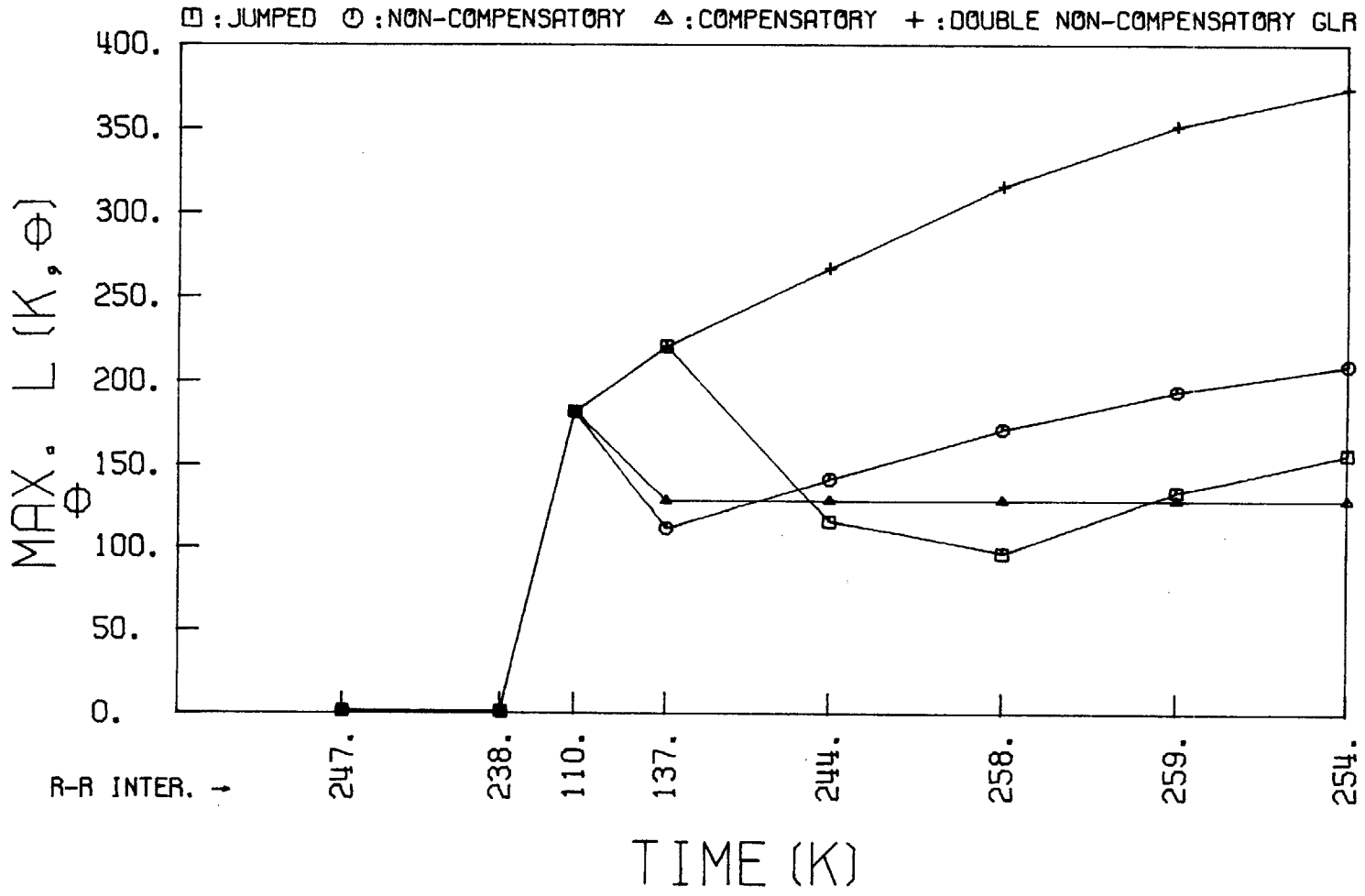

Figure 7.40 GLR Comparisons for Data File #492-1.

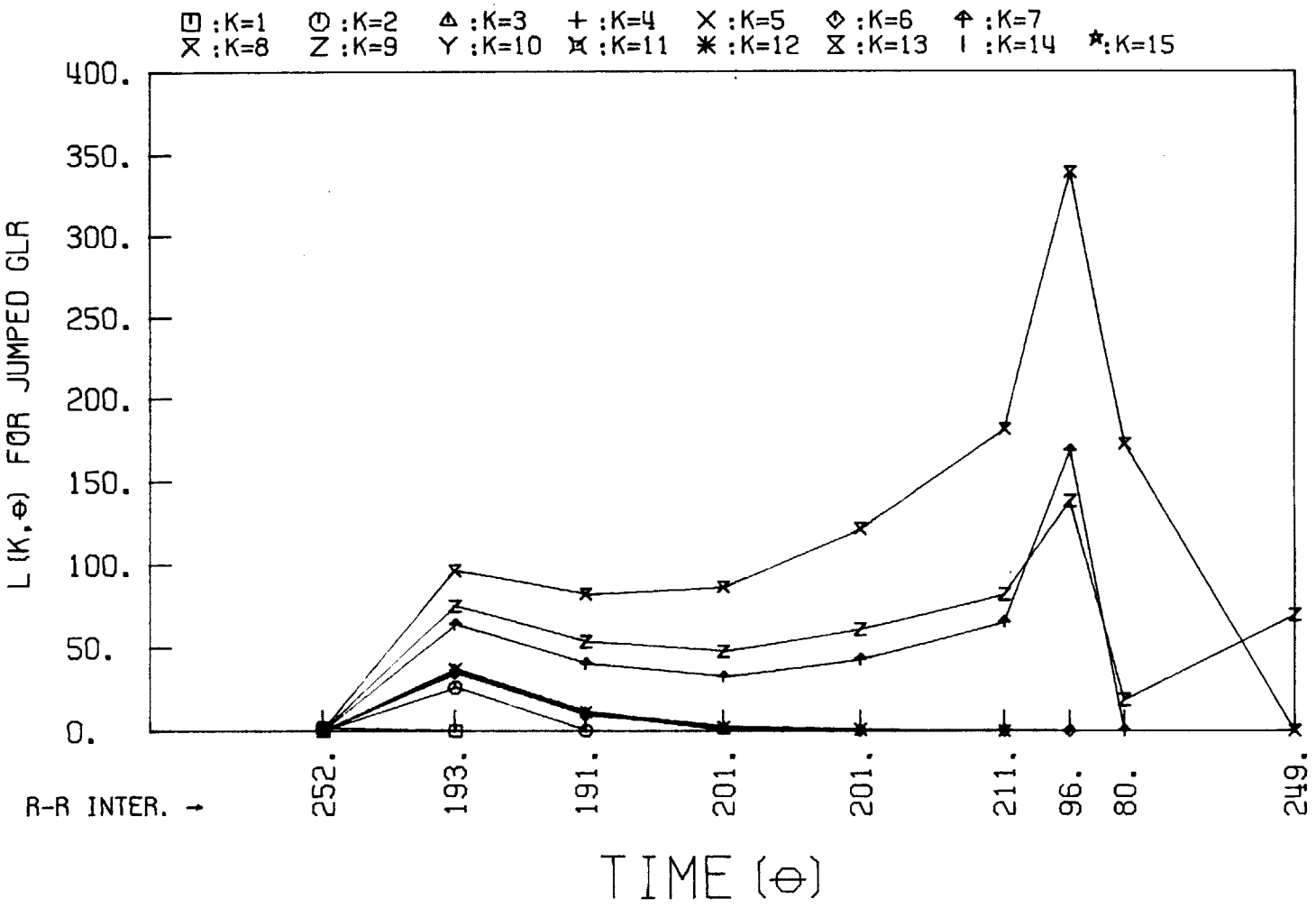

Figure 7.41 Jumped GLR for Data File #534-1

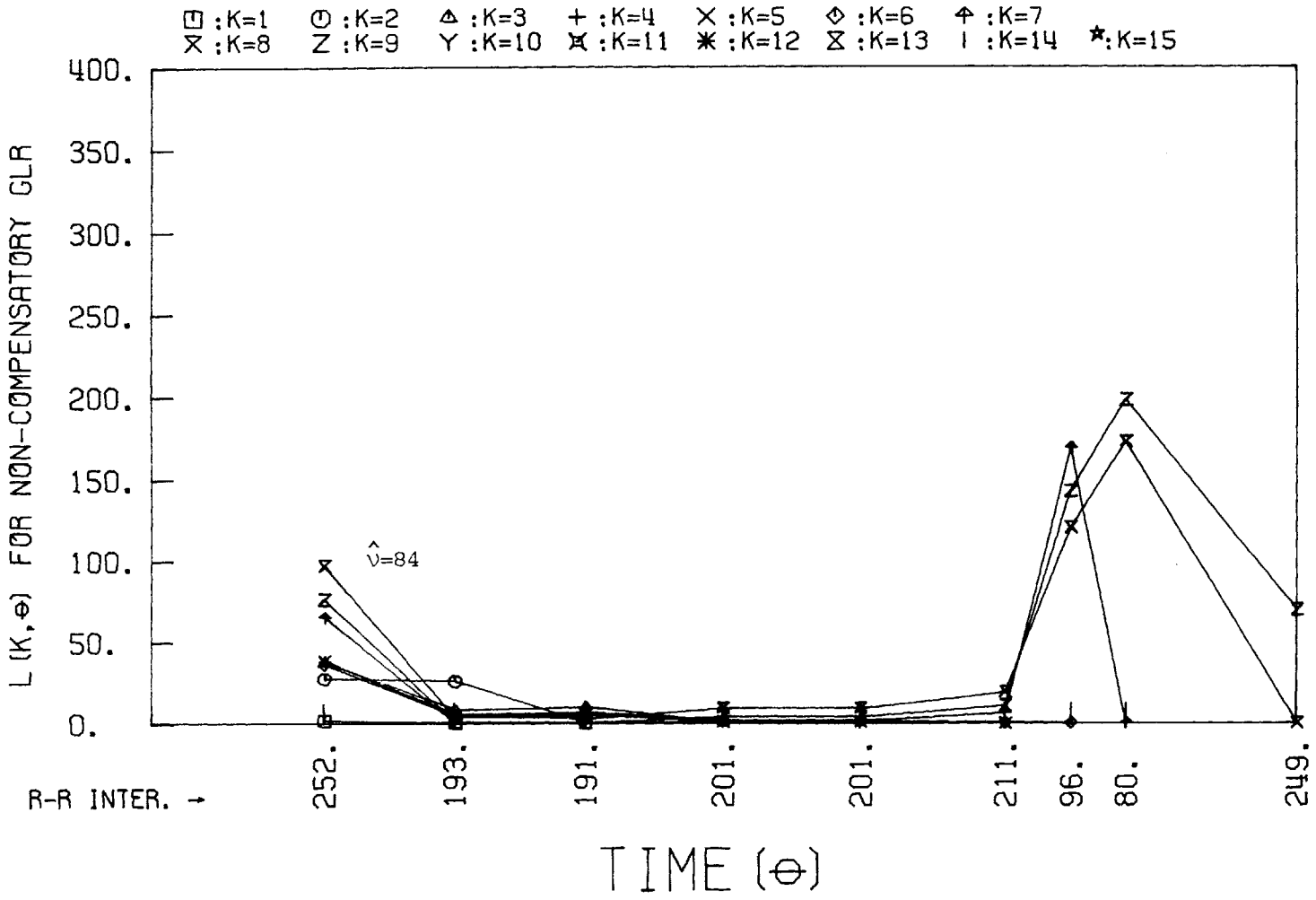

Figure 7.42 Non-Compensatory GLR for Data File #534-1

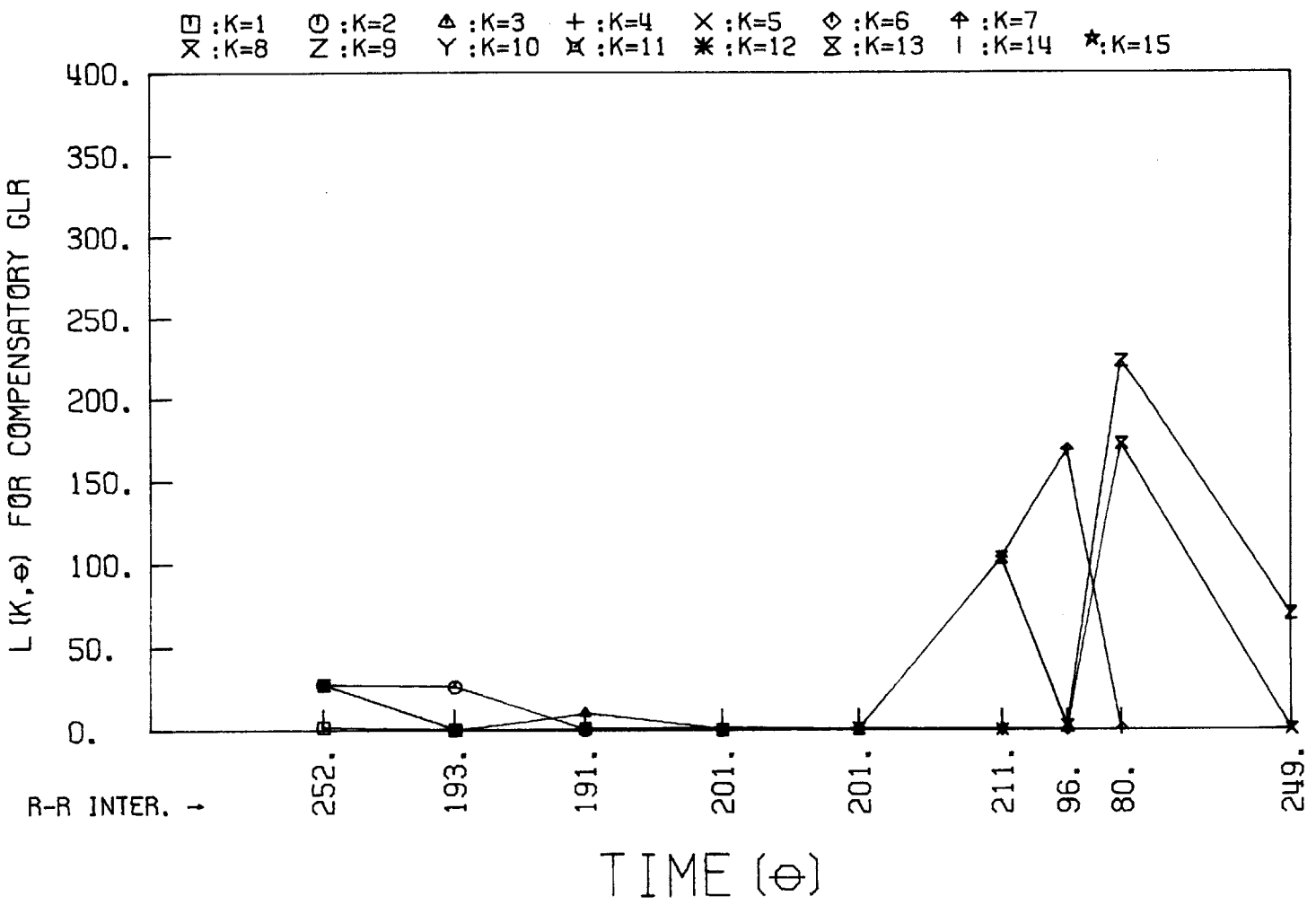

Figure 7.43 Compensatory GLR for Data File #534-1

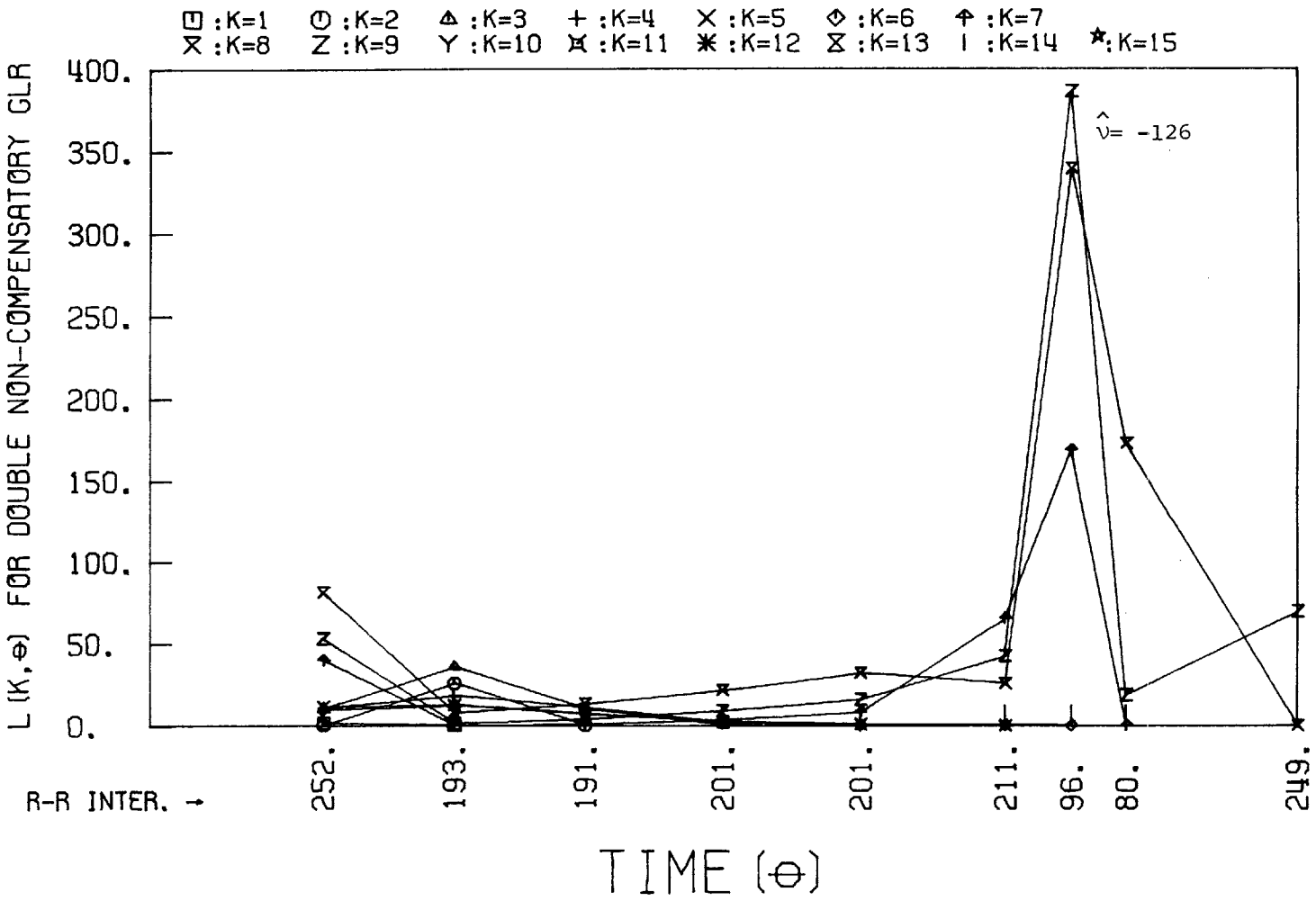

Figure 7.44 Double Non-Compensatory GLR for Data File #534-1.

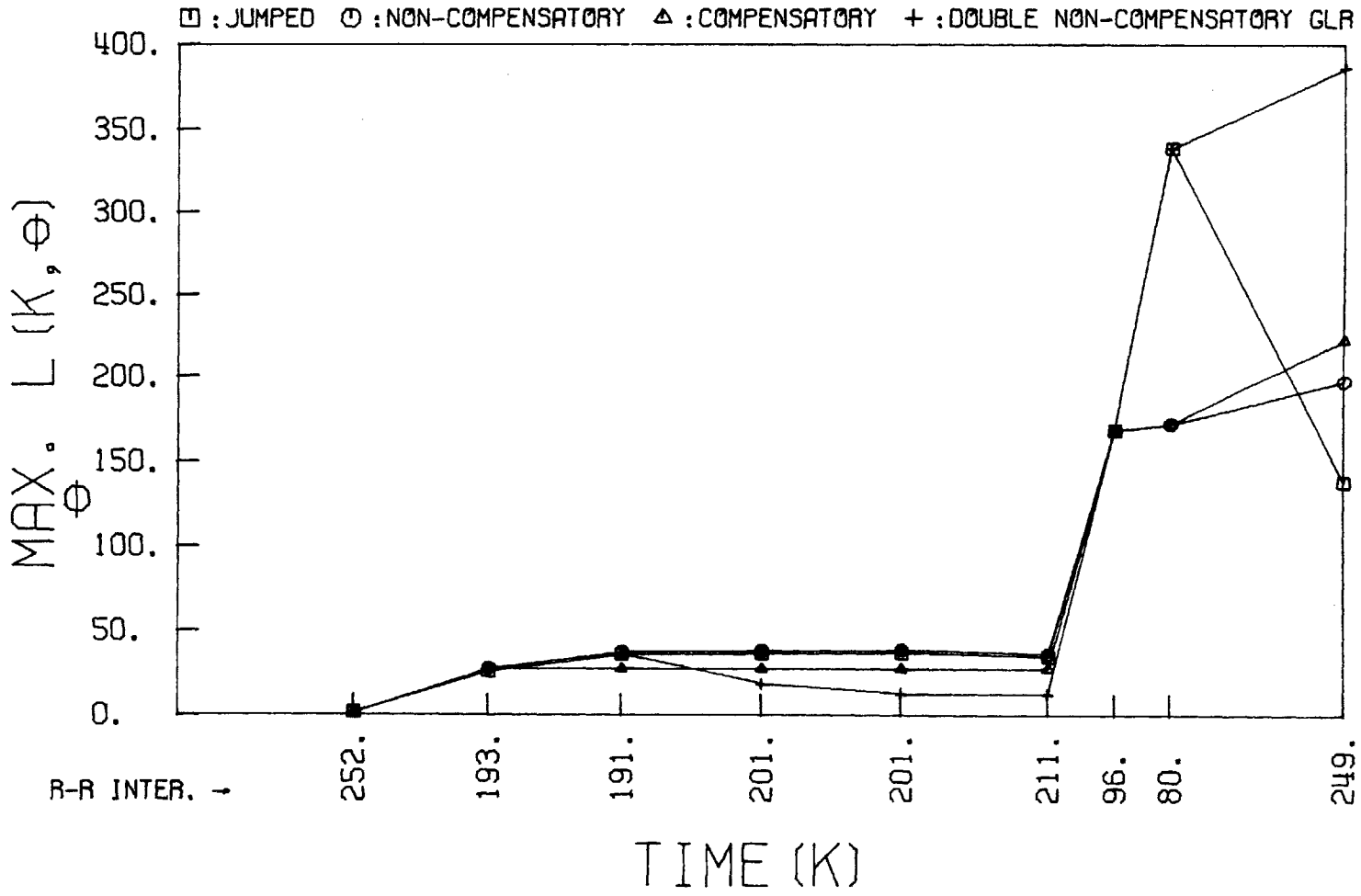

Figure 7.45 GLR Comparisons for Data File #534-1.

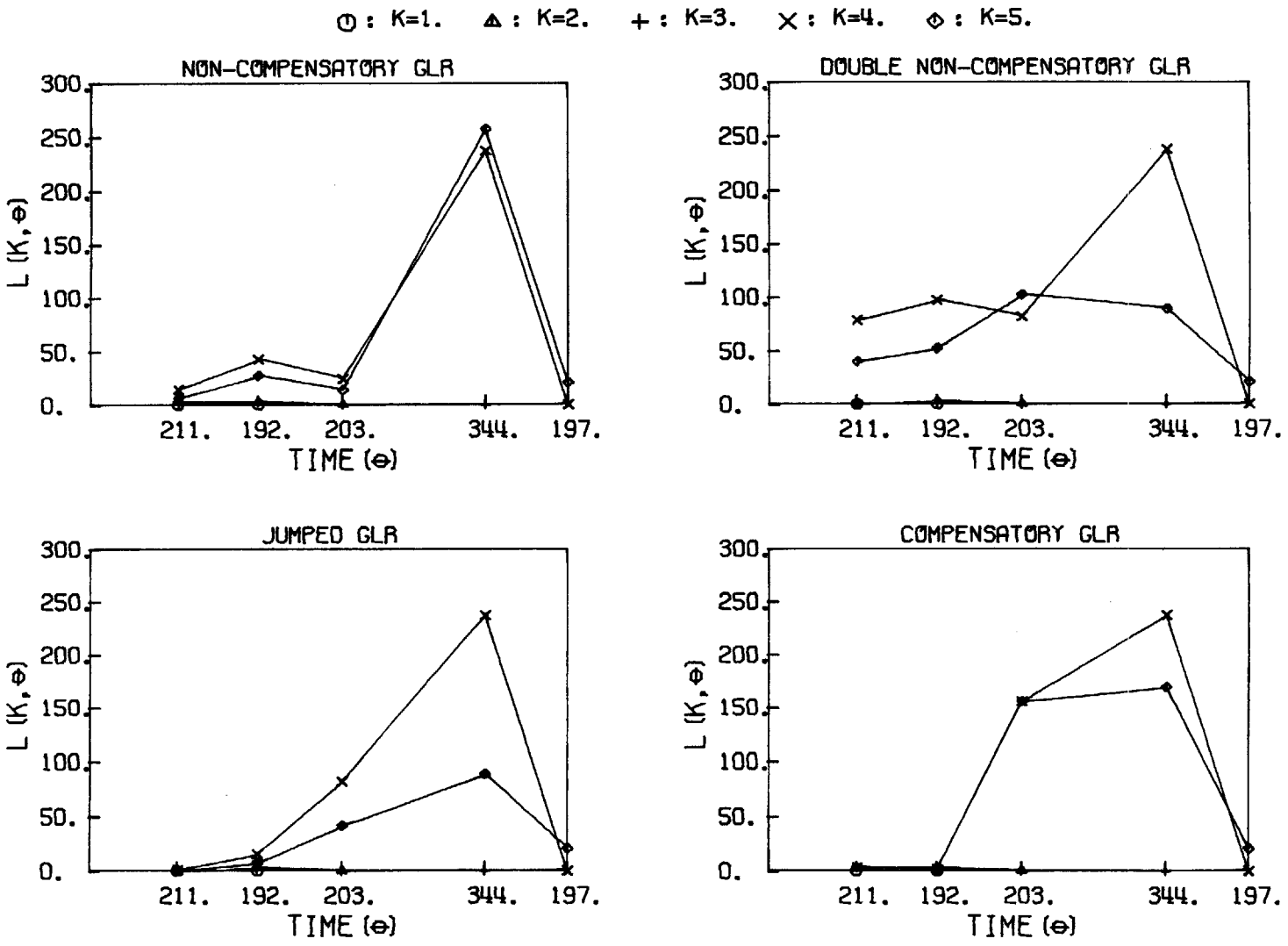

Figure 7.46 Sliding Window GLR for Data File #463, without Filter Reinitialization (T=1).

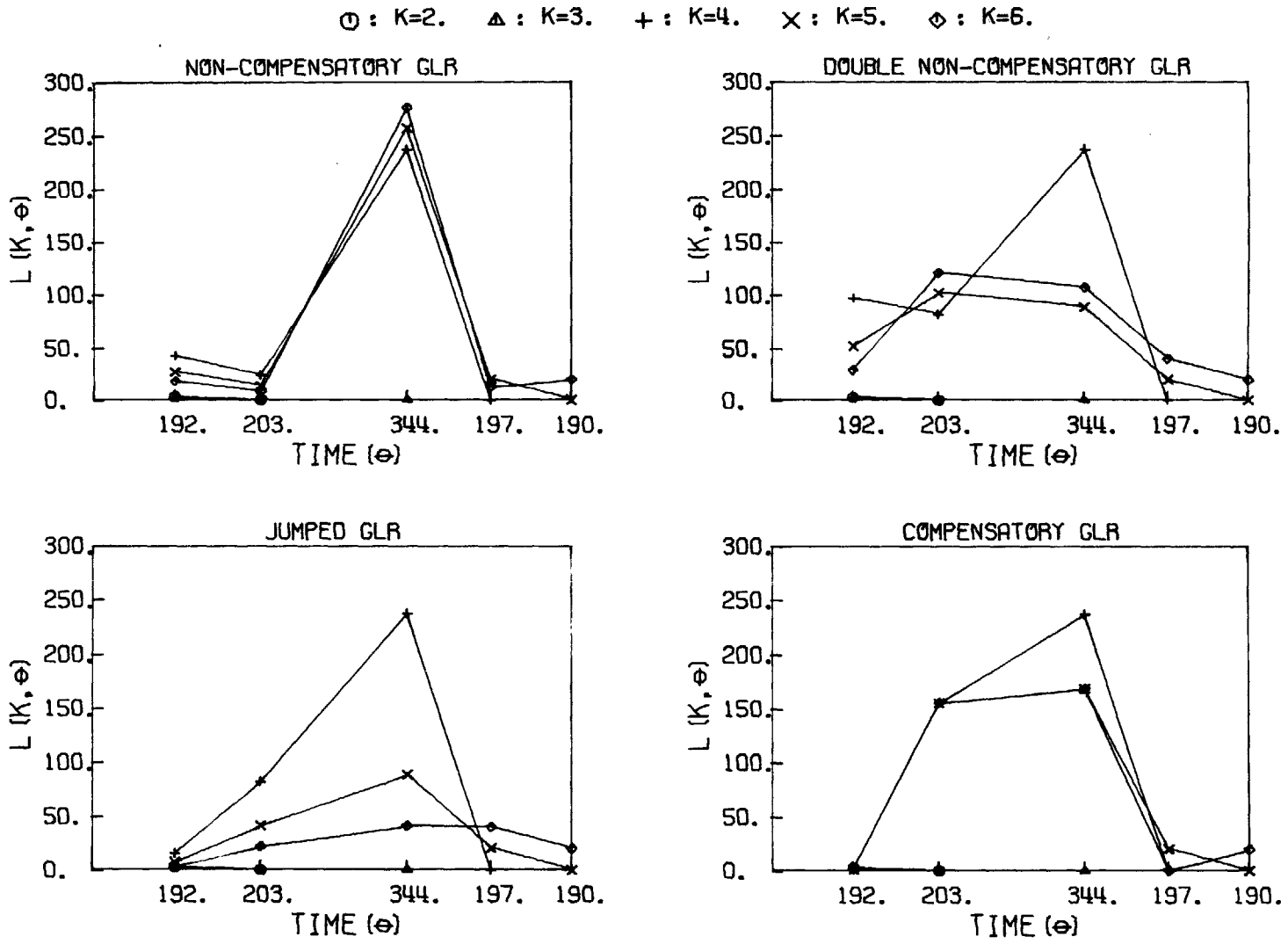

Figure 7.47 Sliding Window GLR for Data File #463, without Filter Reinitialization (T=2).

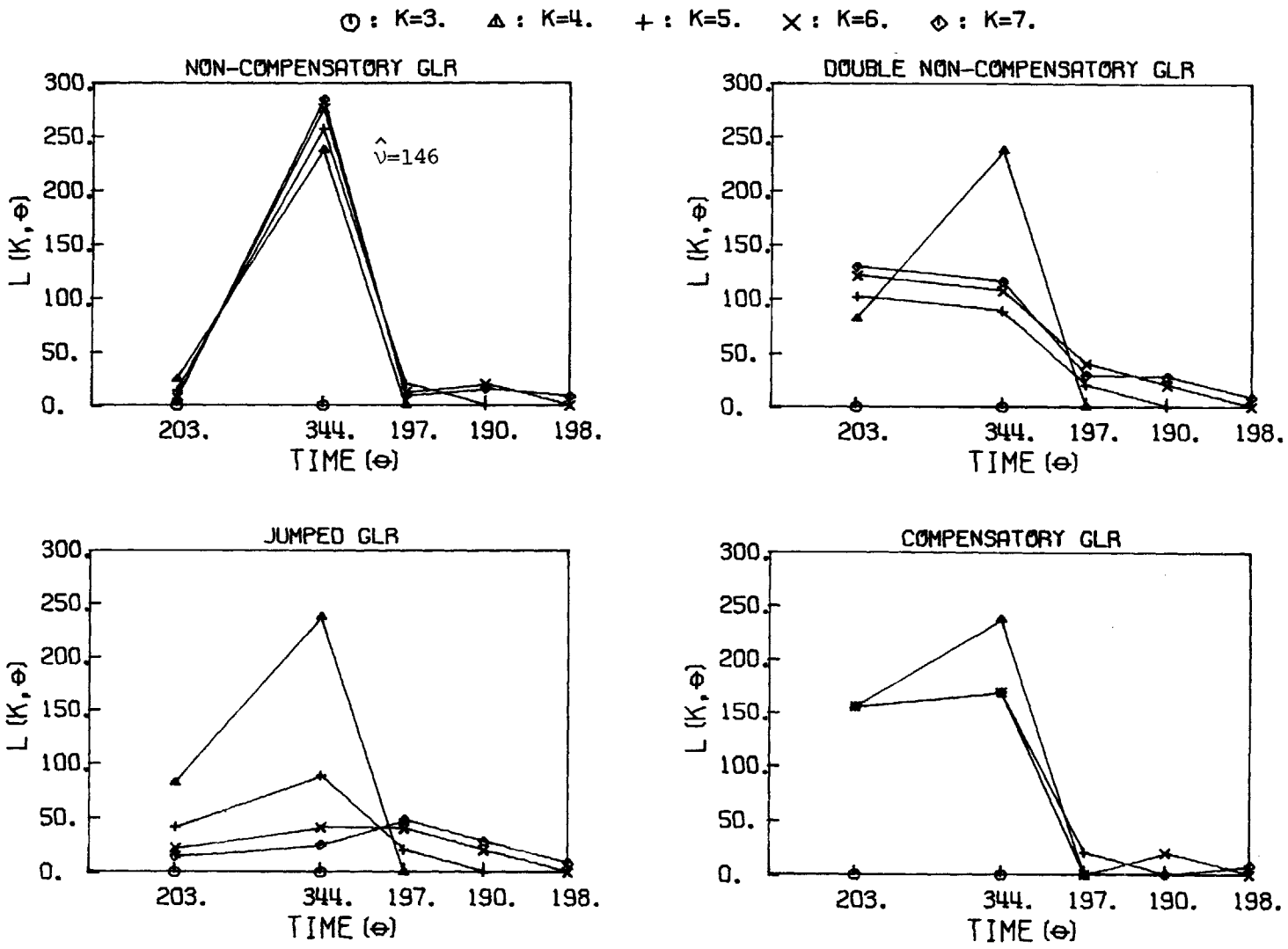

Figure 7.48 Sliding Window GLR for Data File #463, without Filter Reinitialization (T=3).

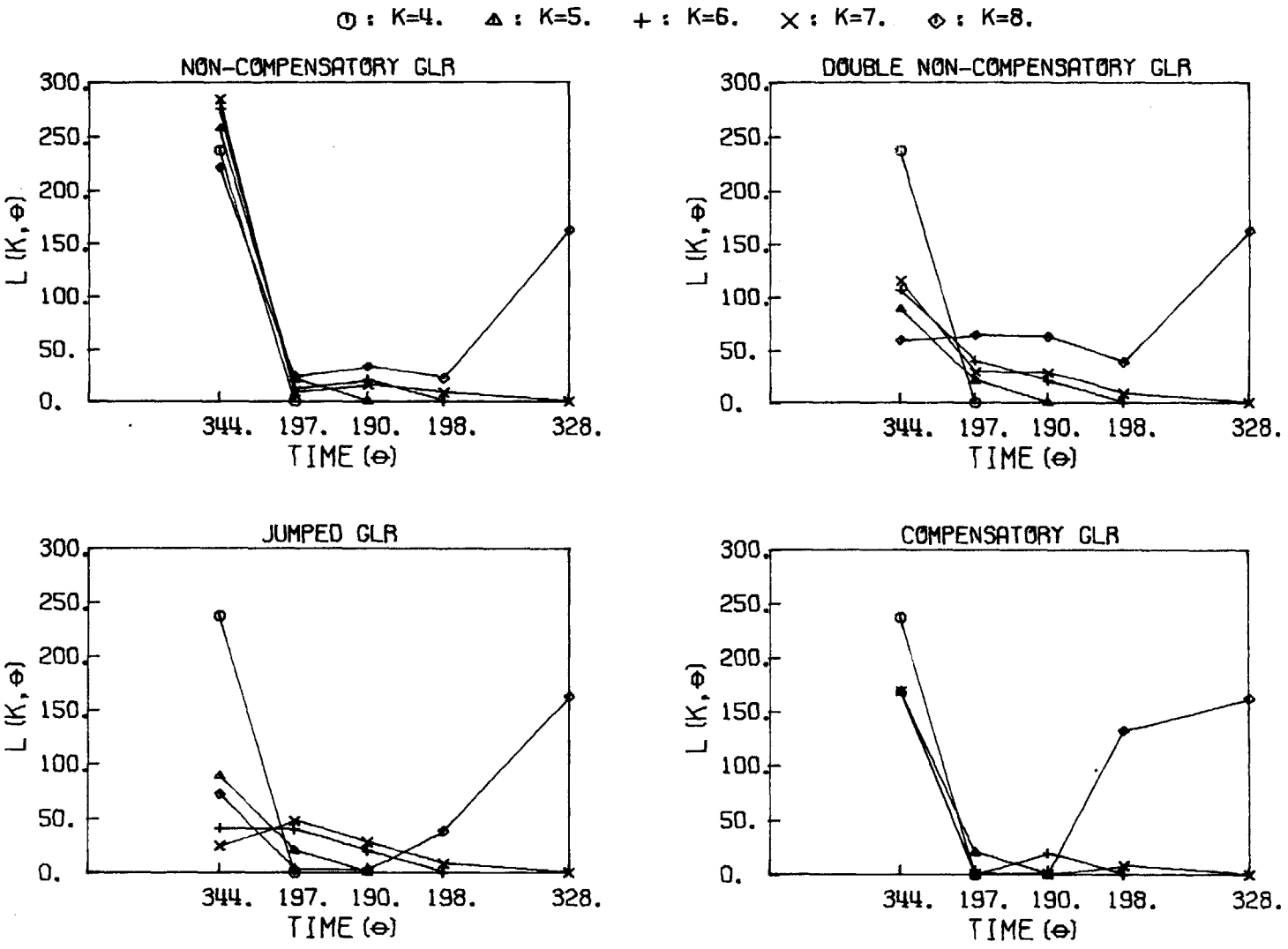

Figure 7.49 Sliding Window GLR for Data File #463, without Filter Reinitialization (T=4).

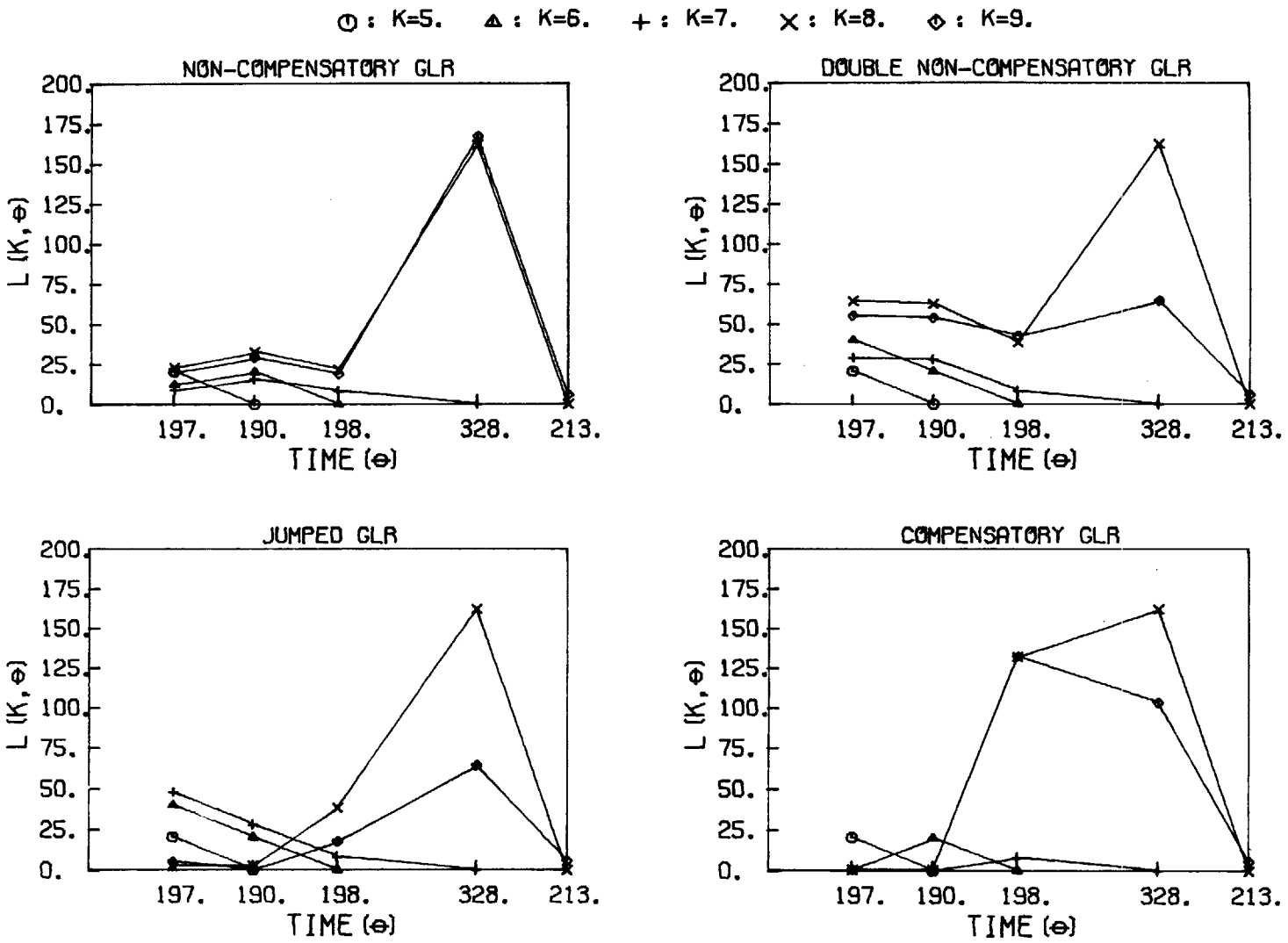

Figure 7.50 Sliding Window GLR for Data File #463, without Filter Reinitialization (T=5).

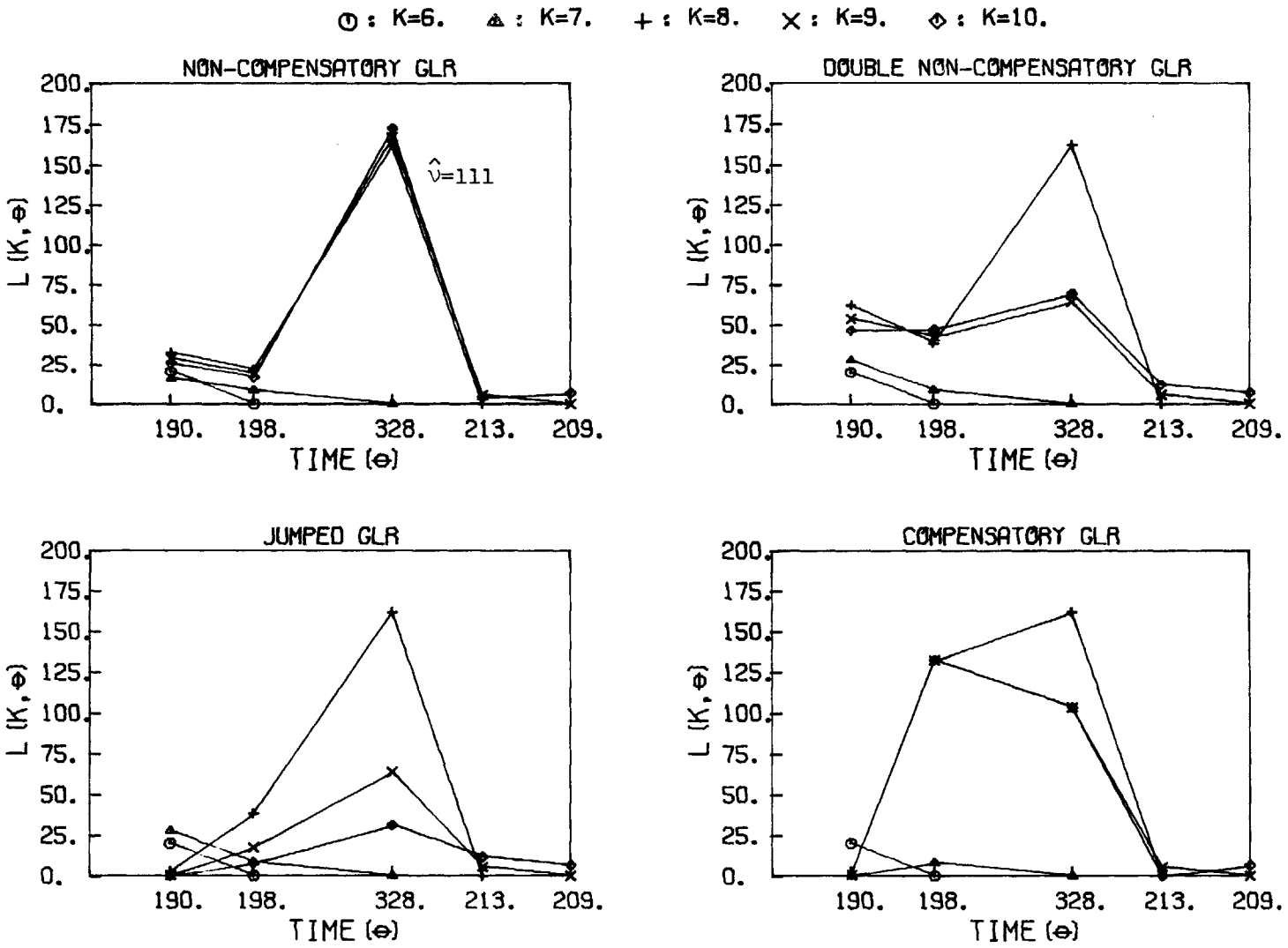

Figure 7.51 Sliding Window GLR for Data File #463, without Filter Reinitialization (T=6).

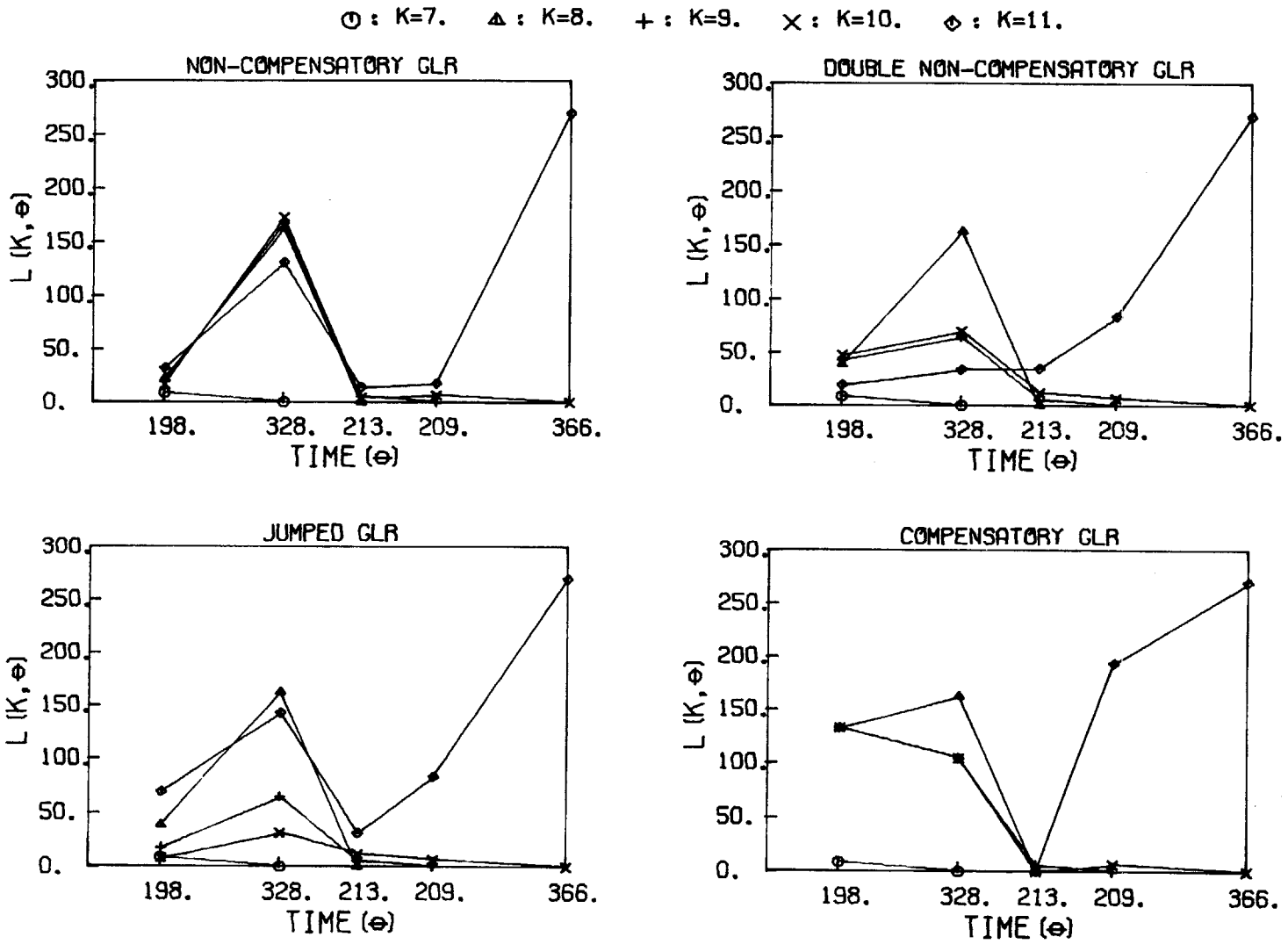

Figure 7.52 Sliding Window GLR for Data File #463, without Filter Reinitialization (T=7).

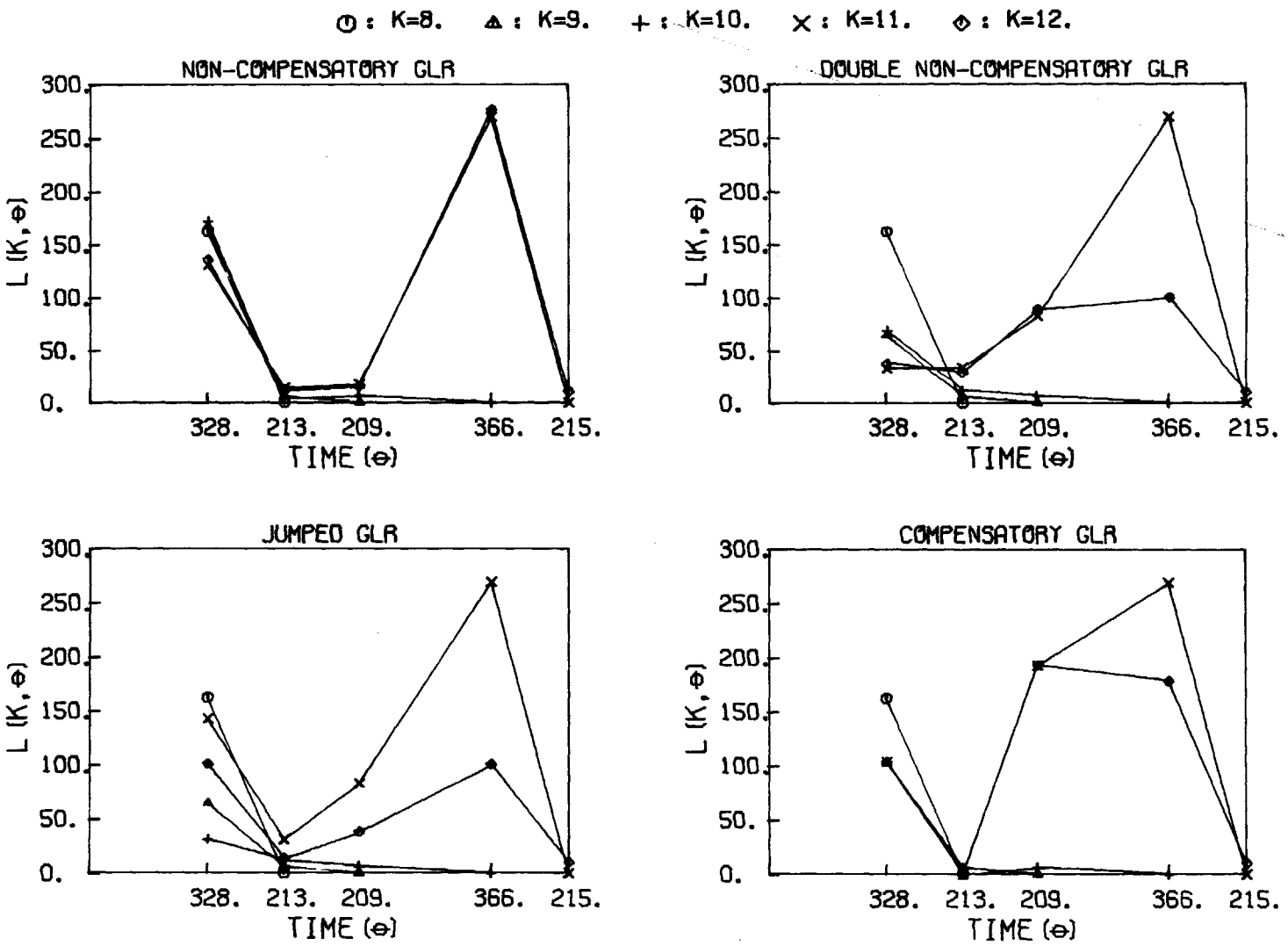

Figure 7.53 Sliding Window GLR for Data File #463, without Filter Reinitialization (T=8).

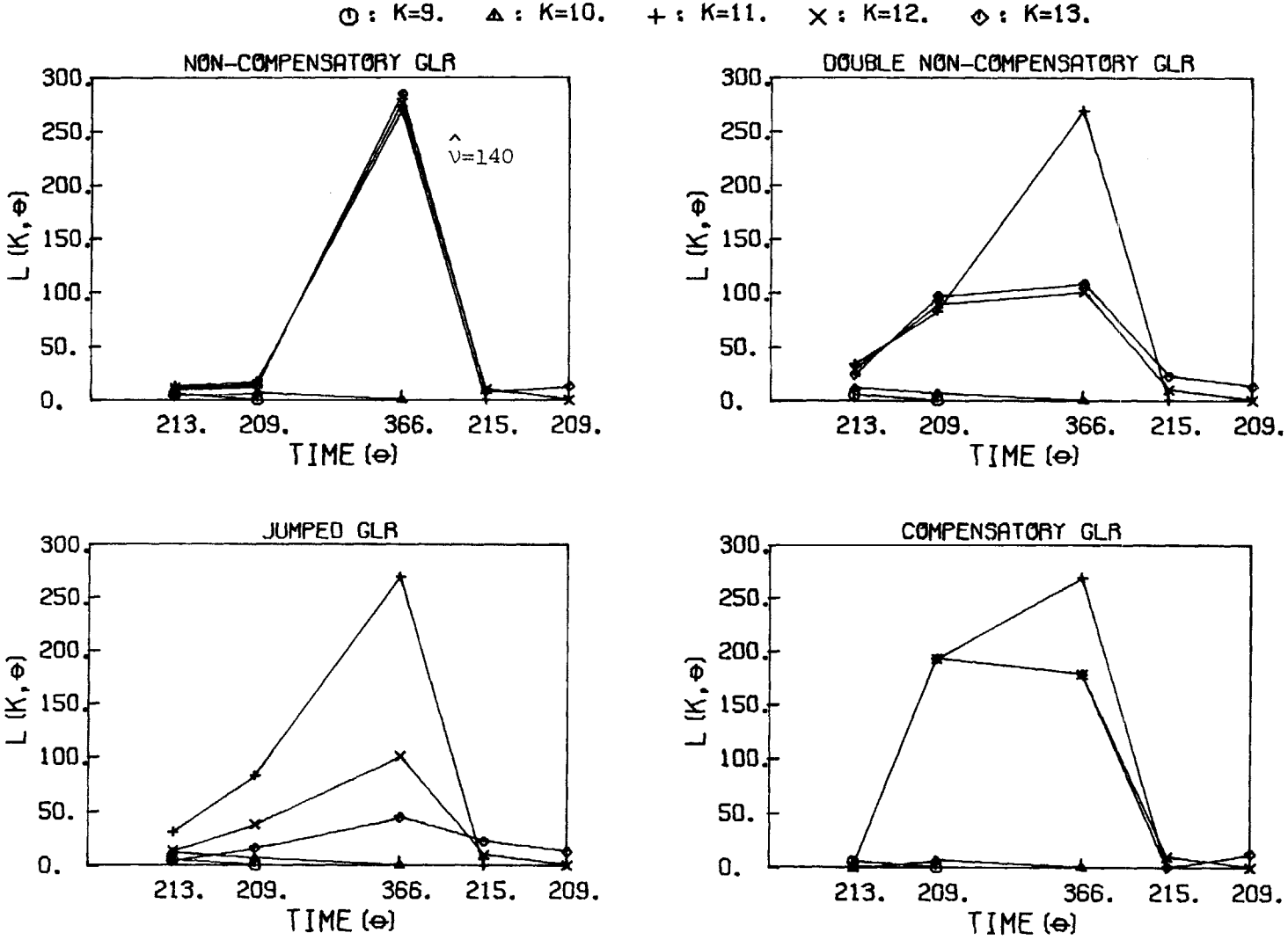

Figure 7.54 Sliding Window GLR for Data File #463, without Filter Reinitialization (T=9).

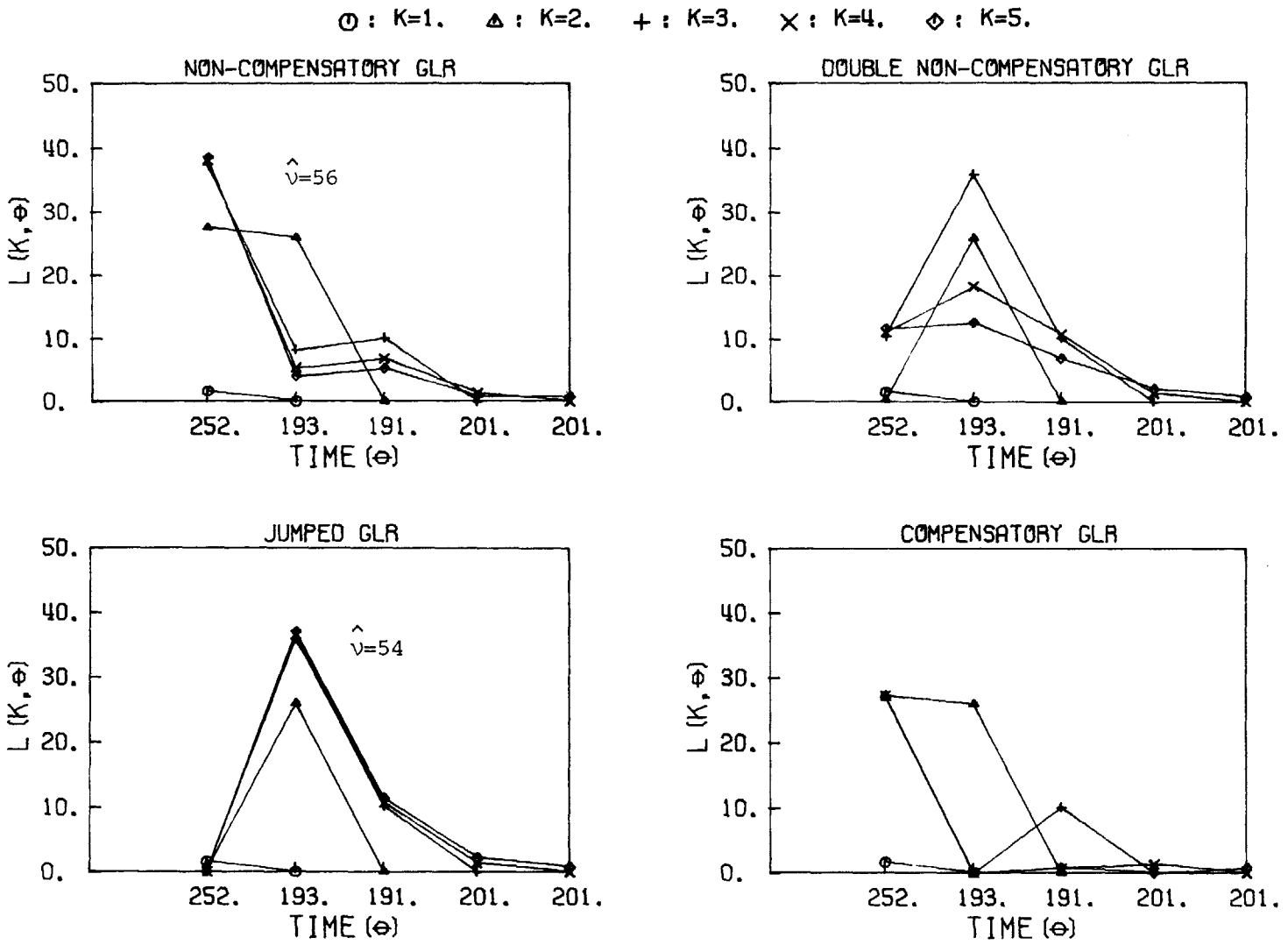

Figure 7.55 Sliding Window GLR for Data File #534-1, without Filter Reinitialization (T=1).

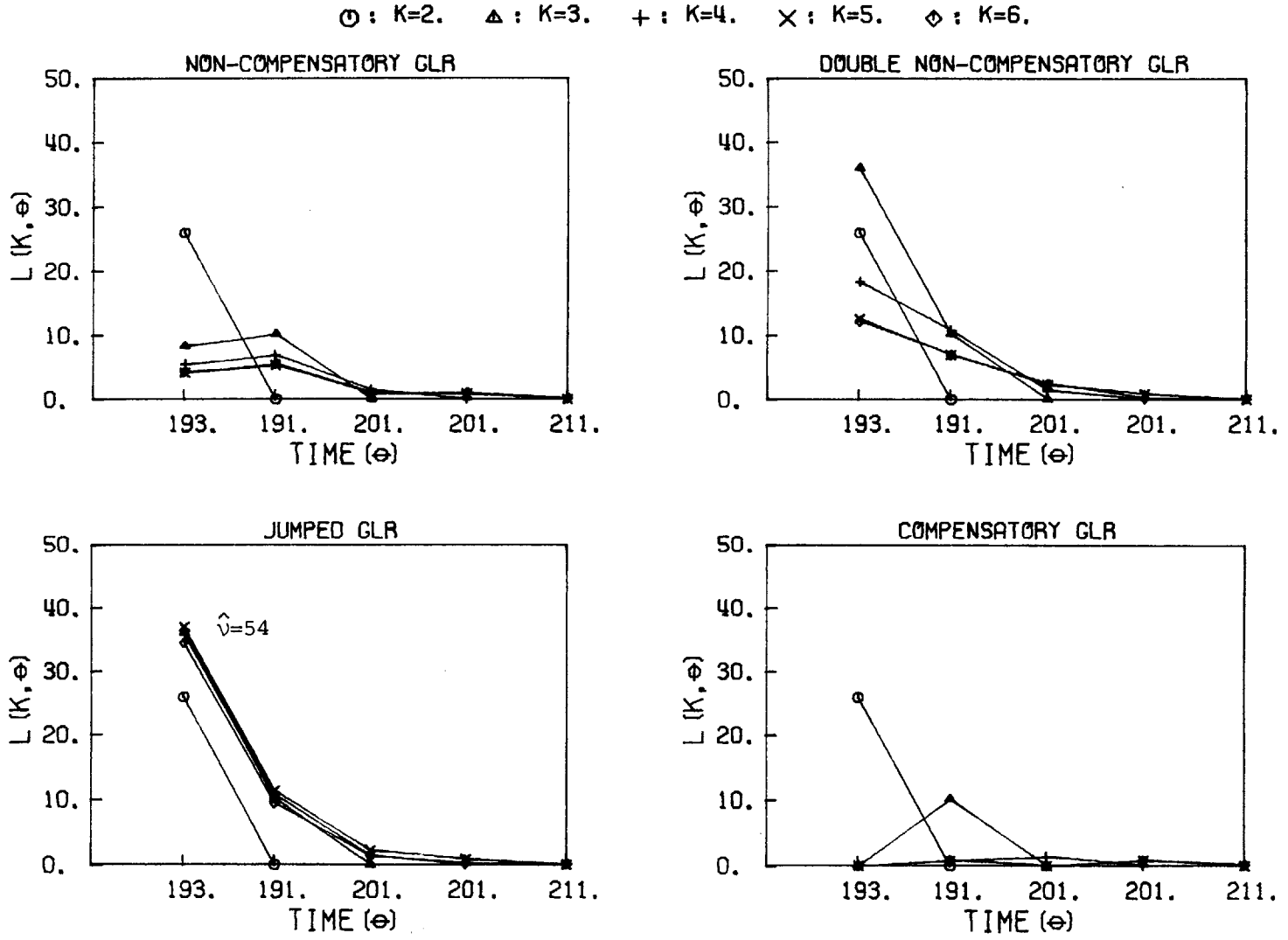

Figure 7.56 Sliding Window GLR for Data File #534-1, without Filter Reinitialization (T=2).

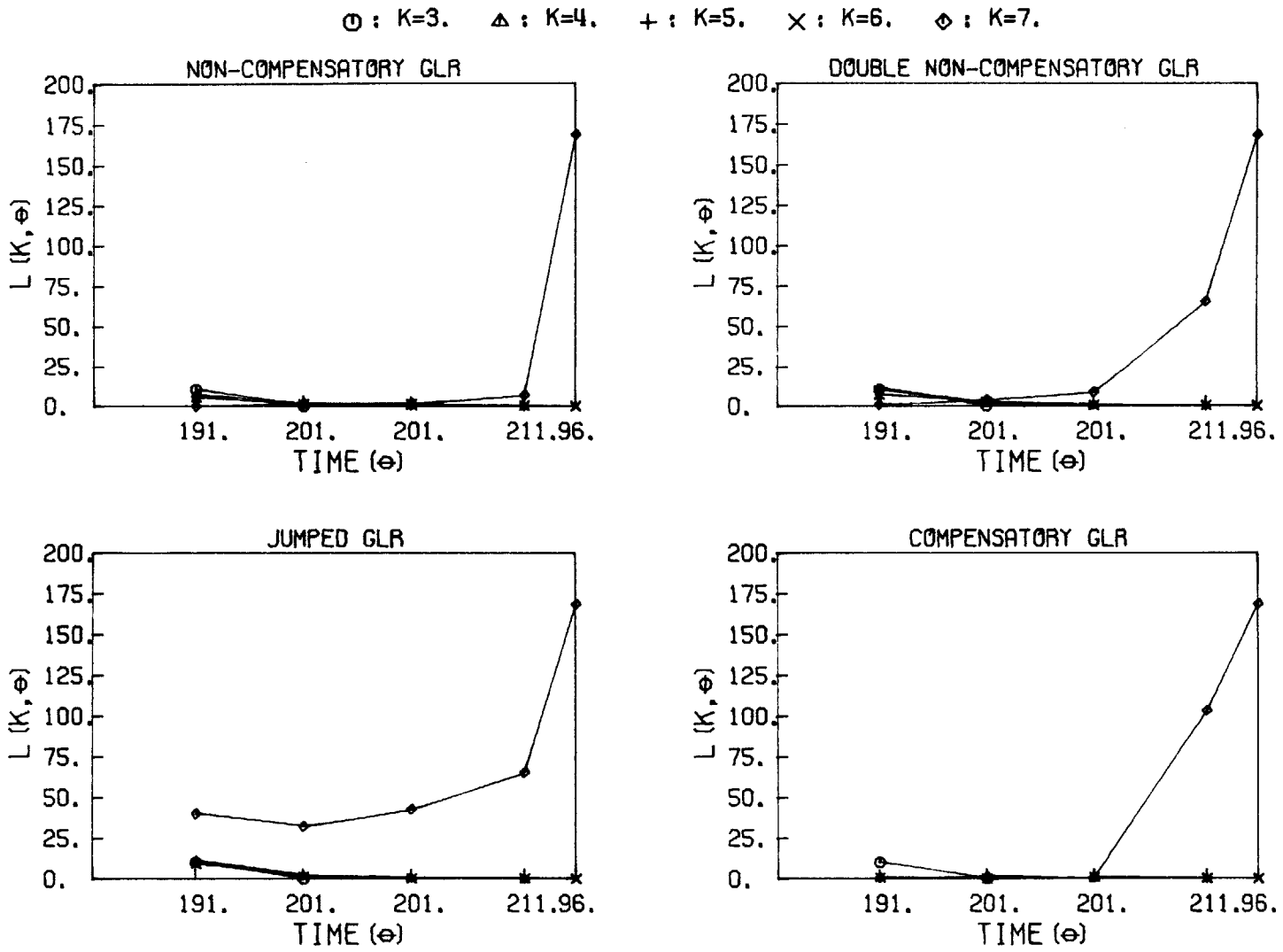

Figure 7.57 Sliding Window GLR for Data File #534-1,without Filter Reinitialization (T=3).

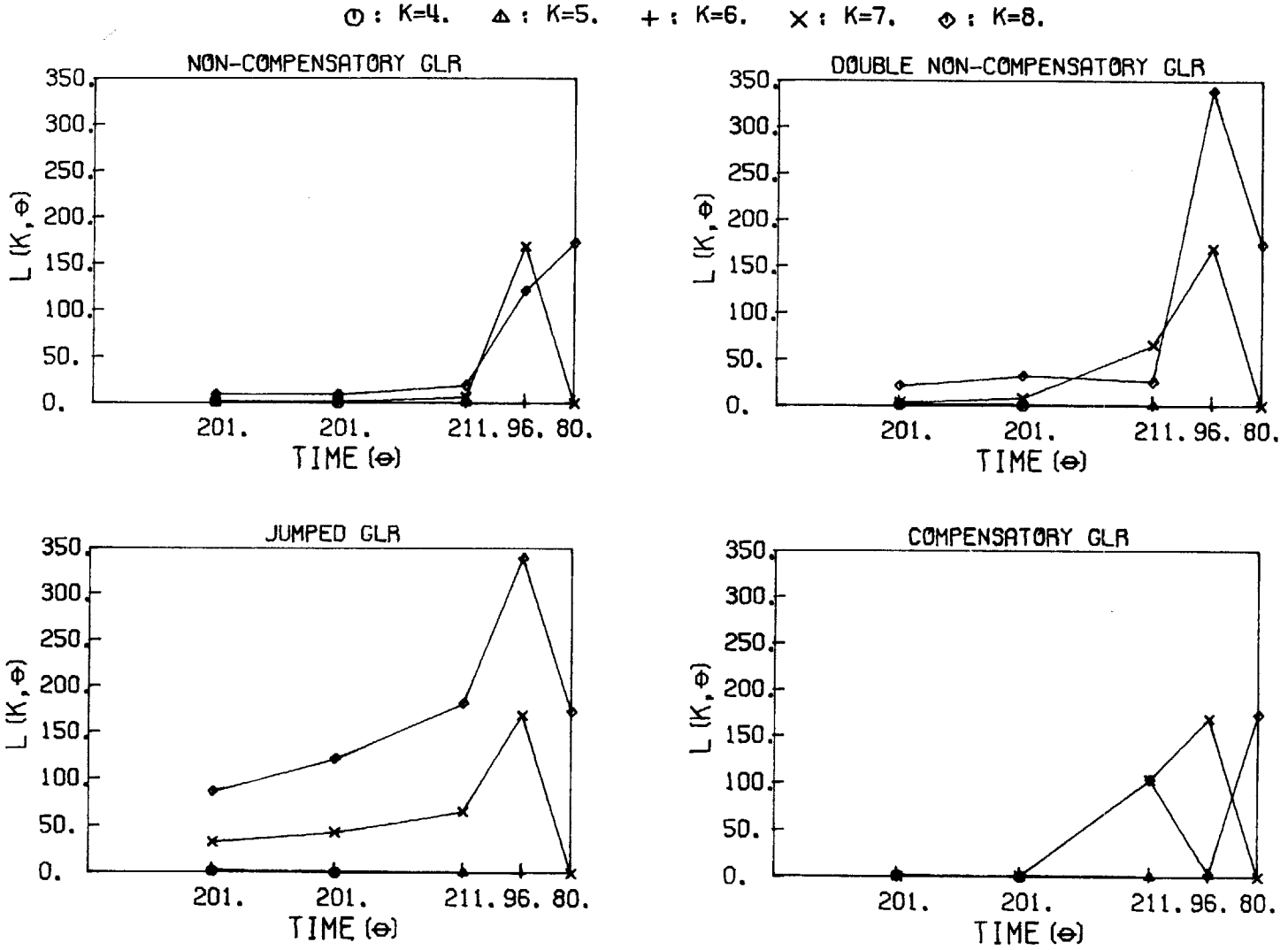

Figure 7.58 Sliding Window GLR for Data File #534-1, without Filter Reinitialization (T=4).

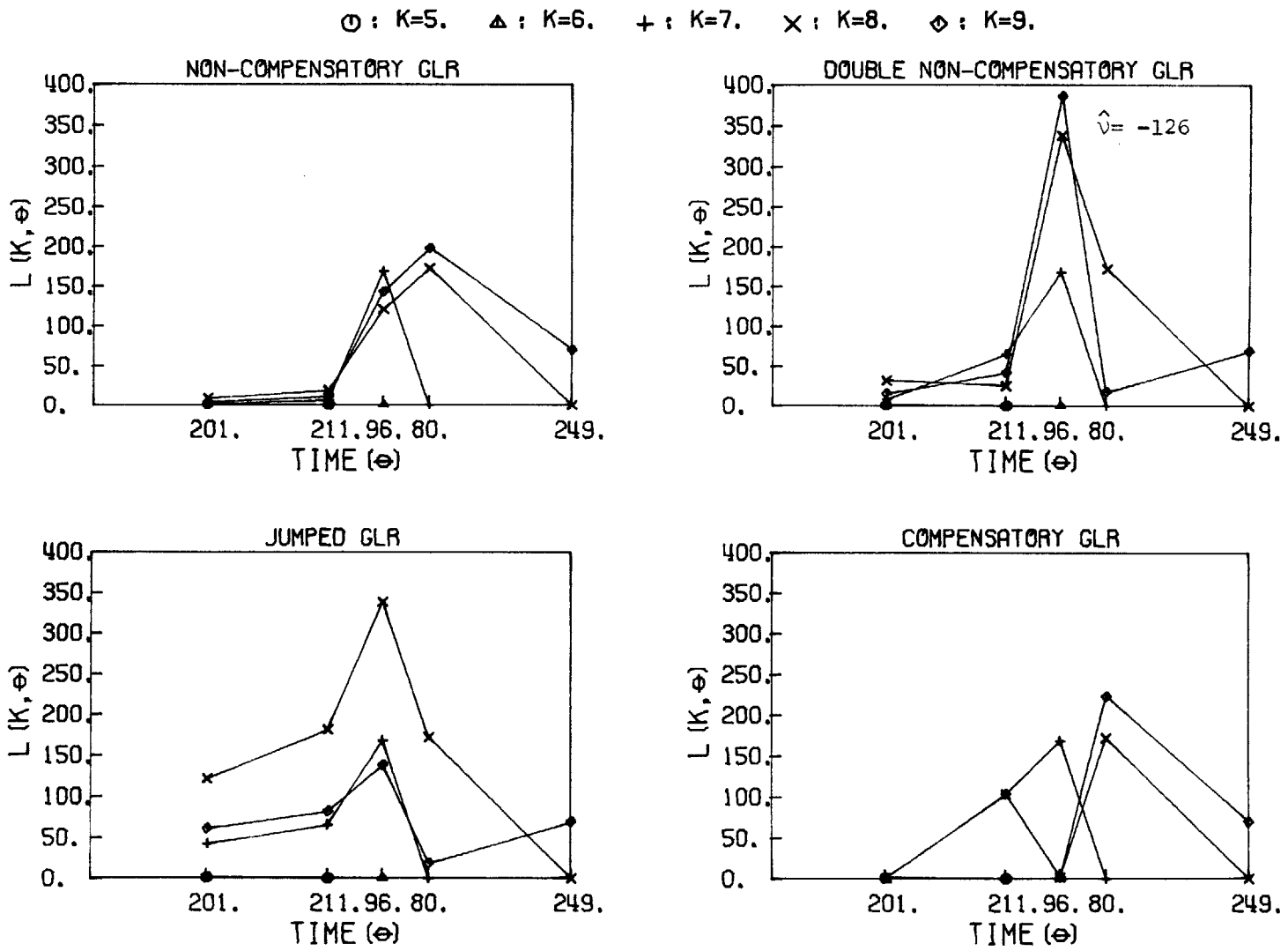

Figure 7.59 Sliding Window GLR for Data File #534-1, without Filter Reinitialization (T=5).

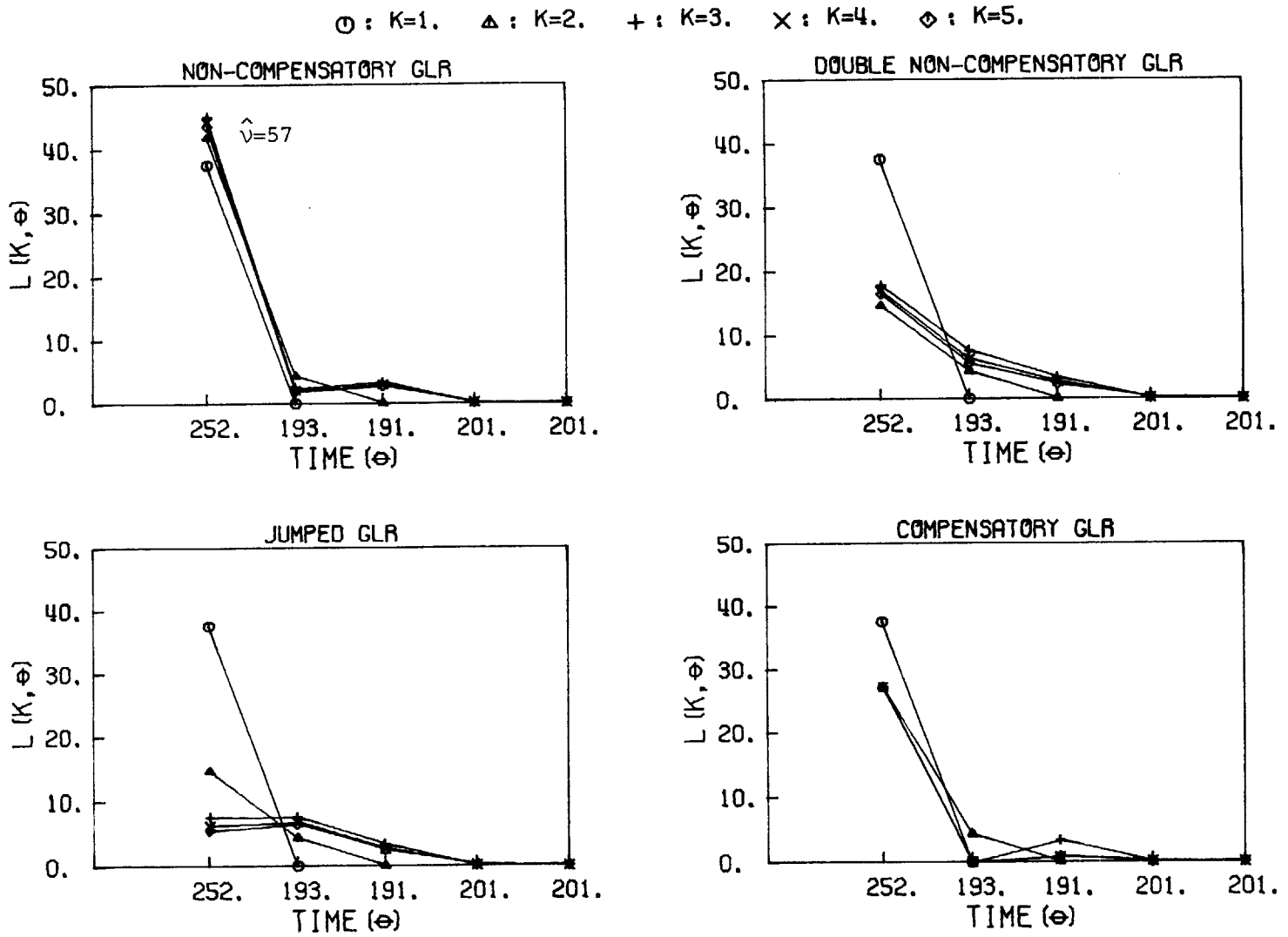

Figure 7.60 Sliding Window GLR for Data File #534-1, with Filter Reinitialized at P_o=32, x_o=192 (T=1).

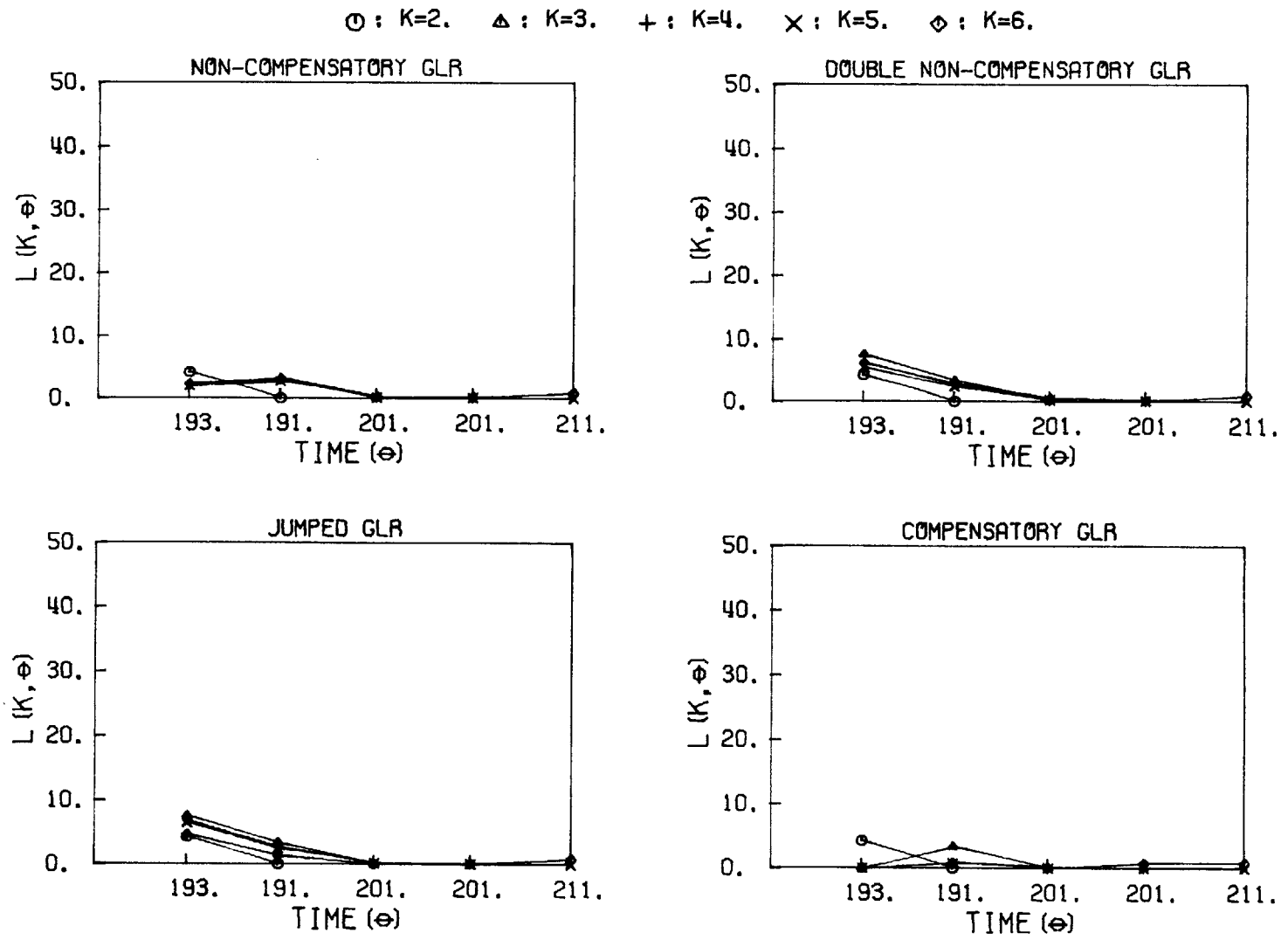

Figure 7.61 Sliding Window GLR for Data File #534-1, with Filter Reinitialized at P_o=32, x_o=192 (T=2).

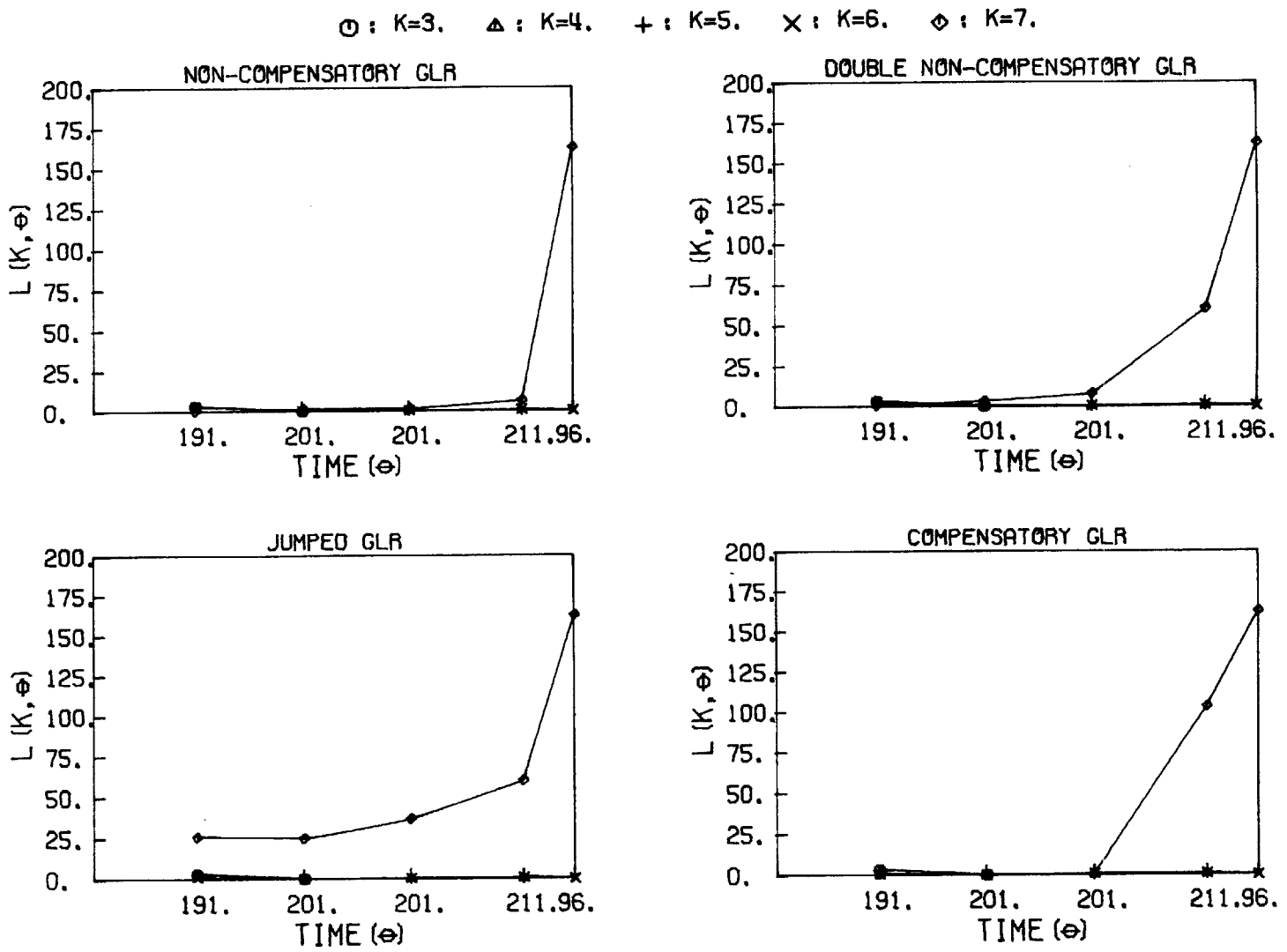

Figure 7.62 Sliding Window GLR for Data File #534-1, with Filter Reinitialized at P_o=32, x_o=192 (T=3).

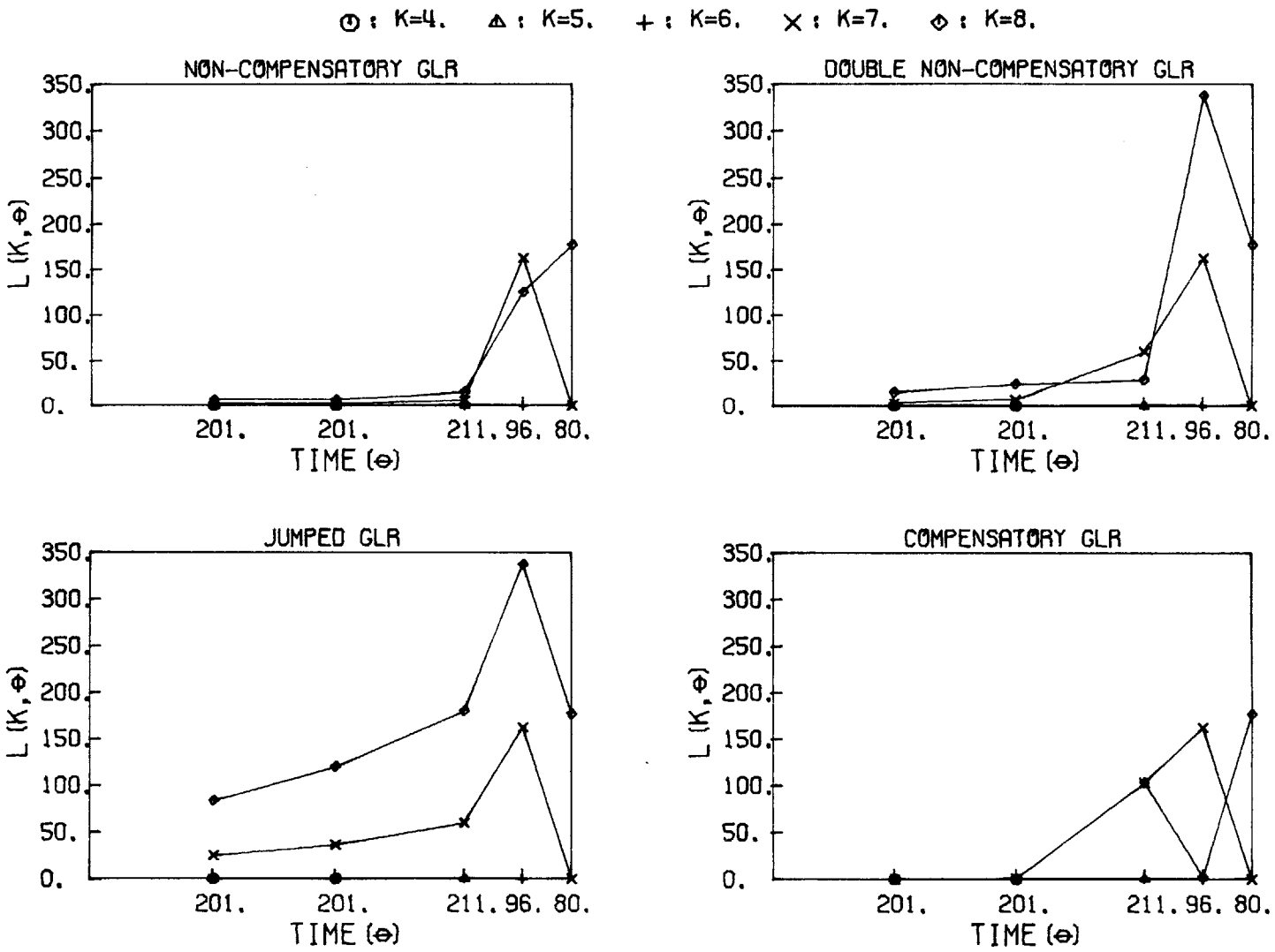

Figure 7.63 Sliding Window GLR for Data File #534-1, with Filter Reinitialized at P_o=32, x_o=192 (T=4).

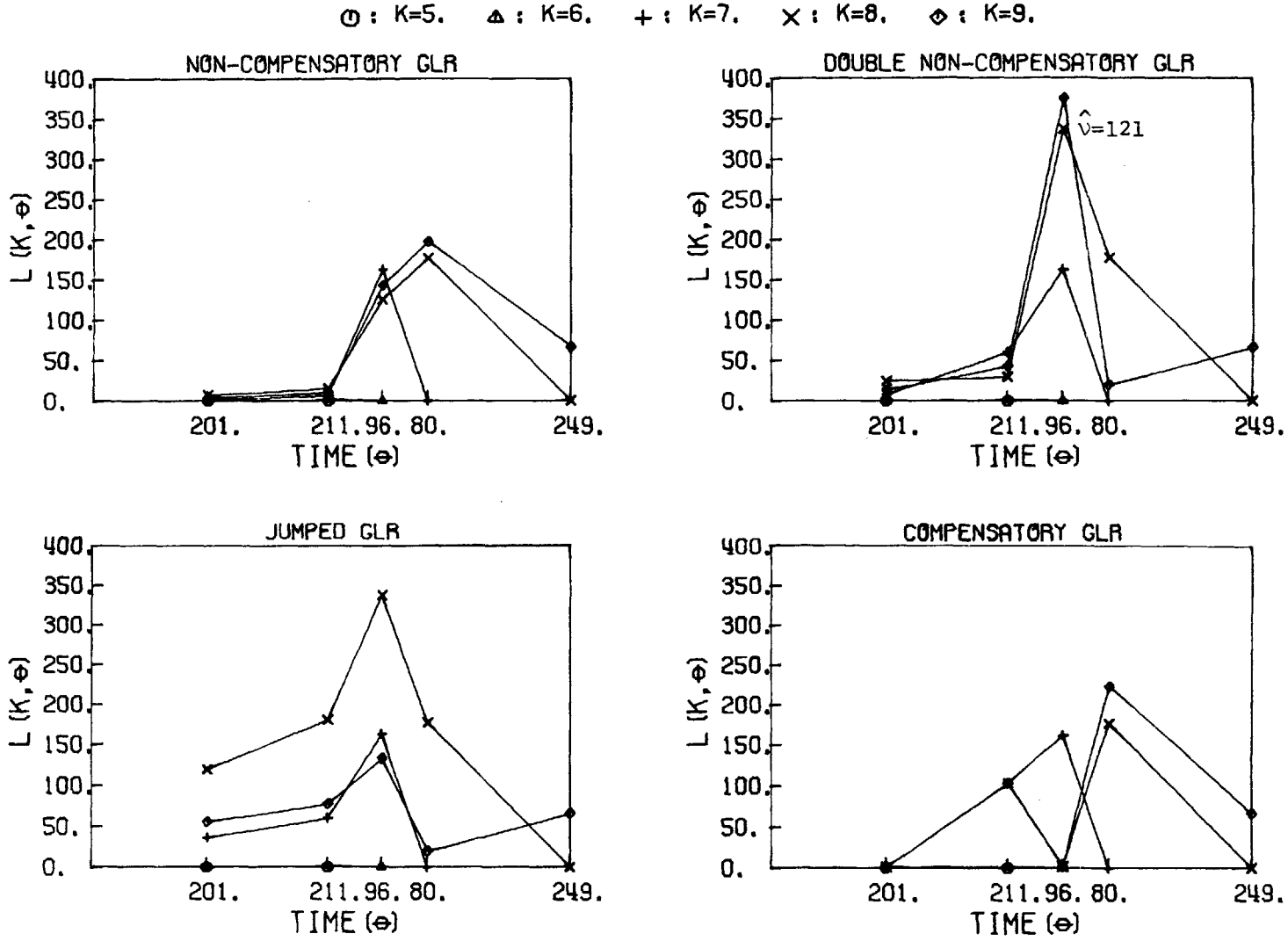

Figure 7.64 Sliding Window GLR for Data File #534-1, with Filter Reinitialized at P_o=32, x_o=192 (T=5).

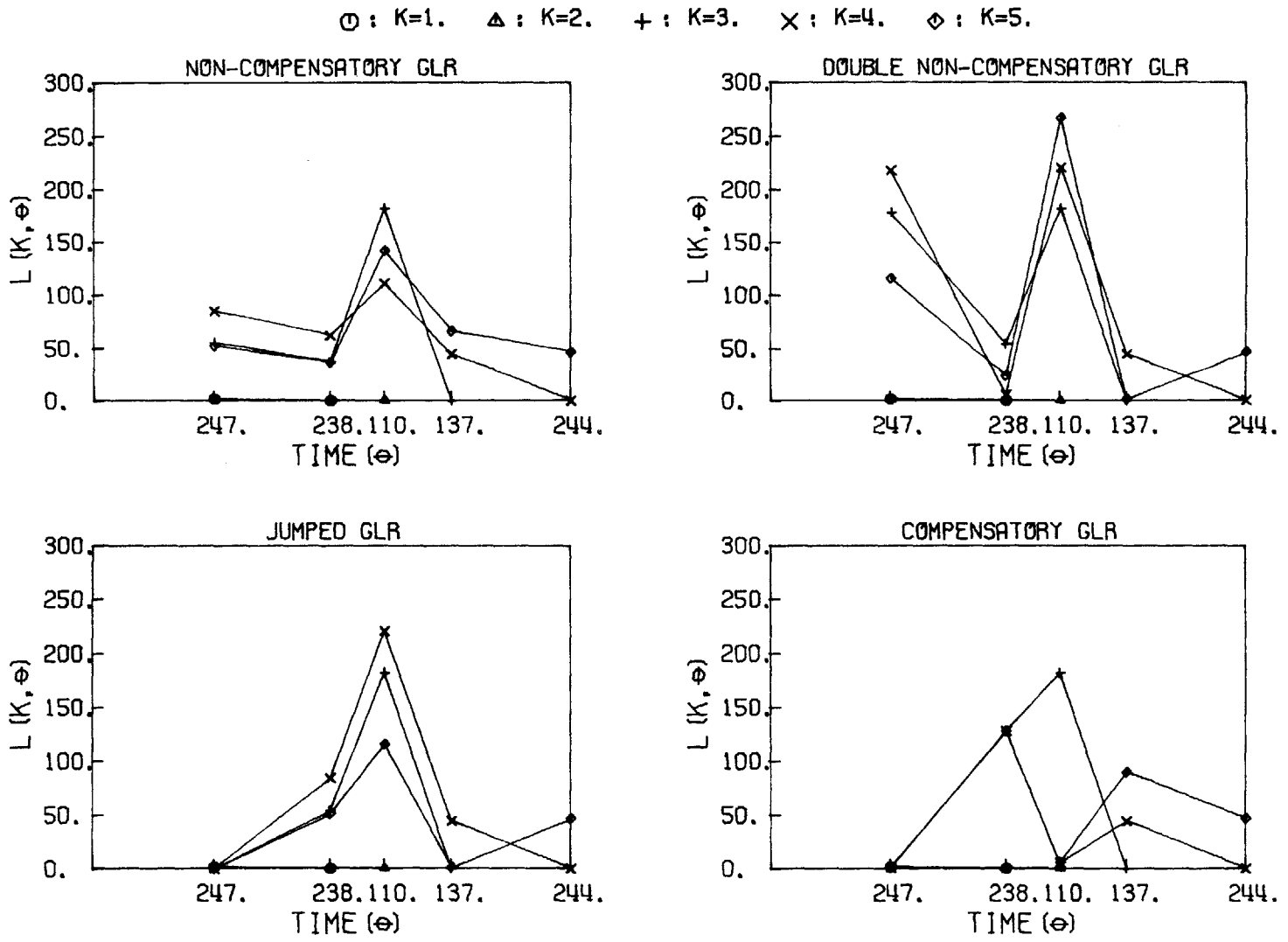

Figure 7.65 Sliding Window GLR for Data File #492-1, without Filter Reinitialization (T=1).

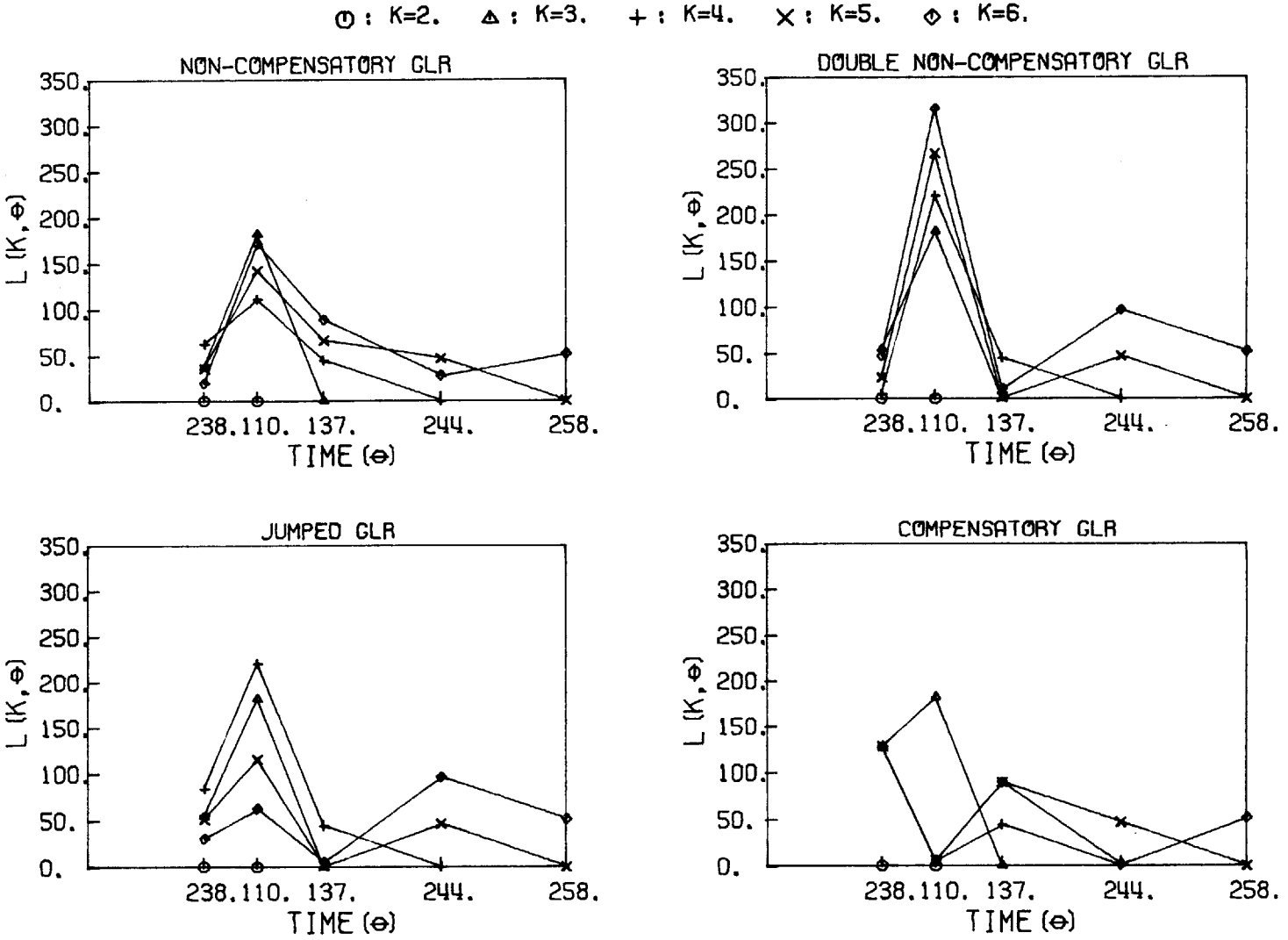

Figure 7.66 Sliding Window GLR for Data File #492-1, without Filter Reinitialization (T=2).

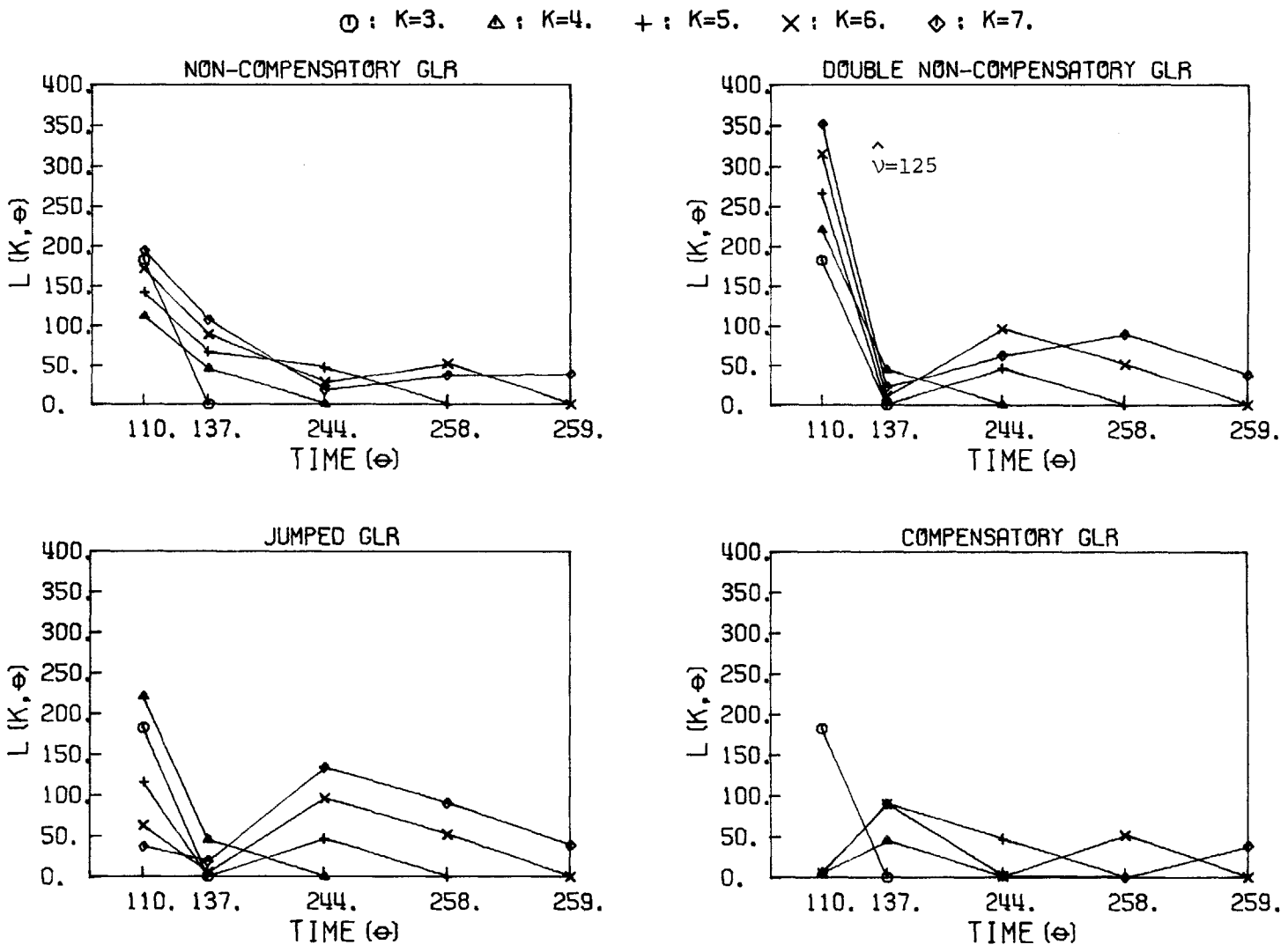

Figure 7.67 Sliding Window GLR for Data File #492-1, without Filter Reinitialization (T=3).

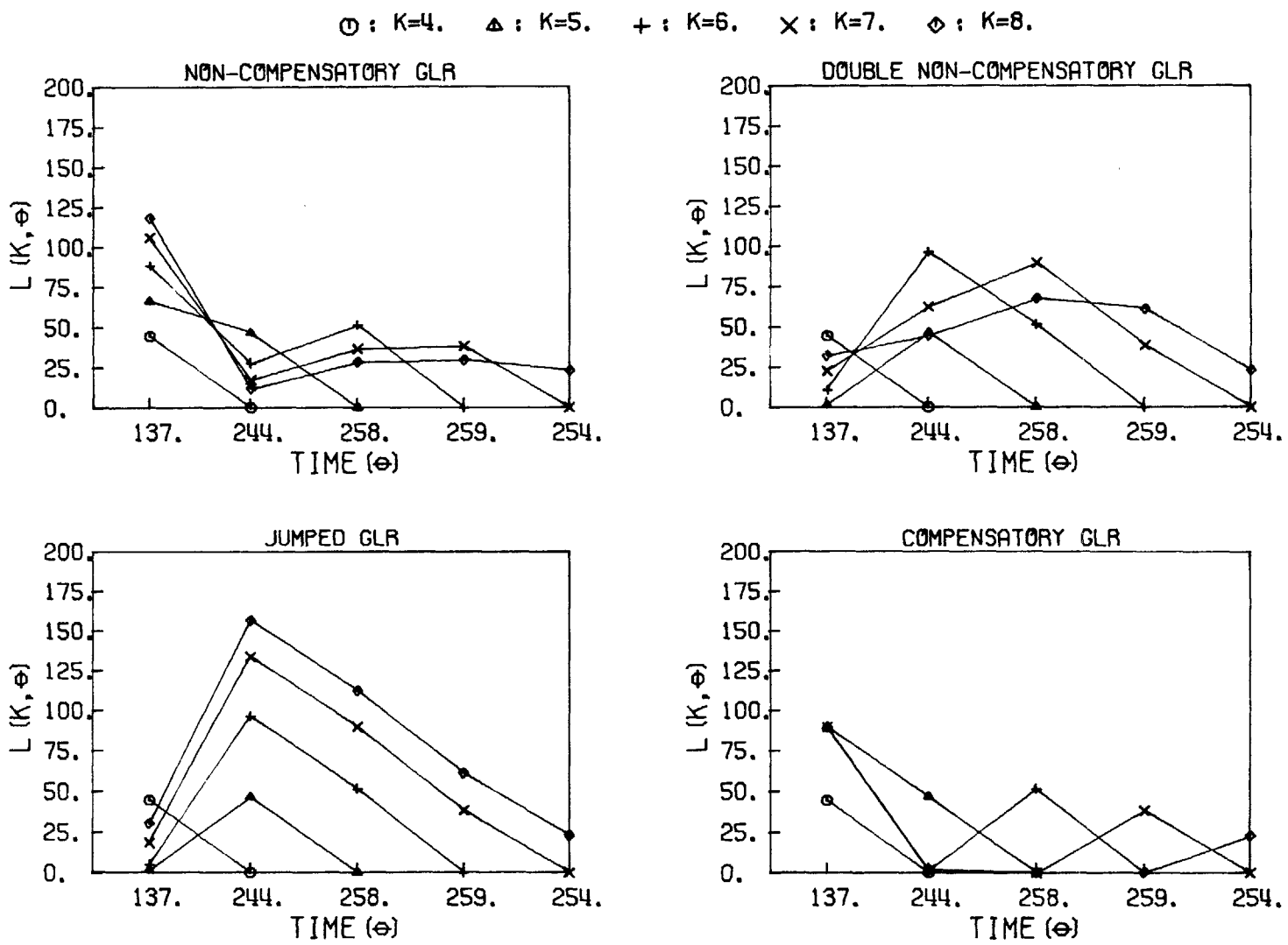

Figure 7.68 Sliding Window GLR for Data File #492-1, without Filter Reinitialization (T=4).

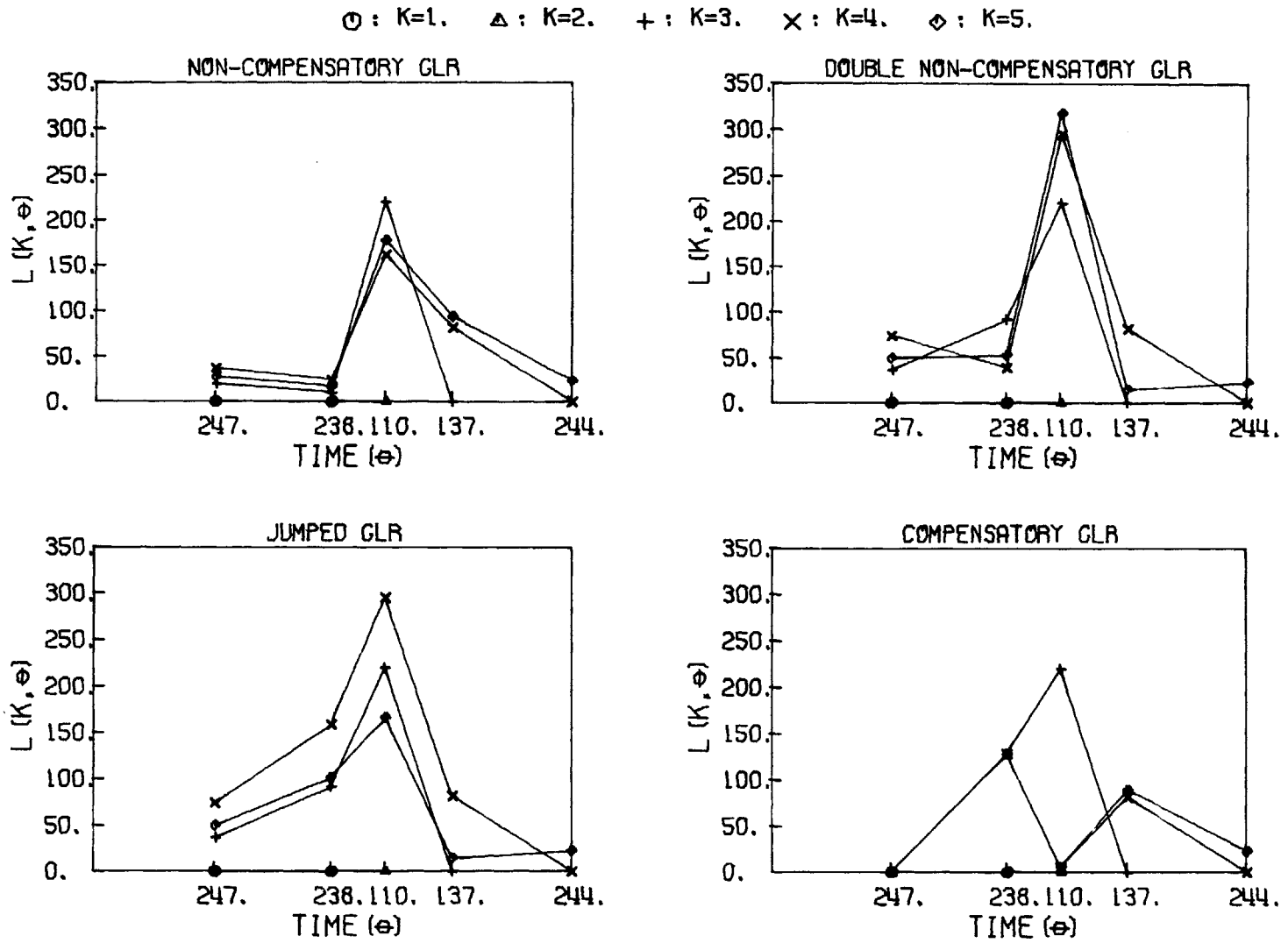

Figure 7.69 Sliding Window GLR for Data File #492-1, with Filter Reinitialized at P_o=32 and x_o=242.5 (T=1).

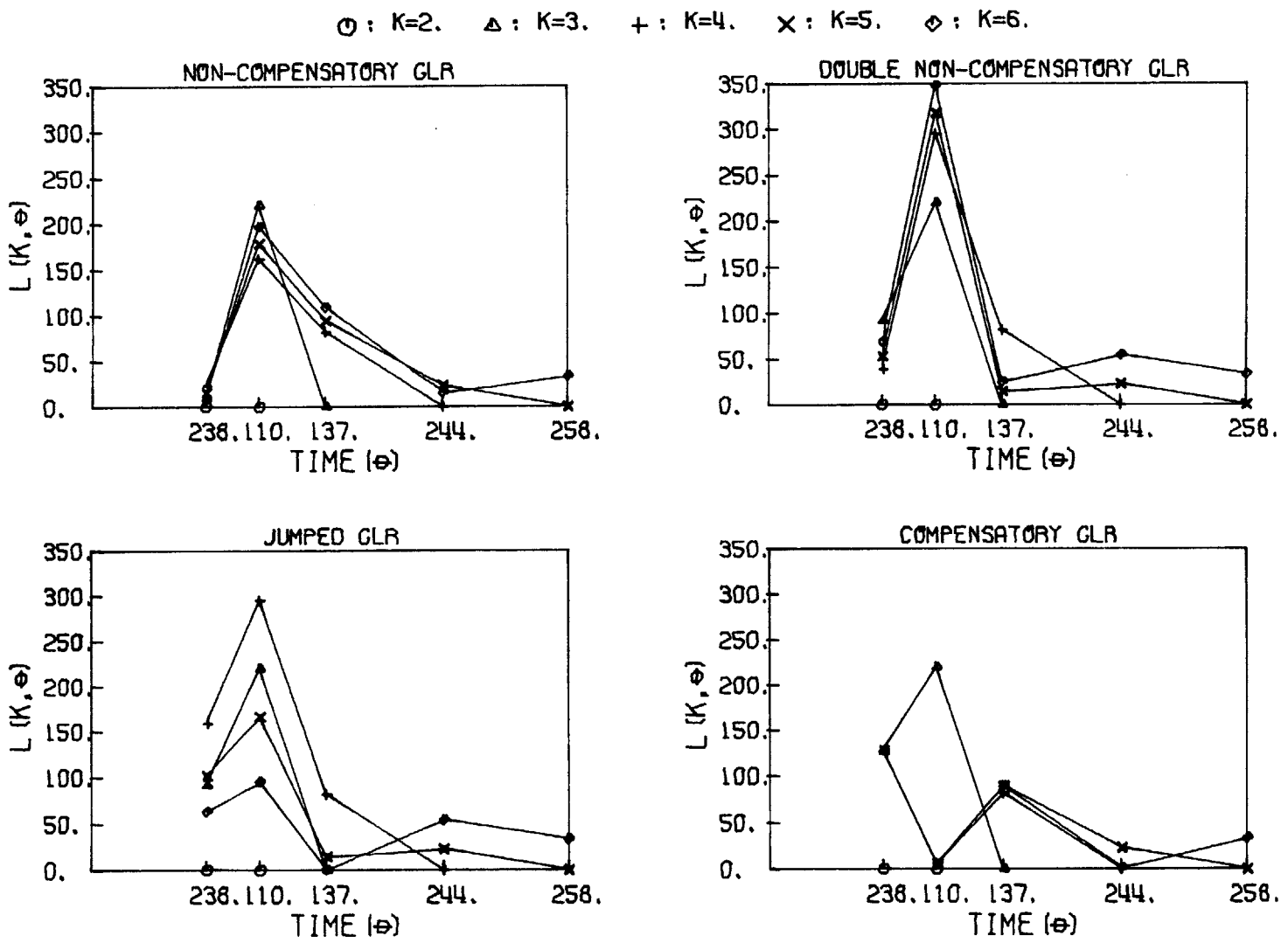

Figure 7.70 Sliding Window GLR for Data File #492-1, with Filter Reinitialized at P_o=32 and x_o=242.5 (T=2).

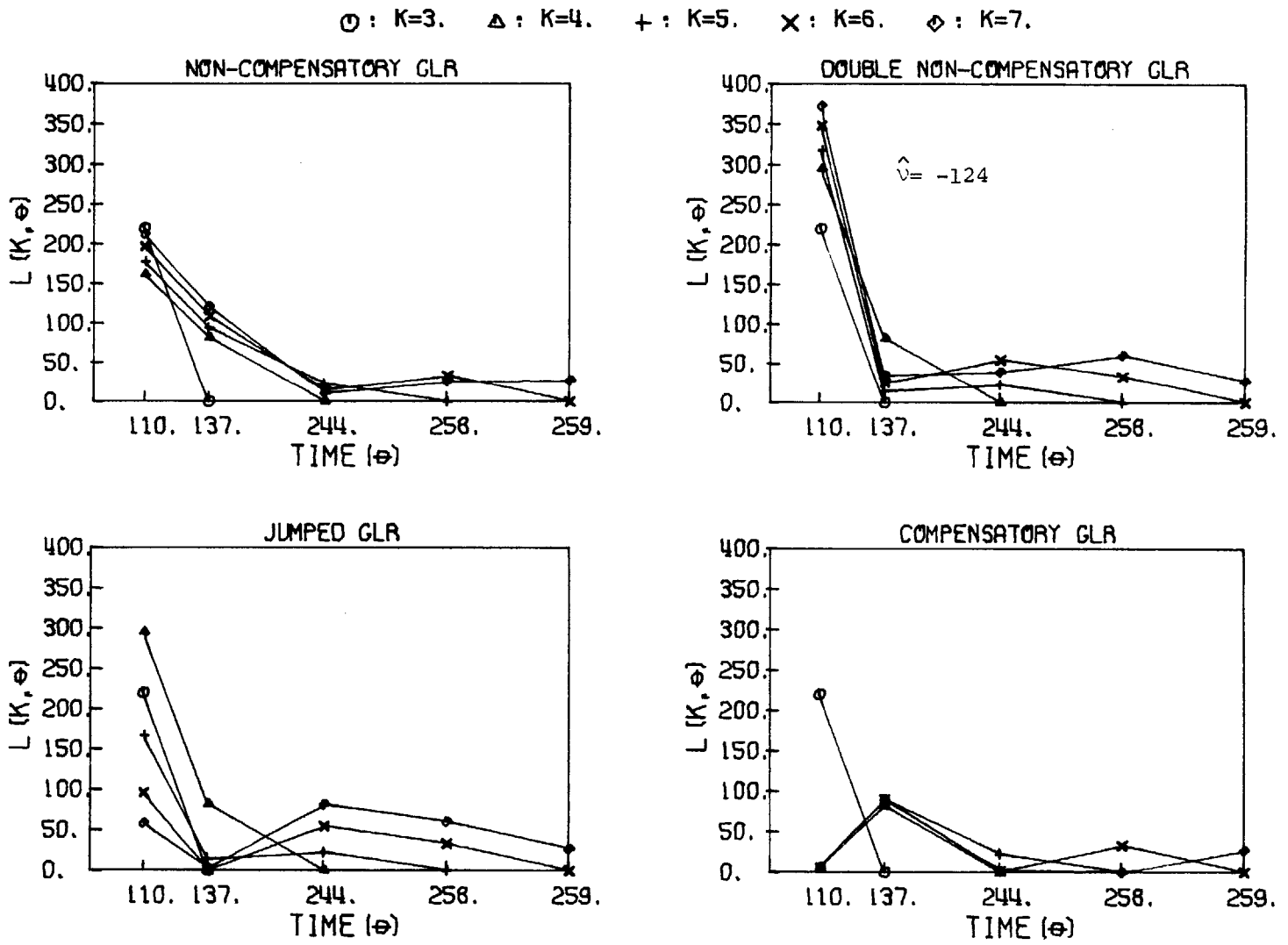

Figure 7.71 Sliding Window GLR for Data File #492-1, with Filter Reinitialized at P_o=32 and x_o=242.5 (T=3).

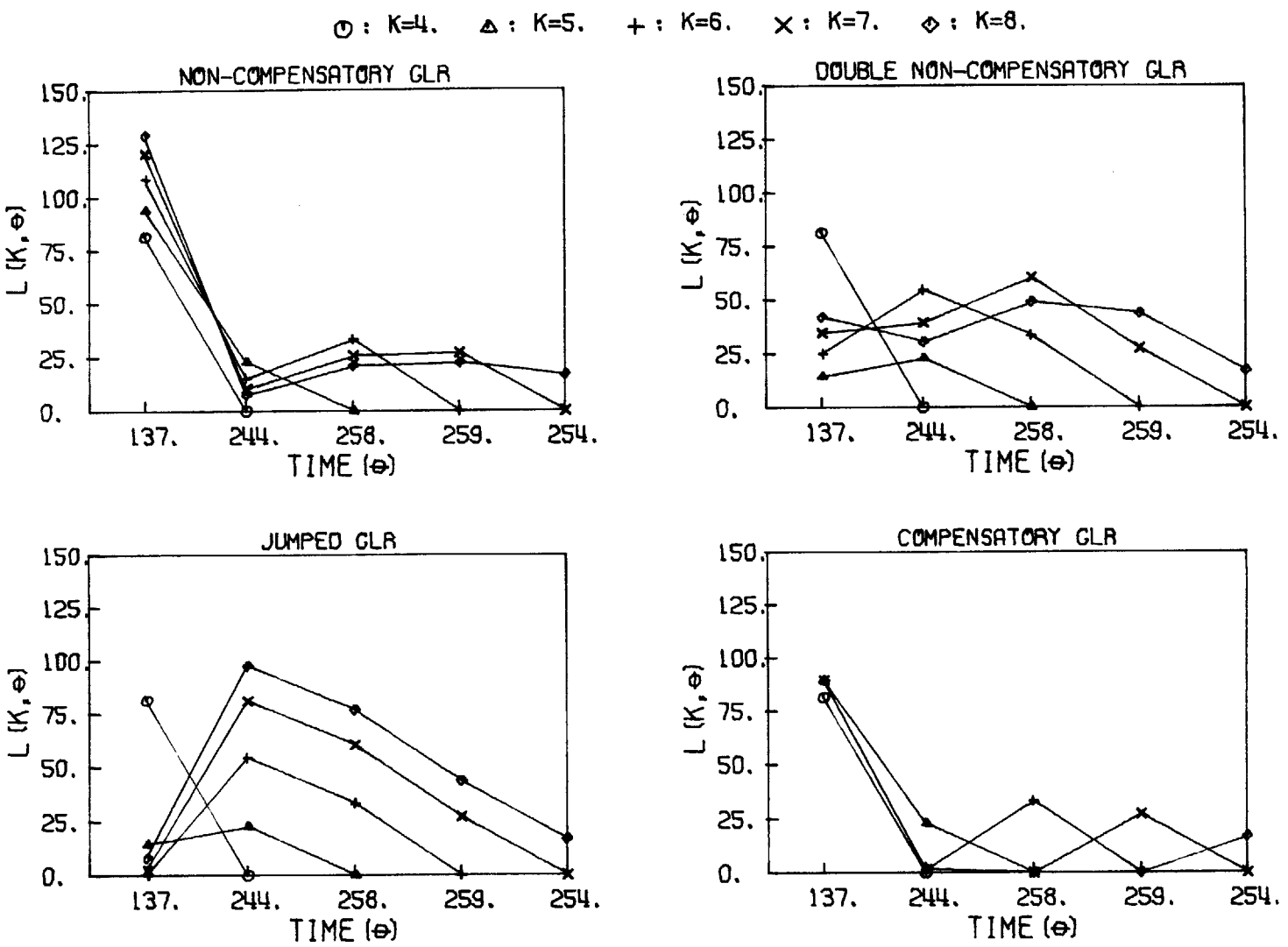

Figure 7.72 Sliding Window GLR for Data File #492-1, with Filter Reinitialized at P_o=32 and x_o=242.5 (T=4).

CHAPTER 8

CONCLUSIONS AND RECOMMENDATIONS

In this thesis, a new approach to development of an automated computer program for the detection and classification of cardiac arrhythmias involving the use of powerful statistical techniques has been studied. The principle results and conclusions of this work are given in the following:

(1) A robust, simple procedure for the determination of fiducial points of the QRS complexes for ECG/VCG has been developed. This fiducial point detector has been tested on a variety of data and good performance has been obtained.

(2) The development of methods for performing rhythm analysis is facilitated by first categorizing the arrhythmias into several classes based on certain clearly identified dynamical characteristics. An attempt was made to categorize cardiac arrhythmias into different classes, based on the use of R-R intervals only. For the persistent rhythms, four classes are identified: small variation, large variation, bigeminy, and trigeminy. For the transient events, four ectopic classes, namely, rhythm shift, non-compensatory beat, compensatory beat, and double non-compensatory beat, are proposed.

(3) Further and more quantitative information about the manifestation of various arrhythmias was obtained by the statistical analysis of the available R-R interval data. Certain simple statistics were computed and two simple graphic display tools, namely, the R-R interval histogram, and the scatter diagram, were employed. These statistics provide us with useful information in the design of the

mathematical models for different arrhythmia classes.

(4) We have shown that several important cardiac disorders can be modeled by a low-order linear stochastic dynamical system for the R-R intervals. These include normal sinus rhythm, sinus tachycardia, sinus bradycardia, atrial fibrillation, bigeminy, trigeminy, PAC, PVC, sinus arrest, SA block, AV block, and interpolated beats. The parameters of the models can be selected to best match the associated statistical characteristics of the cardiac arrhythmia classes. Based on the mathematical models, powerful statistical techniques are available and easily implemented for efficient detection and classification of persistent rhythms (e.g., normal sinus rhythm), and ectopic events (e.g. PVC's)

(5) An algorithm based on multiple model hypothesis testing of a set of Kalman filter residuals has been developed and works quite well in classifying persistent rhythms. A different Kalman filter is used for each persistent rhythm class. Detection of persistent rhythms generally occurred within five heart beats. Detection of switches in persistent rhythms was achieved by using an outlier test, and the desired detection performance was made fast and accurate by reinitializing the Kalman filter parameters and the probabilities for the various rhythm classes.

(6) A generalized likelihood ratio (GLR) testing technique was developed and implemented for the detection and classification of transient events on top of normal sinus rhythms. Extensive tests have been performed on available data. Initial test results suggest that the GLR detection technique is promising. Detection of multiple

ectopic events was achieved by using a "sliding window" GLR detector of window width 5. Using this narrow window we can isolate events that are spaced at points wider than the window width, and thus better detection performance can be obtained. The problem of the detection of ectopic events that occur at the start of a record was overcome by reinitializing the GLR detector.

The results of this work suggest several areas of further research as well as continued development of present ideas. Specifically:

(1) More ECG/VCG data should be tested to evaluate the fiducial point detector in a wide variety of situations. These tests will either be used to adjust parameters of the present detector, or suggest more robust detector designs. For instance, a noise burst of high amplitude, and high frequency may be identified as a QRS complex by the present fiducial point detector. If this should happen, a measure of the width of the QRS complex is necessary. A declaration that an R-wave has been detected will not be made unless the width of the possible QRS complex exceeds a preset value. In addition, in this study, detection has been done using only a single lead. A detector utilizing several or all leads of the ECG/VCG record should be developed and tested.

(2) Since only a limited number of data files were tested, further R-R interval statistical tests will be necessary to get the best estimate of the dynamical model parameters.

(3) Further tests are needed for the multiple model hypothesis testing system to determine the optimal set of filter parameters, which include the measurement noise, initial state estimate, and

initial error covariance for each of the persistent rhythm filters, such that the underlying persistent rhythm associated with each record being tested will be detected and classified in the shortest time, and with the greatest accuracy. Furthermore, the detection and estimation of the multiple model hypothesis testing system is done using causal models. That is, estimates of model states and a posteriori probabilities use only past and present data. However, the detection performance may be improved if one uses non-causal models, which employ future data to perform the detection and estimation. Thus a non-causal detection system should be developed and tested.

(4) For the transient rhythm classes proposed in this study, a GLR window width of at least three is needed in order to distinguish each classes. Therefore a window width of five was choosen for the GLR detector system in this study. However the test results show that a window width of three should do as well. Using a smaller window width will not only reduce the computations of the likelihood ratios, and separate the multiple ectopic events, but also simplify the logic for classifying different transient rhythm classes. Thus if the detection performance is not degraded a smaller window width is more desirable. Furthermore, it appears that it is feasible to use only a window width of two for the GLR system. In this case, a rhythm shift will be identified by the detection of more than two consecutive double non-compensatory beat. Using this window width the computations and classification logic will be further simplified. A GLR detector using a window width of two should be implemented and tested.

(5) The Kalman filter models now have no driving noise, so that the gains will approach to zero asymptotically. Driving noise could be included to produce non-zero steady state gains, or techniques such as age-weighted filtering could be used.

(6) The multiple model hypothesis testing system and the GLR detection system must be integrated together in an overall system for the detection and classification of arrhythmias. At the beginning of the record both the multifilter and GLR detector should be running. When an ectopic event is detected by the GLR detector, additional logic will be used to determine type of arrhythmia. The multiple models may have to be reinitialized when an ectopic event occurs such that accurate and fast detection can be obtained. However the exact configuration and the detailed logic will be determined only as experience with more actual data is gained.

(7) The arrhythmia detection and classification system considered thus far has only utilized the R-R interval information. Thus, a PVC may not be distinguishable from other prematures (since their interval sequence patterns may look identical). In this case the wave shape information should be considered, since PVC's have aberrant QRS's and this can be used to distinguish from other prematures. Therefore, a classification system utilizing the waveshape information should be developed and integrated in the rhythm analysis system.

(8) Extensions should be made to include both P-R and P-P intervals, which require the development of a P-wave detector. Once these intervals are known the present techniques used for R-R interval data

can be extended in a straight forward manner by simply defining higher order dynamical models with the R-R, P-R, and P-P intervals as the components of the state.

(9) The detection of another arrhythmia class -flutter and fibrillation- in which there is an unusually large amount of high frequency energy will need some type of high pass digital filter. To do this, the diagnostic characteristics and spectral character of this class of arrhythmias must be studied.

REFERENCES

1. Waller, A., "A Demonstration of Electromotive Changes Accompanying the Heart Beat", J. Physiol. 8:229, 1887.

2. Wenckebach, K.F., "Zur Analyse des Unregelmassigen Pulses", Z. Klin. Med. 37:475, 1899.

3. Burch, G.E., and De Pasquale, B., A History of Electrocardiography, Year Book Medical Publ., Chicago, 1964.

4. Wartak, J., Computers in Electrocardiography, Charles C. Thomas, Ill., 1970.

5. Scher, A.M., Young, A.S., and Meredith, W.M., "Factor Analysis of the Electrocardiogram; A Test of Electrocardiographic Theory; Normal Leads", Circ. Res. 8:519, 1960.

6. Noran, L.G., Flowers, N.C., and Brody, D.A., "Principle Factor Waveforms of the Thoracic QRS Complex", Circ. Res. 15:131, 1964.

7. Young, T.Y., and Huggins, W.H., "On the Representation of Electrocardiograms", IEEE Trans. Bio. Med. Electron. BME-10:86, 1963.

8. Frank, E., "An Accurate, Clinically Practical System for Spatial Vectorcardiography", Circ. Res. 13:737, 1956.

9. Burch, G.E., and Winsor, T., A Primer of Electrocardiography, Lea and Febiger, Phila., 1966.

10. Simonson, E., Differentiation Between Normal and Abnormal in Electrocardiography, C.V. Mosby, St. Louis, 1961.

11. Neufeld, H.N., et.al., "The Use of a Computerized ECG Interpretation System in an Epidemiologic Study", Meth. Inform. Med. 10:85, 1971.

12. Pipberger, H.V., "Computer Analysis of the Electrocardiogram" in Computer in Biomedical Research (Edited by Waxman, B.D., and Stacy, R.V.), P.377. Academic Press, New York, 1965.

13. Willems, J.L., and Pipberger, H.V., "Arrhythmia Detection by Digital Computer", Comp. Biomed. Res. 5:263, 1972.

14. Caceres, C.A., Steinberg, C.A., Abraham, S., et.al., "Computer Extraction of Electrocardiographic Patterns", Circ. Res. 25:356, 1962.

15. Caceres, C.A., "Electrocardiographic Analysis by a Computer System", Arch. Intern. Med. 111:196, 1963.

16. Caceres, C.A., and Rikli, A.E., Appendix I in Diagnostic Computers, p.77, Charles C. Thomas, Springfield, 1969.

17. Arvedson, O., "Automatic interpretation of ECGs with the Digital Computer" in Digest of the 7th International Conference on Medical and Biological Engineering, P.107, Stockholm, 1967.

18. Bonner, R.E., and Schwetman, H.D., "Computer Diagnosis of Electrocariograms. II, A Computer Program for EKG Measurements", Comp. Biomed. Res. 1:366, 1968.

19. Bonner, R.E., and Schwetman, H.D., "Computer Diagnosis of Electrocardiograms. III, A Computer Program for Arrhythmia Diagnosis ", Comp. Biomed. Res. 1:387, 1968.

20. Pordy, L., Jaffe, H., Chesky, K., Friedberg, C.K., Fallowes, L., and Bonner, R.E., "Computer Diagnosis of Electrocardiograms. IV., A Computer Program for Contour Analysis with Clinical Results of Rhythm and Contour Interpretation", Comp. Biomed. Res. 1:408, 1968.

21. Bonner, R.E., Crevasse, L., Ferrer, M.I., and Greenfield, J.C., "A New Computer Program for Analysis of Scalar Electrocardiograms", Comp. Biomed. Res. 5:629, 1972.

22. Smith, R.E. and Hyde, C.M., "Computer Analysis of the Electrocardiogram in Clinical Practice" in Electrical Activity of the Heart (Edited by Manning, G.W. and Ahuja, S.P.), P.305, Charles C. Thomas, Springfield, 1969.

23. Macfarlane, P.W. "ECG Waveform Identification by Digital Computer", Cardiovasc. Res. 5:141, 1971.

24. Wolf, H.K. and Rautaharju, P.M., "An On-Line Program for Acquisition and Analysis of Resting and Exercise Electrocardiograms" in Proceedings of the XIth International Vectorcardiography Symposium (Edited by Hoffman, I.), P.231, North Holland, Amsterdam, 1971.

25. Wartak, J., Milliken, J.A., and Karchmar, J., "Computer Program for Diagnostic Evaluation of Electrocardiograms", Comp. Biomed. Res. 4:225, 1971.

26. Pryor, T.A., Russel, R., Budkin, A. and Price, W.G., "Electrocardiographic Interpretation by Computer", Comp. Biomed. Res. 2:537, 1969.

27. Watanabe, Y.M., and Y. Okamoto N., et.al., "On-Line Computer Diagnosis of Arrhythmias on ECG Using Small Scale Digital Computer System", Jap. Circ. J. 33:129, 1969.

28. Bailey, J.J., et.al., "A Method for Evaluating Computer Programs for Electrocardiographis Interpretation", Circ. Res. 50:73, 1975.

29. Gersch, W., Eddy, D.M., and Dong, E., "Cardiac Arrhythmia Classification: A Heart-Beat Interval-Markov Chain Approach", Comp. Biomed. Res. 4:385, 1970.

30. Gersch, W., Lilly, P., and Dong, E., "PVC Detection by the Heart-Beat Interval Data - Markov Chain Approach", Comp. Biomed. Res. 8:370, 1975.

31. Haisty, W.K., Batchlor, C., Cornfield, J., and Pipberger, H.V., "Discriminant Function Analysis of RR Intervals: An algorithm for On-Line Arrhythmia Diagnosis", Comp. Biomed. Res. 5:247, 1972.

32. Tsui, E.T., and Wong, E., "A Sequential Approach to Heart-Beat Interval Classification", IEEE Trans. Inform. Theory, IT-9:596, 1975.

33. Chiang, B.N., Perlman, L.V., Ostrander, L.D., and Epstein, F.H., "Relationship of Premature Systoles to Coronary Heart Disease and Sudden Death in the Tecumsah Epidemiologic Study" Ann. Inter. Med. 70:1159, 1969.

34. Leblanc, A.R., and Roberge, F.A., "Present State of Arrhythmia Analysis by Computer", Can. Med. Assoc. Jour. 108:1239, 1973.

35. Gustafson, D.E., Johnson, T.L. and Akant, A., "Cardiogram Analysis and Classification Using Signal Analysis Techniques", C.S. Draper Lab Report R-853, September, 1974.

36. Akant, A., "Processing of Cardiograms for Pattern Recognition", S.M. thesis, Dept. of Electrical Engineering, M.I.T., June, 1974.

37. Gustafson, D.E., Willsky, A.S. and Wang, J-Y., "Cardiac Arrhythmia Detection and Classification Through Signal Analysis", C.S. Draper Lab Rept. R-920, July, 1975.

38. Wadsworth, G.P., and Bryan, J.G., Introduction to Probability and Random Variables, McGraw-Hill, New York, 1960.

39. Kalman, R.E., "A New Approach to Linear Filtering and Prediction Problems", Trans. ASME, Ser. D, J. Basic Eng. 82:35, 1960.

40. Lainiotis, D.G., and Park, S.K., "On Joint Detection, Estimation and System Identification: Discrete Data Case", Int. J. Control 17-3: 609, 1973.

41. Athans, M., and Willner, D., "A Practical Scheme for Adaptive Aircraft Flight Control Systems", Symposium on Parameter Estimation Techniques and Application to Aircraft Flight Testing, NASA Flight Research Center, Edwards AFB, Calif. April, 1973.

42. Van Trees, H.L., Detection, Estimation, and Modulation Theory, Part I, Wiley, New York, 1968.

43. Willsky, A.S. and Jones, H.L., "A Generalized Likelihood Ratio Approach to Estimation in Linear Systems Subject to Abrupt Changes", Proc. of the 1974 IEEE Conference on Decision and Control, Phoenix, Ariz., November, 1974.